Analysis and Assimilation of Temperature and Altimetry Data in the North Atlantic Ocean

Stephen M. Grey

Doctor of Philosophy
The University of Edinburgh
1999

Declaration

This thesis has been composed by myself, and all work reported herein is my own except where otherwise stated.

Stephen M. Grey

Acknowledgements

I'd like to thank my supervisor, Keith Haines, for his help and support throughout this project. Thanks also to members of the Department of Meteorology for the help I have received and for creating a good, friendly atmosphere in which to work. Thanks to Doug Smith of the UK Meteorological Office for providing the historical temperature data on which much of this work is based.

This work was supported financially by the Natural Environment Research Council and a CASE award from the Rutherford Appleton Laboratory.

Abstract

Observations of subsurface temperatures in the North Atlantic between 1950 and 1994 have been analysed to investigate interdecadal variability. Previous studies have concentrated on the more plentiful sea surface temperature data or on limited hydrographic data. Here, all subsurface temperature data, principally from bathythermographs, are used to investigate the development and evolution of temperature anomalies.

During most of the period, a dipole feature was seen. The western subtropical gyre and the ocean north of 50°N were occupied by anomalies of opposite sign. These regions appear to show a cycle of warming and cooling with a period of approximately 30 years but the data record is too short to determine whether this is a regular oscillation. There is evidence of propagation of temperature anomalies along the paths of the major upper ocean currents, namely along the Gulf Stream and North Atlantic Current and also along the return currents on the southern edge of the subtropical gyre.

An intense warm anomaly on the northern edge of the subtropical gyre developed between 1988 and the end of the data in 1994. The Gulf Stream front became steeper and isotherms were depressed by up to 150m. This is consistent with a stronger Gulf Stream and an intensification of the circulation of the subtropical gyre. This is compared with a cold anomaly in 1966–1972 which is opposite in nature, indicating a weaker subtropical gyre circulation.

A scheme developed by Cooper and Haines (1996) has been employed to assimilate sea level anomaly data from the TOPEX/POSEIDON altimeter with a climatological hydrography of the North Atlantic. The aim was to use this model-independent and computationally cheap method to create a hydrography representing the ocean at the time of the observations. Resultant hydrographies were compared with XBT observations to assess the assimilation scheme and determine its limitations and whether modifications are necessary. These findings may also be useful for future application of the scheme with ocean models.

It was found that the climatology needed adjustment to make it consistent with the period, 1993–1995, from which the mean surface height is determined. After this correction, the scheme was quite successful in recreating the permanent thermocline but the mixed layer and seasonal thermocline could not be satisfactorily reproduced. Spatially filtering the sea level anomaly data to remove seasonal effects improved the success in the permanent thermocline.

Contents

1 Introduction 1
- 1.1 The North Atlantic . . . 3
  - 1.1.1 The Subtropical Gyre . . . 4
  - 1.1.2 Circulation in the northern North Atlantic . . . 6
  - 1.1.3 The formation and ventilation of the thermocline . . . 8
  - 1.1.4 Convection and formation of mode waters . . . 11
  - 1.1.5 Mesoscale Eddies . . . 12
- 1.2 Satellite Altimetry . . . 15
  - 1.2.1 TOPEX/POSEIDON . . . 18

2 Hydrographic Data 20
- 2.1 Levitus Hydrography . . . 20
- 2.2 Lozier Hydrography . . . 21
  - 2.2.1 Filling in Holes . . . 23
  - 2.2.2 Smoothing . . . 25
  - 2.2.3 Smoothing results . . . 29
- 2.3 Comparison of Lozier and Levitus hydrographies . . . 30
- 2.4 Representativeness of the Hydrographies . . . 32

3 Interannual and interdecadal variability of ocean hydrography 36
- 3.1 Introduction . . . 36
- 3.2 The North Atlantic Oscillation . . . 37
- 3.3 Studies of hydrographic variability . . . 39
- 3.4 Sea surface temperature variability . . . 48
- 3.5 Variability of the position of the Gulf Stream and North Atlantic Current . . . 54
- 3.6 Variability in Ocean Models . . . 56
- 3.7 Summary and Discussion . . . 59

4 Interdecadal variability of subsurface temperature in the North Atlantic 63
- 4.1 Hydrographic temperature data . . . 63
- 4.2 The objective analysis mapping technique . . . 66
- 4.3 Comparison of XBT mapping with previous studies . . . 67
  - 4.3.1 Comparison with Levitus (1989b) . . . 67
- 4.4 Decadal variation of subsurface temperatures . . . 72

4.4.1 Evolution of temperature anomalies between 300 and 500m depth, 1950–1994 . . . 74
4.4.2 Evolution of temperature anomalies between 100 and 250m depth, 1950–1994 . . . 83
4.4.3 Discussion of temperature anomalies . . . 88
4.5 Temperature anomalies in the subtropical gyre . . . 92
4.5.1 The warm anomaly in the Gulf Stream 1988–94 . . . 93
4.5.2 Cold anomaly in the Gulf Stream 1966–72 . . . 97
4.6 Summary and Discussion . . . 99
4.6.1 Propagation of anomalies . . . 101
4.6.2 Events in the subtropical gyre . . . 102

5 Assimilation of Altimetry with Climatological Hydrography 105
5.1 Introduction . . . 105
5.2 Methods of assimilating altimetry . . . 106
5.3 Sea Level Anomaly Maps . . . 109
5.4 Assimilation Scheme . . . 109
5.4.1 Sea Surface height and water column mass . . . 110
5.4.2 Vertical displacement of water columns . . . 111
5.5 Producing new hydrographic fields . . . 114
5.6 Comparison with XBTs . . . 119
5.6.1 Evaluation of assimilation scheme . . . 121
5.6.2 Amendments to the assimilation scheme . . . 122
5.6.3 Best Possible Fit . . . 124
5.7 Summary . . . 125

6 Assimilation Results 126
6.1 Introduction . . . 126
6.2 Atlantic Results . . . 126
6.2.1 Results of Assimilation . . . 128
6.3 Long-term variability of hydrography . . . 133
6.3.1 Results for correction of hydrography for long-term variability 135
6.4 Mixed-Layer Effects . . . 137
6.4.1 Assimilation of Sea Surface Temperatures . . . 141
6.4.2 Filtering out the Steric Component . . . 143
6.4.3 Results of assimilation accounting for steric height changes 146
6.5 Assimilation with Levitus 1994 Climatology . . . 151
6.6 Other problems . . . 152
6.6.1 Spatial differences . . . 152
6.6.2 Advection . . . 154
6.6.3 Errors in the Altimetry . . . 155
6.6.4 Barotropic Mode . . . 156
6.7 Summary of Results from North Atlantic . . . 157
6.8 Pacific Results . . . 161
6.8.1 Results . . . 166
6.9 Discussion . . . 170

7 Conclusions **173**
7.1 North Atlantic Hydrography 173
7.2 Interdecadal Variability 174
7.2.1 Further work 175
7.3 Assimilation of altimetry with climatological hydrography 176

A Mapping Technique **179**

Chapter 1

Introduction

In the past century the oceans have received growing attention from the scientific community. Covering over two thirds of the Earths surface, their importance to the global climate cannot be overstated, acting as a vast reservoir and transporter of heat. Despite the expanding research, there is still much that is unknown about the physical oceans. Due to the vast size and inaccessibility of the world's oceans, observations can only give a limited picture of their structure and circulation.

Advances in technology has aided the study of the oceans through development of, for example, expendable bathythermographs which are cheap, accurate and easy to deploy so that they can be used to collect data from merchant ships as well as specific research cruises. More recently, advances in remote sensing is allowing accurate observation of the ocean from satellite. Although satellites can only observe properties of the sea surface, they can give unprecedented coverage and continuous data collection.

Due to its position between Europe and North America, the North Atlantic is the most observed ocean in the world. For this reason, it has been the subject of many studies of ocean dynamics and processes. The North Atlantic also has a large influence on climate. The Gulf Stream and North Atlantic Current, which transport warm waters from the tropics, are among the major influences on the climate of Northern Europe, particularly the British Isles, being largely responsible for our mild winters. The North Atlantic Current is the largest oceanic transporter of heat northward in the Northern Hemisphere (Talley 1984). The North Atlantic is also a site of water formation, for example deep water formed by convection in the Labrador Sea is transported widely throughout the North

Atlantic and also to other oceans around the world (Talley and McCartney 1982).

The initial purpose of this research was to test the assimilation method of Cooper and Haines (1996) with a climatological hydrography of the North Atlantic. The aim being to combine the hydrography, which describes the long-term mean state of the whole ocean in terms of temperature and salinity, with sea surface height determined from satellite altimetry which vary with time but only directly tell us about the surface. The results of this assimilation are new hydrographic fields which hopefully better represent the ocean at the time of the altimetric observations. These could be useful in situations where one might normally use a climatological hydrography, such as the initialisation of a model, but wish it to be relevant to a particular time. This method is independent of any model and is therefore very computationally inexpensive.

Another motivation for employing the assimilation in this way is to evaluate the method of combining SSH with hydrography and the usefulness of altimetry for correcting hydrographic fields. This method isolates the assimilation from a model, so we can assess it on its own without any complicated effects of a model. Hence, we can see how well the simple assimilation can recreate the state of the ocean by comparing the results with in situ measurements such as expendable bathythermographs. We can then determine problems and limitations of the assimilation scheme and any modifications that need to be made. These findings may then be more useful for the application of the assimilation scheme with a model.

This method requires a climatological hydrography as the starting point. The usual climatology which is used is Levitus (1982) or the updated version Levitus (1994). Another, newer climatology is Lozier et al. (1995) which is a climatology specific to the North Atlantic and has been produced by averaging hydrographic observations on potential density surfaces, rather than depth surfaces, which avoids unrealistic mixing of water masses. This climatology, in the form in which it was obtained, was unsmoothed and had gaps in the data. Before it could be used effectively these gaps were filled and the data smoothed.

In the course of the assimilation experiments it was found that there were persistent differences between the XBTs deployed in the years 1993–1995 (the years for which TOPEX/POSEIDON altimetry is available), and the climatology which

had been built up from all observations from 1900 to 1990. It was found that the differences were due to large, decadal time-scale variation in the hydrography of the North Atlantic. This led to an investigation into interdecadal variability. The structure of the thesis does not follow the chronology of the research but is arranged in the following, more logical, manner.

In this chapter the North Atlantic is introduced and the hydrography and circulation briefly discussed and also the dynamics of mesoscale eddies, which are relevant to the principles of the assimilation scheme and to comparisons with altimetry maps. This chapter also contains an overview of satellite altimetry and the TOPEX/POSEIDON satellite.

In chapter 2 the climatological hydrographies, Levitus (1994) and Lozier et al. (1995), are described. Also described are the methods of filling in the holes in the Lozier dataset and smoothing it on potential density surfaces.

Chapters 3 and 4 are concerned with interdecadal variability in hydrography. Chapter 3 introduces and reviews previous studies of interdecadal variability. In chapter 4, subsurface temperature measurements taken over the 45 years from 1950 to 1994 inclusive are analysed to investigate interdecadal variability in the North Atlantic.

In chapter 5 altimetry assimilation scheme is described, the methods by which it is used with climatological hydrography, and how it is evaluated against instantaneous XBT observations. In chapter 6, the results of the assimilation experiments are presented. Chapter 7 is a discussion and conclusions from the work and proposals for further work.

1.1 The North Atlantic

The North Atlantic basin is shown in figure 1.1 with some of the features and regions important to this study labelled. In this section the main near-surface circulation is described with some of the processes occurring in the ocean such as deep water formation and mesoscale eddies. The circulation in the North Atlantic is dominated by the subtropical gyre and the subpolar gyre.

1.1.1 The Subtropical Gyre

The circulation of the subtropical gyre dominates the North Atlantic between the latitudes of 15 and 45°N. The circulation is wind driven, with prevailing westerly winds over the northern gyre and the easterly trade winds over the south. Hence, the circulation is anticyclonic, which in the northern hemisphere is clockwise. The western boundary current of the subtropical gyre is the Gulf Stream and waters recirculate by a broad flow including the Azores and Canaries Currents.

The Gulf Stream

The waters in the Gulf Stream originate from the equatorial Atlantic and the recirculated waters of the subtropical gyre as illustrated in figure 1.2 taken from Schmitz and McCartney (1993). Some of the south equatorial current is diverted by the north Brazilian coastline, is joined by the recirculated subtropical gyre waters, and enters the Caribbean Sea. This water continues on through the Yucatan Channel into the Gulf of Mexico. From here, some of the water joins the circulation of the Gulf Of Mexico but most goes directly to the Florida Straits and out into the North Atlantic where it becomes the Gulf Stream. Some of the deeper waters from the South Atlantic are unable to enter the Caribbean Sea because the passages between the islands of the Lesser Antilles are not deep enough. These waters form part of the Antillean Current, which runs on the eastern side of the Antillean island chain, and then joins the Gulf Stream after it emerges from the Florida Straits.

From the Florida Straits, the Gulf Stream flows northward along the continental slope until it reaches Cape Hatteras. At Cape Hatteras the current separates from the coast and continues in a wide arc to the end of the Grand Banks southeast of Newfoundland (45°W). Figure 1.2 shows an estimation of the mean flow but the Gulf Stream does not follow a constant path. Upstream of Cape Hatteras, the current is constrained by the topography and so meanders are small. However, after Cape Hatteras, in the open ocean, the path of the Gulf Stream is very variable with time and meanders of amplitude greater than 300km are common. Often these meanders 'pinch off' creating mesoscale eddies on either side of the current. Meanders and eddies are large enough to be identified by

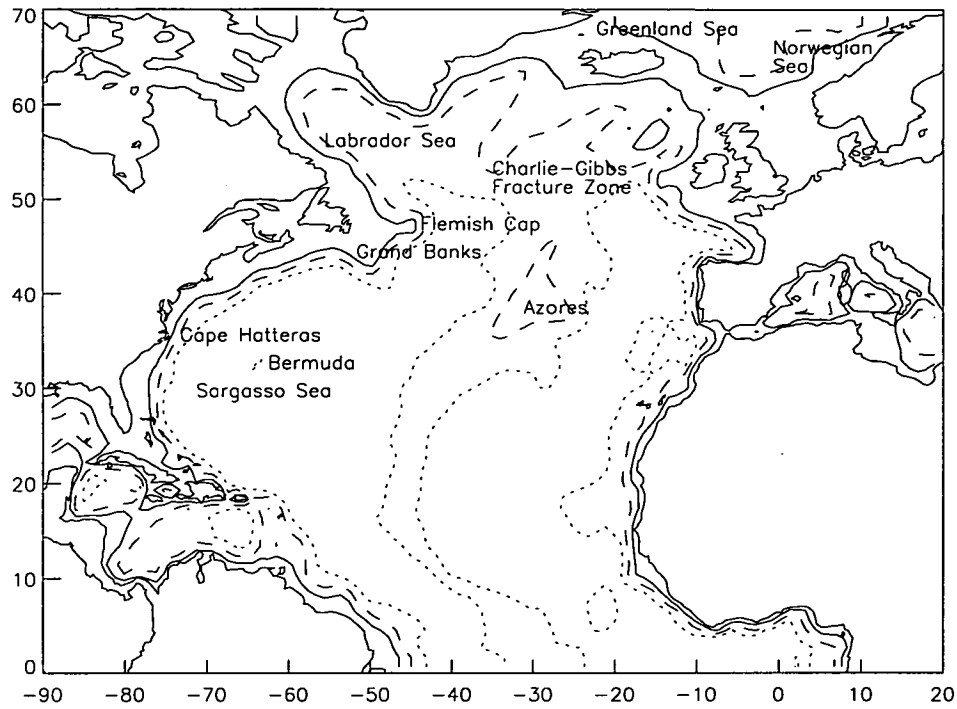

Figure 1.1: The North Atlantic Ocean with some areas and features referred to in the thesis. Contours show 1000m, 2500m and 4000m isobaths.

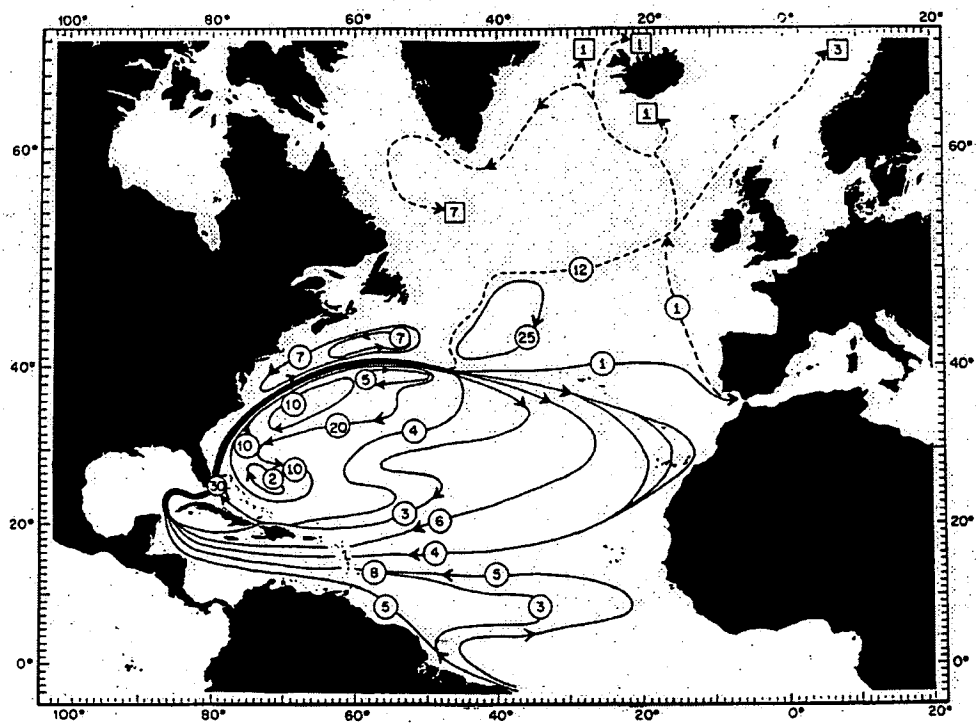

Figure 1.2: Near surface currents of the North Atlantic showing the flow of waters of temperature greater than 7°C. Taken from Schmitz and McCartney (1993). The numbers on the streamlines denote approximate transport in sverdrups.

satellite altimeters and in the North Atlantic are the cause of the greatest temporal variations in sea surface height. Section 1.1.5 discusses mesoscale eddies in more detail. To the north of the Gulf Stream there is a narrow cyclonic gyre between the Gulf Stream and the coast of the USA and Canada. These slope waters are very cold compared to the Sargasso Sea waters on the other side of the Gulf Stream.

The volume of transport of the Gulf Stream changes along its length due to contributions from the recirculation of the Sargasso Sea. The flow coming out of the Florida Straits is well known to be approximately 30Sv (Worthington 1976, Schmitz and McCartney 1993). The volume of the flow reaches a maximum at about 65°W where the flow has been estimated as being between 100Sv (Schmitz and McCartney 1993) and 150Sv (Worthington 1976). The current gradually broadens and becomes more diffuse.

At the southeast corner of the Grand Banks, the current now splits in two, part carrying on eastward and forming the broad currents of the eastern subtropical gyre and part turning to the northeast, the North Atlantic Current. The southward flow of the eastern subtropical gyre is known as the Canary Current.

1.1.2 Circulation in the northern North Atlantic

The North Atlantic Current flows northeast after it has split from the rest of the Gulf Stream and follows the continental slope east of the Grand Banks. After passing the Flemish Cap there is a permanent meander in the current at approximately 50°N 45°W called the 'Northwest Corner' (Worthington 1976). Here, the current goes northwest and almost doubles back on itself before continuing eastward and northward towards Scotland and up into the Norwegian Sea. Figure 1.3 from Krauss (1986) shows a more detailed map of the currents of the northern North Atlantic.

Figure 1.2 shows some of the North Atlantic Current is part of a 'northern gyre' around 45°N 40°W. This was proposed by Worthington (1976) and has also been adopted by Schmitz and McCartney (1993). However, there is little evidence that this recirculation exists and other authors have suggested other schemes. The schematic shown in figure 1.3, proposed by Krauss (1986), was based on trajectories of satellite-tracked buoys and hydrographic sections and is similar to

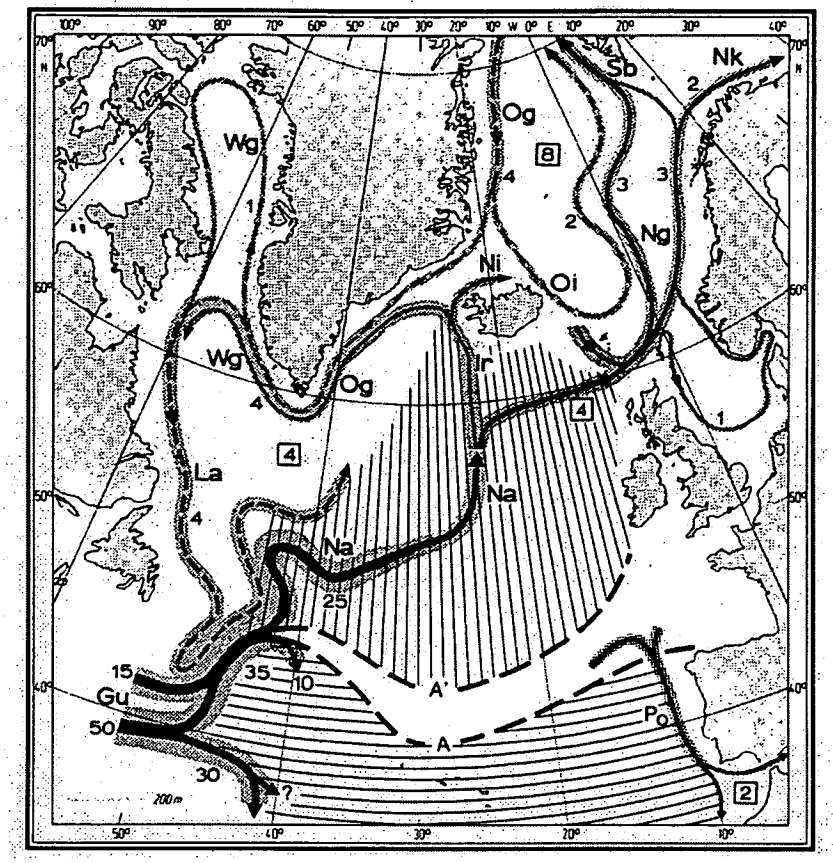

Figure 1.3: Surface currents in the northern North Atlantic. Taken from Krauss (1986). The currents are labelled; Gu, Gulf Stream; Na North Atlantic Current; Ir, Irminger Current; Og, Wg, East and West Greenland Currents; La, Labrador Current; Ng, Norwegian Current; Ni, Oi, North and East Iceland Currents.

an earlier plan by Dietrich et al. (1975). This scheme is also supported by the results of Belkin and Levitus (1996). Beyond the 'Northwest Corner' the current is very broad and diffuse and the paths in figure 1.3 just give an indication of the general flow direction.

After the bifurcation of the Gulf Stream, there is a further branch off the North Atlantic Current flowing southeastward towards the Azores where it rejoins the circulation of the subtropical gyre. After this branching, Krauss states that the North Atlantic Current contributes no more to the subtropical gyre. As the current flows northeastward there is a branch northward towards Iceland, the Irminger Current. At Iceland this current splits into the North Iceland Current and a westward current which joins the East Greenland Current which flows southward from the Arctic Ocean. This then flows round the southern tip of Greenland then for some way northward along the west coast before looping

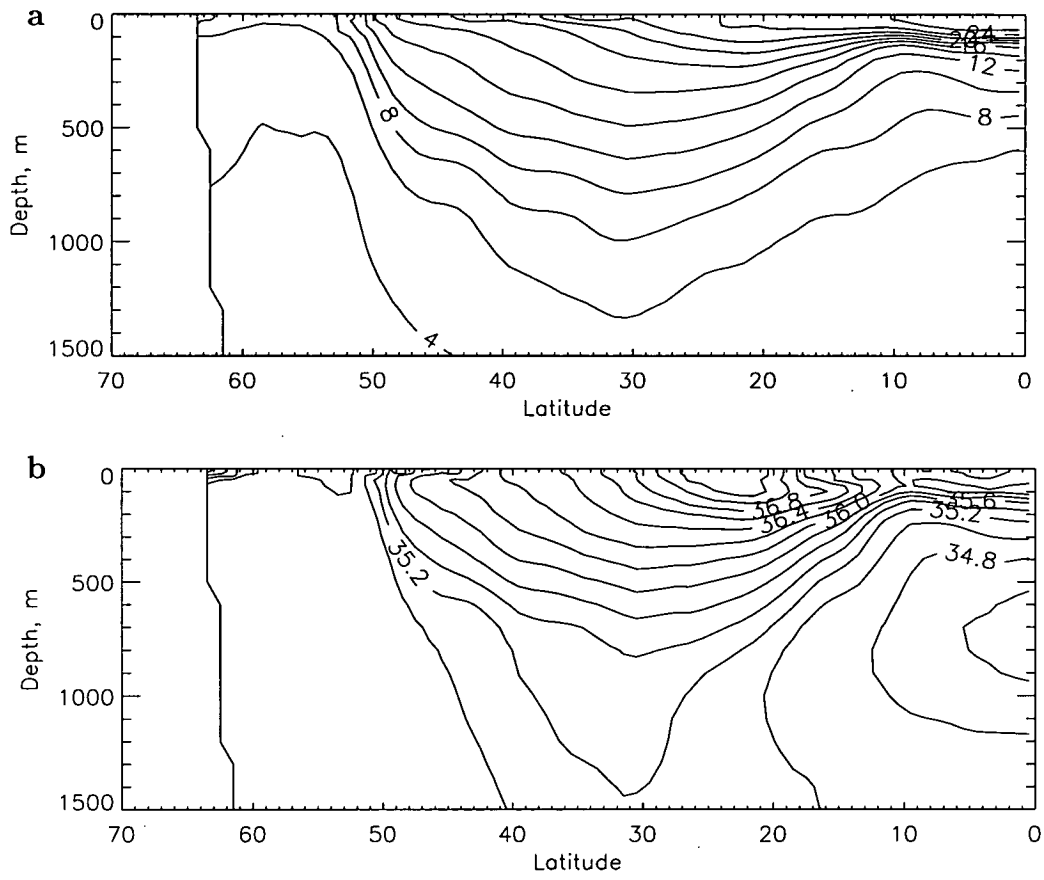

Figure 1.4: Cross-sections along 40°W in the North Atlantic showing **a)** the thermal structure of the ocean, contours are separated by 2°C and **b)** the salinity field, contours are separated by 0.2 psu. Taken from the smoothed Lozier climatology described in Chapter 2.

round to join the Labrador Current. The North Atlantic, Irminger, Greenland and Labrador Currents circulate around the subpolar gyre.

1.1.3 The formation and ventilation of the thermocline

Figure 1.4 shows the climatological subsurface structure in the North Atlantic along 40°W of temperature and salinity. Figure 1.4a is a typical North–South cross-section revealing the changes in temperature with depth and latitude. The most noticeable features are the very steep and shallow thermocline of the tropics, the deep bowling of isotherms of the subtropical gyre between approximately 15° and 50°N then the poorly stratified waters of the subpolar gyre in the north. The salinity also decreases with depth in the thermocline although in some places, particularly the tropics, there is a maximum is at about 100m depth. The tropics,

the subtropical gyre and the subpolar gyre also have distinctive salinity structures with the maximum in the southern subtropical gyre.

The general meridional circulation in the North Atlantic is driven by convection in the north. The surface waters are strongly heated by the sun in the equatorial regions. As they are advected northwards they gradually lose heat to the atmosphere. The cooling of the waters also deepens the mixed layer by convective over-turning. The convection at high latitude forms the deeper waters which are advected back toward the equator. In the tropics there is an overall upwelling of water as there is divergence of the surface waters due to Ekman flow. This produces the very steep thermocline and shallow mixed layer.

This work is concerned with intermediate depths – the upper 700m of the ocean – which is in the thermocline over most of the ocean. How the water in the thermocline is formed and how the temperature and salinity properties are set are therefore very important.

Figure 1.5a is a schematic diagram illustrating how surface waters are subducted to form the subsurface water structure (Stommel 1979). Wind shear at the surface produces convergence in the Ekman layer, the layer directly influenced by the wind. The convergence results in Ekman pumping, the forcing of water downward. As this water moves southward it moves underneath the warmer and lighter waters. This formation occurs most in the winter months when the mixed layer is deepest (Stommel 1979). Water subducted into the thermocline outwith winter is mostly re-entrained into the mixed layer in the following winter.

There have been several studies developing the theory behind the subsurface water structure and the thermocline. Rhines and Young (1982) presented a theory of wind-driven circulation, focusing on the subtropical gyre. Their theory reproduced the bowling of isopycnal layers and the shift of the gyre centre northward with depth, features consistent with observations of the subtropical gyre.

The theory of the ventilation of the thermocline was developed by Luyten et al. (1983). In their model, the waters of the thermocline are formed in winter where the isopycnals outcrop and, moving southward, are subducted into the main thermocline. Their model has Ekman pumping as the only forcing which drives the subduction of water. Williams (1989) proposes that the mixed layer and air-sea interaction also play a role. Figure 1.5b is taken from Williams (1989)

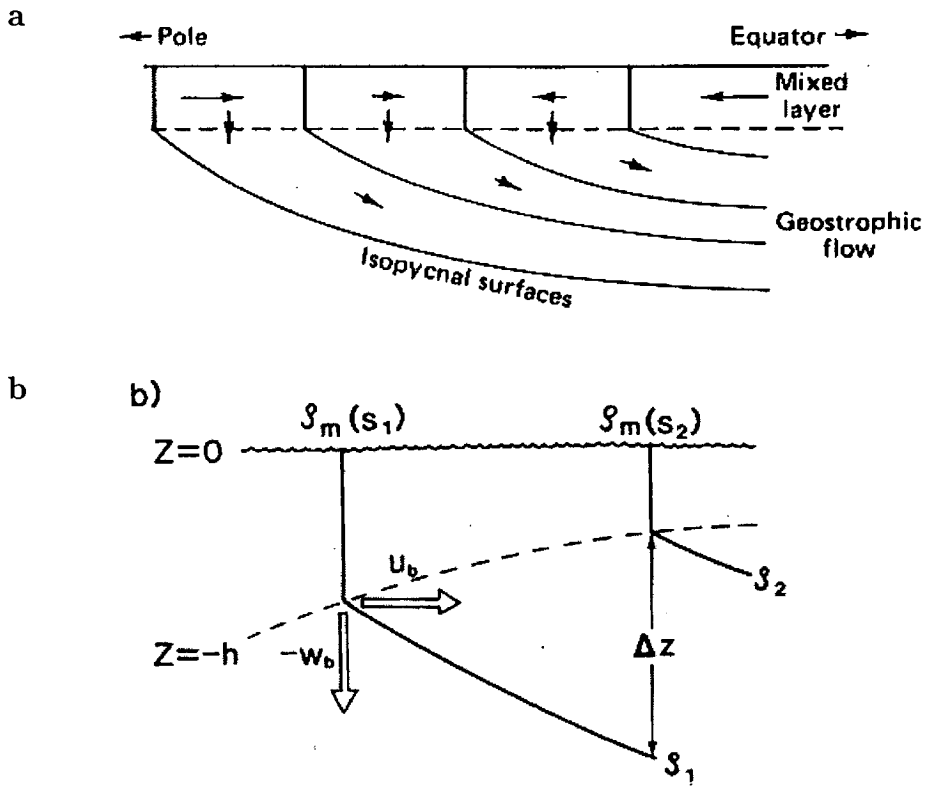

Figure 1.5: **a)** A schematic representation of the meridional circulation showing convergence in the surface layers pumping water down into the thermocline along isopycnal surfaces (Stommel 1979). **b)** A cross-section showing how water is subducted into the thermocline from the mixed layer from Williams (1989). Solid lines are isopycnals and the dashed line indicates the bottom of the mixed layer. The arrows show advection of water, the downward flow is from Ekman pumping.

and shows how the thermocline waters are formed from the mixed layer where the isopycnals outcrop in winter. From the equator northward, the winter mixed layer deepens as cooling of the surface waters produces convective overturning. As figure 1.5b illustrates, water is subducted into the thermocline both by Ekman pumping (labelled $-W_b$ in the diagram) and horizontal advection (U_b). In the real structure of the ocean shown in figure 1.4 the waters of the thermocline are formed where the isotherms outcrop, they are subducted and move southward along isopycnal surfaces which approximately follow the isothermals.

Once water has been subducted, it is separated from the surface by less dense layers. In the ocean, below the mixed layer, there is little mixing between water masses of different densities because diapycnal diffusion is small. Therefore, subducted waters retain their properties, such as temperature and salinity, they

acquired when they were last in contact with the surface.

Hence, the properties and structure of subsurface waters are determined by the atmospheric and oceanic conditions when those waters were formed and subducted. Here, air-sea interaction set the temperature and salinity of the water and also the depth of the mixed layer. Sea temperature is influenced by solar heating and sensible and latent heat fluxes. Air-sea heat fluxes are determined by the temperatures of ocean and atmosphere and also very strongly by the wind. Wind greatly increases both sensible and latent heat loss from the sea surface. Salinity is controlled by evaporation and precipitation. The mixed layer depth is set by convection by surface cooling and wind stirring. The mixed layer of the ocean deepens and cools at higher latitudes which has a strong influence on ventilation.

The properties of subducted water are therefore defined at the surface where the waters are formed. The largest variation of surface properties is the change with latitude. As figure 1.4 illustrates, sea surface temperature decreases away from the equator with the most rapid change at the Gulf Stream front. Salinity also varies with latitude but has a maximum in the southern subtropical gyre. Northwards from here it decreases, again the maximum gradients is across the Gulf Stream front. There is, of course, spatial variability of surface properties other than just with latitude, a result of the North Atlantic circulation. Surface temperature fields from the Lozier and Levitus climatologies are shown in figures 2.3 and 2.4 in the next chapter.

1.1.4 Convection and formation of mode waters

In the North Atlantic there are two sources of water formation by convective processes. One is in the Sargasso Sea southeast of the Gulf Stream (Worthington 1959) and the other is in the Labrador Sea (McCartney and Talley 1982, Talley and McCartney 1982).

On the northern edge of the Sargasso Sea, surface waters are regularly cooled in winter to just below 18°C. Convection creates a deep mixed layer, up to 400m deep, of homogeneous water. At other times of the year this is capped by warm waters. The layer is advected southward and spread throughout the Sargasso Sea. Due to the remarkable consistency of its properties, it is known as '18° water'

and can be seen widely throughout the subtropical gyre as a thick layer of water about 200m thick centred at a depth of approximately 300m.

The centre of the subpolar gyre in the Labrador Sea is an area of very deep convection. Waters from the North Atlantic Current are carried northward by the Irminger Current and then westward around Greenland until they reach the Labrador Sea. As they do so they are repeatedly cooled in winters, gradually increasing in density. The winter mixed layer becomes deeper and a wedge of homogeneous water is created. In the Labrador Sea, this water has been cooled to a temperature of around 3.5°C and convection in the winter reaches depths of typically 1500–2000m.

The deep water mass that is formed is known as Labrador Sea Water and is carried southward by the deep western boundary current. Some of the water is carried southward to the Caribbean Islands and beyond. Some Labrador Sea Water gets drawn into the Gulf Stream and North Atlantic Current system which brings it into the ocean interior. This water gets mixed with other waters, particularly Mediterranean outflow waters, and forms a layer known as Upper North Atlantic Deep Water (Curry et al. 1998).

1.1.5 Mesoscale Eddies

Mesoscale eddies are by far the strongest time-dependent features of the ocean. In most regions of the ocean, particularly the strong currents, eddies are by far the greatest source of temporal variability. Wyrtki et al. (1976) estimated eddy kinetic energy was considerably larger than mean flow kinetic energy in all parts of the ocean. In some places eddy KE was estimated to be 40 times the mean flow KE.

Eddies are generated in the strong shear currents such as western boundary currents and equatorial current systems. In the North Atlantic, the Gulf Stream is a major source of mesoscale eddies and is used here as an example.

Eddies are formed in the Gulf Stream by baroclinic instability. Meanders in the current pinch off, enclosing an area of water. Warm core eddies are formed when water from the south side of the current, Sargasso Sea water, is pinched off and becomes surrounded by cold slope water. Cold-core eddies are formed vice versa. Such eddies contain very strong rotational geostrophic currents.

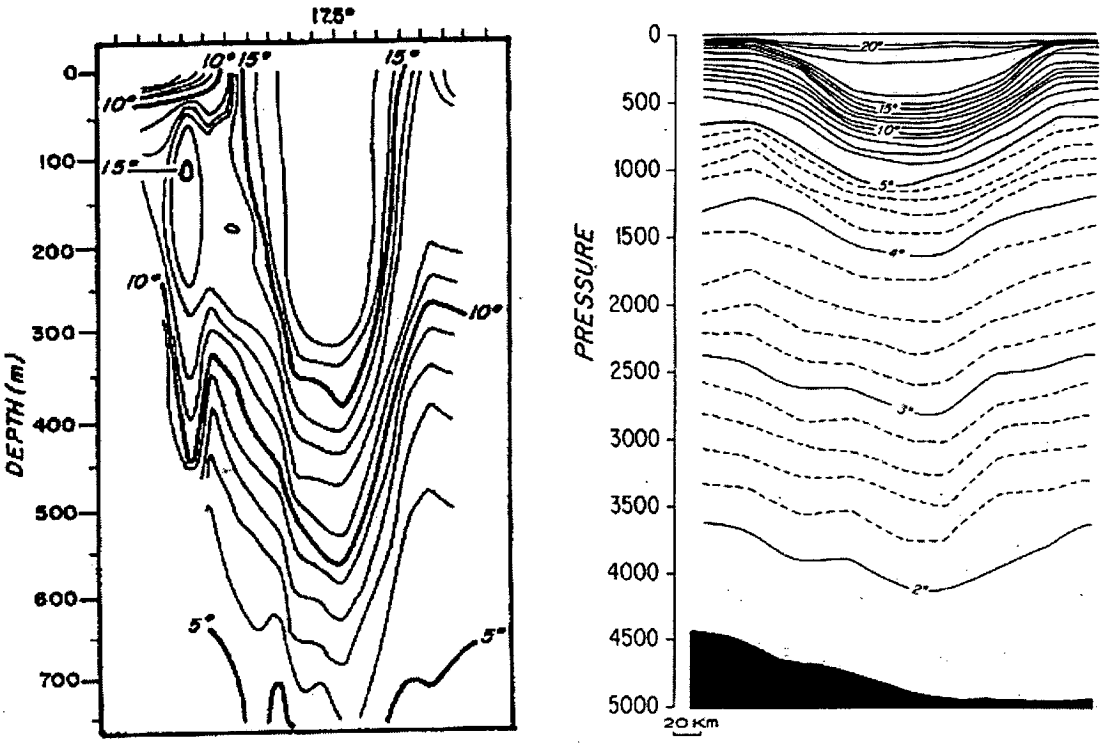

Figure 1.6: Observed temperature cross sections of two Gulf Stream warm core eddies from Dewar (1986) and Joyce (1984) respectively.

The size of mesoscale eddies is typically of the order of the Rossby radius of deformation which is the scale of motion at which rotation and stratification have approximately the same effect. The Rossby radius of deformation has a dependence on the planetary vorticity parameter, f, such that mesoscale eddies decrease in radius with latitude. Gulf Stream eddies have radii of the order of 100km. The lifetime of mesoscale eddies can be several years during which they can travel basin scale distances and are thus distributed to other regions of the ocean.

Figure 1.6 shows examples of temperature cross-sections through two typical warm core eddies from Dewar (1986) and Joyce (1984). The isotherms can be seen to bow towards the centre of the eddy, where the warm waters are concentrated. The second eddy was observed in September and is capped by a shallow warm mixed-layer.

Warm core eddies are anti-cyclonic and have a domed sea surface. At the centre of an eddy, the sea surface is higher than the surrounding ocean by the order

of tens of centimetres. Hence, on surface of constant geopotential, close to the sea surface, hydrostatic pressure is greater in the centre of the eddy than outside. This, of course, drives the geostrophic flow. As the water in the eddy is warmer and therefore less dense, the pressure increases less rapidly with depth than outside the eddy. Thus, pressure gradients between the eddy and surrounding ocean decrease with depth and consequently geostrophic flow also decreases. By the base of the thermocline, typically approximately 1000m depth, differences in hydrostatic pressure between inside and outside the eddy have become very small.

Cold core eddies are the opposite of warm core eddies. Isotherms are domed upwards within the eddy and the sea surface level is depressed. Therefore near surface pressure will be lower in the centre of the eddy than outside. Again, pressure gradients on levels decrease as the denser, colder waters in the eddy counterbalance the low surface pressure.

As figure 1.6 illustrates, isotherms in the permanent thermocline are separated by more or less the same vertical distance inside and outside of the eddy. In these warm core eddies, more warmer water has been introduced at the top and consequently there is less cold water right at the bottom. The isotherms of the permanent thermocline are simply displaced vertically, downward for a warm core eddy and upward for a cold core eddy. The sea surface height signal of an eddy reflects this displacement and the change in mass of the water column that it has produced. Cooper (1995) described a simple model of a mesoscale eddy and found that it had a weak potential vorticity signal which is consistent with little vertical compression of expansion within the water column.

Air-sea interaction

Eddies consist of a volume of water which has been isolated from its original water mass and has moved to be surrounded by a different water mass. It will therefore experience new atmospheric forcing at the surface which will be different to that experienced by the water mass of its origin (Dewar 1986, Williams 1988). Generally, warm core eddies experience heat loss to the atmosphere and cold core eddies heat gain. Here, the symmetry between warm and cold core eddies breaks down. Surface warming of cold core eddies will just produce a thin, warm mixed-

layer capping the water column. However, surface cooling of a warm core eddy will, by convective overturning, lead to cooling of the entire mixed-layer.

Surface heat fluxes on an eddy and changes in the mixed-layer do not greatly affect the surface height signature of an eddy. Firstly, changes in the permanent thermocline affect a much larger mass of water. While mixed-layer depths are of the order of 100m, the permanent thermocline is typically 1000m deep. Secondly, eddies experience the same atmospheric conditions as the surrounding ocean so that, in time, air-sea fluxes act so as to create similar mixed-layers in open ocean as in the eddy. Hence, the sea level difference between eddy and surrounding water mass informs us more about the deeper changes in the permanent thermocline than the mixed-layer.

Cooper (1995) and Cooper and Haines (1996) exploited these properties of eddies as the basis for their method of assimilation of altimetry. They assumed hydrostatic balance and that changes in pressure on the bottom topography are negligible which is true except for strongly barotropic flow or shallow water. With these assumptions, it is then possible to interpret variations in observed sea surface height as reflecting variations in the mass of the underlying water column.

1.2 Satellite Altimetry

For many years, the only means to study the ocean was from making *in situ* observations from ships. Due to the vast size of the oceans, good coverage was impossible. Instruments on satellites can now be used to measure sea surface temperature (AVHRR and ATSR) or sea surface height (TOPEX/POSEIDON, ERS-1 and ERS-2). Although remote sensing from satellites can only measure properties of the sea surface, they provide the opportunity to continually observe oceans all over the globe.

Satellite altimeters are now able to measure accurately the height of the sea surface. This is determined, after correction for atmospheric conditions, from the return time of a radar pulse reflected off the sea surface directly below the satellite (figure 1.7.)

Measurement of sea surface height is extremely useful as gradients reflect the underlying current. Continued observation of the ocean surface can be used to

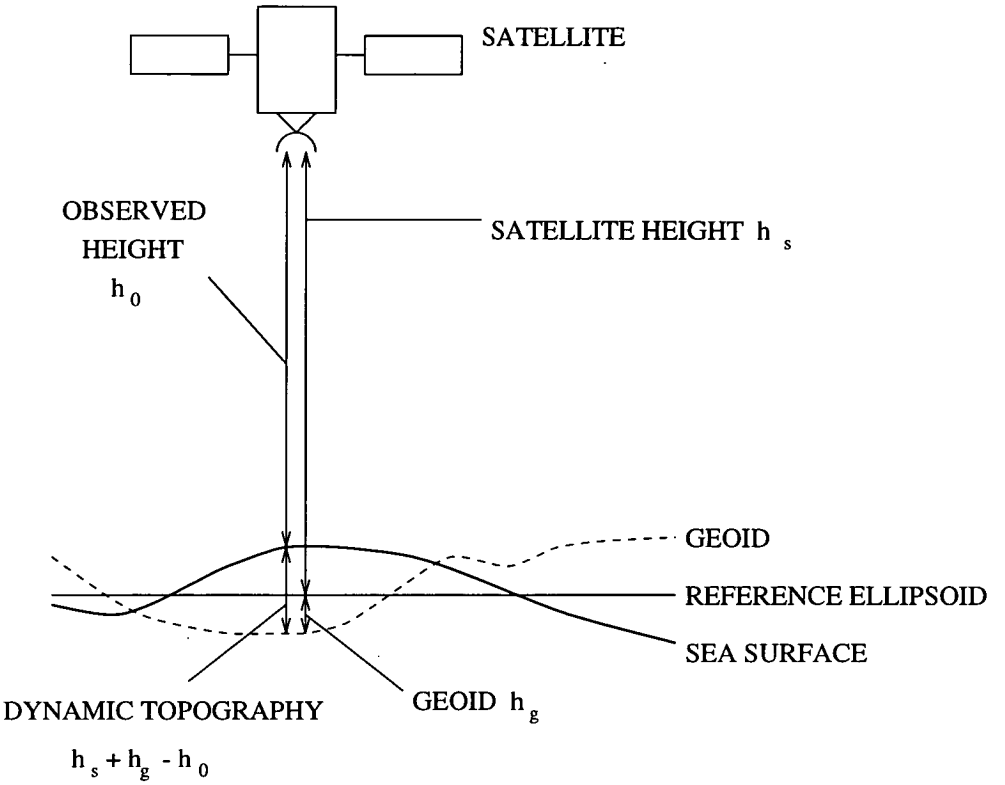

Figure 1.7: Satellite observation of the sea surface height.

investigate the ocean circulation and also changes in currents over time.

There have been several satellite missions dedicated to altimetry. The earlier missions were GEOS 3 (1975 – 1978), Seasat (1978) and Geosat(1985 – 1989) (Cheney 1995). TOPEX/POSEIDON (1992 –) is the latest satellite purely devoted to altimetry but there are also altimeters aboard the European satellites, ERS-1 (1991 –) and ERS-2 (1996 –).

Figure 1.7 illustrates how the sea surface height is measured relative to a reference ellipsoid. This measurement will suffer from instrument errors and errors from the atmospheric correction. There will also be errors from uncertainties of the satellite orbit. The observed sea surface height is a result of the geoid, tides and the dynamic topography which reflects movements of water masses in the mixed-layer and thermocline and is the component of SSH that we are interested in.

The geoid is the sea surface height of ocean if it was at rest. This is a surface of constant gravitational potential. This is not a perfect ellipsoid as irregularities in the Earth's structure create a distorted gravitational field. In order to determine

the dynamic topography, the geoid must first be subtracted. Geoid models have improved greatly in recent years, partly in response to the need created by advanced altimeters. The original geoid used with early TOPEX/POSEIDON data was the OSU91A model (Rapp et al. 1991). Newer geoids developed specifically for the TOPEX/POSEIDON were the Joint Gravity Model-1 (JGM-1) and the Joint Gravity Model-2 (Nerem et al. 1994) which were then improved to make the JGM-3 geoid (Tapley et al. 1996). This has now been adopted as the official geoid for TOPEX/POSEIDON data.

Geoid errors are the most significant error in the derivation of dynamic topography since current geoid models can only account for large scale variations of the Earth's gravitational field (Tapley et al. 1994) although they are improving. Because of these unavoidable geoid errors, satellite altimetry is often used for examining time variations in sea surface height and gradients rather than absolute values.

Another component of the sea surface height comes from the tides. An early model which was used for more than a decade was the Schwiderski model (Schwiderski 1980a,b). After the Geosat mission an improved model was produced by Cartwright and Ray (1990,1991). After the launch of TOPEX/POSEIDON with its unprecedented accuracy, several tidal models have been released. Andersen et al. (1995) reviews and compares 12 such models from 1994. More recent models are assessed by Shum et al. (1997) who states that all models agree to within 2–3cm in the deep ocean.

The sea surface height is also affected by the atmospheric pressure above it (Gill and Niiler 1973). As atmospheric pressure increases, the sea level is depressed. This is known as the "inverted barometer" effect. The local inverse barometer correction is used to account for this effect in altimetric observations. Wunsch and Stammer (1997) review the inverted barometer effect and Gaspar and Ponte (1997) check the validity of the local inverse barometer correction against TOPEX/POSEIDON data.

One of the greatest problems in making accurate altimetric observations is the need to know the orbit of the satellite as precisely as possible. On the earlier altimetry missions this was by far the largest source of error. The orbit is calculated by a combination of tracking of the satellite and models of the orbit trajectory.

The latter can be improved after observations have been made so that orbit errors of the Seasat and Geosat missions have since been reduced to 20cm and 10cm respectively (Cheney 1995).

1.2.1 TOPEX/POSEIDON

Altimetric data used in the assimilation experiments here have come from the TOPEX/POSEIDON satellite. This mission was specifically designed to measure sea surface heights accurately enough to study ocean circulation (Fu et al. 1994, Cheney 1995). The satellite was launched on the 10th August 1992 and began collecting scientific data on the 23rd September 1992. The satellite was built, launched and run as a collaboration between NASA and the French space agency, CNES.

The satellite has two altimeters on board. The main instrument is a dual-frequency radar altimeter based on the altimeters on board the previous Seasat and Geosat missions. Taking measurements at two frequencies helps to reduce the errors caused by ionospheric free electrons. The other altimeter is an experimental device using new technology, a single-frequency solid state altimeter. Its advantages are that it is lightweight and requires low power which may be useful for future missions. The two altimeters share the same altimeter so cannot be used at the same time. After the verification phase, the experimental altimeter is used for one cycle in ten.

The choice of orbit configuration is crucial with spatial and temporal resolution in competition. The compromise is a orbit with a repeat period of 9.916 days (nominally 10 days) and a track separation of 316km at the equator. The inclination of the orbit is 66° which allows observation of most of the global ocean.

The chosen altitude of the orbit is 1336 km. A high altitude orbit was chosen to reduce atmospheric drag and gravity forces acting on the satellite which introduce errors in the orbit. The satellite is tracked by two methods and also an experimental system. The satellite has a laser retroreflector array on board which is used with an array of satellite ranging stations on the ground. The other operational tracking system on board is the Doppler orbitographer and radiopositioning integrated by satellite (DORIS) receiver which receives microwaves transmissions from a network of ground stations. This allows the satellite to be tracked for

about 80% of the time. The experimental tracking system is a Global Positioning System (GPS) demonstration receiver which works with the GPS constellation. This system allows continuous, precise tracking of the satellite. These tracking methods are combined with orbit models for determination of the complete orbit (Nouël et al. 1994).

In the planning stages of the TOPEX/POSEIDON mission, the budget for random errors was specified to be a RMS value of 13.7cm. After the first year of operation, Fu et al. (1994) reported that the random errors from the instrument were 3.2cm and from the orbit determination, 3.5cm. This gives a total random error of 4.7cm which is a considerable achievement. Hence, for the first time, a satellite altimeter is in operation which provides continuous measurements of the sea surface height accurate enough to allow study of ocean circulation.

Chapter 2

Hydrographic Data

A climatological hydrography describes a mean three-dimensional structure of ocean properties. It may include concentrations of oxygen or nutrients for example but in this case the useful information is temperature and salinity. The hydrographies in use in this work are Levitus (1994) which covers the whole world ocean and Lozier et al. (1995) which is a climatology of the North Atlantic alone. These describe the mean built up from observations spanning several decades and from all times of year.

2.1 Levitus Hydrography

The Levitus (1994) hydrography is an updated version of the Levitus (1982) *Climatological Atlas of the World Ocean* including more recent observations. The original Levitus (1982) hydrography was a comprehensive atlas covering the whole world ocean built up from all oceanographic station data (SD), mechanical bathythermographs (MBT) and expendable bathythermographs (XBT) available from the National Oceanographic Data Center, Washington D.C. This climatology and the updated Levitus (1994) version is still used as a standard in the oceanographic community.

The atlas contains information of temperature, salinity and oxygen content for the world ocean to a depth of 5500m. It includes seasonal information of temperatures and salinities and also the annual mean which is the data set used here.

The annual mean is compiled from all NODC data after quality control. As the world ocean is so expansive, it is extremely difficult, even over many years,

to observe it all extensively. In some areas, such as busy shipping lanes and more accessible regions, the data are well concentrated and a good mean representation can be compiled. However, many areas are less frequented, particularly the southern ocean but also large areas of other oceans. Observations get more scarce with depth. Fortunately water properties in the deeper ocean do not vary very rapidly in comparison to surface and intermediate depth waters.

The objective analysis procedures used by Levitus to produce one-degree resolution gridded property fields from the irregularly distributed raw data is based on influence radii. All observations within the influence radius of the grid-point contribute to the assigned property value, dependent on the distance from the grid-point. This produces a smoothed resultant dataset. The smallest influence radius used in the procedure is 771km giving large scale smoothing. While this amount of smoothing is required for remote, poorly observed regions, the same influence radii were used in areas with an abundance of observations and where property gradients are large. The result is a very smooth and comprehensive data set but small scale features are unresolved and sharp changes in properties are smoothed out.

2.2 Lozier Hydrography

Lozier et al. (1995) is an annual mean climatology of the North Atlantic. This has been produced from 143,879 hydrographic stations from the National Oceanographic Data Center (NODC). These are all the North Atlantic station data available from 1904 to April 1990 which is 60% more data than Levitus (1982).

Lozier et al. (1995) produced one-degree resolution maps of mean pressure, temperature, salinity and oxygen on selected potential density surfaces. These fields have been produced by averaging the original irregularly spaced data onto a regular grid on potential density surfaces. The fields were also smoothed on potential density surfaces and on much smaller scales than Levitus, improving the resolution of smaller features and preserving steep gradients. The advantage of averaging and smoothing on potential density surfaces rather than depth surfaces is that as mixing of water masses in real ocean processes is predominantly isopycnal, artificial mixing of water properties is avoided. In the previous work,

Lozier et al. (1994) it was found that averaging data on pressure surfaces where isopycnals were inclined produced water properties that were dissimilar to *in situ* observations and that such problems were avoided by isopycnal averaging.

Unlike Levitus, where all observations within an influence radius of the grid-point were used, Lozier et al. (1995) only averaged data within a one-degree square around the grid-point. All observations within the square received equal weighting regardless of distance from the grid-point. After the averaging, the gridded data were then smoothed in a two stage process. The first stage was based on density of observations per grid-point, thus data-scarce areas received greater smoothing. The scale of the smoothing was nowhere greater than 3 degrees. The scale of the second stage was uniformly 2 degrees. Therefore the scales of the smoothing were in the range 100–300km compared to Levitus' 771km.

Lozier et al. (1995) presented data arranged on potential density surfaces but the dataset obtained from Woods Hole Oceanographic Institution held data on depth levels. The data are gridded with one degree resolution in both latitude and longitude with the points located in the centre of a degree box. The boundaries of the data are 90°W and 20°E in longitude and 0°N and 70°N in latitude. The data are on 79 depth levels. These are at depths of 0, 10, 20, 30, 50, 75, 100, 125, 150, 200, 250, 300m and every 100m thereafter. Bottom depths are typically about 5000m.

These data were produced by the Lozier team by averaging as described above and then projecting onto depth surfaces. However, no smoothing was performed on the data. In compiling the gridded data set, points were only given values of temperature and salinity if there were ten or more observations within the degree square around the grid-point. Thus there are several grid points where there are no data producing holes in the grid. These holes become larger and more widespread at greater depth.

The data set was not smoothed in any way other than by averaging station data within a grid square onto the grid-point. The station data have been observed at many different times of year and spanning 9 decades. The data are so irregularly spaced in time and the natural variability so great that averaging over one 1°x1° square is insufficient to remove all the variability. Thus the data set shows large small scale variations which need some smoothing in order to gain a

good representation of the mean state of the North Atlantic.

Figure 2.1 shows two temperature maps from the surface and 1000m depth from the original Lozier hydrography. There are many gaps in the data, the number and size of which increase with depth. They are concentrated in the centre of the ocean. These maps also reveal the noisiness of the data. This is more obvious at the surface, where temperatures are more variable due to seasonal effects and air-sea interaction.

These problems of missing data and noise have had to be resolved before the hydrography could be used. Following Lozier et al. (1995) all processing of the data has been performed on potential density surfaces.

2.2.1 Filling in Holes

The large gaps in the gridded data were the first problem to be rectified. Fortunately, station observations are concentrated in areas where water properties vary rapidly on horizontal planes. Most large gaps in the data are located in the middle of the North Atlantic, in the subtropical gyre. Here, temperature and salinity have a low spatial variability so it is possible to interpolate to assign values to points with no data.

As mentioned earlier, the interpolation has been carried out on isopycnal surfaces. In order to do this, the whole data set was re-projected onto isopycnals, then the gaps filled and then projected back onto depth surfaces. Projecting onto isopycnals was done by linearly interpolating in vertical profiles. Thus a three-dimensional array of properties on isopycnals was produced. In the deep ocean, potential density varies very slowly with depth so linear vertical interpolation will introduce errors. In cases where the potential density levels were too distant vertically the holes were filled in by interpolation on depth levels instead of isopycnals. The filling method is still the same.

Holes were filled by a simple interpolation procedure based on data immediately surrounding the missing point. As the grid is regular, each point has eight neighbouring points in a square around it. Each missing point is given the mean value of temperature and salinity of its immediate neighbours if there are five or more good data points surrounding it on a plane (isopycnal or depth surface in deep water.) If there are less than five valid surrounding points then the missing point

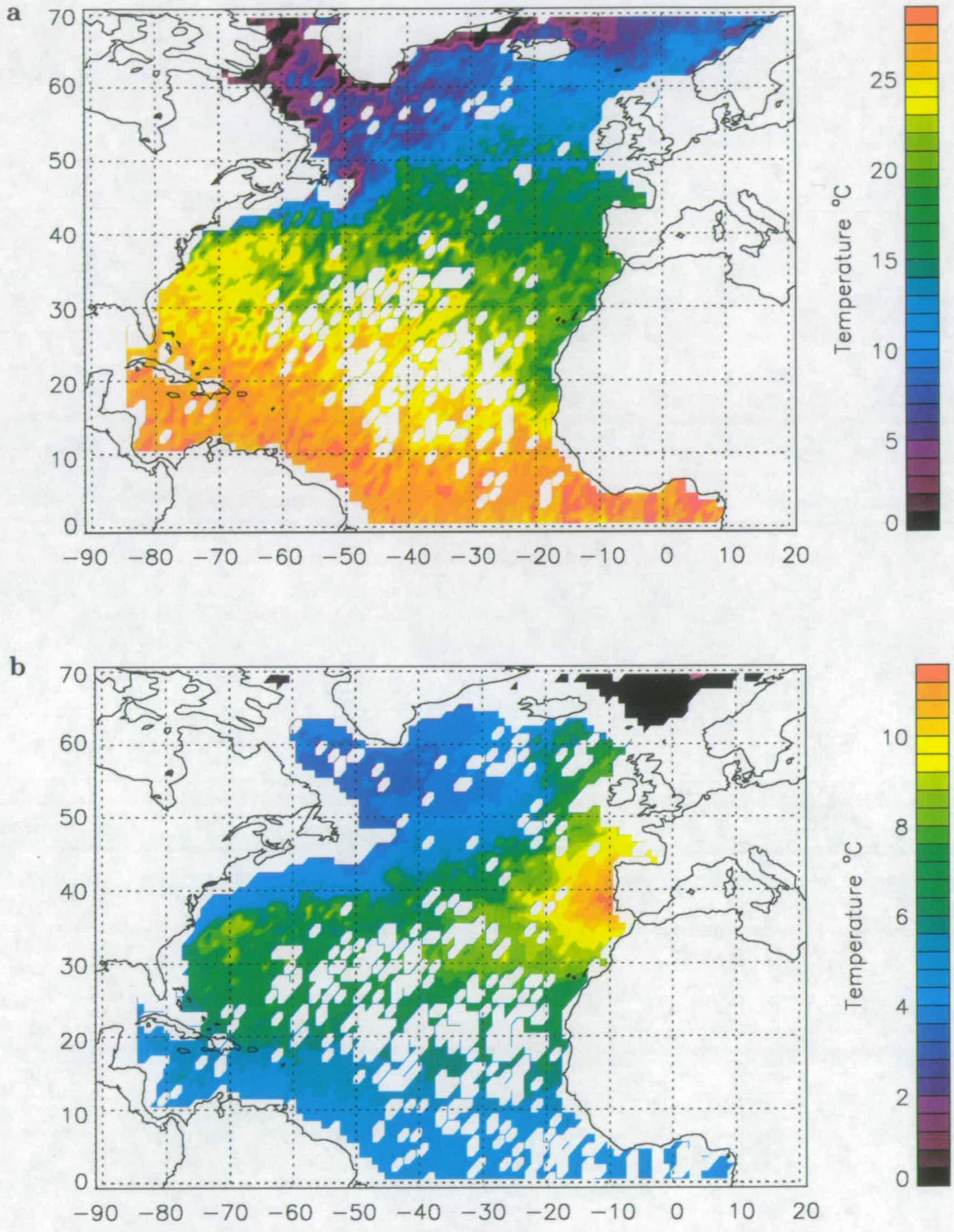

Figure 2.1: Maps of temperature from the original Lozier hydrography at **a)** the surface **b)** 1000m depth.

is left blank. This procedure is repeated several times until no more can be filled. When this happens and there are still some obviously absent grid-points, the interpolation method is passed over once with a limit of four surrounding points contributing to filling in a point. Then more passes of the five point minimum fill are made. After many passes most of the holes are filled.

Its is impossible to tell which holes are due to missing data and which are actual topography. In order to get around this problem, the topography from Levitus 1994 is imposed upon the Lozier data set after all the filling. The interpolation still leaves some small gaps at the bottom of the ocean. It may be necessary to fill these in with Levitus 1994 data.

2.2.2 Smoothing

The smoothing process involves three stages. The first stage removes any peaks, the second smoothes the temperature, salinity and depth of isopycnal surfaces and the third smoothes the depth of the isopycnals again. Two methods of smoothing the data on potential density surfaces have been developed.

1st Method

The first method is similar to the filling in scheme. The gridded data are projected onto density surfaces, and temperature, salinity and depth of the isopycnals are recorded. All of these three properties are smoothed by a simple one-degree block average of the area surrounding each point. The smoothed data are then re-projected onto depth levels.

The isopycnal surfaces are spaced 0.1 kg m^{-3} apart. In the thermocline this is sufficient resolution to prevent inaccuracies being introduced by the vertical interpolation. Deeper down the potential density gradient is less steep so interpolation may introduce errors. When the 0.1 kg m^{-3} isopycnals become further than 300m apart then the projecting onto isopycnals is abandoned and smoothing is done on depth surfaces.

This projection onto isopycnals is also used for the peak removal process. The raw data are very spiky and there are some obvious rogue data points so a smoothing method which removes any peaks is used. If a property at a point is higher or lower than any of the points immediately surrounding it, the property is set

to the nearest of those points.

Care needs to be taken at the surface and at the bottom when re-projecting onto depth surfaces from isopycnal surfaces. Here there will only be information from the one isopycnal above or below the point. At the surface, if all points above the uppermost isopycnal are given the T and S properties of that isopycnal then the ocean-wide mean sea surface temperature will be reduced with each smoothing. Therefore, at the surface, any point above the highest isopycnal is given the mean of the sea surface properties from a nine-box. At the bottom points are simply smoothed horizontally on z-surfaces.

The second stage smoothing by this method is the same as described except only the depth of the isopycnal is smoothed and not temperature and salinity.

There are a few problems with this approach. The linear vertical interpolation onto isopycnal surfaces may introduce errors. Deep down this is a problem where isopycnals become far apart and it has been found that the interpolation onto potential density surfaces and back onto depth levels has introduced some significant systematic changes which are not due to smoothing. Thus, in the first stage, where the isopycnals become greater than 200m apart, smoothing is performed on horizontal depth surfaces. In the second stage, no smoothing is carried out where the isopycnals become greater than 200m apart.

Another problem is that all isopycnals have to be referenced to the same level. In this case the reference level is the ocean surface. However, temperature and salinity affect the density of sea water as well as pressure. Two water masses with different T and S properties may have the same density at a given depth, but pressure will affect them differently – compressibility varies for water masses with different properties. If they are brought to the surface, their densities are likely to be different. Therefore, when considering the potential density of water masses it is important to choose a reference level close to depths of the masses under examination. In this smoothing method, this is not possible and errors may be introduced byt using the surface as a universal reference level.

Due to these problems, a second method was devised which does not rely on fixed potential density surfaces and does not reference all potential densities to the surface.

2nd Method - Local Density Smoothing

The second method is simpler and avoids large scale projection and re-projection. It will also work better, it is hoped, by isopycnal smoothing in deep water.

The principle of this method is to consider the density field local to the point being smoothed. Figure 2.2 illustrates the method employed. Smoothing is small scale, just involving adjacent grid-points. There are two stages to this smoothing scheme, the first stage smoothes temperature and salinity on isopycnal surfaces and the second stage smoothes just the depth of the isopycnal surfaces.

Figure 2.2 shows a grid-point on a depth level (solid line) and the eight surrounding points, each point has a temperature and salinity. The first step of the process is to find the mean in situ density of the nine grid-points. Then, by interpolation vertically along the water columns, the position of a surface which has a potential density (referenced to the depth level) equal to the mean density is determined. This potential density surface is shown on the diagram as the dashed lines. The new, smoothed values assigned to the central grid-point are the means of the temperatures and salinities of the nine water columns where they are intersected by the potential density surface.

The second stage of the smoothing finds the mean density and the potential density surface as before. However the new property values are determined from where the potential density surface intersects the central water column only. This, in effect, smoothes the isopycnal surfaces.

This method has several advantages over the first in that it can be used at all depths in the same way. It also does not have a problem with a reference for the potential temperature as this can be taken as the depth of the z-surface under consideration. The simplicity of this scheme is also attractive.

With this method as well as the first, there are problems with the surface. When looking for the nine-box mean density on a water column, this isopycnal may have out-cropped. Therefore the information from this point is lost. The effect is an mean drop in SST across the ocean and is quite significant. To combat this, if the chosen isopycnal outcrops on more than four of the nine boxes examined, the mean SST for the nine-box is assigned to the point under consideration.

There are some problems at depth with this method. The potential density

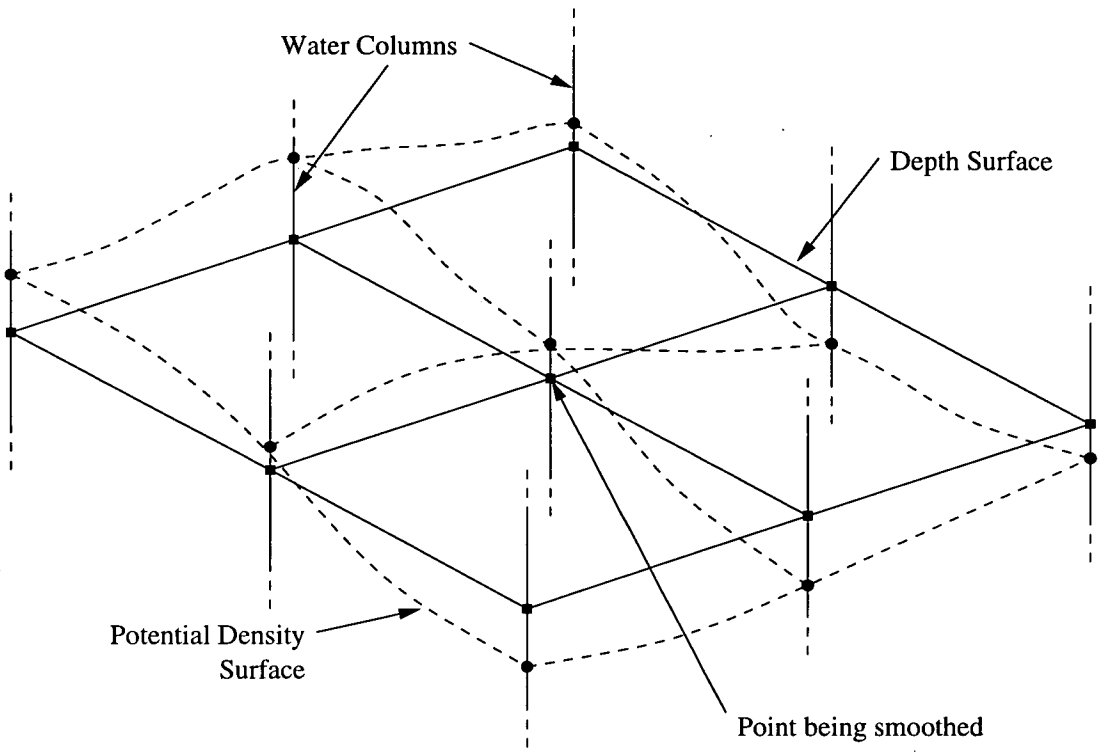

Figure 2.2: Illustrating the local density smoothing method. A square of nine data points on a depth level from a hydrography and the isopycnal surface with density equal to the mean of the nine grid-points.

gradient becomes very small deep down. This means that when looking up and down a water column, it may be a few levels to find the required potential density. In the Eastern Basin, at the outflow from the Mediterranean, while the vertical gradient of potential density decreases and becomes quite flat below 1000m, the temperature and salinity gradients are still quite steep. So a small variation in potential density will require going up the water column a long way, where the temperature and salinity will have changed more. This introduces large errors in the smoothing routine. The smoothing still works well where T and S are smoothed in the first stage but in the second stage where only isopycnal depth is smoothed this creates noisiness below about 1500m.

In order to solve this problem it was decided to limit the second stage smoothing to 1500m and above. However, as below this level the properties are still too noisy, simple smoothing of temperature and salinity on depth surfaces was used. This does go against the ideal of only smoothing on isopycnal surface but such a compromise is necessary in the second stage smoothing. The first stage still

smoothes on isopycnal surfaces at all depths. The stronger smoothing in the second stage at depths greater than 1500m is reasonable because in the deep ocean properties vary slowly in space and there are fewer observations which contributed to the hydrography.

There was some concern that this sharp transition between local density smoothing and horizontal smoothing could create discontinuities and possible unstable water structure but investigation of water columns showed this not to be the case.

2.2.3 Smoothing results

The two smoothing schemes give very similar results which is expected and good, a significant difference would indicate a flaw in one or other method. In the majority of the ocean both have had good success in removing the noise-like variations. With both methods, the surface still retains some irregularity, but I am unwilling to smooth any further. The second scheme appears to produce a slightly smoother, more natural looking, hydrography in these difficult surface layers. In some uses of the hydrography, the retained unevenness in the extreme upper ocean may cause problems but it is largely confined to the top 100m. For the purposes for which the hydrography is employed in this work, these slight variations are negligible. It is more important that properties at intermediate depths, in the permanent thermocline, are smooth.

A crucial area is the Gulf Stream, where there are steep horizontal temperature and salinity gradients. When deciding how much smoothing to apply to a hydrography, it is important to remove the small-scale, noise-like, variations but we must try not to smooth out real features such as the front. In comparing these two smoothing schemes the second produces a front with a slightly steeper gradient. This is a little better.

The local density method allows smoothing in the first stage at all depths on isopycnal surfaces, whereas the first cannot when the defined isopycnals become too far apart. Even the second method has problems with the isopycnal depth smoothing stage by the outflow of the Mediterranean. The best approach for deep water smoothing is the local density as is allows at least some isopycnal smoothing. The second method also performs better in the north where the water is poorly stratified and property gradients are slow.

In all further work where the smoothed Lozier hydrography is used, it is the local density smoothing method that has been employed.

2.3 Comparison of Lozier and Levitus hydrographies

We now have two smooth climatological hydrographies to work with in the North Atlantic. Figure 2.3 shows the surface temperatures of the unsmoothed, with missing data filled in, and the smoothed Lozier and figure 2.4 shows Levitus 1994 surface temperatures.

The unsmoothed Lozier has a lot of noise-like variability which is largely removed by the smoothing, although at the surface there is some unevenness remaining. The Levitus surface temperature field is very smooth but the sub-arctic front is not as sharp as the smoothed Lozier. Figure 2.5 shows meridional cross sections of temperature through the hydrographies. The jaggedness of the isotherms shows in the unsmoothed Lozier field illustrates the irregularity which can be seen to be worst near the surface. Below the surface, the smoothing has been very effective and the smoothed Lozier appears no more uneven than Levitus 1994.

However, figures 2.5 does illustrate the advantage of the Lozier hydrography over Levitus 1994. Between 40° and 50°N is the sub-arctic front. The unsmoothed Lozier shows this as a very steep gradient which is spread out a bit by the smoothing. Levitus, however, shows very broad isotherms, the front has been smoothed out considerably.

Another difference is a feature displayed by the Lozier hydrography at about 50°N. This small dip in isotherms is caused by a permanent meander in the North Atlantic Current called the North-West Corner (Worthington 1976, Krauss 1986) where the current briefly turns to the north-west before turning round again to the east. This feature is completely missing in the Levitus 1994 field.

The salinity field for Lozier and Levitus hydrography is given in figure 2.6. As with the temperature cross-sections, the sub-arctic front is very sharp in the unsmoothed Lozier, smoothed out slightly in the smoothed version and quite spread in Levitus 1994.

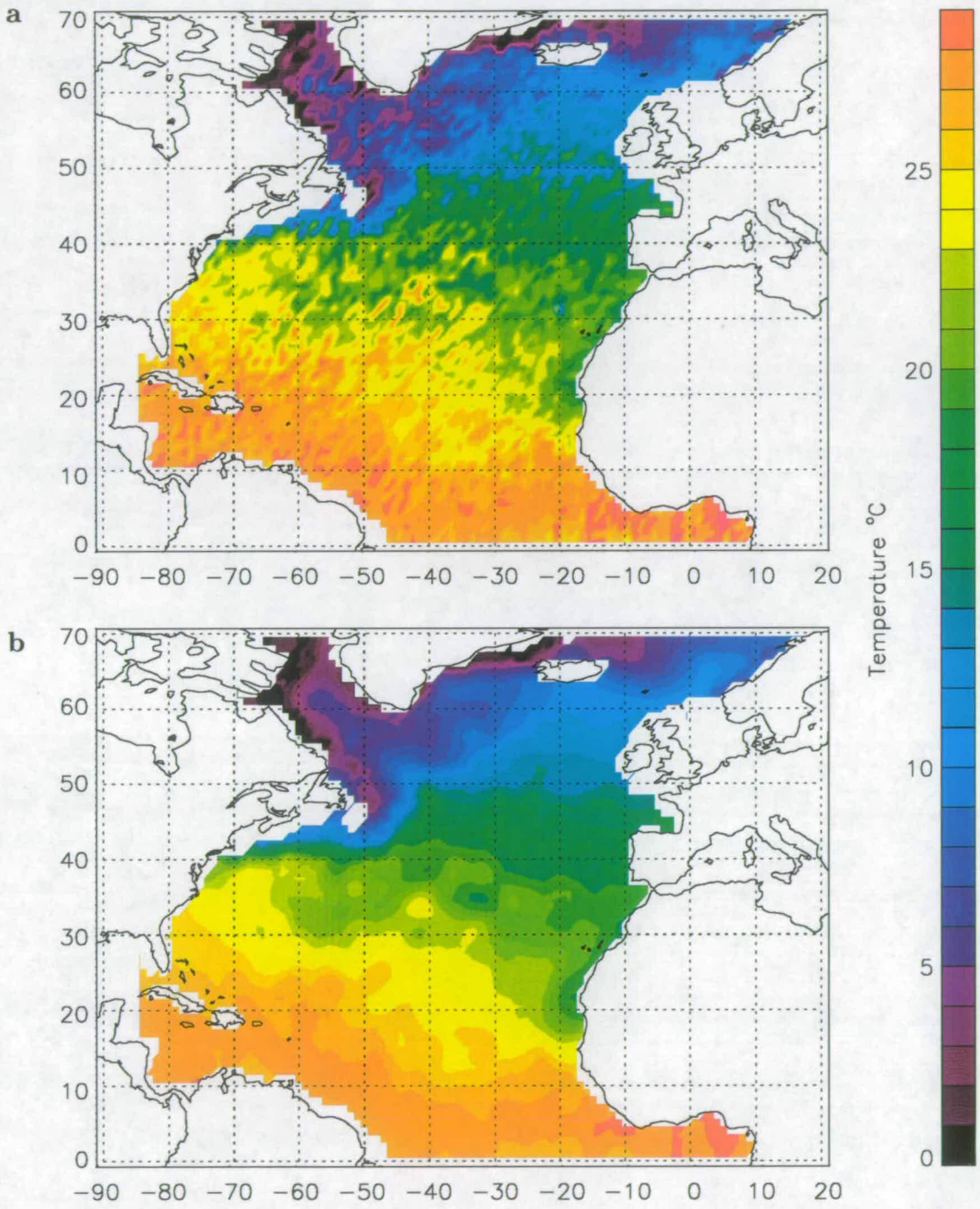

Figure 2.3: Surface temperatures from the Lozier climatology **a)** filled data gaps, unsmoothed **b)** smoothed by the local density smoothing scheme.

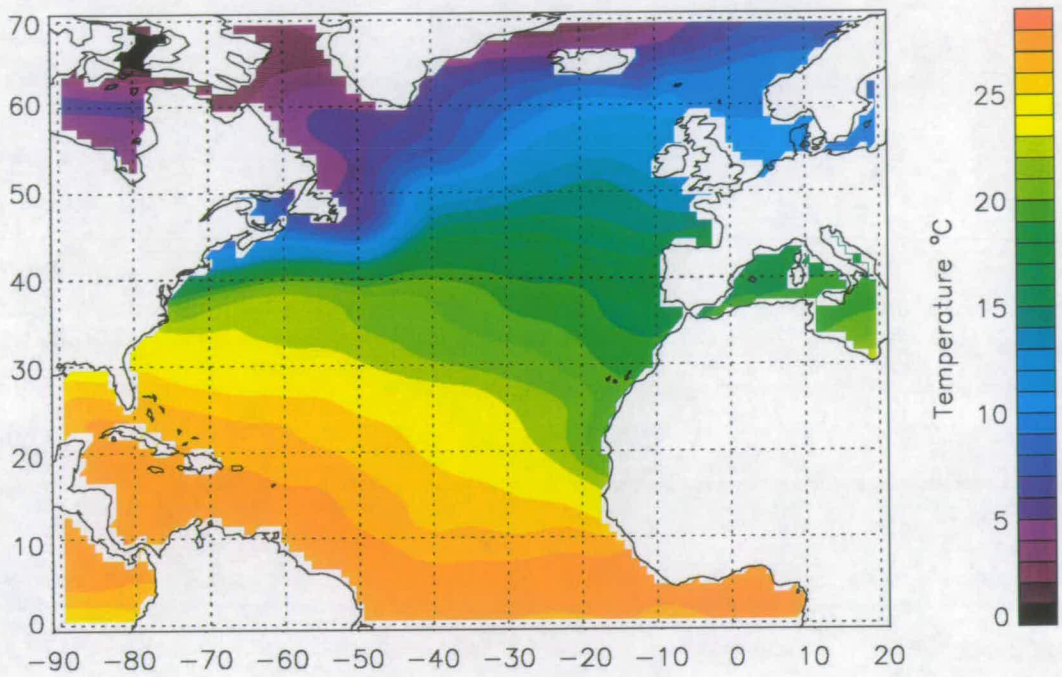

Figure 2.4: Surface temperatures from Levitus 1994 climatology.

With any smoothing there has to be a compromise. It is necessary to remove noise and unwanted random variation, but smoothing inevitably alters the data and changes real features. In the smoothing I have performed on the Lozier dataset, I have attempted to use as small scale smoothing as possible, it does seem that the large-scale smoothing employed by Levitus is excessive in the North Atlantic.

2.4 Representativeness of the Hydrographies

A concern with such climatological hydrographies is how representative of the actual ocean they are. As observations are so scarce, the datasets have had to be built from all available historical data which are very irregularly scattered in both time and space. It follows that the data that contributed to one square may be dominated by a particular year and season whereas the next square may be built from data of entirely different years or seasons. Therefore there will be sampling biases in the observational data, obvious seasonal variations will affect the mean datasets as will inter-annual changes. This is recognised in Levitus (1982) and it was accepted that the results cannot strictly be considered to be a long-term

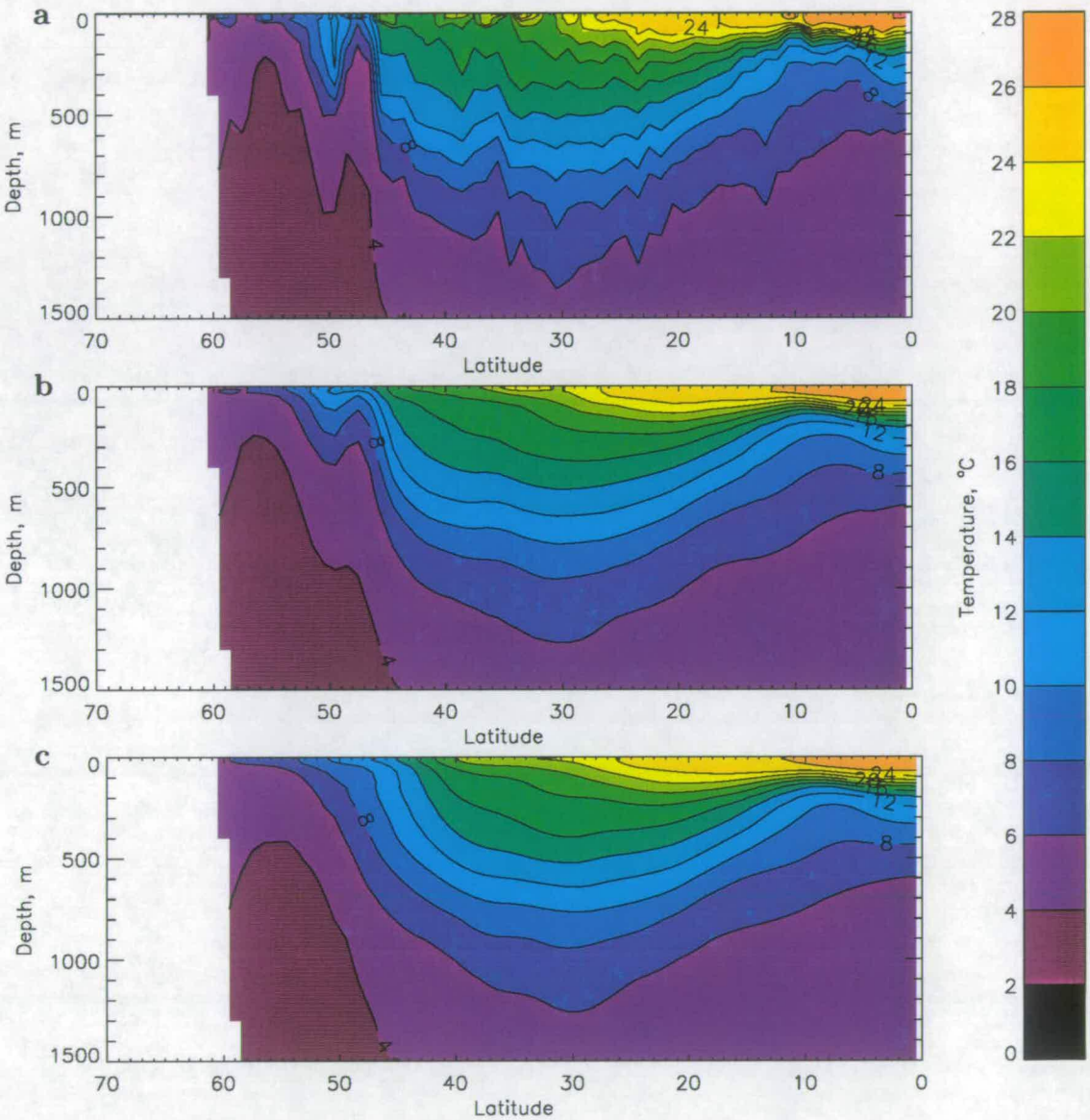

Figure 2.5: Meridional cross section showing temperature along 43°W from **a)** unsmoothed Lozier **b)** smoothed Lozier **c)** Levitus 1994

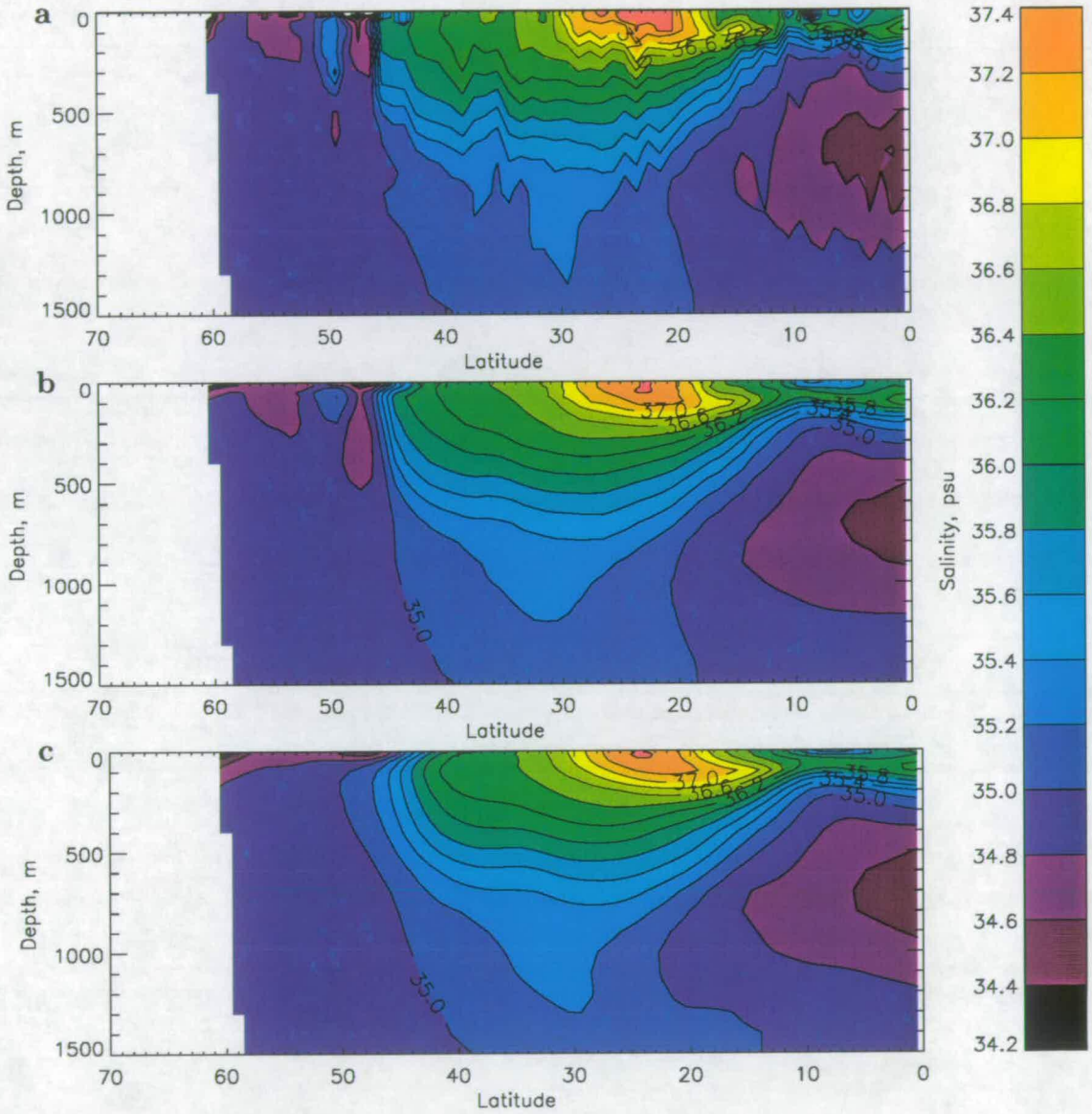

Figure 2.6: Meridional cross section showing salinity along 43°W from **a)** unsmoothed Lozier **b)** smoothed Lozier **c)** Levitus 1994

climatological mean.

These problems can be seen in the unsmoothed Lozier gridded dataset. The hydrography shows considerable grid-point scale variations giving the data a very noisy appearance. Levitus uses extensive smoothing to overcome this and gives the proviso that his climatology is only representative of larger scale features in the ocean. The Lozier dataset had to have some smoothing to remove the noisiness of the fields. This did have the effect of smoothing the sharp front along the Gulf Stream but as the Gulf Stream does meander in its path a mean climatology will, by its very nature, be a smoothed representation. As the Lozier et al. (1995) climatology considered the North Atlantic on its own with its high density of observations relative to the other oceans of the world, smaller smoothing scales could be used which should give a better representation of small scale features and sharp property gradients.

Inter-annual variability will have consequences for the use of a climatology. These data sets represent a smoothed mean state of oceans over several decades, biased towards the times when the taking of observations was most prolific, that is in more recent decades, particularly the seventies. However, as reviewed in chapter 2, there is a lot of observational evidence for considerable inter-annual and longer time-scale variability. Therefore, it is likely that a mean climatology will have large differences from the mean of a given year or even series of years.

Ocean models are often initialised using climatological hydrographies, however, due to these inter-annual or interdecadal variations, these may not be appropriate to the period the model is being employed to study. It would, therefore, be advantageous to adapt the climatology to the period under consideration.

Chapter 5 describes the assimilation of satellite altimetry with climatology. The altimetric data used are sea level anomalies, that is variations of sea surface height from a three year mean observed level. The mean is taken from the complete years 1993 to 1995. For the assimilation, it is assumed that this three year mean is equivalent to the sea surface height consistent with the climatology. However, as the investigations into long term ocean variability indicate, this may not be a valid assumption. In the next chapter, the climatologies are compared to XBT observations to determine how representative the climatologies are, look at long term variations and determine if they need adapting before use.

Chapter 3

Interannual and interdecadal variability of ocean hydrography

3.1 Introduction

The climatological hydrography is an estimate of the mean state of the ocean over the period of observations which have contributed to it. However, the oceans are not constant, there is considerable variability over a wide range of time-scales. The North Atlantic is the most observed ocean making it an obvious choice to study variability. It is also a very important ocean as its circulation is a large transporter of heat. The climate of Northern Europe is dominated by the Atlantic and the North Atlantic current which brings warm water from the tropics to its shores. The North Atlantic is also important to the global climate as in the northern hemisphere it is the largest oceanic transporter of heat to high latitudes (Talley 1984). The North Atlantic also responsible for the formation of deep waters which can be advected all around the globe. The study of variability in the North Atlantic is therefore of importance. In chapter 4 changes in subsurface temperatures in the North Atlantic are investigated. In this chapter, as an introduction to the results presented in the next chapter, previous research into North Atlantic variability is reviewed.

As the oceans are closely linked to the atmosphere, variability in atmospheric conditions will have a strong effect on the oceans and several authors have attempted to relate ocean variation with atmospheric changes. The North Atlantic Oscillation is the most dominant mode of variability in the atmosphere over the North Atlantic ocean and a brief overview of this phenomenon is given in the first

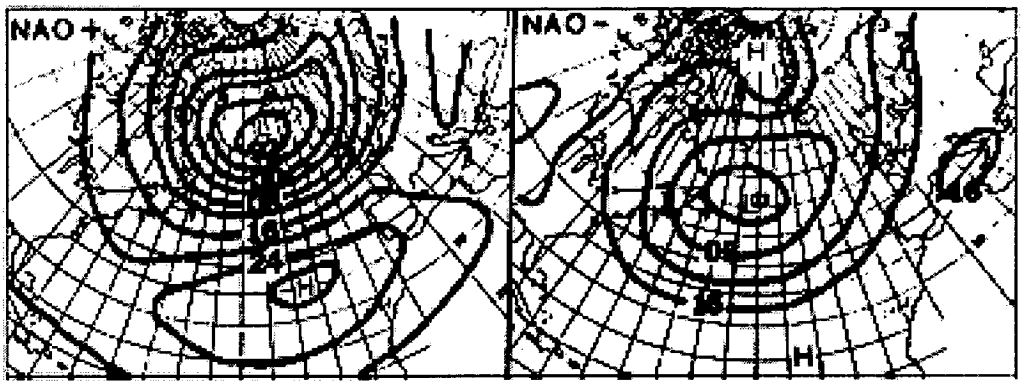

Figure 3.1: The North Atlantic Oscillation. The two panels show examples of sea level pressure at the extreme high and low state of the North Atlantic Oscillation. Taken from Deser (1996).

section.

The second section is a review of observed changes in the subsurface hydrography of the North Atlantic. Section 3.4 looks more specifically at recent research on variability of sea surface temperatures, observations of which are much more abundant than of subsurface water properties. Section 3.5 covers the variation in the position of currents in the North Atlantic. Section 3.6 reviews results of experiments with ocean and coupled ocean-atmosphere models used to study the causes of oceanic variability.

3.2 The North Atlantic Oscillation

The atmosphere over the North Atlantic exhibits a dominant pattern of variability known as the North Atlantic Oscillation (NAO), most notable in winter months (Walker and Bliss 1932, van Loon and Rogers 1978). The normal mean atmospheric state over the North Atlantic is characterised by a large subtropical high pressure region centred near the Azores and a low pressure cell over Iceland and Greenland. The NAO is an oscillation of the strengths and positions of these features on interannual and interdecadal time scales.

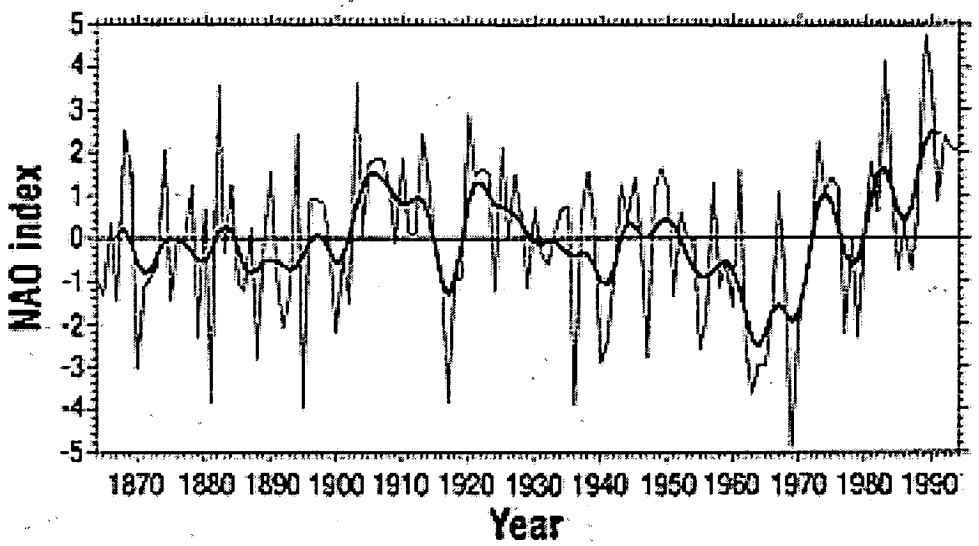

Figure 3.2: An index of the North Atlantic Oscillation produced from the difference of normalised winter (December to March) pressures between Lisbon, Portugal and Stykkisholmer, Iceland from Hurrell (1995). The thick line represents the index after low-pass filtering to remove fluctuations with periods of less than 4 years.

Figure 3.1, taken from Deser (1996), shows sea level pressure maps of the two extreme modes of the NAO. In the high NAO state (left panel), both the Azores High and the Icelandic Low are at their most intense giving rise to strong westerlies across the North Atlantic. This brings milder winters to Northern Europe but there are strong, cold northerly winds over northeastern America and the Labrador Sea. In the positive NAO state, the trade winds are also stronger than average.

During the low state of the NAO, the Icelandic low moves southward and weakens and a high pressure is introduced over Greenland. Northern Europe experiences colder conditions in these periods while easterly winds, warmed by the ocean, give Labrador a milder climate.

The NAO is most noticeable in the winter when it accounts for more than 36% of the variance of the mean December to March sea level pressure field (Hurrell 1995) but it can be detected in every month of the year (Barnston and Livezey 1987). Figure 3.2 shows an index of the North Atlantic Oscillation based on the difference in mean winter sea level pressure between Lisbon, Portugal and

Stykkisholmer, Iceland. This index shows that the oscillation varies on both interannual and interdecadal time-scales.

As the NAO is the most important long-term oscillation in atmospheric conditions over the North Atlantic it will have a strong influence on the North Atlantic Ocean and is likely to be related to some of the ocean's variability. The NAO will clearly have an effect on surface temperature from both temperature of the air mass above the ocean, and the strength of the wind affecting heat fluxes and causing stirring of the surface layers. Changes in winds will also influence the currents, changing transports and possibly the directions of the currents.

3.3 Studies of hydrographic variability

The North Atlantic is the most observed ocean in the world and so has received the greatest attention for the study of variability. Evidence of variability in the thermohaline structure had been discovered as early as the beginning of the century when Helland-Hansen and Nansen (1909) reported evidence of changes in the amount of North Atlantic water in the Norwegian Sea. This work was later added to by Helland-Hansen (1934) with more data showing continued variability.

Talley and Raymer (1982) documented the variability of the Eighteen Degree Water in the North Atlantic subtropical gyre. This large, uniform, mass of water is formed south and east of the Gulf Stream and forms a thick band centred around 300m depth (Worthington 1959). Studying hydrographic data from the Panulirus station (32°10′N, 64°30′W), Talley and Raymer (1982) found variations in the properties of this water mass with time. Between 1955 and 1964, 18° water was regularly renewed with a temperature of 18°C and salinity of 36.5 psu. After 1964 until 1972 the properties changed gradually to 17.1°C and 36.4 psu and then from 1972 to 1975 formation of this water mass, stopped completely in this area. After 1975 renewal continued, forming waters at 18°C and 36.5 psu again.

As part of the International Geophysical Year (IGY), transatlantic sections of temperature and salinity were obtained at 24°30′ N in 1957 and 36°16′ N in 1959. These latitudes were occupied again in 1981 and the large scale changes reported by Roemmich and Wunsch (1984). They found ocean-wide warming between depths of 700m and 3000m in both sections to a maximum of 0.2°C, although the

temperature difference patterns are not the same for both sections. In the upper waters both sections show some cooling, a narrow band at 200m at 24°N but a thicker, stronger band between 100 and 700m at 36°N. At 36°N the positive and negative changes are in balance but at 24°N the whole section averages 0.03°C warmer.

An interesting result of their analysis is that historical temperature–salinity relationships were maintained; where temperature had increased, salinity had also increased. Changes in temperature often occurred by changes in volumes of water masses, lifting or lowering isotherms. The warming is due to an increase in volume of 4–12°C water and a decrease in the deep 2–4°C water pushing isotherms downward.

The section at 24°N across the subtropical North Atlantic was again occupied in 1992 and reported by Parrilla et al. (1994). They found that, compared to the earlier surveys in 1957 and 1981, temperatures continued to increase between 800 and 2500m depth. The maximum rate of increase, at 1100m depth, is 1°C per century. East of about 55°W the warming from 1981 to 1992 occurs over almost all depths. West of this longitude, the warming is confined to above 2000m with cooling below. There also is a band of cooling between 300 and 800m depth across all the ocean east of 67°W.

Over the whole period between 1957 and 1992, the bands of warming above 2500m and cooling below are remarkably uniform across the entire ocean. The deep cooling of waters is less intense than the warming, thus the overall heat content along this section has increased.

Bryden et al. (1996) conducted a more detailed study of the three occupations of this section including examination of salinity as well as temperature. While before 1981, temperature–salinity relationships were maintained and warming on a constant depth level was due to downward displacement of isopycnal surfaces, between 1981 and 1992, the depth of isopycnals did not change significantly. However, during the latter time period, the temperature and salinity on isopycnal surfaces increased, hence the warming from 1981 to 1992 is mostly due to changes in the water characteristics.

Roemmich and Wunsch (1984) also recognised some of the difficulties encountered in observing long-term variability of the oceans. IGY and 1981 sections only

provide a snapshot of the state of the North Atlantic at two particular instances. It is impossible to determine from these whether the changes are real long-term trends or a result of natural short-term variability. Roemmich and Wunsch (1984) indicated that short time-scale eddies were the most significant source of error. In order to study large scale changes they smoothed the data horizontally with a 1000km wide Gaussian filter. However, a small intense eddy locally may change the water temperature at some depth by a few degrees, which when smoothed, will produce a significant change in the fields. Small scale eddies can be identified in the sections by comparing the patterns of temperature and salinity at the different times and it was found that these sections were not affected by eddy noise.

One of the most significant variations in northern North Atlantic hydrography was the "Great Salinity Anomaly" of the 1970s. This event involved a dramatic decrease in salinity observed in the northern North Atlantic. By examining hydrographic data from a variety of sources, Dickson et al. (1988) traced this anomaly as it circulated around the subpolar gyre.

The anomaly was first detected as a strong cooling and freshening of waters east of Greenland and north of Iceland in 1968. This anomaly was advected southwards by the East Greenland Current and round to the west coast of Greenland by 1969–70. Now in the subpolar gyre, the salinity minimum followed the Labrador slope current reaching the Grand Banks by about 1971–72. At this point the feature joins the North Atlantic Current. From here repeat measurements were scarce and it was difficult to track the progress of the anomaly but evidence suggested that a salinity anomaly arrived at the Rockall Channel in the eastern North Atlantic around 1975. By now the anomaly had spread over a wide area. The Irminger current brought a freshening to waters south of Iceland in 1976 and the anomaly was detected off Norway in 1977–78. The anomaly continued to be advected until it eventually arrived back in the Greenland Sea in 1981–82. Dickson et al. (1988) estimated that its overall propagation around the subpolar gyre had occurred at about 3cm s^{-1} which is consistent with average current speeds.

The anomaly as it was first observed in the Greenland sea had a depth of 200–300m. It kept this depth as it entered and circled round the Labrador Sea. After joining the North Atlantic Current system salinity minima were detected

at depths down to 800m in the eastern North Atlantic.

The original source of this fresh anomaly was attributed to a persistent anomalous atmospheric pattern during the 1960s which resulted in an unusually strong northerly wind component over the Greenland sea. This increased the flow of the East Greenland and East Iceland currents and also increased the proportion of cold, fresh polar waters contained in them. As the salinity of the waters in the Greenland Sea fell below the critical value of 34.7psu the water was not dense enough to convect during winter cooling. Thus, as the cold fresh surface layer could not mix with the warmer and more saline lower layer, its anomalously fresh and cold nature was further preserved.

Dickson et al. (1988) described the difficulties involved in compiling the evolution of the "Great Salinity Anomaly" and indeed establishing that the salinity minima observed at several different locations were part of the same phenomenon. The main problem is with paucity of data. To track the progression of a feature requires repeat measurements at several sites. Dickson et al. (1988) were hampered in their investigation by gaps in the time series of conductivity-temperature-depth (CTD) measurements carried out at ocean weather stations Charlie (52°45′N, 35°30′W) and Juliet (52°30′N, 20°00′W) just as the anomaly reached them. This emphasises that to determine the origin and evolution of variations in ocean properties, good resolution of data is needed in both time and space.

Three studies (Levitus 1989a, Levitus 1989b, Levitus 1989c) examined hydrographic records of the North Atlantic from the National Oceanographic Data Centre, Washington D.C., for the pentads 1955–59 and 1970–74. Objective analysis techniques were used to map temperature and salinity data from Nansen bottles and CTD casts. The resultant fields, on depth surfaces and cross-sections, from the two pentads were compared to investigate changes.

The first paper (Levitus 1989a) examined salinity changes between the two periods in the upper 150m of the North Atlantic. He found that in 1970–74 the subpolar gyre was fresher by as much as 0.5psu than in 1955–59. This is consistent with Dickson et al. (1988) as in 1970–74 the Great Salinity Anomaly was circulating around the subpolar gyre. The majority of the area of the subtropical gyre had also freshened by smaller amounts. An area on the north edge of

the subtropical gyre, south of Newfoundland and Nova Scotia had increased in salinity over this time by up to 0.4psu.

Levitus (1989b) compared temperature and salinity at intermediate depths between the periods of 1955–59 and 1970–74. It was found that between 500m and 1300m, the North Atlantic subtropical gyre was colder and fresher in the latter pentad than in the former and this was attributed to an upward displacement of isopycnal surfaces. The western subpolar gyre was found to have warmed and become more saline. This underlies the fresher waters at 150m reported by Levitus (1989a) and Dickson et al. (1988). The presence of the Great Salinity Anomaly in the subpolar gyre in the early 1970s with less dense water suppressed convection. Therefore, underlying warmer saltier waters will not have mixed as much with the cold fresh surface waters, giving rise to the observed anomalously warm and saline conditions. East of 40°W, the waters were slightly colder and fresher. Changes were of the order of 0.5°C and 0.025psu.

Levitus (1989b) investigated similar depths to the analyses presented here. The study is reviewed further in section 4.3.1 and compared to results obtained by our analysis including expendable bathythermographs (XBTs).

The final paper in this series (Levitus 1989c) detailed the changes in temperature and salinity in the deep North Atlantic between the two pentads. At 1750m depth it was found that most of the North Atlantic had increased in temperature by about 0.1°C and salinity by 0.025psu. There was one tongue of water in the east, off the coast of Spain between 30°N and 50°N and east of 35°W where the water had cooled and freshened by similar amounts. Levitus (1989c) also looked at cross-sections along 24.5°N and 36.5°N and found that while the periods under consideration were slightly different the fields were in general agreement with Roemmich and Wunsch (1984).

As with Roemmich and Wunsch (1984) it is difficult to draw any conclusions as to whether these changes are a linear trend or part of a cycle. To find the evolution of such features requires more than just snapshots of the hydrography.

The raising of potential density surfaces in the subtropical gyre in 1970–74 compared with 1955–59 described by Levitus (1989b) implies a weakening of the circulation around the gyre. Greatbatch et al. (1991) used Levitus' hydrographic data, along with wind stress data and a diagnostic model, to investigate changes

in the circulation between the these pentads. It was found that the circulation around the subtropical gyre had weakened in the latter period as had the cyclonic circulation in the continental slope region between the Gulf Stream and Atlantic Canada. These effects combined to produce a Gulf Stream 30 Sv weaker in 1970–74 than in 1955–59. No significant changes in transports around the subpolar gyre were found.

Antonov (1993) analysed all available data from Nansen bottles and CTD/STD casts between 1957 and 1981 in both the North Atlantic and the North Pacific to determine linear changes in temperature. Examining the depth range of 300 to 3000m he found that in both oceans temperature in the upper waters to about 500m depth had decreased. In the North Atlantic, below 800m there was a statistically significant rise in temperatures by approximately 0.1°C per 25 years. In the North Pacific, however, no significant changes occurred overall below 500m. The North Atlantic observations of general warming concur with the observations of the 24°N section reported by Roemmich and Wunsch (1984).

Few studies of interdecadal variability in hydrography have used data from MBTs and XBTs, most use CTDs and bottle casts. Levitus et al. (1994) analysed all available temperature data of the North Atlantic between 1947 and 1990 at 125m depth. Temperature anomalies were objectively mapped for each year. These fields were then examined with the empirical orthogonal function (EOF) technique.

The most significant result is that temperature anomalies in the subtropical gyre are opposite in sign to the subpolar gyre. From 1954 to 1965 much of the subtropical gyre cooled while the subpolar is became warmer. After 1965 both these trends switched sign. This may be an oscillating process whose period is longer than the 44 years of observations. Levitus et al. (1994) also identified a quasi-decadal oscillation with the peak in the spectrum at 13 years which can also be seen in the record of temperatures from ocean weather station 'C' (Charlie). The loading pattern of this oscillation shown by the EOF analysis has a large positive region in the northern and eastern North Atlantic, and negative regions in the southwest and north of 60°N.

In a review of subsurface variability in the temperature and salinity structure of the world ocean, Levitus and Antonov (1995) particularly emphasised the

North Atlantic as it is the most observed ocean. They presented time-series of temperature measurements of the deep ocean from Ocean Weather Station 'C' (52°45′N, 35°30′W) in the subpolar gyre and Station 'S' (formerly 'Panulirus', 32°10′N, 64°30′W). In the depth range 1000–1500m, Ocean Weather Station 'C' showed increasing temperatures until about 1973 after which temperatures fell until the end of the record in 1990. In the subtropical gyre, Station 'S' showed linearly increasing temperatures at 1750m from 1960 onwards.

Maps of linear changes during the period 1966–90 show warming south of about 45°N and cooling to the north at 100m depth, both of the order of 0.1-0.2°C. At 400m depth all of the northern North Atlantic and the eastern Atlantic exhibits cooling of about 0.1°C. There is an area of warming in the western subtropical gyre which extends in a tongue along the path of the Gulf Stream.

Levitus and Antonov (1995) conclude by stating that the North Atlantic has undergone a major redistribution of heat and salinity since at least 1960. They emphasise the need for repeated measurements of ocean properties to monitor further changes in subsurface water structure.

Joyce and Robbins (1996) report the results of the time series of temperature and salinity measurements taken at station 'S' throughout its long, by oceanographic standards, duration. They found that in the thermocline, temperature and salinity changes were highly correlated and mainly due to either vertical movements of the thermocline by up to ±30m, or by meridional movements of the horizontal gradients along the southern edge of the subtropical gyre. Long-term changes in the thermocline depth range (500–1000dbar) show a significant cooling from the start of the time series in 1954 to a minimum in 1970. From 1970, temperatures rose slightly and then stayed roughly constant through to the end of the data in 1995.

In the deep waters, 1500–2500dbar, Joyce and Robbins report a persistent long-term warming throughout the time series. By extending the time series using data collected in the area before station 'S' was established, they found that the increase in temperature continued from 1920 to 1995 at a rate of about 0.5°C/century. Comparisons of two meridional sections from the IGY and 1985 passing close to station 'S' show that this warming trend is widespread.

The changes in the deep waters observed at Bermuda have been traced back

to their formation in the Labrador Sea by Curry et al. (1998). The Labrador Sea is a region of normally deep convection in the winter and is the source of Labrador Sea Water (LSW). The depth of the convection is typically between 1000–2000m. After formation, LSW is advected southward by the boundary current. It then splits, part continuing along the Deep Western Boundary Current and part advected by the Gulf Stream and North Atlantic Current, becoming mixed with warmer, saltier waters from other origins, and brought into the ocean interior (Talley and McCartney 1982). Thus, the characteristics of the waters in the basin interior affected by LSW, known as Upper North Atlantic Deep Water (UNADW), will depend to some extent on the conditions under which the LSW was formed. An increase in the volume of LSW advected from the subpolar gyre will create colder and fresher and thicker UNADW and conversely it will be thinner, warmer and saltier when LSW outflow is reduced.

The properties of the LSW will depend on the atmospheric conditions at the time of formation and on the properties of the water advected into the Labrador Sea from elsewhere. Curry et al. (1998) relate the depth of convection, and thickness of LSW, with the North Atlantic Oscillation. At periods of high NAO index, the atmospheric conditions over the Labrador sea are characterised by strong, cold northerly winds (figure 3.1) which increase the depth of the convective overturning by increased cooling of the surface and by increased wind stirring. Convection was weak at the end of the 60s after a long period of negative NAO winters but has increased greatly to an unprecedented depth of 2300m in 1993–95 after a period of high NAO winters (Dickson 1997).

Anomalous ocean conditions have also affected the LSW thickness. The appearance of the "Great Salinity Anomaly" in the Labrador Sea in 1968–72, accompanied by anomalously low winds, shut down convective overturning completely. This was repeated in the early 1980s when another low salinity anomaly entered the Labrador Sea, capping the cold dense waters to such an extent that even strong winds associated with a high NAO index could not create deep convection.

Curry et al. (1998) examined the relationship between the depth and temperature of the LSW at its formation with the temperature of the deepest layer 1500–2500m observed at station 'S' near Bermuda. They found that the tem-

perature of the deep water at station 'S' in the subtropical gyre was negatively correlated with the source thickness of the LSW lagged by six years. The general increase in temperatures recorded at Bermuda from 1922 to 1987 are accompanied by an overall thinning of LSW from 1928 to 1983. After this time the LSW has cooled and thickened and, since 1988, Station 'S' temperatures have also decreased.

XBTs in the western North Atlantic were used by Molinari et al. (1997) to study variability in the period 1966 and 1995. The XBT temperatures were averaged by month onto a 2° latitude by 4° longitude grid and time series of temperature anomalies were compiled by detrending and filtering to emphasise longer time periods. This was done at 0, 100, 200, 300 and 400m depths. 31 rectangles in the western subtropical gyre (within 16° and 44°N, 80° and 64°W) contained enough data to construct time series.

Time series of anomalies averaged over all 31 boxes show three warm and three cold periods at 100 and 200m but only two of each at 300 and 400m. Meridional cross sections of temperatures through the subtropical gyre show that during positive anomaly events isotherms deepened throughout the section, and rose during negative anomalies.

Molinari et al. (1997) attempted to link the transitions between warm and cold periods with transitions in a detrended North Atlantic Oscillation index. They found that at the surface and 100m depth these transitions occurred at nearly the same time. At 300m and 400m three events (1971, 1976 and 1988) coincided with NAO transitions. Periods of positive NAO index coincided with positive subsurface temperature anomalies.

Reverdin et al. (1997) investigated variability in the North Atlantic subpolar gyre from station salinity and temperature data. It was found that although variability was stronger at the surface, variations in properties were coherent to a depth greater than the deepest mixed-layer in the late winter.

Reverdin et al. (1997) also examined the spatial coherence of the variability of salinity. They found that the same pattern explains 70% of the variance and that salinity anomalies propagate from the west of the subpolar gyre to the northeast. This agrees with the evolution of the "Great Salinity Anomaly" described by Dickson et al. (1988). Reverdin et al. (1997) propose that the origin of these

salinity anomalies are the slope currents of the Labrador Sea. They also found correlations with atmospheric circulation, with weakened westerlies at 55° and weaker northwesterlies over the Labrador Sea, associated with warmer and more saline waters.

3.4 Sea surface temperature variability

The studies mentioned in the last section have all been based on hydrographic records of subsurface ocean properties. Sea surface temperature data are far more plentiful than subsurface observations which should allow better investigation of their variability. It is obvious that SSTs will be strongly influenced by the atmospheric conditions with which they are in contact. They show strong seasonal variations which must be taken into consideration when investigating interannual to interdecadal variability to ensure that data do not have any unwanted seasonal bias.

The sea surface temperature is affected by solar radiation, sensible heat exchanges and latent heat. Wind also has an affect, strong winds will increase exchanges of sensible and latent heat. Wind stress also has an indirect effect on SSTs by stirring the surface water which may increase the depth of the mixed-layer thus entraining colder water from below. It is not so clear, however, how much SSTs affect the atmosphere and there has been some speculation that ocean changes may lead atmospheric changes in some circumstances. Several investigations, particularly in the North Atlantic, have examined interdecadal variability in SSTs and related it to atmospheric conditions.

Bjerknes (1964) studied sea surface temperature and sea level pressure variations, particularly the NAO, in the North Atlantic to determine their relationships and the mechanisms of air-sea interactions. He considered both interannual and interdecadal variability.

On interannual time-scales Bjerknes found that from the Azores to Iceland, SST variability was negatively correlated with the local strength of the prevailing westerly winds. This correlation was about equal all the way from the Azores to Iceland. Clearly in the short term, higher wind speeds increase the transfer of heat, both sensible and latent, from the ocean to the atmosphere.

Bjerknes examined changes over longer time-scales by comparing North Atlantic sea surface temperatures during three pentads, 1894–98, 1920–24 and 1930–34. 1920–24 was within an extended period of high NAO index whereas in the other two pentads, it was low. Between 1894–98 and 1920–24 the ocean cooled north of 50°N in agreement with the short time-scale observations that increased winds lead to cooler SSTs. In 1930–34 when the westerlies had dropped in intensity, the northern North Atlantic had warmed.

In contrast to the cooling north of 50°N Bjerknes found that between 30°N and 50°N, SSTs had increased from 1894–98 to 1920–24. The strongest warming was on the north edge of the Gulf Stream but warming occurred across almost all the ocean. By 1930–34 this area had further warmed, but only slightly. He concluded that the Gulf Stream and North Atlantic Current respond to more intense winds by increasing in speed and bringing increased volumes of warm water from the tropics.

Deser and Blackmon (1993) described variations of North Atlantic winter SST and surface atmospheric conditions from 90 years of observations. Using EOF analysis, they found an important mode of SST variability to be a dipole pattern with a centre of anomalies of one sign east of Newfoundland, and the opposite sign in the western subtropical gyre. This pattern of oscillation contained components with a period on both interannual and interdecadal scales. EOF analysis of surface air temperatures demonstrates a very similar dipole pattern of variability. Comparison with wind fields shows anomalously strong winds overlying anomalously cold SSTs. Deser and Blackmon also found that periods with greater sea ice in the Labrador sea preceded by $\sim$ 2 years periods of colder than normal conditions east of Newfoundland.

Deser and Blackmon (1993) also identify another mode of variation characterised by a period between 1900 and 1929 of colder SSTs and a period of warmer conditions in 1939-68. A map of the difference in mean SSTs between these periods reveals that the warming occurred in the western North Atlantic and extended in a tongue along the path of the Gulf Stream to about 40°W. This change was accompanied by a change in the NAO from a high phase to a low. The most significant changes in the wind fields between these periods occurred downstream of the SST anomalies leading Deser and Blackmon to suggest that the cause of

the warming was due to changes in ocean currents rather than local winds.

Kushnir (1994) also studied North Atlantic SSTs, concentrating on long term variability. Time series of mean SSTs in zonal bands reveal basin scale changes during this century. Before 1920, SSTs were less than normal but began to rise after this time across all the ocean. Over most of the ocean an anomalously warm period lasted from the 1930s to the 1960s. North of 30°N, a cold period was again entered in the mid-to-late sixties which then continued to the end of the data in 1985. South of 30°N SSTs remain reasonably constant.

Kushnir investigated the spatial pattern of these SST changes by comparing mean SSTs from four 15 year periods. The warm years of 1925–39 were compared to the cold years 1900–14, and 1950–64 (warm) compared to 1970-84 (cold). Thus the patterns of pre-war warming and post-war cooling are shown. The years before and after the second world war were considered separately as SST measurement practises changed at about that time. In both cases, Kushnir presented the warm period minus the cold period. The patterns for the warming and the cooling are similar with changes over most of the ocean. The greatest changes for both transitions are in the north and both show a band of change along the Gulf Stream. If only winter months are used in this analysis, large changes are particularly prominent along the Gulf Stream, around Iceland and in the Labrador sea.

While the three SST studies reviewed above have all related some SST variability to the effects of local atmospheric conditions, all have also noted that non-local processes may be responsible for much of the long-term variability in SSTs. Kushnir (1994) notes that the lack coherence between interdecadal patterns of SSTs and sea level pressures may indicate that interdecadal variability is caused by basin-scale dynamical interaction between ocean and atmosphere. Deser and Blackmon (1993) suggested that warming along the path of the Gulf Stream and North Atlantic Current was due to changes in ocean circulation. However, in contrast to Bjerknes (1964), Deser and Blackmon (1993) found that warm temperatures in the Gulf Stream coincided with weaker winds.

These three studies have only looked at SST changes as stationary features. Hansen and Bezdek (1996) investigated SST in the North Atlantic to study the development and evolution of SST anomalies. They considered only extreme

features, those in the upper and lower deciles of anomaly time series. Between 1945 and 1992, five cold and nine warm anomalies were identified. These are in general agreement with the warm and cold periods found by previous research, (Deser and Blackmon 1993, Kushnir 1994) but show the features in more detail.

McCartney et al. (1996) also examine and describe SST anomalies in the same way as Hansen and Bezdek (1996). Figure 3.3 is taken from McCartney et al. (1996) and illustrates the method by which anomalies are tracked. The growth, migration and decline of the anomalous features can be clearly seen.

Hansen and Bezdek (1996) tracked the evolution, temporally and spatially, of these extreme SST anomaly events. They found considerable propagation of anomalies in the North Atlantic, following the paths of the major surface currents. In the northern North Atlantic, anomalies travelled along the Gulf Stream and North Atlantic Current until reaching the Norwegian sea. Anomalies were also detected moving around the subpolar gyre. A cold anomaly first seen in 1970 in the Labrador Sea can be identified as the thermal signature of the "Great Salinity Anomaly".

South of 40°N, anomalies followed the currents of the subtropical gyre. One cold feature which started off Florida in 1968 completed almost a full circuit of the subtropical gyre in about 8 years. There were some anomalies originating on the eastern border of the ocean which spread out north and south along the European and North African coasts.

A typical size of anomaly was about 20° across in latitude or longitude and they lasted between 3 and 10 years. The speed of travel (1–3 km day^{-1}) was found to be less than the speed of the near surface currents. This raises questions over the mechanisms that create and move these anomalies but Hansen and Bezdek could not propose a solution.

Hansen and Bezdek also comment that previous analyses using compositing, epochal differencing and EOF do not show the scales and evolution of these features very well. Their representation of yearly maps of SST anomalies presents a clear representation from which to study the temporal and spatial development of these features.

Following on from the principle that a component of SST anomalies may be advected, Sutton and Allen (1997) examined wintertime SST anomalies along the

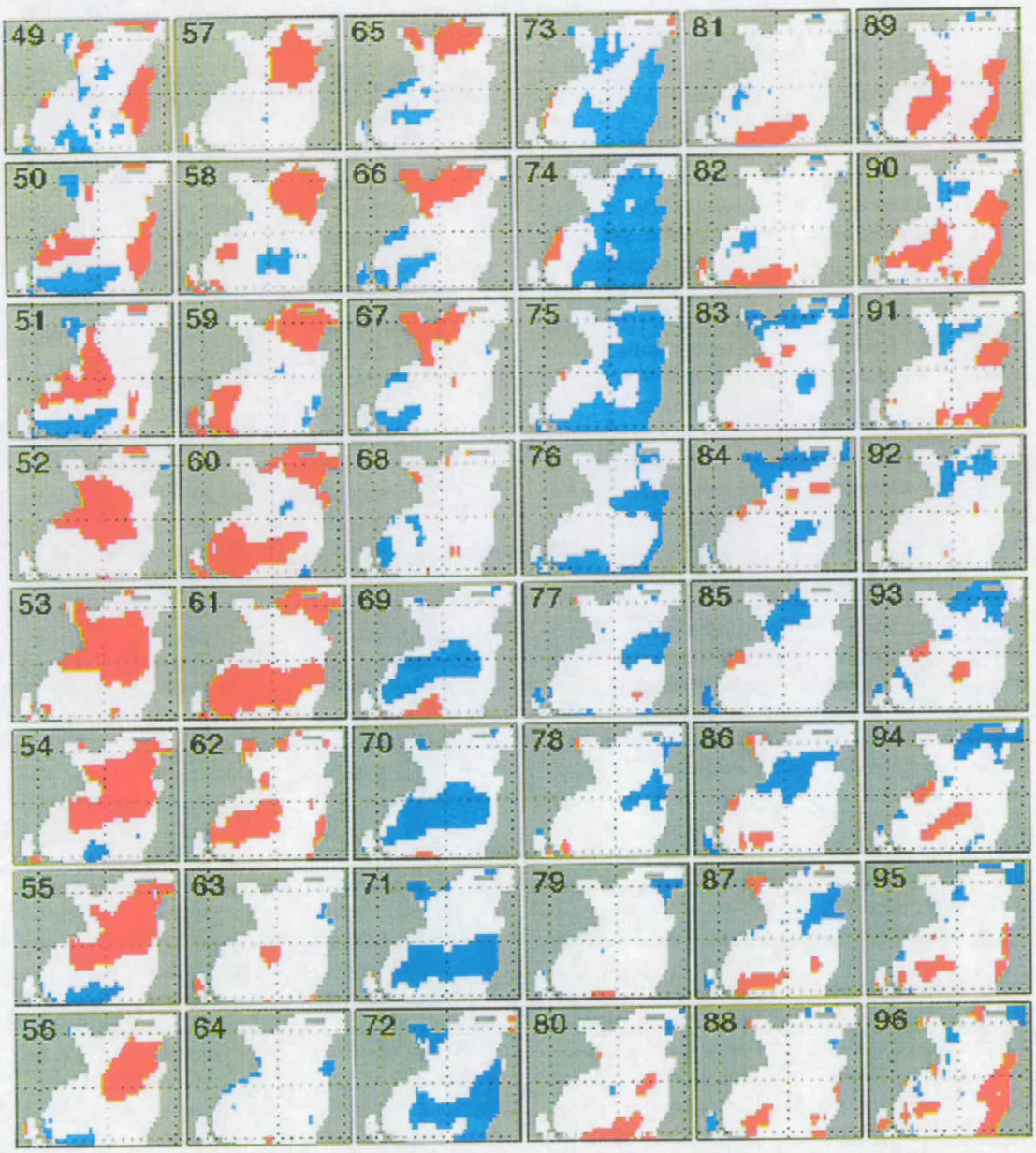

Figure 3.3: The evolution of extreme cold (blue) and warm (red) SST events in the North Atlantic between 1949 and 1996. Taken from McCartney et al. 1996.

Gulf Stream and North Atlantic Current. Alternating warm and cold anomalies are tracked from the Western Atlantic off Cape Hatteras to the northwest of Scotland. This propagation takes about nine years across the North Atlantic at an average speed of $\sim$ 1.7cm s^{-1}. This is considerably slower than the surface current at the centre of the Gulf Stream. Sutton and Allen suggest that the velocity of SST anomalies may be determined by the slower subsurface currents or by the weaker currents either side of the main Gulf Stream.

A power spectrum of Gulf Stream winter SST anomaly time series reveals a peak at 12–14 years. These periods of variability coincide with a dipole-like pattern of sea level pressure variability over the North Atlantic. Warm SSTs off the eastern sea-board of the United States coincide with stronger than normal westerlies over the mid-Atlantic. The large contrast in winter between the cold land and warm SSTs off the US coast fuels storm development. A warm SST anomaly here would enhance storm formation. The observed pressure dipole and strengthened westerlies is consistent with the theoretical response of the mean flow to an enhanced storm track (Hoskins 1983). Sutton and Allen also found that cold SST anomalies in the mid-Atlantic (40–50°N) were correlated with warm anomalies off the US east coast and in the tropical Atlantic. The cause of this is attributed to increased heat-flux due to the stronger westerlies in mid-latitudes and stronger trades over the tropics.

The progression of the warm SST anomaly after it leaves the storm formation region, along with associated atmospheric patterns and SST anomalies, were tracked using regression analysis. At a lag of 2 years, the warm anomaly has moved only a small amount, the pressure anomaly dipole has weakened and the northern cold anomaly has advected along the path of the North Atlantic Current. After 4 years the warm anomaly has moved along and split as the Gulf Stream bifurcates, part has travelled southward with the recirculation and part has followed the North Atlantic Current. At this time, a cold anomaly has developed in the Gulf of Mexico. At a 6 year lag, the warm anomaly has been further advected by the circulation and the Gulf of Mexico cold anomaly has spread into the storm formation region off the US. As a response to this, the sea level pressure anomaly dipole has reappeared with the opposite sign.

The research presented by both Hansen and Bezdek (1996) and Sutton and

Allen (1997) has shown that to understand the causes and evolution of sea surface temperatures, it is necessary to study both the spatial progression of features and their development with time. To do this requires good data coverage over the ocean over many years. Sea surface temperatures are relatively plentiful, particularly in the North Atlantic.

The study of subsurface property changes is, of course, much more difficult. As described, many studies of hydrographic changes have compared just snapshots (Roemmich and Wunsch 1984, Levitus 1989b) or examined only one, well observed region (Molinari et al. 1997). To investigate the changes in subsurface changes using methods similar to Hansen and Bezdek (1996) and Sutton and Allen (1997) is difficult and results will be less accurate and less conclusive.

However, throughout this century, observations have been regularly made of subsurface temperatures using Nansen bottles, CTDs, MBTs and XBTs and the quantity, coverage and depth ranges have been considerably increased in the latter half century. It is therefore very worthwhile investigating climatic change in the North Atlantic, the most observed ocean, using all of this thermal data.

3.5 Variability of the position of the Gulf Stream and North Atlantic Current

Some smaller scale variability of ocean properties is due to meanders and migrations of ocean currents and the fronts associated with them. Lateral migration of currents and ocean fronts results in changes in temperature at locations in the vicinity of the front. A northward shift of the North Atlantic Current, for example, will bring warmer waters from the south to locations previously occupied by a cold water mass. These changes are evident on temperature anomaly plots and as temperature gradients across fronts can be very large, intense anomalies can be seen.

The path of the north wall of the Gulf Stream has been determined from surface, aircraft and satellite observations since 1966 and recorded in monthly charts. These have been analysed to produce time series of the latitude of the north wall at 6 different longitudes between 65°W and 79°W, up until 1977 (Taylor and Stephens 1980) and to 1996 (Taylor 1996, Taylor and Stephens 1998). Drinkwater

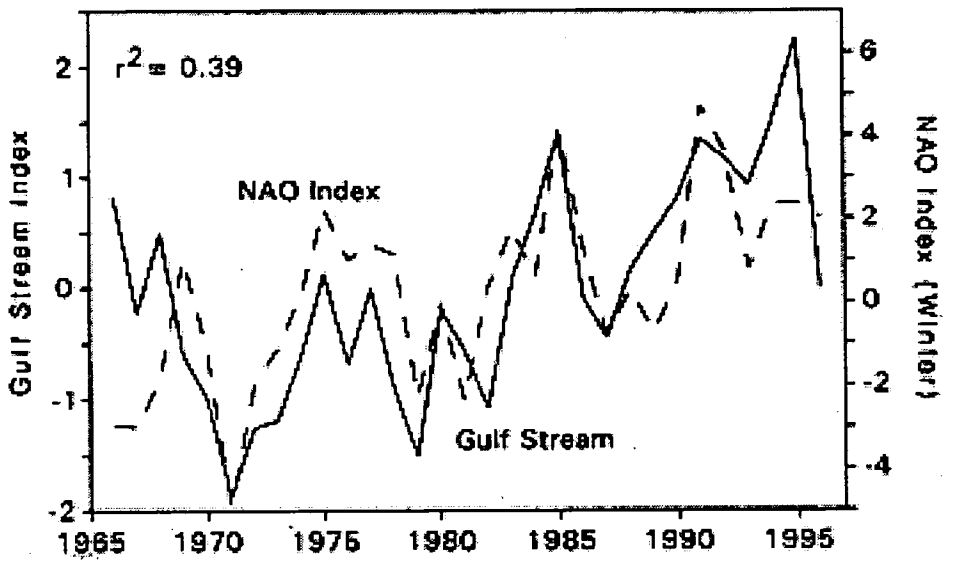

Figure 3.4: Index of the north wall of the Gulf Stream between 65 and 79°W and the NAO index lagged by two years. Taken from Taylor (1998).

et al. (1994) also investigated the position of the Gulf Stream at each degree of longitude between 50°W and 75°W from the 1970s to 1992. Drinkwater's analysis is in good agreement with Taylor's.

Taylor (1996) used principal components analysis to determine the pattern of variation common to all six longitudes and determined that the first principal component could be regarded as representative of the variation of all this section of the Gulf Stream. There is considerable variation of this index on seasonal, interannual and interdecadal time-scales. However, there is little coherence with the mean annual cycle, i.e. seasonal variations are smaller than interannual variations (Taylor 1995). The standard deviation of the variations of the first principal component was 0.04° of latitude at 79°W increasing eastwards to 0.37° of latitude at 65°W. Taylor and Stephens (1998) used the same analysis technique to produce an index of the Gulf Stream position from the most recent data.

In both Taylor (1996) and Taylor and Stephens (1998), attempts have been made to relate the Gulf Stream position to atmospheric conditions. Taylor and Stephens (1998) reported a link between the latitude of the Gulf Stream and the North Atlantic Oscillation. They found that their position index was correlated with the NAO index from Hurrell (1995) lagged by 2 years. This is illustrated in figure 3.4. The high state of the NAO, with stronger mid-latitude westerlies and

trade winds, was linked to a northward shift of the Gulf Stream, between 65 and 79°W, two years later. While they stated that the mechanism that connected these events is not clear, it is likely that the delay is due to the adjustment of the ocean circulation to the atmospheric winds.

Belkin and Levitus (1996) studied the position of the North subpolar Front near the Charlie-Gibbs fracture zone which is associated with the North Atlantic Current. Hydrographic data were obtained from repeat occupations of three sections crossing the front covering the period from 1976–1985.

The results show that the position of the front can change very rapidly. The westernmost transect, between Ocean Weather Station Charlie and St. John's, Newfoundland showed the North subpolar Front move south in 1976–77 and then shift dramatically northward by 250–300km in 1978–79 and 1980–81, each time returning southward later the same year. Downstream of these events, the easternmost section (OWC Charlie - Cape St. Vincent, Portugal) revealed a northernmost location of the front in 1976–77 followed by sharp southward movements of the front in 1978–79 and 1980–81. The time series does not extend long enough to determine whether this coherence continues. The sections also detect the passing of the "Great Salinity Anomaly" in the 1970s and another large salinity anomaly in the 1980s.

3.6 Variability in Ocean Models

Several authors have employed ocean models or coupled ocean-atmosphere models to try to recreate variations observed in the oceans and gain a better understanding of the mechanisms behind such variability.

Delworth et al. (1993) investigated interdecadal variability of the thermohaline circulation in a coupled ocean-atmosphere model of the North Atlantic. In a model run over 600 years they found an irregular oscillation in the strength of the thermohaline circulation with a broad time-scale of about 50 years. The sea surface temperature patterns associated with this oscillation are similar to the patterns of observed SST variations described by Kushnir (1994).

Delworth et al. state that this oscillation appears to be driven by density anomalies in the northern sinking region (approximately 52–72°N) and smaller

anomalies in the larger rising region at lower latitudes. The horizontal transports associated with the gyre circulation also play a significant role. They suggest that the cause of the oscillations are mostly due to oceanic processes although they state that the atmosphere's role requires further investigation.

Latif and Barnett (1994) and Latif and Barnett (1996) reported an interdecadal oscillation in a coupled model of the North Pacific. The oscillation was sustained by a feedback loop involving the subtropical gyre in the ocean and the Aleutian Low in the atmosphere. An enhanced circulation of the subtropical gyre leads to anomalously warm near-surface waters brought up along the Kuroshio and Kuroshio Extension. The atmospheric response to this is a weakening of the Aleutian Low and the associated westerly winds. In the short term, air-sea heat flux is reduced, acting as a positive feedback to the warming. However, the reduced winds cause a winding down of the subtropical gyre and so the transport of warm water from the tropics is lessened. It is this delayed feedback that moves the cycle into its opposite phase with a cold SST anomaly occurring in the Kuroshio and extension.

Figure 3.5 shows the circulation of heat content anomalies around the North Pacific subtropical gyre from Latif and Barnett (1994). Alternate upper ocean warm and cold anomalies are seen to rotate around the subtropical gyre with a period of about 20 years. This is considerably slower than the advection.

Grötzner et al. (1998) investigated a similar decadal cycle in a coupled GCM of the North Atlantic. This oscillation produced similar effects to variability of SSTs observed in the North Atlantic (Deser and Blackmon 1993, Sutton and Allen 1997). However, the model period was found to be 17 years as opposed to the spectral peak at 12 years for the observed oscillation.

In the North Atlantic, the feedback loop between the subtropical gyre and the atmospheric circulation is similar to the Pacific oscillation but there are differences. As mentioned by Sutton and Allen (1997), the atmospheric response to a warm anomaly off the east coast of the United States is a strengthening in the pressure dipole which increase the mid-latitude westerlies and the trade winds. This partly acts to spin-up the gyre, which is a positive feedback, but also creates cold anomalies in the eastern subtropical ocean which travel westward with the gyre circulation until they replace the original warm anomaly in the Gulf Stream

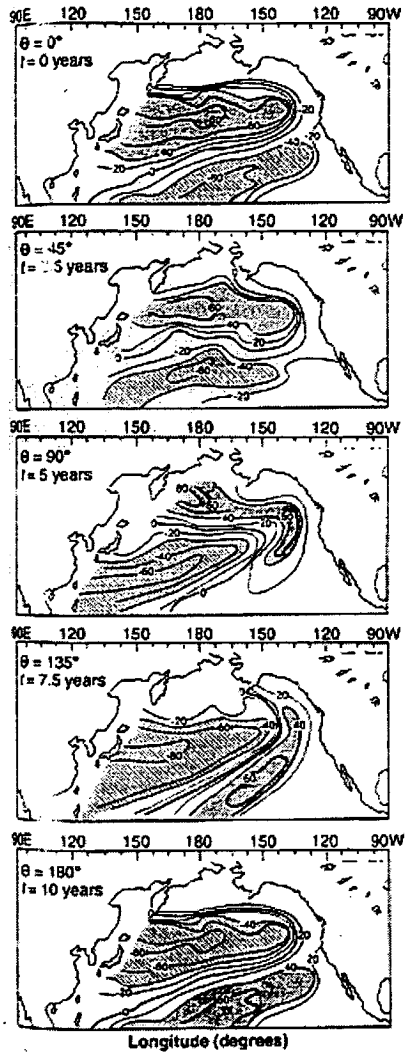

Figure 3.5: The progression of heat content anomalies around the subtropical gyre. The panels show different stages of the cycle. Units are °C m. Taken from Latif and Barnett (1994).

region. This then provides the negative feedback in the oscillation.

Zorita and Frankignoul (1997) also examined interdecadal variability in a 325 year run of a coupled model of the North Atlantic Ocean. They found two distinct modes of variability with periods of 20 and 10 years. The 20 year mode occurs throughout the thermocline to about 1000m and has a pattern with opposite signs either side of 30°N and another sign change at 50°N although the amplitude of variations in the far north are small. This mode is not detected in the atmosphere alone and they find no evidence of an ocean to atmosphere feedback. Zorita and Frankignoul suggest that this mode is a passive ocean response to atmospheric

variations.

Zorita and Frankignoul relate the 10 year mode, which is confined to the surface layers, to the 20 year mode of variability found by Latif and Barnett (1994) in their coupled model of the North Pacific. They find a similar feedback loop between subtropical gyre and atmosphere with the response time of the gyre defining the length of the period. As with Grötzner et al. (1998) the model SST pattern of variability is similar to observations of North Atlantic SSTs reported by Deser and Blackmon (1993).

Halliwell (1998) studied the effect on winter SSTs in the North Atlantic of atmospheric circulation anomalies by forcing an ocean model with the observed winds from 1950 to 1992. The resultant simulated SSTs agree quite well with observed SSTs. Halliwell also found that atmospheric patterns with strong subtropical high and subpolar low, create intense westerlies and the ocean flow around the subtropical gyre is increased leading to anomalously warm SSTs in the Gulf Stream region. These strong winds, accompanied by strong trade winds, also lead directly to cooling of the surface. These results agree very well with Sutton and Allen (1997).

As observations of the real ocean are sparse, have been taken irregularly, and only during the last century, it is very difficult to observe variability. Analysing the causes and evolution of climatic changes within the ocean is difficult with such a short and limited data set. Ocean models can be run over many years and property changes examined at all depths. Thus, although they may not represent the oceans completely accurately, they may help us to understand the processes that contribute to variability. They can also be used to test ideas of variability.

The patterns of variability identified in these coupled models may be related to variations seen in observations of the North Atlantic. This might help in the explanation of anomalous features in the temperature fields and their evolution.

3.7 Summary and Discussion

The investigations of temperature and salinity observations reviewed here show that there is considerable variability in the North Atlantic both at the surface and also in deeper waters. Measurements of sea surface temperatures in the

North Atlantic have been taken for over a century now which has allowed several studies of their variability often in conjunction with atmospheric conditions. The abundance of such data across the ocean has allowed the use of techniques such as EOF analysis.

Subsurface data have been more limited and consequently study of variability is more difficult. Examining the development of changes and anomalies in the structure of the ocean is very difficult from such relatively few data from only the last 40 to 50 years.

The overall linear trend in the ocean over the last half century has been a general warming south of approximately 45° and a cooling to the north (Roemmich and Wunsch 1984, Antonov 1993, Levitus et al. 1994, Levitus and Antonov 1995, Bryden et al. 1996, Joyce and Robbins 1996). A dipole pattern such as this is often seen in maps of temperature changes with the western subtropical gyre showing an anomaly of one sign and the subpolar gyre of the other sign. This pattern is evident in the comparison of the pentads 1955–59 and 1970–74 at intermediate depths by Levitus (1989b) and in the linear trend of temperatures shown in Levitus and Antonov (1995). In the study of temperature variability at 125m by Levitus et al. (1994), this pattern is the loading pattern of the first EOF, accounting for 32% of interannual variability. A similar pattern is also seen in SSTs (Bjerknes 1964, Deser and Blackmon 1993, Kushnir 1994).

Several studies have attempted to examine the advection of anomalies by ocean currents. By piecing together data from a number of sources, Dickson et al. (1988) managed to follow the path of the "Great Salinity Anomaly" as it circulated around the subpolar gyre. This was also be seen in other papers, Levitus (1989a) reported that the subpolar gyre was considerably fresher in 1970–74 than in 1955–59. Reverdin et al. (1997) showed that temperature and salinity anomalies could be traced as they were advected around the subpolar gyre.

The most comprehensive study of the propagation of temperature anomalies was Hansen and Bezdek (1996). This clearly showed the evolution and propagation of SST anomalies as they followed the paths of the major North Atlantic currents. This kind of propagation is missed by EOF techniques and comparison between periods which is the usual way to investigate interannual or interdecadal variability. Sutton and Allen (1997) investigated the propagation of SST anoma-

lies along the Gulf Stream and North Atlantic Current. These took nine years to traverse the ocean which, as Hansen and Bezdek (1996) also found, is slower than the surface flow in the centre of the current.

Several studies tried to correlate oceanic changes with atmospheric conditions. On shorter time-scales, such as interannual, the relation between wind speed and SSTs is clear. Bjerknes (1964), Deser and Blackmon (1993), Kushnir (1994) and Sutton and Allen (1997) all agree that stronger than normal winds increase the loss of heat from the ocean to the atmosphere leading to cooler SSTs. In this mechanism, SSTs are governed by local effects.

On interdecadal time-scales there is evidence that ocean-atmosphere interactions produce more complicated effects. Particular attention has focused on the effects of long term changes in the NAO. Bjerknes (1964), Kushnir (1994) and Sutton and Allen (1997) have proposed that after a few years of high NAO state, the enhanced westerly winds in mid-latitudes act to spin up the subtropical gyre, leading to a stronger Gulf Stream. This brings up more warm waters from the tropics leading to a positive SST anomaly in the western subtropical gyre and along the Gulf Stream. Only the results of Deser and Blackmon (1993) contradict this mechanism finding that even on longer time-scales warmer temperatures in a tongue along the Gulf Stream coincided with lighter winds. However, Bjerknes (1964), Kushnir (1994) and Sutton and Allen (1997) all found that the NAO is positively correlated to SSTs in the western subtropical gyre on decadal and longer time-scales. This mechanism is supported by experiments of Halliwell (1998) in which an ocean model is forced with different atmospheric circulation anomalies.

Sutton and Allen (1997) proposed that SST anomalies were part of a cycle maintained by ocean-atmosphere feedback. A warm anomaly in winter off the east coast of America, leads to an enhanced storm track which then leads to an increase in the NAO index. This acts to spin up the gyre acting as a positive feedback. The negative feedback is from increased trade winds creating colder SST in the eastern subtropical Atlantic which is advected westward until it replaces the warm anomaly in the Gulf Stream region. This hypothesis is supported by results from coupled ocean-atmosphere models (Latif and Barnett 1994, Zorita and Frankignoul 1997, Grötzner et al. 1998). The period of the oscillation is de-

termined by the response time of the subtropical gyre. Sutton and Allen (1997) find the period to be about 13 years in real SST data, whereas in the models Grötzner et al. (1998) found it to be 17 years and Zorita and Frankignoul (1997) about 10 years.

Change in the atmospheric forcing, acting to increase or decrease the circulation around the subtropical gyre, will also have an effect on subsurface temperatures. Levitus (1989b) found temperatures in the subtropical gyre in 1970–74 were colder than 1955–59 because isopycnal surfaces had lifted. Greatbatch et al. (1991) showed that this was related to a reduced circulation of gyre. Molinari et al. (1997) also showed that temperatures in the subtropical gyre were correlated to the NAO, high NAO coincided with warmer temperatures beneath the surface layers. When the gyre is spun up by stronger westerlies associated with a high NAO state, isopycnals within the gyre are lowered bringing down warmer water.

Studies of subsurface variability have been limited by the paucity of data available. Many studies have just compared repeated occupations of sections (Roemmich and Wunsch 1984, Bryden et al. 1996) or hydrographic data from two different periods (Levitus 1989a,b,c). These show that there has been considerable changes between observations but it is impossible to tell whether this is a trend or part of an oscillation.

Dickson et al. (1988) noted the difficulty of determining that a variation in salinity observed at isolated locations in the northern North Atlantic was in fact the same feature moving around the ocean. Hansen and Bezdek (1996) produced a time series of maps of SST anomalies in the North Atlantic which, for the first time, showed the development, evolution and propagation of anomalies.

Bathythermograph observations are the most plentiful source of data from the subsurface ocean. However, only a few previous studies have made use of BT data. In the next chapter, subsurface temperature data from bathythermographs and other sources are used to map temperature changes in the North Atlantic since 1950.

Chapter 4

Interdecadal variability of subsurface temperature in the North Atlantic

4.1 Hydrographic temperature data

Determining climatic change in the hydrography of the oceans extremely difficult due to the size and depth of the oceans. The most commonly measured hydrographic property is temperature by mechanical bathythermographs (MBTs) and expendable bathythermographs (XBTs). Many previous investigations of hydrography and variability, such as Levitus (1989b), have used data from Nansen casts or conductivity-temperature-depth (CTD) casts. While these record both temperature and salinity of water masses and often measure properties to great depths, they are relatively scarce and very unevenly spread in time and space. In this study, bathythermograph data provide most of the temperature information used as they are much more abundant, allowing study of temperature changes with greater accuracy and resolution in both time and space. Some data have also come from Nansen bottles and CTD casts.

Mechanical bathythermographs were the original method to measure the ocean temperature at several depths and were usually deployed from research ships, often only from local research cruises. Most MBTs measured temperatures to a depth of only 295m. Therefore, in the 1950s and early 1960s, although many MBT observations were made, they tended to be concentrated around the coast and only measured the upper ocean temperatures.

Since the mid-1960s, MBTs have been superseded by XBTs which are conve-

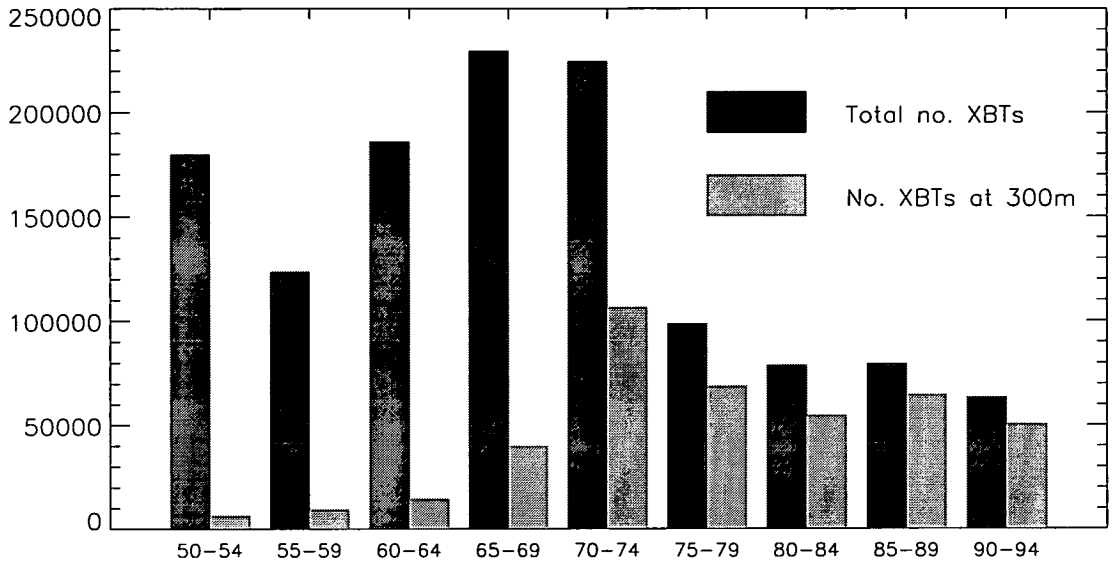

Figure 4.1: Numbers of MBTs or XBTs deployed in the North Atlantic during 5 year periods from 1950 to 1994. Dark grey blocks show the total number of MBTs/XBTs and light grey blocks show numbers reaching to 300m or deeper.

nient to deploy. Earlier XBTs measured temperatures to 450m depth but more recent XBTs go down to 798m with some going deeper. XBTs are often now deployed from merchant ships so it is possible to obtain more widespread temperature data. While the total number of XBTs has not increased, they are more widespread and measure a greater depth range.

Figure 4.1 shows the numbers of MBTs or XBTs taken in the North Atlantic in each pentad from 1950 to 1994 and the number reaching 300m or deeper. As can be seen, the total number of observations in each pentad are high until 1975 after which numbers are drastically decreased. However, measurements below 300m are very small in number in the earlier pentads, reaching reasonable levels in the late 1960s. The investigation of the temperature of waters at intermediate depth, which is a region of particular concern in this study, will be severely limited in the earlier years. However, coverage is very good in the latter half of the period.

The locations of all MBTs/XBTs in the pentads 1950–1954 and 1990–1994 are shown in figure 4.2. In the 1950–1954 period, there is a high density of data off the east coast of America but in the more remote parts of the ocean, the sampling is very low. The coverage in the latter period is much more even and there are few large gaps.

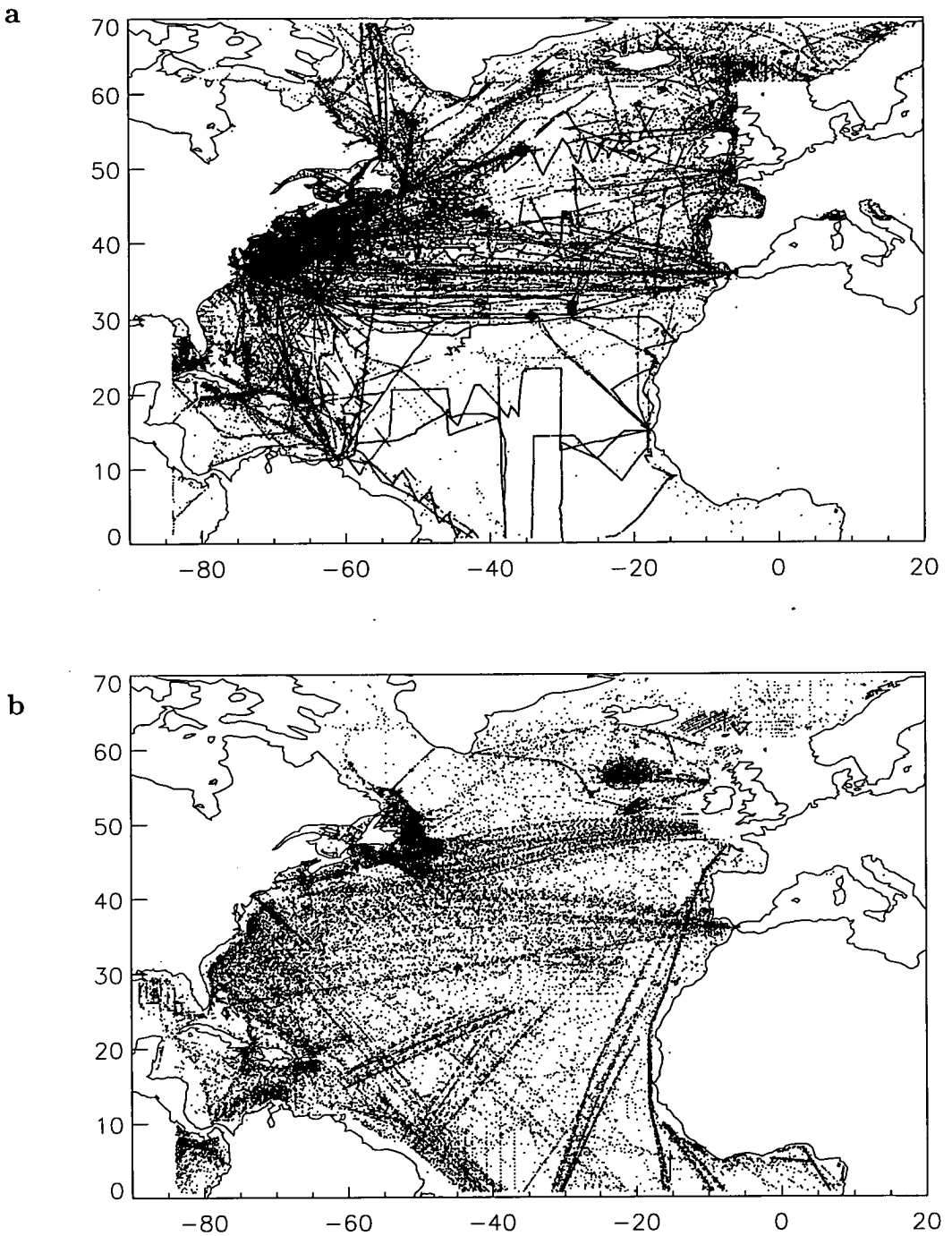

Figure 4.2: Distribution of MBTs/XBTs in **a)** 1950–1954 and **b)** 1990–1994.

The XBTs have temperatures recorded on the same standard depths used by Lozier et al. (1995) and Levitus (1994) in the upper 1500m of the ocean so no vertical interpolation needs to be performed to map on these levels. The next section describes the method of mapping by objective analysis.

4.2 The objective analysis mapping technique

Objective analysis is a method of producing fields on a regular grid from irregularly spaced data (Bretherton et al. 1976, Levitus 1982, Roemmich 1983, Levitus 1989b). This method has been used to produce all the fields of temperatures presented in this chapter.

The scheme is an advance on the basic mapping technique described in section A using differences between the observations and a first estimate of the field. The value at gridpoint A_{ij} is computed as the sum of the first guess G_{ij} and a correction, C_{ij}. The correction is calculated from all the data within the influence radius, R by,

$$C_{ij} = \frac{\sum_{s=1}^{N} Q_s w_s}{\sum_{s=1}^{N} w_s} \tag{4.1}$$

where Q_s is the difference between the observation at point s and the first guess at that point. The weighting function w_s is found from

$$w_s = \exp\left(-\frac{r_s^2}{(R/2)^2}\right) \tag{4.2}$$

for all points whose distance, r_s from the grid point i, j is less than the influence radius, R.

The process is usually iterative, employing successively smaller influence radii with each iteration and using the product of the previous iteration as the first guess. This still requires an initial field for the first guess of the first iteration. To produce his Climatological Atlas of the World Ocean Levitus (1982) used four iterations. The initial first guess field was created by zonally averaging the observed data in each ocean basin. The influence radii used in each iteration were 1541, 1211, 881 and 771km respectively.

The first guess fields used in the analyses presented here have been taken from the smoothed Lozier et al. (1995) climatological hydrography (see chapter 2). As this hydrography has good resolution and will be close to the product fields, only one iteration is required.

In the calculation of the value Q_s, the difference between the observation at point s and the first guess at that point, the nearest first guess grid point to point s is used. Employing interpolation to determine a better first guess at point s was tried but was found to produce no significant improvement.

This method is used to create both temperature maps at different depths and cross-sections to show temperatures at depths through the ocean along the line of a meridian or a parallel. These are mapped in the same way as the depth level maps, with XBT temperatures within a horizontal radius of each grid-point contributing to it. There is no smoothing between depth levels.

4.3 Comparison of XBT mapping with previous studies

There have been several previous studies of hydrography and interdecadal variability. It is worthwhile comparing their results with the analysis of bathythermographs presented here. In this way we can assess the effectiveness of the mapping and analysis techniques employed here and discover where these data and analysis methods can add to the previous investigations.

4.3.1 Comparison with Levitus (1989b)

Levitus (1989b) documented differences in temperature, salinity and in situ density in the North Atlantic between the pentads 1955–1959 and 1970–1974. This study covered the ocean between 250m and 2000m depth and was based on hydrographic casts, mainly Nansen bottles with some salinity/conductivity-temperature-depth (S/CTD) casts. These data allow the study of both temperature and salinity and extend to large depths but are very sparse which restricts the accuracy and resolution of variability studies.

Levitus (1989b) produced temperature maps for the pentads 1970–74 and 1955–59 at depths of 250m, 500m and 1000m by objective analysis. He performed one

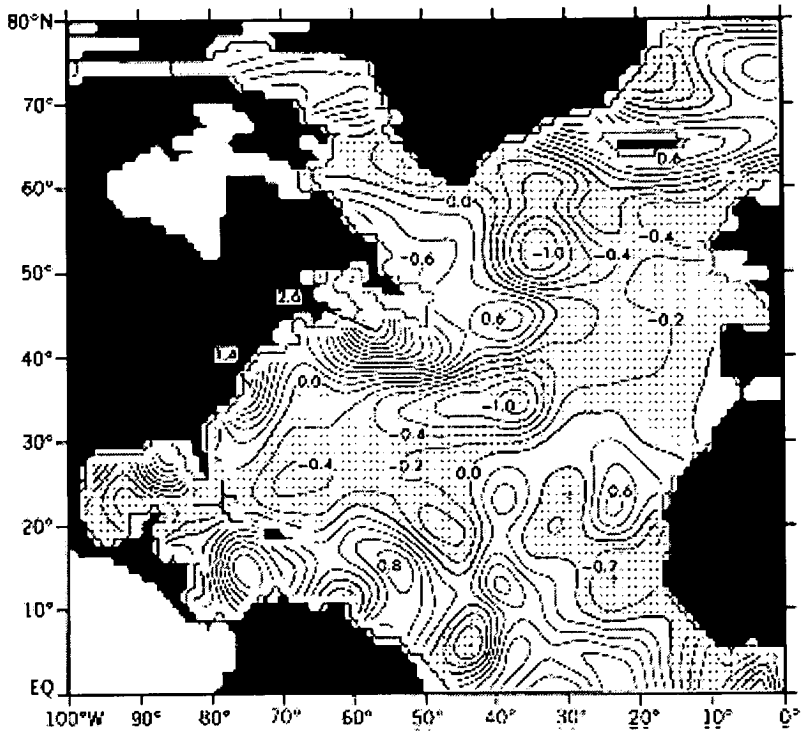

Figure 4.3: Mean temperature during 1970–1974 minus 1955–1959 at 250m depth from Levitus (1989b). Shading indicates negative values. Contours are at 0.2°C intervals.

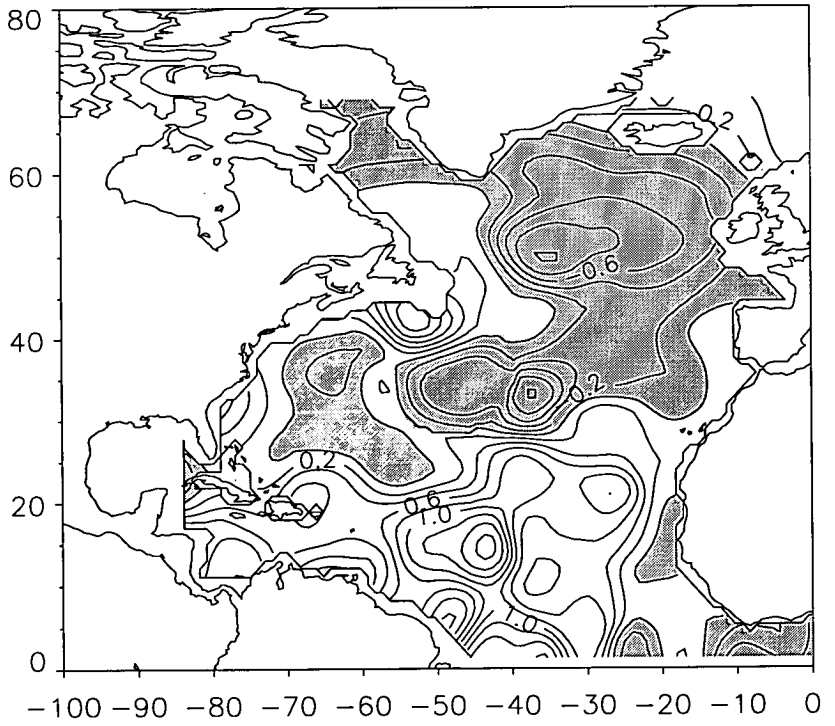

Figure 4.4: Mean temperature during 1970–1974 minus 1955–1959 at 250m from present study. Grey shading indicates negative values. Contours are at 0.2°C intervals.

iteration of the objective analysis procedure, using the climatological fields from Levitus (1982) as the first guess. The influence radius was the smallest used by Levitus (1982), 771km. Fields of temperature, salinity and density were made for each pentad. For each depth or section the field for 1955–59 was subtracted from 1970–74. Figure 4.3 is the temperature difference between the pentads 1970–74 and 1955–59 at 250m depth from Levitus (1989b).

Figure 4.4 shows the equivalent analysis from the data used here. The influence radius employed was the equivalent of 7° of longitude at the equator which is 778km. The smoothed Lozier climatology was used as the first guess but as it is the temperature differences between pentads that are produced, the first guess field is cancelled out. Therefore there is little difference between the analysis procedure used here and that used by Levitus. Any differences should be due to the different data sets used, primarily the use of XBTs. The 250m depth level has been chosen for comparison as at this depth more data from MBTs and XBTs are available.

On large scales, the two are similar. In both plots the latter pentad is cooler in the northeast with a band reaching south and west into the subtropical gyre indicated by dot or grey shading. The peak of cooling at 35°N 35°W is in the same place and of the same magnitude as is the peak at 50°N 35°W.

The two analyses also both show warming in the western subpolar gyre and along the eastern seaboard of North America. South of 20°N the two maps appear to be very different. However, they both contain considerable small scale noise-like variation, probably due to the scarce data in this area. It is perhaps not surprising to see these differences. Levitus (1989b) states that he does not consider small scale features as they may be based on only a few data, on erroneous data or on data taken in a small, transient feature such as an eddy which is not representative of the ocean during the five year period.

Figure 4.5 shows temperature differences in a latitude section across the North Atlantic at 24.5°N from Levitus (1989b) and compiled from the data used here. The overall agreement is very good. Both demonstrate the general cooling in the subtropical gyre and slight warming in the east of 30°W and below 300m. Differences between the data sets should be largest in the upper 500m where temperatures from XBTs and MBTs are available. Below this depth most data

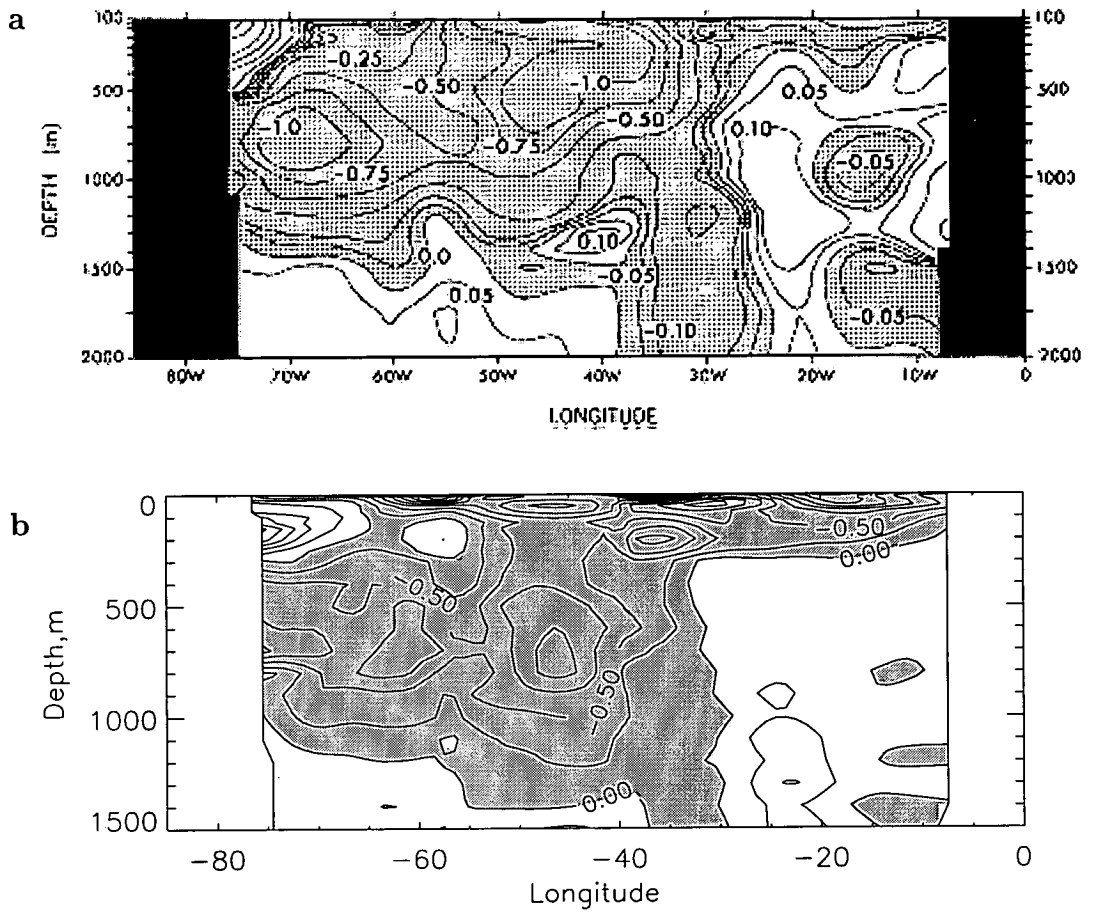

Figure 4.5: Mean temperature difference, 1970–1974 minus 1955–1959 along Latitude 34.5°N **a)** Levitus (1989b) **b)** new analysis. Shading indicates negative values. Contours are in °C. In **b** they are at 0.25°C intervals.

are from CTDs and bottles and should be based on the same observations. That there are some small differences indicates that the data are not exactly the same even at these depths. Differences between these two fields are all small-scale, such as the small warming region around 60°W which is also noticeable in figure 4.4 interrupting the cooling which is prevalent throughout most of the subtropical gyre.

North-south sections of temperature differences from Levitus and the new analysis are shown in figure 4.6. Again, they agree with the major features and discrepancies confined to only small areas. The large cooling region between 30 and 40°N is of similar magnitude and extends to the same depth. In the new analysis there is a small intense region south of 10°N with a minimum of −2°C. As it is

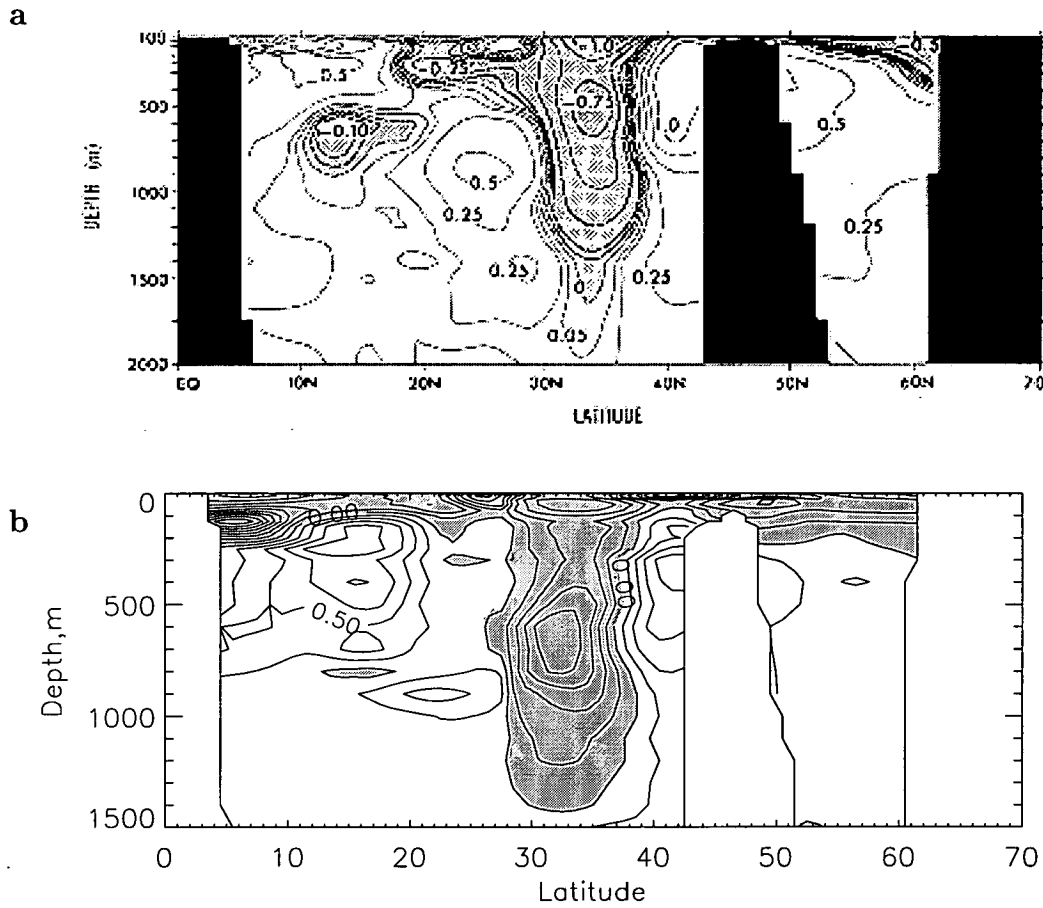

Figure 4.6: Mean temperature difference, 1970–1974 minus 1955–1959 along Longitude 49.5°W **a)** Levitus (1989b) **b)** new analysis. Shading indicates negative values. Contours are in °C. In **b** they are at 0.25°C intervals.

small and over a very narrow depth range it is almost certainly an example of an erroneous or unrepresentative observation in one of the pentads.

It is not possible to declare that one analysis provides the 'correct' representation of the difference between these two pentads. Both are just the best estimate of the true change from the available data. Since the analysis is essentially the same for each, situations where they do not agree are due to the differences in the data sets from which they have been compiled. The discrepancies between the examples shown give an indication of the kind of errors we can expect from the low coverage of the ocean which the observations provide. This comparison also demonstrates the spatial scales at which features can be assumed to be real. Inconsistencies between maps and sections from Levitus (1989b) and the

new fields are confined to small scales of typically $\sim 10°$. Features significantly larger than this are likely to be reliable. Figures 4.3 and 4.4 disagreed most in the poorly sampled tropical region of the North Atlantic, south of 20°N which may indicate that derived temperature fields in this region should be treated with some caution.

4.4 Decadal variation of subsurface temperatures

In this section, temperature data from bathythermographs and other subsurface temperature observations of the North Atlantic are examined to detect changes during the period between 1950 and 1994. Following Hansen and Bezdek (1996), variability is investigated by producing a chronology of temperature anomaly maps and cross-sections. Attention is concentrated on the upper ocean where data are more plentiful. We also wish to study, in particular, climatic changes below the layer directly influenced by interactions with the atmosphere, i.e. below the maximum depth of the winter mixed-layer.

Temperatures from the XBT measurements were objectively analysed to give fields of mean temperature during 5 year periods on depth surfaces, or mean temperatures over a range of depths, and along latitude and longitude sections. As the data are sparse, each field is produced by mapping five years of observations. The radius of influence chosen for these maps is 3° or 330km and the first guess used in the objective analysis procedure is the smoothed Lozier et al. (1995) climatological hydrography described in chapter 2. This influence radius is smaller than that used by Levitus (1989b) but as we are using bathythermographs as well as CTD and bottle casts, more data are available for this study. The 3° radius was chosen because for most of the period, it is sufficient to produce complete, smooth absolute temperature fields with good resolution. A small radius is also an advantage as it reduces the influence of erroneous data or data collected during a short lived but intense event which is not representative of the five year period. With a small smoothing scale grid points more than 6 degrees away can be considered truly independent. Thus, features whose scale is larger than this are likely to be significant events.

Temperature fields and variations are presented as anomalies from the mean

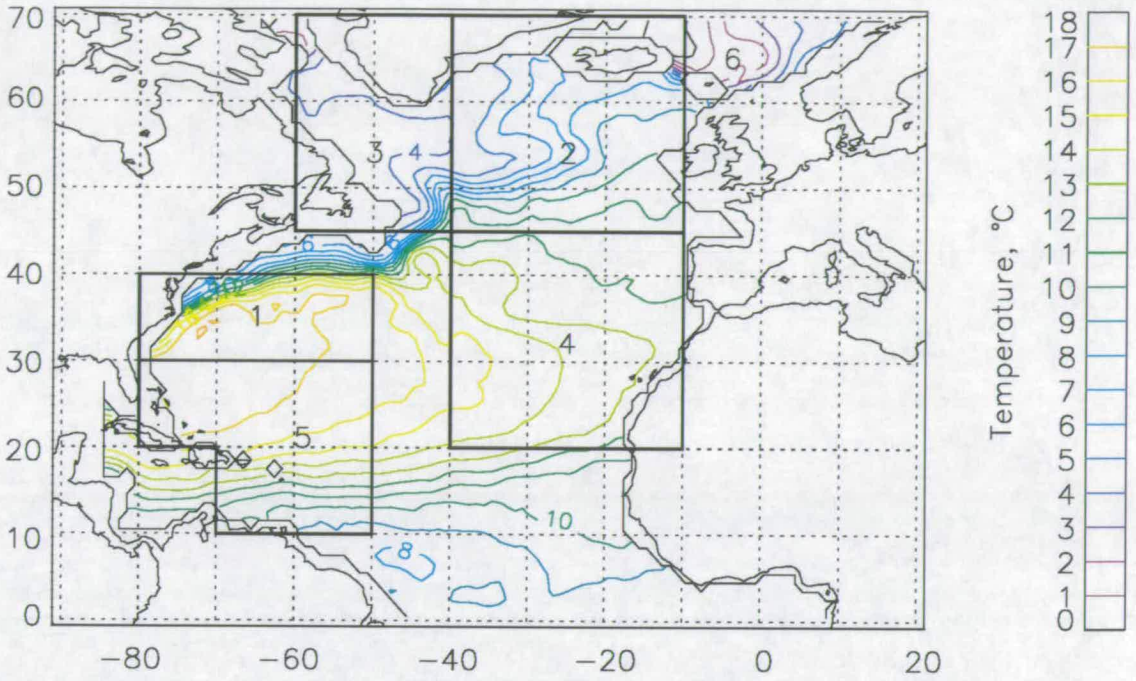

Figure 4.7: Mean temperature at 400m for 1950–1994. The numbered regions are areas from which time series of temperatures are calculated.

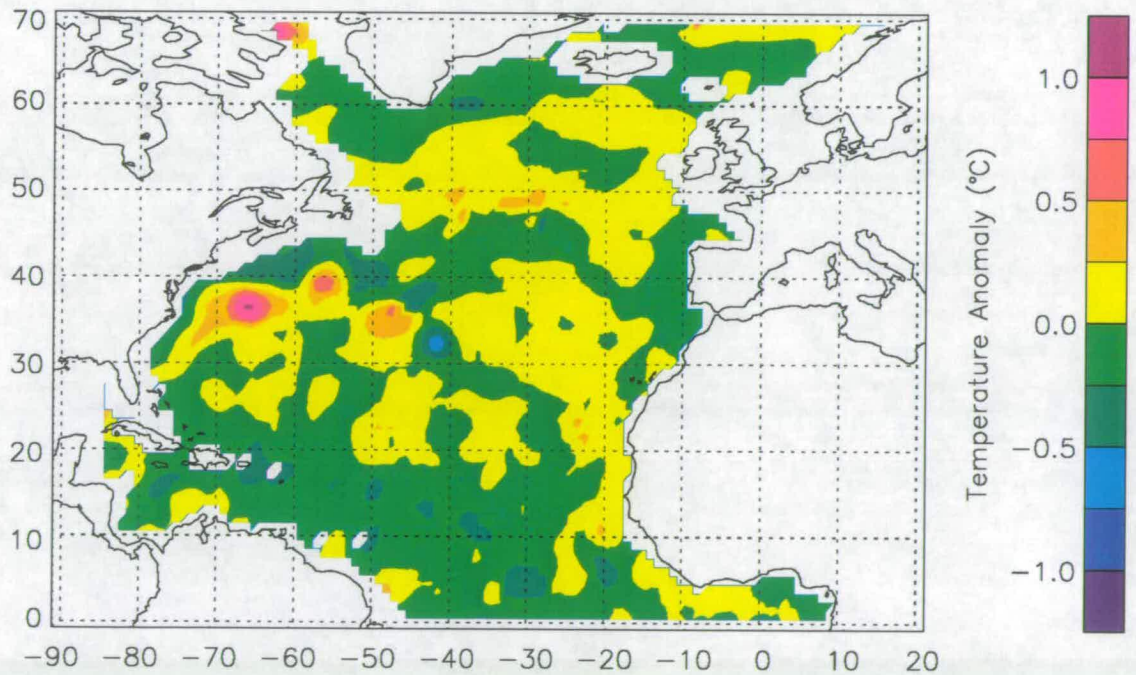

Figure 4.8: The difference between the average of nine separate pentad temperature fields and the field mapped straight from all data. The depth level is 400m.

temperature field over the 45 years from 1950 to 1994. Fields are produced for each five year period from which the 45 year mean is subtracted to give a field of temperature anomalies. To produce their climatologies, both Levitus (1982) and Lozier et al. (1995) collected all data available together and then averaged. However, as more data were taken during some years than others (figure 4.1), the resultant hydrographies are biased to those periods when data were more plentiful, such as the 1970s. To avoid this bias, in this study, data were objectively mapped to produce nine non-overlapping pentad means from 1950 to 1994 (1950–54, 1955–59 etc) which were then averaged to produce the 1950–1994 mean. The map of mean temperature at 400m depth is shown in figure 4.7.

Figure 4.8 shows the difference between the mean temperature field at 400m calculated from the nine pentads and the field calculated from objectively mapping all data from 1950–1994. Most of the large scale differences are small in amplitude, less than 0.25°C. The most noticeable features are along the line of the Gulf Stream which result from the meandering nature of the current. At 37°N 66°W, the unbiased mean is 1°C warmer than the 1950–94 mean. Figure 4.1 shows that the early seventies were the years most rich in data. At this time Taylor and Stephens (1998) report that the mean position of the Gulf Stream is abnormally far south which would result in cooler waters in this area. Levitus (1989b) also shows that the subtropical gyre was anomalously cold in 1970–74. The differences between the mean fields are consistent with a bias toward this period in the field mapped straight from all data.

Maps showing mean temperature over a range of depths were produced by first mapping temperatures at each level and then averaging over all the levels in the chosen range. Where there are no data contributing to a given grid point at any of the depths, the grid point is given a null value. Averaging over a number of depth surfaces will produce smoother maps as the effect of one erroneous temperature in a temperature profile is reduced.

4.4.1 Evolution of temperature anomalies between 300 and 500m depth, 1950–1994

Figures 4.9–4.11 show mean temperature anomalies averaged over the depths of 300, 400 and 500m. Each map shows the mean anomaly from a five year period.

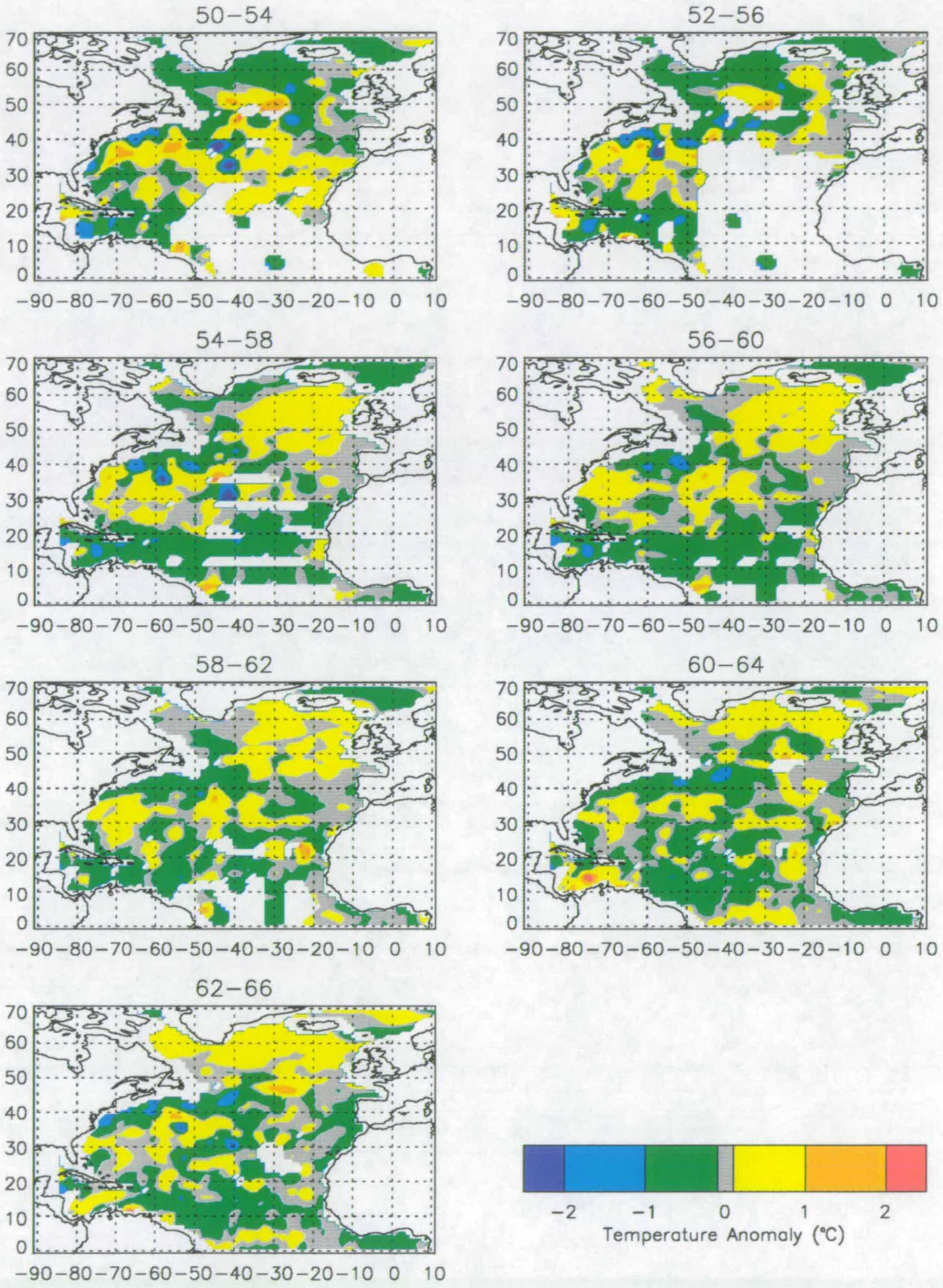

Figure 4.9: Mean temperature anomaly over the depth range 300–500m.

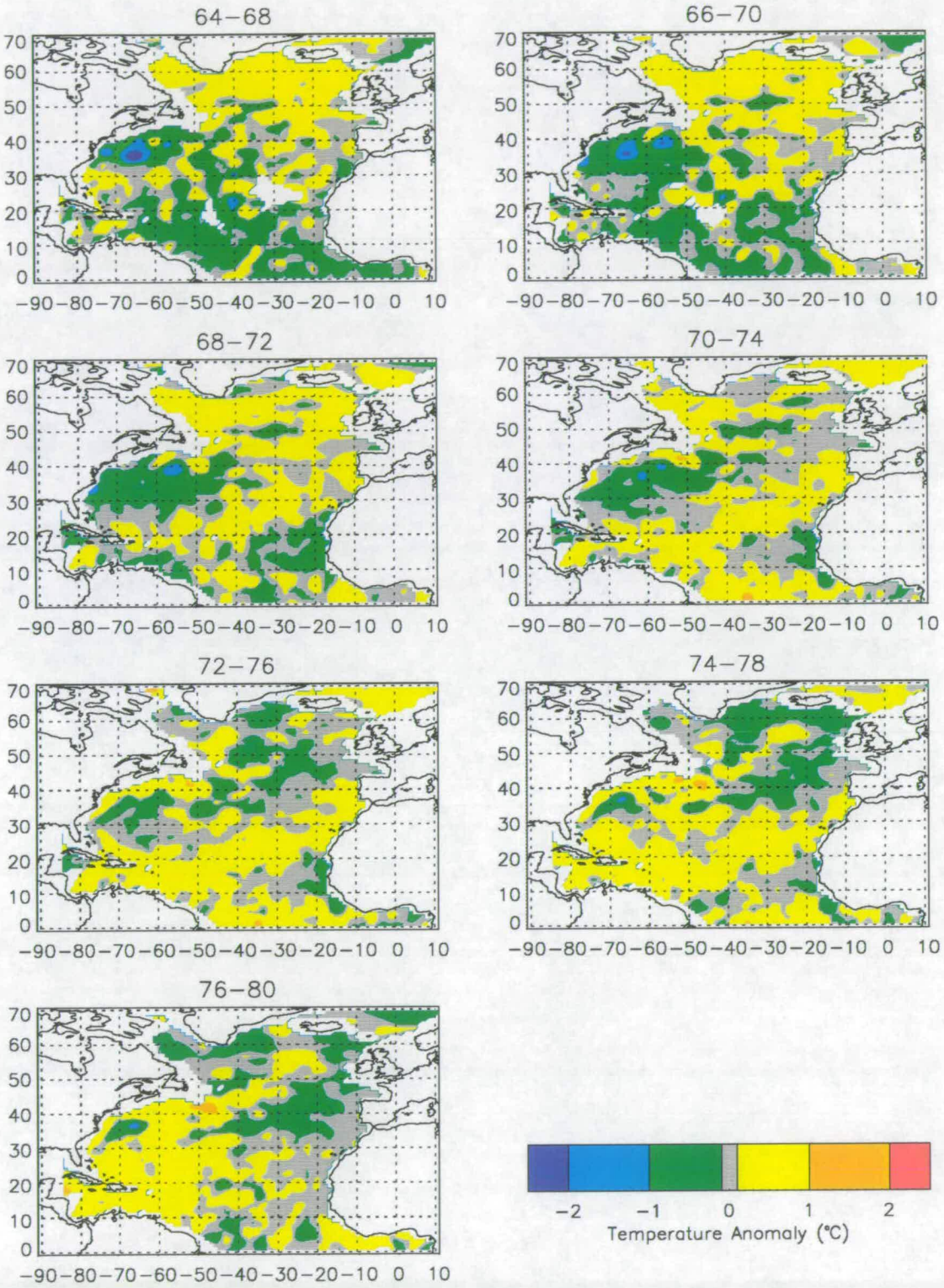

Figure 4.10: Mean temperature anomaly over the depth range 300–500m.

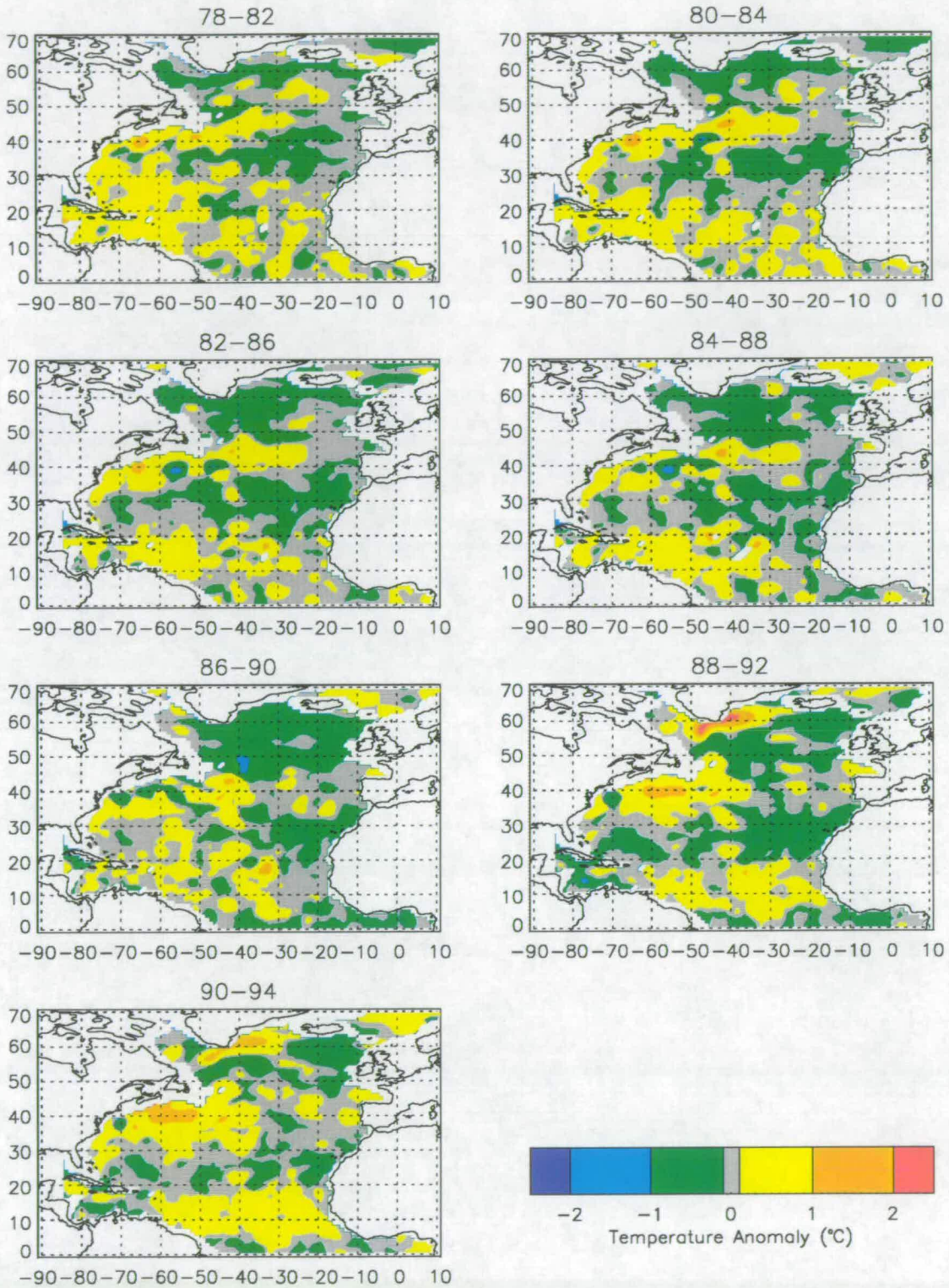

Figure 4.11: Mean temperature anomaly over the depth range 300–500m.

The starting times of maps are two years apart so each period overlaps both the previous and the next by three years. It is necessary to average five years of data to produce each map so that there are enough data for a complete, smooth map. Contour ranges have been chosen to emphasise large scale anomalies which may be quite small in amplitude. It is the development, evolution and progression of these large scale features that is of interest here. When water masses advect through the ocean they do not always continue at one level, hence maps of anomalies over a range of depths may help to track their progression more effectively. However, it is worth noting that the temperature anomaly maps shown in figures 4.9–4.11 are very similar to, though smoother than, maps of temperature anomaly at 400m only.

In the early years, data are very sparse, resulting in very large gaps in the anomaly maps. The early maps are also very noisy making it difficult to pick out large scale features and trends.

At the start of the period, 1950–56, although the maps are very noisy, the subtropical gyre appears to be occupied by a warm anomaly whereas north of 40°N the ocean is mostly cooler than normal. The 1954–58 map reveals that a warm anomaly was developing in the northeast. The tropics, south of 20°N, are cool across the whole width of the ocean at this time.

The subtropical gyre and most of the main body of the ocean cools over the next ten years. By 66–70 a strong cold anomaly has developed in the subtropical gyre, west of 40°W. The presence of this anomaly in 1970–74 contributes greatly to the large cooling from the 1955–59 pentad reported by Levitus (1989b). The tropics have remained cool overall.

The warm anomaly in the north persists and begins spreading into the Labrador Sea in 60–64. The warm anomaly becomes larger and in the 66–70 map occupies all the northern North Atlantic and a considerable part of the eastern ocean, north of 20°N and east of about 45°W. The evolution of this anomaly is very interesting. The northern section retreats westward, cooling first in the east then later in the Labrador sea. The anomaly possibly moves southward along the slope current where, in the 72–76 map, the ocean off the North American east coast has warmed. The warm anomaly also moves over into the Norwegian Sea, occupying the basin from 1968 to about 1978.

The eastern branch of the warm anomaly starts moving southeastward across the North Atlantic. In the anomaly fields from 68–72 to 74–78 the warm anomaly appears to propagate across the ocean, following the southern branch of the subtropical circulation until it occupies the western subtropical gyre in 76–80. At the same time the tropics have also warmed.

As the warm anomaly moves away from the north and east, the cold anomaly in the western North Atlantic moves northwest, along the path of the Gulf Stream and North Atlantic Current and into the northeast of the map area. This cool anomaly then spreads into the Labrador Sea. The 74–78 and 76–80 anomaly maps are approximately opposite in sign to the maps ten years earlier, 64–68 and 66–70.

The patterns during the 1980s are not so clear as in the 1970s, partly due to a reduction in data collection. Throughout the 1980s the cold anomaly has a firm grip on the northern region, appearing to be strongest in 86–90 and declining later. This anomaly also seems to extend into the eastern North Atlantic as the warm anomaly did previously. Although in most of the fields since 82–86 there looks to be a movement of the eastern cold anomaly across the Atlantic, the evidence that this is occurring is weak. This progression certainly is not as striking as the prior warm anomaly.

Throughout almost all the maps in figure 4.11 there is a band of warm water along the path of the Gulf Stream. This may be the result of a northward shift of the path of the Gulf Stream. Taylor and Stephens (1998) presents a gradual northward movement of the Gulf Stream throughout the 1980s and early 1990s (figure 3.4) although his results are confined to the current between 65 and 79°W. In the period 1988–94 a very intense anomaly develops on the northern edge of the subtropical gyre. The extent of this anomaly is not very large but it is more intense than any other anomaly between 1950 and 1994. This area is particularly well sampled so the feature is reliable. It is strongest between 50 and 65°W.

During this latest third of the period, the tropics have been mostly in a warm phase. This has the appearance of suppressing the westward propagation of the eastern cold anomaly in the 1980s and in 90–94 the combination of warm tropics and an expanding warm region in the northern subtropical gyre seems to squeeze out the insurgent cold anomaly.

In the 88–92 map a very warm anomaly is shown immediately offshore of southern Greenland, however, as this area is not very well observed (figure 4.2) it is probably the result of a few spurious data.

A notable feature in most of these maps is that there is a dipole effect, with the western subtropical gyre and the northern (north of 50°N) ocean occupied by anomalies of opposite sign. Patterns similar to this have been noticed by other authors, in SSTs by (Deser and Blackmon 1993), in hydrographic data (Levitus et al. 1994, Levitus and Antonov 1995) and also in coupled models (Zorita and Frankignoul 1997). This appears to be a very significant mode of oscillation. Often accompanying the northern anomaly is an anomaly of the same sign in the eastern Atlantic. The anomaly in the eastern region starts to emerge slightly after that in the north.

There is evidence that the anomalies propagate along the paths of ocean currents in a similar manner to SST anomalies reported by Hansen and Bezdek (1996) (figure 3.3). Although no connection in the timing of the SST anomalies and those at depth can be detected, the movement of the features are similar. Hansen and Bezdek observed SST anomalies travelling along the Gulf Stream and North Atlantic current and into the northeast. This can be seen in the 70–74 to 74–78 maps in figure 4.10. Northern anomalies can also be seen spreading into the Labrador Sea and possibly into the Norwegian Sea.

The other major track taken by SST anomalies in figure 3.3 is that crossing the Atlantic from east to west along the southern part of the subtropical gyre circulation. At 300–500m depth a warm anomaly is clearly seen to cross the ocean during the 1970s. This circulation is also similar in appearance to the oscillation in a coupled model of the North Pacific reported by Latif and Barnett (1994) (figure 3.5).

Figure 4.7 showed six areas which have been defined to analyse the temperatures as time series. The time series of mean temperature anomalies averaged over 300–500m within these boxes are presented in figure 4.12. Each point represents the mean temperature in a five year period, essentially the time series have been smoothed with a five year box-car filter. The mean of each time series is given and represented by the horizontal lines.

Box 1 covers the northern subtropical gyre. The early years are neither warm

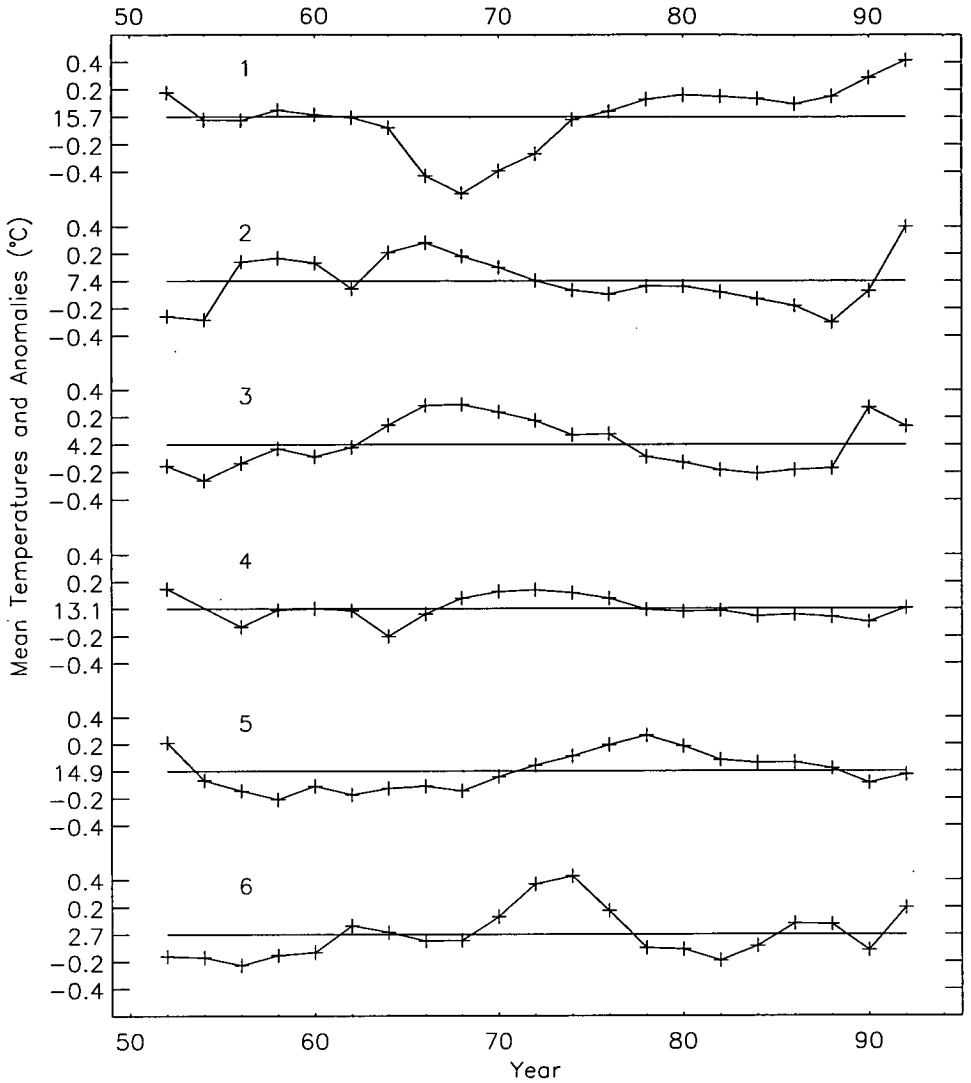

Figure 4.12: Time series of temperatures from the areas indicated in figure 4.7. The ordinate shows the mean temperature for the region and temperature anomaly. Temperatures are the mean for the depth range 300–500m.

nor cold, but in 1962 the intense cold period begins and lasts until 1974 after which the area is continuously warm to the end of the data.

Region 2 is in the northeast, down stream of area 1. Starting off cold, it rapidly enters a warm phase which lasts until 1972 just as the cold anomaly in region 1 is declining. This suggests the progression of the cold anomaly along the Gulf Stream and North Atlantic Current into region 2.

Region 3 represents the Labrador Sea and has a similar form to region 2, starting cold then warming from 1962 to 1976 and then entering a cold phase. The transitions from warm to cold periods occur after those in region 2 by approx-

imately 6 years. This is consistent with waters in region 2 spreading along the Irminger and east Greenland currents into the Labrador Sea.

Region 4 in the east Atlantic also lags behind region 2 and shows the same changes, although the anomalies are of a smaller amplitude. There is no strong current which would explain a transition of an anomaly from region 2 to region 4 but perhaps the same processes along the Gulf Stream and North Atlantic Current that set up an anomaly in the northeast also produces the eastern anomaly later by the slower return currents in the eastern basin.

In the anomaly maps of the 1970's a warm anomaly was clearly seen to traverse the Atlantic and move into the southern subtropical gyre. This is illustrated in the time series when a warm anomaly in region 5 develops after the one in region 4. The maps also suggest that a warm anomaly in the tropics may also play a role in the warming of region 5. The cold and warm anomalies in region 5 also seem to predate those in region 1, the northern subtropical gyre. This is also unsurprising and completes the cycle about the subtropical gyre.

Region 6 is a small area in the Norwegian sea. As it is small and there are relatively few observations made here, the time series is not very reliable. However, there is a very strong warm anomaly occupying the region between about 1970 and 1977 which is just after the warming of region 2.

The time series from regions 1 to 5 all show cycles of cold and warm anomalies which appear to have a period of approximately 30 years. Unfortunately, the time span of data records is not long enough to determine whether this is a repeating cycle or just a feature of this particular time span. However, it is worth noting that this oscillation appears to be present in all these regions, with different phase.

Throughout most of the ocean, the water masses in the depth range analysed here, 300–500m, are part of the permanent thermocline. The anomalies seen here may be caused by changes in the water masses in the permanent thermocline or, more likely, by the depression or rise of the thermocline. The properties of the water masses in this depth range are strongly affected by changes in the ocean above and by changes in circulation such as the spinning up or spinning down of the subtropical gyre.

To better determine the cause of temperature anomalies the depth structure of the changes must be analysed. In the next section, anomalies in the layer above,

100–250m, are investigated.

4.4.2 Evolution of temperature anomalies between 100 and 250m depth, 1950–1994

Figures 4.13–4.15 show temperature anomalies integrated over 100m to 250m. In parts of the ocean this layer is often within the mixed-layer and is thus directly affected by seasons and interactions with the atmosphere. Seasonal affects have not been accounted for in the analysis.

Overall, this level is similar to the 300–500m layer but there are some differences. The warm anomaly in the northeast during the late 1950s and 1960s is stronger in the upper layer but begins to decay away earlier (1966-70). The cold anomaly in the subtropical gyre develops earlier and becomes much more widespread. It also starts to spread earlier and, in contrast to the lower layer, is clearly seen to move across the ocean into the east and northeast.

The prominent warm feature in the lower layer that crosses the Atlantic from the east to the west is absent from the 100–250m maps. However the warming of the subtropical gyre in the 1970s starts earlier and appears to be stronger. At this time (70-78) the cold anomaly that has moved into the north is stronger and larger than below, occupying all of the north and most of the east and overlying the warm region below.

In the 1980s the cold anomaly still occupies the north and is stronger and larger than in the lower level. However it declines faster and is very small by 88–92. The warm anomaly in the subtropical gyre disappear in 80–84 but then begins to be re-established and grows until by 90-94, most of the North Atlantic is in a warm phase.

In a similar manner to the cold anomaly of 68-72, this warm feature developing in the subtropical gyre moves along the paths of the North Atlantic current into the northeast and along the return currents of the gyre into the eastern ocean. It appear that this path is stronger in the upper layer than the lower. It may be that as the waters move along the northward and eastward currents the deeper waters are rising into the upper layer.

Figure 4.16 shows time-series from the 100–250m layer in comparison with those from the 300-500m layer. Roughly, the lower and upper layer have similar

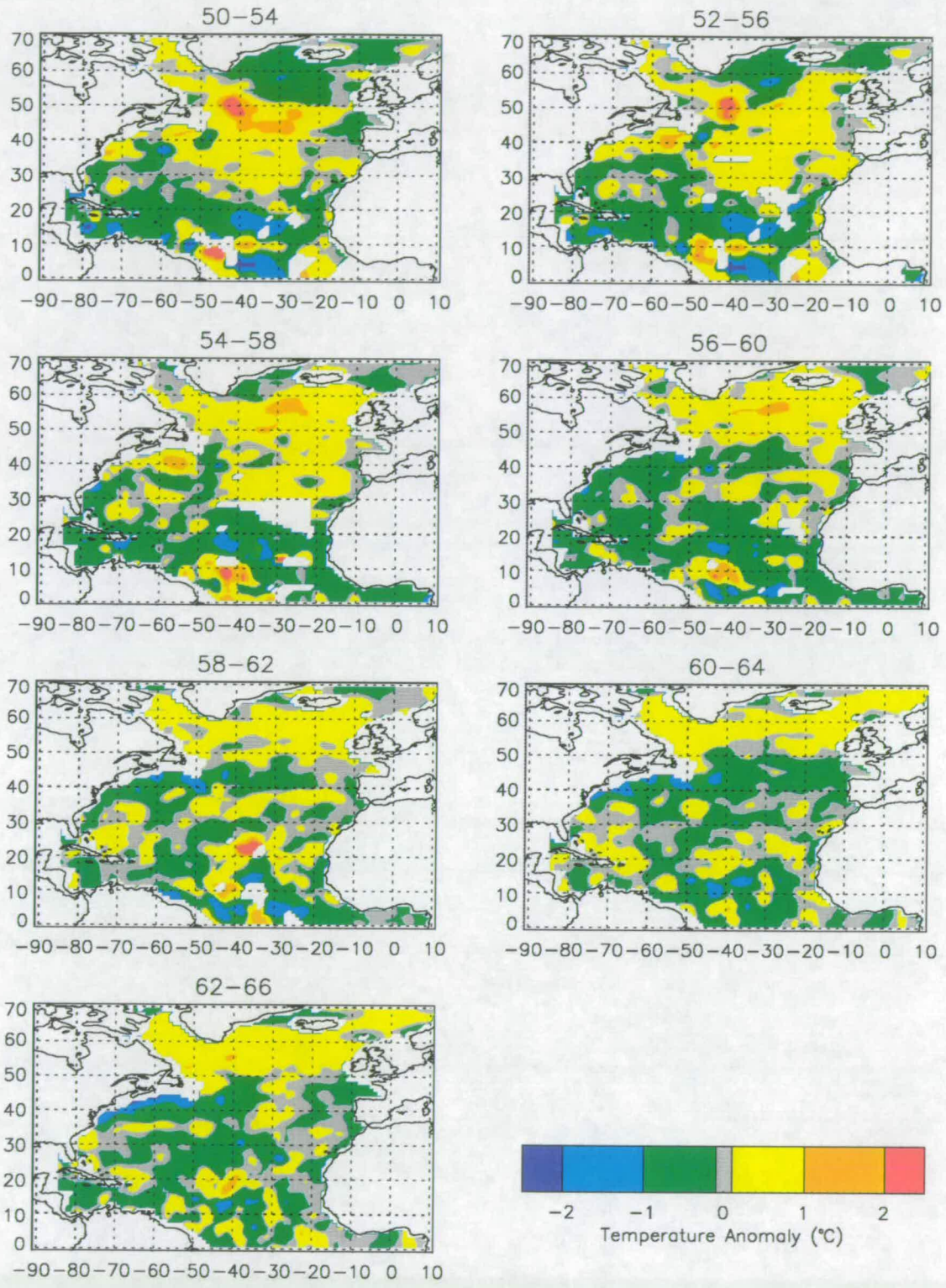

Figure 4.13: Mean temperature anomaly over the depth range 100–250m.

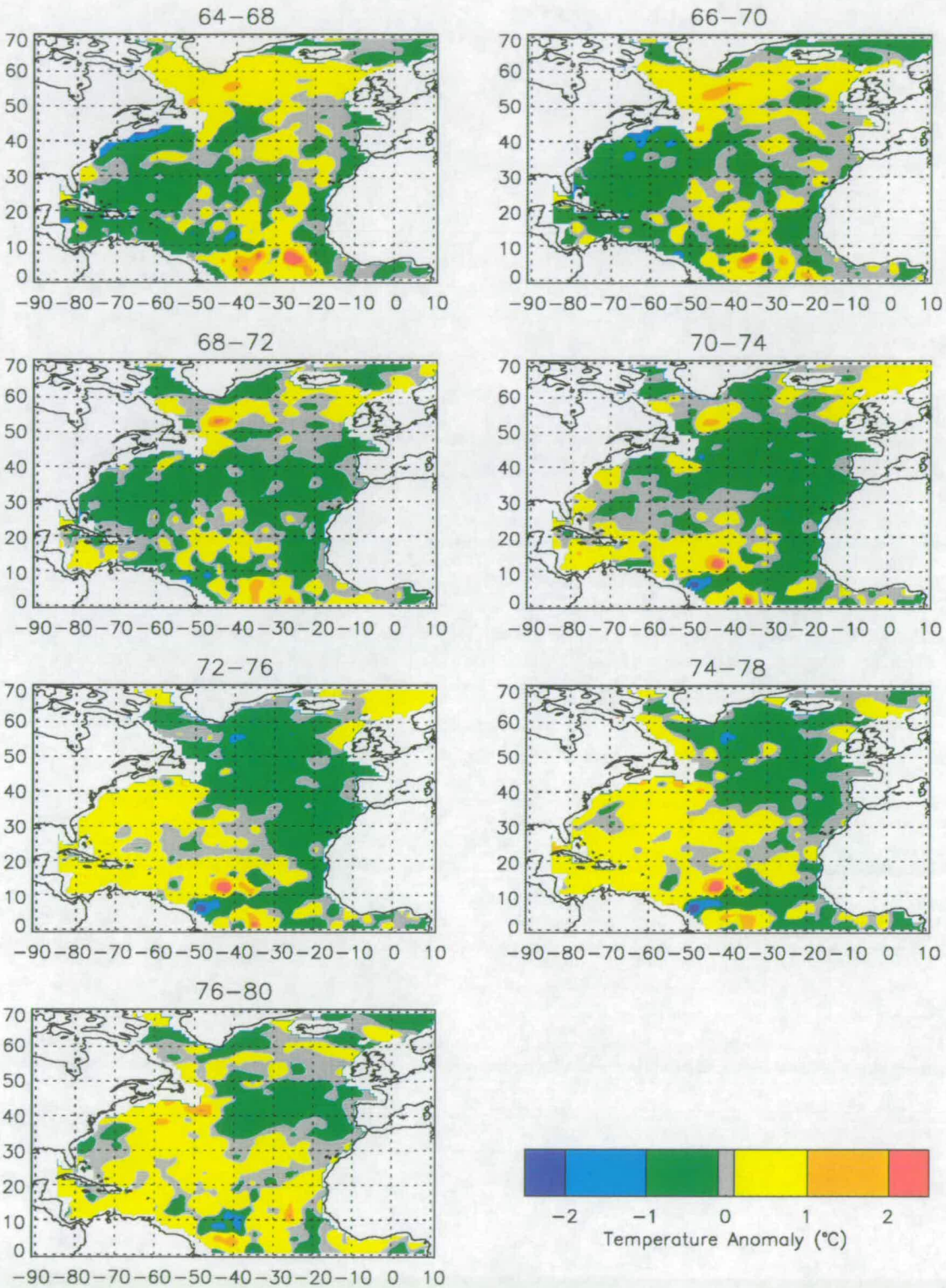

Figure 4.14: Mean temperature anomaly over the depth range 100–250m.

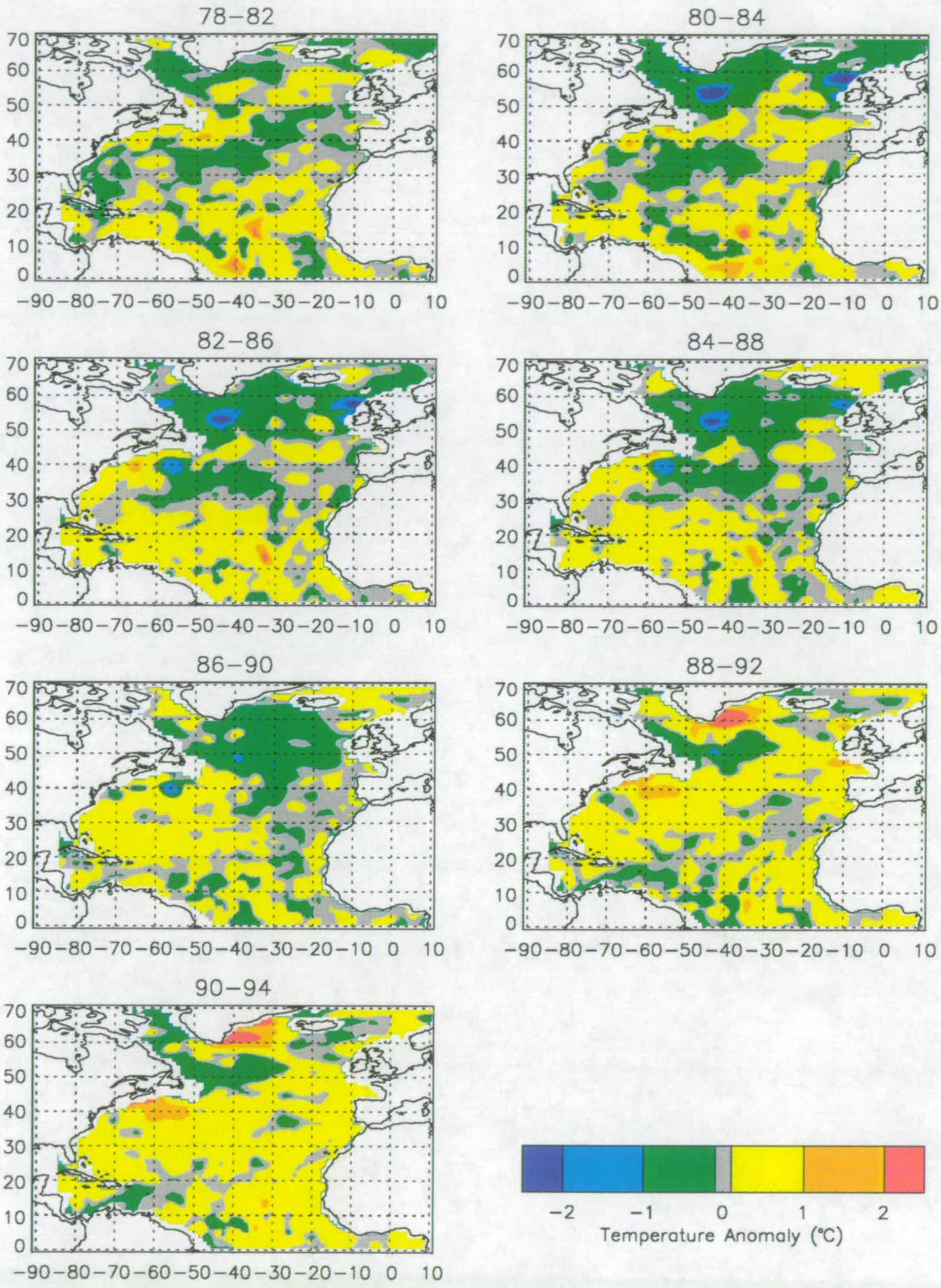

Figure 4.15: Mean temperature anomaly over the depth range 100–250m.

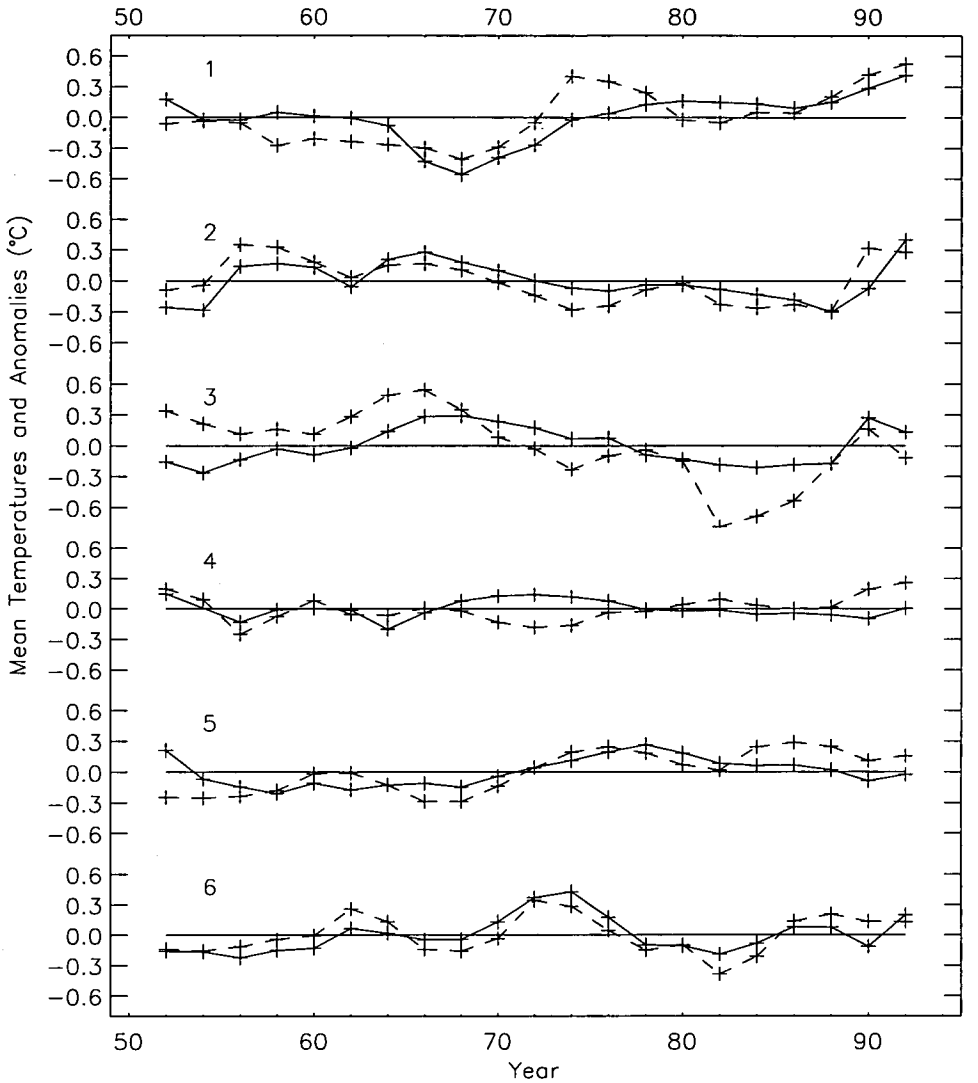

Figure 4.16: Time series of temperatures from the areas indicated in figure 4.7. The solid line is for the lower (300–500m) layer and the dashed line is for 100–250m.

patterns. Possibly the most striking feature of these graphs is that in the first three during the major change from one sign of anomaly to the other, the upper layer leads the lower by approximately 2-4 years. Unfortunately the time series are not long enough to determine whether this is always the case. However, it could be an important feature of the mechanisms which lead to the development of hydrographic changes.

Other differences between upper and lower layers present themselves in these time-series. In region 3 in the first ten years, the anomalies occupying each layer are of opposite signs but they are of similar shape. The cold anomaly in the 1980s

is very much more intense in the upper layer.

The two layers are reasonably similar in region 4, the eastern North Atlantic, except from 1968 to 1978 when the cold anomaly overlies a warm anomaly. The cold anomaly in the upper layer grows while the cold anomaly in region 1, the northern subtropical gyre, is waning demonstrating its progression.

Considering the small quantity of data in region 6 it is perhaps surprising that the two levels display very good coherence. However, this lends credibility to the time series. The waters here are poorly stratified so it is likely that anomalies will penetrate over a number of depths. Another feature of region 6 is that variations occur on shorter time-scales, of the order of about 15 years. It is obvious that there are more influences in this area than just the advection of anomalies from the North Atlantic.

4.4.3 Discussion of temperature anomalies

The above analysis indicates that large scale variations in subsurface temperatures do occur in the North Atlantic. It is more difficult, however, to determine the causes of the observed variability. The three main influences which may contribute to ocean variability are: direct forcing from the atmosphere, advection of temperature anomalies and changes in the ocean circulation.

Changes in ocean properties occur at the surface by air-sea interaction. The ocean surface is warmed or cooled by several actions. The ocean can gain heat from the atmosphere by sensible heat fluxes, lose heat by evaporation or gain heat from solar radiation. Hence, changes in air temperature will cause warming or cooling of the sea surface. The wind also has a very strong effect, increased wind stress leads to greater sensible and latent heat fluxes. Convective overturning caused by cooling and stirring action of the wind lead to the entrainment of upper thermocline waters into the mixed layer and a deepening of the mixed layer. The entrained waters then also influence the properties of the mixed layer.

As discussed in section 3.4, there have been several previous studies investigating the variability of sea surface temperatures and their relationship to atmospheric conditions (Bjerknes 1964, Deser and Blackmon 1993, Kushnir 1994). These studies show that on interannual time scales, sea surface temperatures reflect the overlying wind, stronger winds lead to cooler SSTs.

In this study, it is the subsurface ocean that is being investigated. Hence, for direct atmospheric forcing to have an influence on lower layers it must be transmitted in some way from the surface. This is often achieved by the formation of the mixed layer by convective overturning and wind stirring. The upper layer discussed earlier (100–250m) will be affected by the winter mixed layer throughout most of the ocean. Only in the tropics do mixed layer depths not reach this layer. The lower layer (300–500m) is unaffected directly by the winter cooling in most of the subtropical gyre and along much of the North Atlantic Current. However, along the northern boundary of the subtropical gyre, late winter mixed layer do sometimes reach depths of 400m or more and this is the source of the subtropical mode waters. In the north, mixed layers will deepen to at least the top of this layer in late winter. In the Labrador Sea, convection produces very deep mixed layers, sometimes to depths of up to 2000m (Dickson 1997).

The water masses in the permanent thermocline, below the deepest mixed layer, can only be changed by the atmospheric conditions at the time and location they are formed. Once they have been subducted into the thermocline they are isolated from the atmosphere and water properties are well preserved though the depth of each layer will change. This was described in section 1.1.3. It is difficult to determine from temperature data alone whether atmospheric conditions at the time of formation have altered over time thus changing the thermocline water masses. With the additional information of salinity it would be possible to determine whether water formation had changed the T-S relationships. However, previous studies (Roemmich and Wunsch 1984, Levitus 1989b, Bryden et al. 1996) suggest that T-S relationships do not change much within the subtropical gyre even over several decades and that most temperature anomalies can be explained in terms of vertical displacement of isopycnals.

It is at high latitudes, where winter mixed layers are deep and there is more convection that local atmospheric forcing will have the greatest effect on subsurface temperature. For example, Curry et al. (1998) related convection in the Labrador Sea with the NAO. To examine how much effect local atmospheric forcing has on the subsurface ocean would require simultaneous analysis of the atmospheric conditions in comparison with the observed oceanic variability in the water formation regions. Such experiments are underway in the Labrador Sea to examine

deep convection and its relation to atmospheric conditions (Marshall et al. 1998).

The advection or propagation of sea surface temperature anomalies has been proposed by some authors. Hansen and Bezdek (1996) showed the evolution of strong SST anomalies in the North Atlantic which appear to roughly follow the paths of the major ocean surface currents and Sutton and Allen (1997) revealed SST anomalies travelling downstream along the Gulf Stream and North Atlantic Current. The simplest mechanism for the propagation of anomalies is just advection by the normal circulation.

The time series of temperature anomalies from overlapping pentads (figures 4.9–4.11 and 4.13–4.15) suggest some propagation along ocean currents. On both levels it appears that anomalies which occupy the northeast then spread into the Labrador Sea. The path of this transition appears to follow the Greenland Currents, entering the Labrador Sea from the north. Hence these patterns are consistent with the advection of temperature anomalies. Advection around this path of the Great Salinity Anomaly in the 1970s was found by Dickson et al. (1988).

Along the line of the North Atlantic Current, anomalies develop downstream after one of the same sign has occupied the northern subtropical gyre. In the 300–500m layer the transition of subtropical gyre temperature anomalies along the North Atlantic Current is not so clear. It appears more to be a case of an anomaly in the northeast developing as the subtropical gyre anomaly declines – a distinct movement from one area to the other is not seen. However, in the upper layer, 100–250m, the cold subtropical gyre anomaly of the late 1960s does appear to spread into both the eastern basin and into the northeastern region. Again in the late 1980s and early 1990s the warm anomaly also spreads downstream from the subtropical gyre.

This suggests that temperature anomalies are only advected by the North Atlantic Current system in the upper waters. An anomaly that has propagated from the subtropical gyre northeastward in the upper few hundred metres may then be spread to deeper levels by convection due to deeper winter mixed layers at higher latitudes. This may also explain the lag between layers seen in the time series in figure 4.16.

The third mechanism which could lead to the observed temperature anomalies

is the effect of changes in ocean circulation. The subtropical gyre is a wind driven circulation, maintained by the trade winds on its southern edge and the midlatitude westerlies to the north. As discussed in section 3.2, the atmospheric sea level pressure fields and associated winds do vary significantly on annual and decadal time scales. The dominant mode of variability is the North Atlantic Oscillation, which in its positive state is characterised by stronger westerlies and trade winds than in its negative state (Figure 3.1).

The strengthening of the winds around the gyre will create greater Ekman flow into the centre of the gyre. This convergence of water will raise the sea surface height and also cause downwelling in the gyre centre. This then depresses the bowled isotherms of the gyre further, pushing warmer water downwards. In this scenario we would expect to see a warm anomaly in the subsurface subtropical gyre. With a depression of isotherms in the gyre, the geostrophic currents around the gyre would also increase.

In persistent periods of low NAO and winds, the subtropical gyre would spin down through friction and baroclinic instability. Isotherms would rise in the gyre giving rise to a cold anomaly in the thermocline. However, the mechanisms for spin down are different to spin up so the two phases may not simply be the opposite of each other. In the pentadal analysis we see cold and warm temperature anomalies in the subtropical gyre. These are compared and contrasted in more detail in the next section.

Another consequence of the increased gyre circulation is the faster flow along the Gulf Stream. This will bring more warm water northward from the tropics, which will result in warmer than normal water along the current. So with greater than normal flow, the waters downstream of the subtropical gyre could, after a time, increase in temperature. This could explain how an anomaly develops in the northeast after one of the same sign is seen in the subtropical gyre. Taking the case of the spin up of the gyre, the scenario could go as follows.

The North Atlantic Oscillation is in the positive phase, midlatitude westerlies and trade winds are increased. Isotherms in the subtropical gyre are depressed and circulation increases. The increased transport in the Gulf Stream brings warmer waters from the tropics northward. Eventually this increased flow travels down the North Atlantic Current and warms the northeastern Atlantic. This

warm flow is mostly in near surface waters. The deeper winter mixed layer in the northern North Atlantic spreads the surface temperature anomalies to deeper levels. For a negative NAO phase the weaker circulation would bring less warm water from the south, resulting in a cold anomaly downstream. This theory is consistent with the observations but, with so short a time span of data, it is impossible to determine its validity with much certainty.

Both Bjerknes (1964) and Kushnir (1994) relate changes in temperature of waters along the Gulf Stream and North Atlantic Current to the changing strength of westerlies in the atmosphere. They find that stronger westerlies do indeed lead to warm SSTs along the Gulf Stream, on multi-annual to decadal time scales, although they do not relate this to warming further downstream. If this does occur, it will lag the initial warming in the Gulf Stream and so may not appear in their analysis as relating to the changing wind stress.

The spin-up and spin-down of the subtropical gyre is a non-local effect of atmospheric forcing on the ocean and is a long term phenomenon. It will take several years of a persistent weather pattern to spin-up or spin-down the gyre so variability due to this mechanism will be most significant on decadal and longer time scales. In the data record there are two occasions which may be candidates for gyre spin up or spin down. The first is in the late 60s and early seventies and is a cold event, a spin down. In the late 80s and early nineties there is a warm anomaly in the subtropical gyre, a spin up. These events are examined in more detail in the next section.

4.5 Temperature anomalies in the subtropical gyre

The analyses of subsurface temperatures shown so far have revealed several events. Two of the strongest have appeared in the northern subtropical gyre and are particularly prominent in the first line of the time series shown in figure 4.12. The first is an intense cold anomaly which, at the 300–500m level, lasts from 1964 to 1974. The second is a warm event, starting in approximately 1988 which displays some of the strongest subsurface temperature anomalies observed in the data record.

Data are more plentiful in the later warm event at the depths where the anomalies are most significant and so it is easier to analyse in more detail and explore the evolution of the event more effectively. For these reasons, the 1988–94 warm event is described first and in more detail.

4.5.1 The warm anomaly in the Gulf Stream 1988–94

The temperature anomaly maps 4.11 and 4.15 show the development of a strong warm anomaly on the northern edge of the subtropical gyre. This is the most intense anomaly seen in the North Atlantic during this period. The appearance of a strong anomaly can also be seen in the time series of temperatures in region 1 in figure 4.16. The temperature in both layers increases from 1988 onwards and by 1992 is showing the highest temperature during the whole period. In this section the structure of this anomaly is studied in more detail.

Development of the anomaly at 500 to 700m depth

Figure 4.17 shows temperature anomalies integrated over three year periods and the depths of 500–700m. These are anomalies from the mean of 9 non-overlapping pentads from 1950–1994 as with the layers shown earlier. The anomaly is strongest and most prominent at these depths. The shorter three year periods have been chosen in order to better illustrate the growth and evolution of this feature. However, the use of only three year time periods results in the noisier appearance of the maps.

The 86–88 anomaly map in figure 4.17 shows no strong temperature anomaly in the subtropical gyre. There are several small anomalies but as only a small number of observations are available to produce each map, such small features are likely to be transient phenomena such as eddies.

The 88–90 map shows that there is definitely a warm anomaly building on the northern edge of the subtropical gyre, along the path of the Gulf Stream. It is strongest between 50 and 60°W. By 90–92, the anomaly has expanded and reached its peak intensity with a maximum temperature anomaly of 3°C greater than average. The strongest warming is still confined to a relatively small area between 50 and 65°W but more gentle warming has begun to spread further afield, particularly to the east.

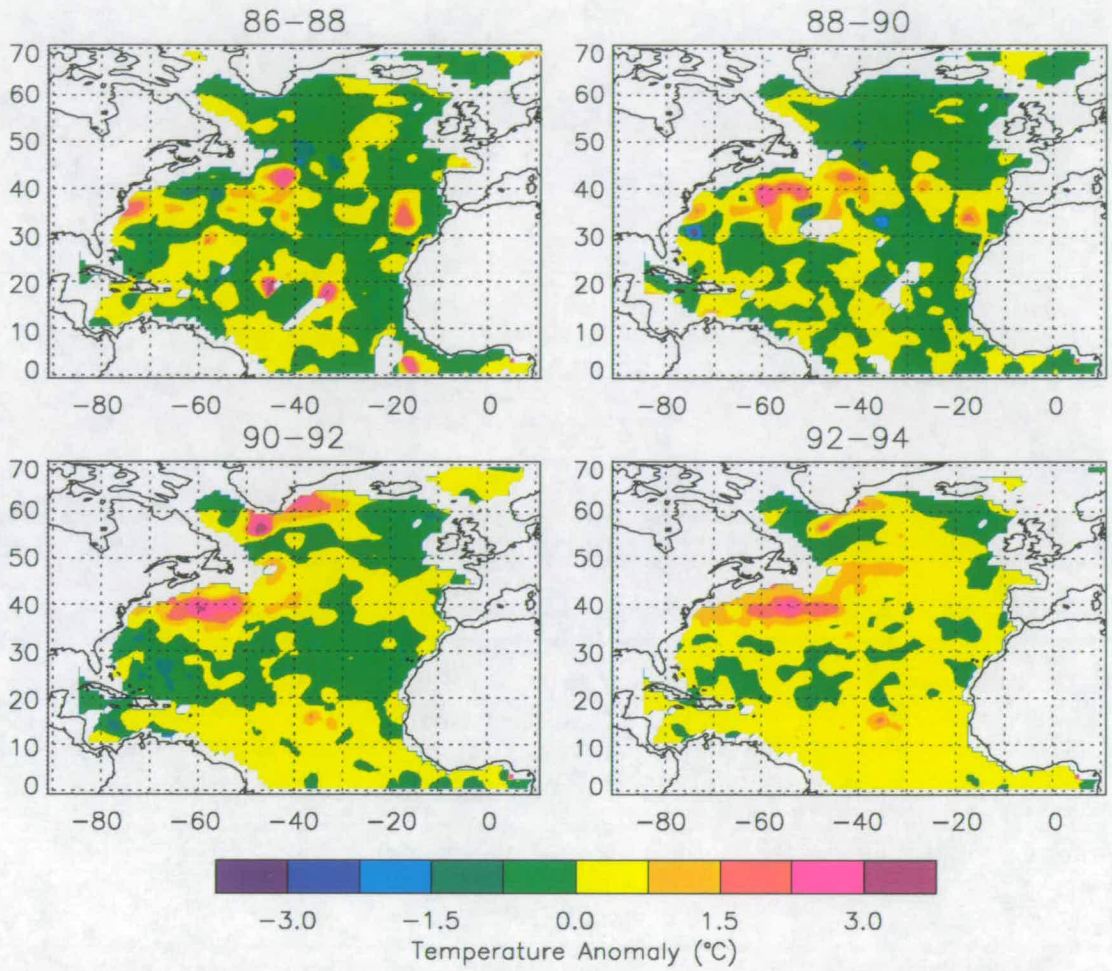

Figure 4.17: Temperature anomaly integrated over 500–700m depths.

The warm anomaly has continued to expand in 92-94 so that temperatures are more than 1.5°C warmer than average in a band centred about 39°N and between 45 and 63°W. A band of warming has also spread north and east along the path of the North Atlantic Current. In fact, by this time, the North Atlantic has warmed slightly all across the ocean at mid-latitudes, 30–50°N.

It is also interesting to note that coinciding with the warming on the northern edge of the subtropical gyre is also some warming to the south of the gyre, from 0 to 20°N.

Depth structure of 1988–94 warm anomaly

Figure 4.18 shows a longitude section at 55°W of mean temperature during the years 1988–94 and the 45 year mean. This section passes through the centre of

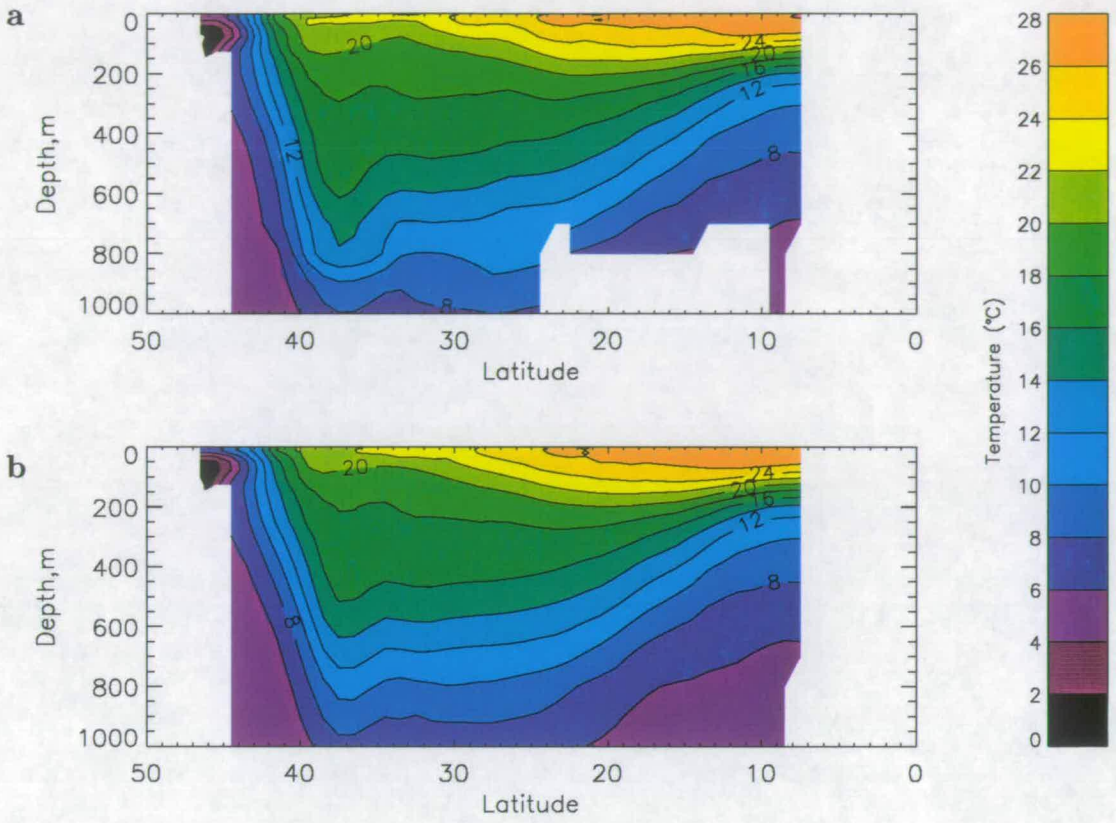

Figure 4.18: Temperature as a function of latitude and depth along 55°W. **a)** 1988–1994 and **b)** Mean 1950–1994.

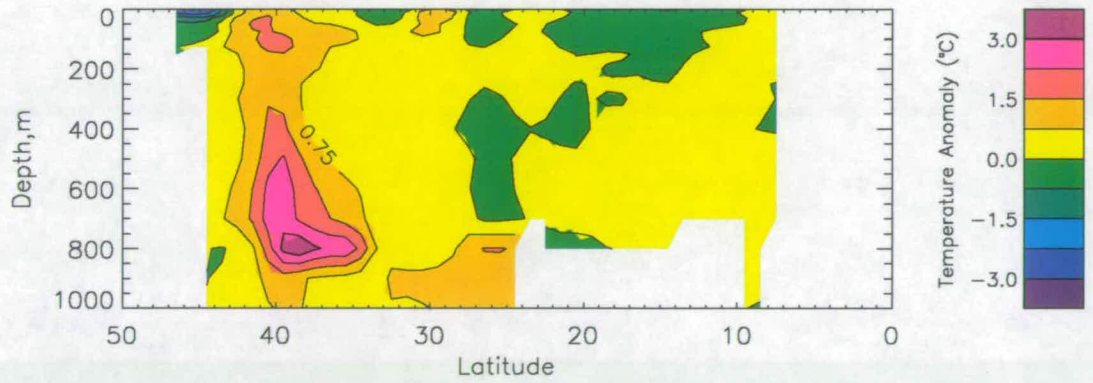

Figure 4.19: Temperature anomaly in 1988–1994 along 55°W

the anomaly south of Newfoundland. Figure 4.19 displays temperature anomalies along this section for 1988–94. Most XBTs in the data used here only report temperatures down to 700m, and data below that level are from the relatively few CTD measurements. Therefore mapped temperatures at 800m and below are not as reliable and may not give significant results.

The major anomaly can easily be seen in figure 4.19 as a vertical band of increased temperatures centred on about 40°N. The anomaly is greatest between 600 and 800m depth. At 800m depth there is a strong anomaly extending southward but as this is only seen at one depth it is assumed to be spurious. Examination of the distribution of data at this point reveals very sparse data and suggests that the mapping procedure at these points will be unevenly influenced by the anomaly to the north.

Comparison of anomaly sections with the temperature sections (figure 4.18) reveals that the most intense part of the feature is located in the steep temperature gradients of the front associated with the Gulf Stream. Isotherms are steeper in 1988–94 than in the average and the front has moved slightly northward. Hence, warmer waters have been introduced.

South of the Gulf Stream the isotherms have been considerably depressed in 88–94 creating much more prominent bowling of isotherms than on average. Isotherms have been displaced downward by up to 100m. In the top 300m extra waters of temperature between 18 and 20°C have been introduced. The sea surface temperature has also increased at this latitude (35-40°N). Below 300m, the thermocline has just been displaced downward. To the south of the bowled isotherms, in the centre of the subtropical gyre, the isotherms have also been depressed by smaller amounts.

The movement northward of the Gulf Stream is consistent with the findings of Taylor and Stephens (1998) (figure 3.4). They found that the position of the north wall of the Gulf Stream between 65 and 79°W was anomalously far north in the early 1990s. The evidence presented here suggests that the path of the current continues to be further north than normal further downstream as well. Taylor also found a good correlation between his Gulf Stream latitude index and a two year lagged North Atlantic Oscillation.

The steepening of the Gulf Stream front and deepening of isotherms indicates

an increase in velocity and transport of the flow of the current. The prominent bowling of isotherms to the south of the Gulf Stream implies enhanced recirculation here. It is clear that the intensity of the subtropical gyre circulation has increased in the years from 1988–94.

The North Atlantic Oscillation gradually increased in index from the 1970s onwards, becoming strongly positive in the late 1980s and early 1990s. This state of the NAO is associated with strong westerly winds in mid-latitudes. These act to spin-up the subtropical gyre (Sutton and Allen 1997, Grötzner et al. 1998, Halliwell 1998) creating greater transport in the Gulf Stream. This in turn will bring warmer waters from low latitudes northward, resulting in warmer SSTs and near surface waters on the northern edge of the gyre.

It would be very useful to examine data from 1995 onwards to investigate the further development of this event.

4.5.2 Cold anomaly in the Gulf Stream 1966–72

Figures 4.10 and 4.12 show that twenty years before the warm anomaly, the subtropical gyre was occupied by a strong cold anomaly. This started developing in the mid-sixties and continued several years into the seventies. Figure 4.16 indicates that the peak was in 1968 at both 100–250m and 300–500m levels. The years 1966–72 have been chosen to study this anomaly as this covers the most intense period and is an equivalent length to that chosen to study the 1988–94 warm event. Although the event appears strong in the time series it is not as intense as the later warm event.

Temperature and temperature anomaly sections along 55°W are shown in figures 4.20 and 4.21. The anomaly section demonstrates an intense band of colder temperatures in the same location as the 1988–94 warming with a maximum at about 500–700m. The structure of the anomaly is very similar, but opposite in sign, to the later warm anomaly.

Isotherms in the Gulf Stream front have become less steep and slightly more southerly. To the south of the Gulf Stream, where normally there is a small dip in the isotherms, isotherms have risen and are flatter through the central subtropical gyre. From these patterns, we can infer that flow of the Gulf Stream has lessened and the strength of the subtropical gyre decreased. This is confirmed by the

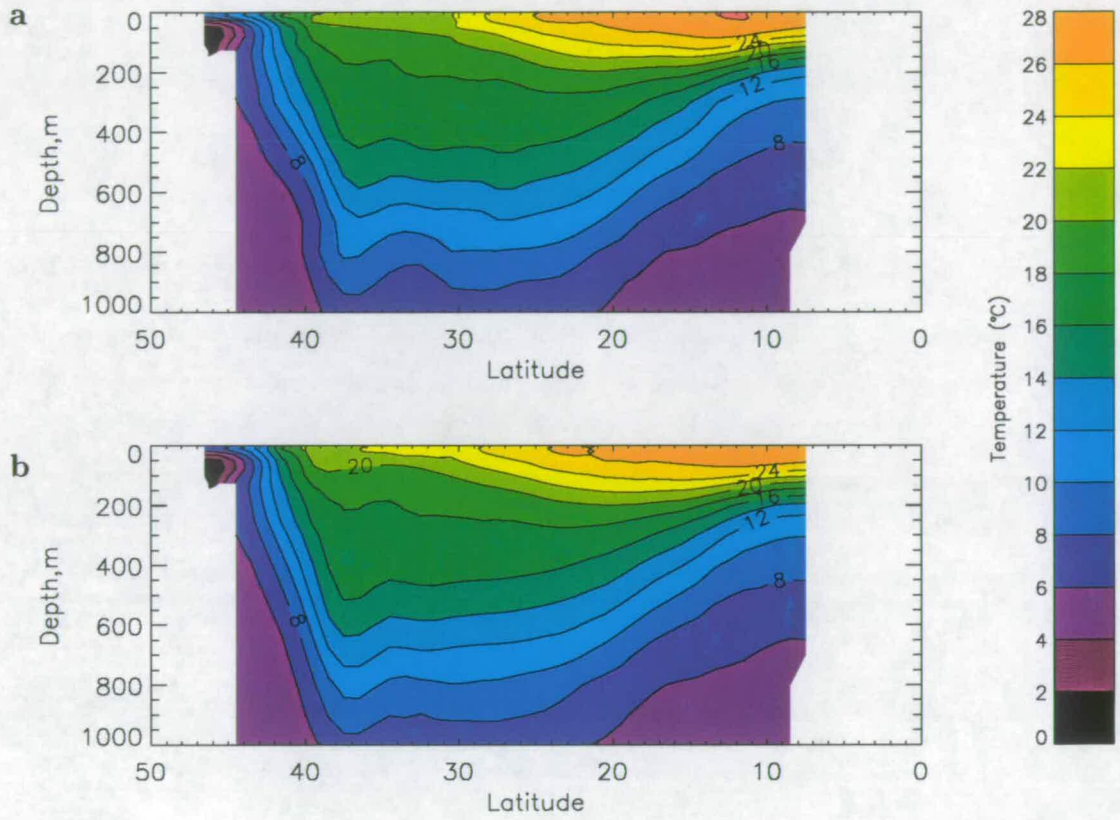

Figure 4.20: Temperature as a function of latitude and depth along 55°W. **a)** 1966–1972 and **b)** Mean 1950–1994.

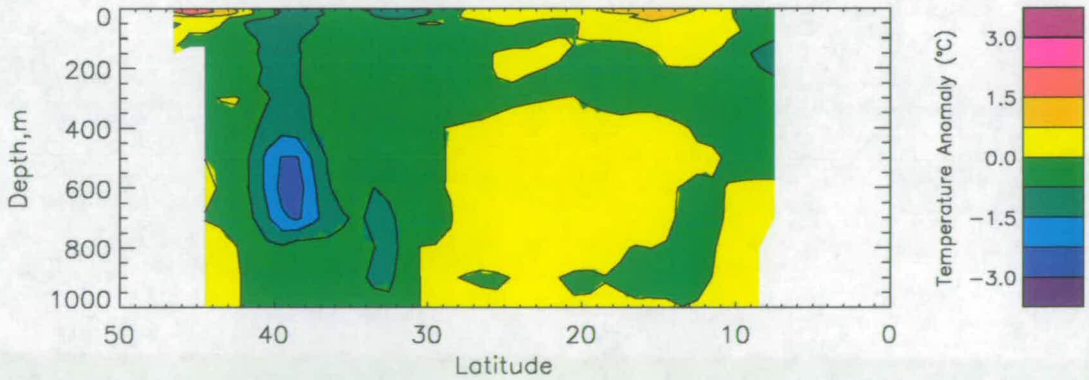

Figure 4.21: Temperature anomaly in 1966–1972 along 55°W

analysis of circulation during 1970–74 by Greatbatch et al. (1991).

The analysis by Taylor and Stephens (1998) shows that the Gulf Stream followed a more southerly path than average in the early 1970s consistent with the analysis presented here. This period in the mid-to-late sixties and early seventies is towards the end of a prolonged period of a low NAO state. The reaction of the subtropical gyre to lower westerly winds would be to slowly spin down the gyre, leading to a less intense Gulf Stream and shallower gradients. Surface waters brought north by the Gulf Stream travel more slowly in this period, have more time to cool and hence, we have cooler surface waters between 30 and 40°N.

The differences between the states of the subtropical gyre at 500–700m in 1966–72 and 1988–94 are illustrated in figure 4.22. The more limited data at these depths of the earlier period is reflected by the noisier appearance and gaps where no data is available.

In the later warm period, the isotherms in the Gulf Stream are much tighter and further north than in the cold period. There are also interesting differences in the centre of the subtropical gyre. In the cold period, the centre of the gyre is more homogeneous with the warmest area in the west. During the warm years, the isotherms have become elongated in a SW–NE direction with the warmest parts of the gyre at this depth in a band running parallel and south of the Gulf Stream. This suggests a changed pattern of circulation around the gyre, particularly the recirculation back from the Gulf Stream southward.

4.6 Summary and Discussion

Changes in the thermal structure of the upper water of the North Atlantic have been investigated showing considerable variation between 1950 and 1994. Producing a time series of temperature anomaly maps has enabled us to see the development and evolution of large scale anomalies.

The analyses presented here are consistent with other studies of hydrographic variability such as Levitus (1989b). Sections in the western North Atlantic similar to those in Molinari et al. (1997) were also produced (not shown here) and were found to be in very good agreement.

The investigation concentrates on layers below the influence of atmospheric

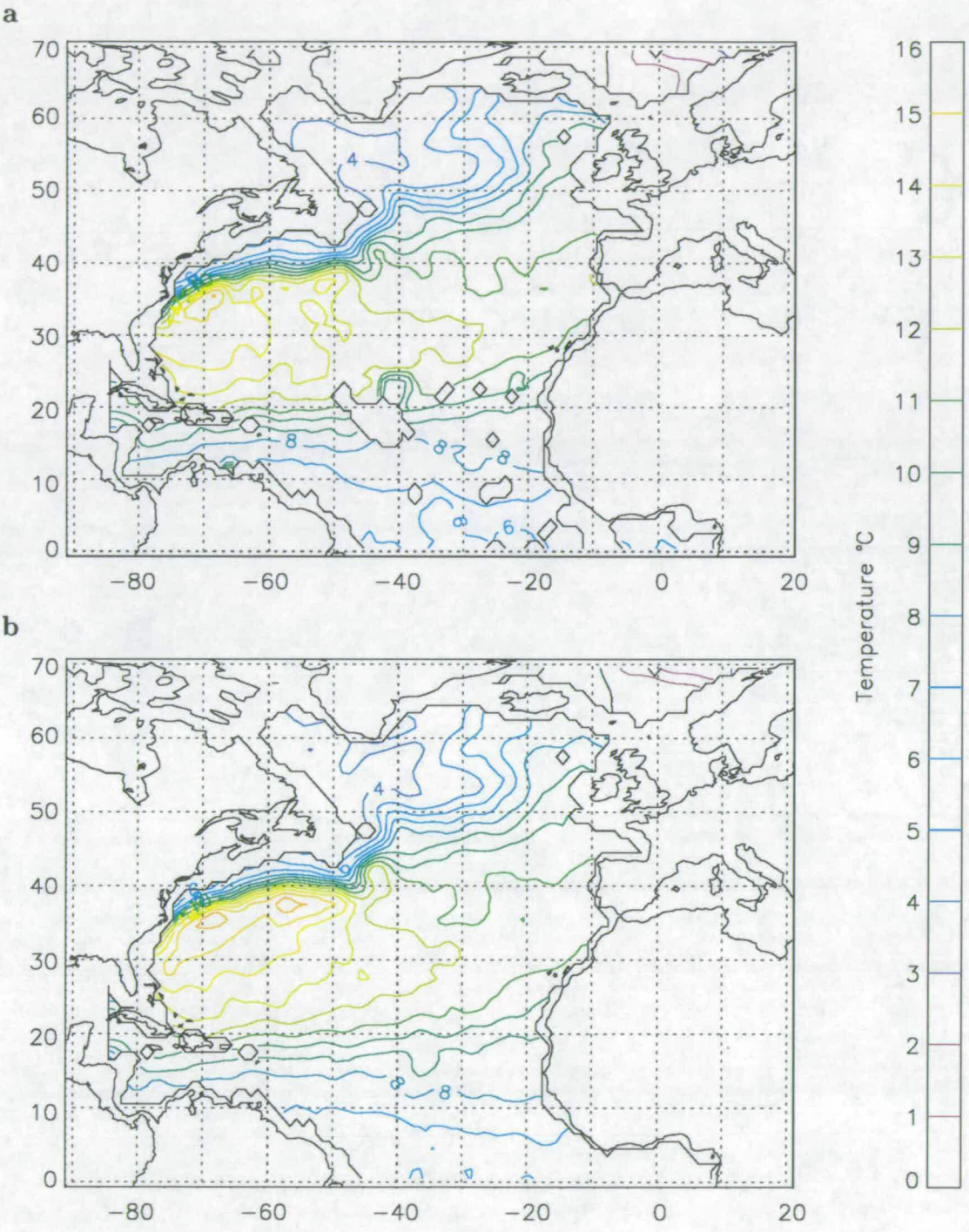

Figure 4.22: Mean temperature integrated over 500–700m. **a)** 1966–72 **b)** 1988–94.

interaction, 300–500m. While at some times in some areas there are no clear large scale anomalies, such as mid-latitudes 1950s, much of the time, strong, well defined anomalies occupy large regions. It was found that when the western subtropical gyre was occupied by an anomaly, the north, and also sometimes the east, was occupied by an anomaly of the opposite sign. This dipole pattern has previously been noticed in SSTs (Bjerknes 1964, Deser and Blackmon 1993, Kushnir 1994) and in hydrographic data (Levitus 1989a, Levitus et al. 1994, Levitus and Antonov 1995).

4.6.1 Propagation of anomalies

There appears to be some evidence of propagation of the anomalies. On several occasions an anomaly occupying one region appears to move along the path of an ocean current, to another part of the ocean. The major transitions that occur are; from western subtropical gyre to the northeast via the Gulf Stream and North Atlantic Current, from northeast to the Labrador Sea via the Irminger Current and following the circulation of the subtropical gyre.

It is not clear how these anomalies are propagated. The transitions are not smooth movements of anomalies like the SST anomalies seen in figure 3.3 from Hansen and Bezdek (1996). In the transition along the Gulf Stream, first an anomaly slowly builds in the subtropical gyre then as it declines in this region it moves northeastward and then builds again in the northeast. It may be better to consider this as the northeast anomaly switching on as the subtropical anomaly switches off rather than a movement of the anomaly. However, in the transition that occurred between 1968 and 1978 there does seem to be a movement of the cold anomaly along the North Atlantic Current.

The movement of anomalies into the Labrador Sea does appear quite natural. There are two good examples when this has happened. The first was a warm anomaly moving at around 1960 and the second, a cold anomaly in about 1976. Although resolution of these features is not easily relied on, the anomalies do appear to take the paths of the Irminger and Greenland Currents.

One of the most striking examples of propagation of an anomaly is that of the warm event in the 1970s which crossed the Atlantic from east to west on the southern fringe of the subtropical gyre. This shows a smooth transition of the

anomaly following the current path of the southern boundary of the gyre.

The mechanism by which the anomalies are advected is not clear. As with Hansen and Bezdek (1996) they travel slower than typical speeds of the currents. These depths, 300–500m, are for most of the North Atlantic in the permanent thermocline. Temperature anomalies here are often due to the displacement of isopycnal surfaces (Roemmich and Wunsch 1984, Levitus 1989b), with physical changes in water mass volumes above. In some way these displacements of the thermocline are transfered from one region to the next.

In the upper layer, the movements of anomalies are similar but appear to precede those in the lower layer. There are some other differences as well. The movement of anomalies along the Gulf Stream and North Atlantic Current is more clear but, interestingly, the warm anomaly in the deeper layer which moves westward in the 1970s is absent.

The time series (figure 4.12) show a cycle of about 30 years in period, but the series is too short to determine whether this repeats. The phases of the time series do support the theory that anomalies pass from one region to another by the current paths.

To conclude, there is evidence suggesting that temperature anomalies below the seasonally affected layer propagate over the ocean and that this propagation occurs along the major currents. There is a possible cycle in temperature of approximately 30 years.

4.6.2 Events in the subtropical gyre

Two strong events have been identified in the subtropical gyre of opposite sign. The first, where subsurface temperatures are anomalously cold occurred in approximately 1964–74 and the second a warm event in 1988–94, although it probably continues after the end of the data in 1994. The cold event was characterised by a shallowing of the gradients of the Gulf Stream front and rising and flattening of isotherms in the subtropical gyre interior. In the warm event, these features were opposite.

These anomalies may be caused by changes in the circulation of the subtropical gyre. Greatbatch et al. (1991) analysed the North Atlantic hydrographies produced by Levitus (1989a,b,c) for the pentads 1955–59 and 1970–74 and found

the Gulf Stream flow was 30Sv weaker in the latter period than the former. Geostrophic currents cannot be calculated directly from these data as we are only looking at thermal data. In order to determine geostrophic currents from hydrography, the density structure is required, which depends on both temperature and salinity. However, by looking at the isotherms, and considering that they will be of similar shape to isopycnal surfaces we can qualitatively infer changes in circulation and current strengths. Vertical displacements of isotherms are here assumed to be the same as displacements of isopycnals. This is a reasonable assumption as T and S properties have been found to be mostly conserved on potential density surfaces (Roemmich and Wunsch 1984, Levitus 1989b).

In the cold period, the Gulf Stream front is less steep than average and the isotherms in the gyre have risen, showing that the circulation has reduced. In the warm period the front is very steep, we have a distinct bowling of isotherms south of the Gulf Stream and deeper than average isotherms in the centre of the gyre. This implies that the gyre has spun-up.

The NAO index in figure 3.2 shows that the cold anomaly came at the end of long period of negative NAO index, which became very extreme. The mid-latitude westerlies would be anomalously light and hence the subtropical gyre would spin-down. The warm anomaly coincides with very high NAO index, hence the subtropical gyre has been spun-up by increased westerly winds and trade winds. Molinari et al. (1997) compared subsurface temperature changes in the western subtropical gyre with the NAO index. They found that warmer temperatures, produced by lowering of isotherms, coincided with periods of high NAO index and lifting of isotherms coincided with low NAO index. This supports the observations and comparisons with NAO presented here. Several other authors have also proposed that the gyre circulation responds to the NAO (Bjerknes 1964, Sutton and Allen 1997, Halliwell 1998, Grötzner et al. 1998).

One effect of the changing circulation is a change in the SST in the northern gyre. The increased flow of the Gulf Stream brings warm water more quickly from the tropics which, as it has less time to cool, results in warmer surface waters along the Gulf Stream (Bjerknes 1964, Sutton and Allen 1997, Halliwell 1998, Grötzner et al. 1998). This theory agrees with the observations of cooler SSTs in the northern gyre in 1966–72 and warmer SSTs in 1988–94.

The warm anomaly in 1988–94 is interesting for several other features as well. The bowling shown in figure 4.18 and the temperature contours in figure 4.22 imply that there has been a change in the pattern of the recirculation south of the Gulf Stream in this period. Although it is difficult to infer the currents from thermal data alone, the pattern of isotherms suggests a stronger recirculation immediately south of the Gulf Stream and the path of the currents is not an arc but is more parallel with the Gulf Stream.

Another interesting feature is the expansion of the warm anomaly along the Gulf Stream and North Atlantic Current shown in figure 4.17. This warm band is caused by a steepening of the front in these locations. It appears that this part of the current also responds to the increased westerly winds associated with a high NAO state, though later than further upstream.

It would be interesting to examine observations from after 1994 to see how the anomaly continues to evolve. After the earlier cold event, the subtropical gyre quite rapidly warmed and the cold anomaly moved downstream into the northeast. It could be that the warming of waters at 500-700m downstream is the start of a similar movement of the warm anomaly.

It is clear that there has been considerable changes in the temperature structure in the 45 years from 1950 to 1994. The available data are sufficient to give us some idea of the variations that have occurred but sometimes the scarcity of data has limited the scope of the investigation. As oceans play a vital role in the worlds climate, particularly the North Atlantic, it is important that any changes are continued to be studied.

Chapter 5

Assimilation of Altimetry with Climatological Hydrography

5.1 Introduction

In this chapter the method of combining a climatological hydrography, discussed in chapter 2, with altimetric measurements is described. The climatology is a description of the mean state of the ocean, giving values of temperature and salinity throughout the ocean. It has been built up from observations taken at many different times so does not represent the ocean at any particular time. Altimetric data reports the time varying state of the ocean but only gives us information about the height of the sea surface. The aim is to combine these two sets of data to recreate the hydrography at the time of the altimeter measurement.

Usually ocean general circulation models with assimilation are used to estimate subsurface fields, e.g. Ezer and Mellor (1997), Drakopoulos et al. (1997). The method used here is independent of a model so is much simpler and less expensive on computer time. The first sections of this chapter describe the altimetric data and the assimilation scheme.

The procedure is evaluated by comparing the pre and post-assimilation hydrographic data with in situ XBT measurements. The comparison of the results of assimilation with in situ data is useful for a number of reasons. Firstly, it will give us an idea how close to the real hydrography we can get by simply combining these two sets of data. It is also an evaluation of altimetric data, giving us an indication of how much the altimetry can be used to constrain an estimate of the subsurface water structure.

The evaluation of the scheme is also very useful to discover problems with the method and amendments that may improve the results. The results of the evaluation and anything that is learnt from applying the assimilation scheme in this way may be useful for its future use with ocean general circulation models.

This chapter describes the assimilation scheme, how it is employed and the experiments to evaluate the method. The results of the comparison with XBTs in the North Atlantic and Pacific oceans and results from amendments to the scheme are presented and discussed in chapter 6.

In this chapter, a brief overview of various assimilation techniques is given first. In section 5.4 the assimilation method used here is described followed by how it is used here to produce new hydrographic fields. Finally, the means by which the results of assimilation are compared with XBTs are detailed.

5.2 Methods of assimilating altimetry

Satellite observations offer unprecedented coverage of the oceans but can only give information about the surface. In order to build a picture of the three-dimensional ocean structure and currents, satellite altimeter measurements have been combined with ocean models. It is hoped that the surface height data together with the dynamics of the models can be used to determine the full three-dimensional fields and circulation.

Several methods have been employed to assimilate satellite altimetry into ocean models. The sea surface height reflects the density structure and currents throughout the water column beneath it so the assimilation has to relate sea level changes to changes in the entire water column.

Earlier methods used the simple approach of updating the model variable representing the sea surface height and allowing the model to transfer the information to deeper levels by the model dynamics between updates. This approach was used by Hurlburt (1986) referring to the method as 'dynamical transfer'. Berry and Marshall (1989) tested this method with a three layer quasi-geostrophic model but found that although the top layer update was transferred well to the second layer, transfer to the bottom layer was weak.

In order to reduce any initialisation shocks created by the sudden change in

surface layer properties, the technique of nudging was developed (Holland and Melanotte-Rizzoli 1989, Verron 1992, Blayo et al. 1994). This method introduces the observations over a period of time rather than all at once. Over several time steps the surface variable to be adjusted is pushed towards the value determined from the observation. Verron (1992) also found that this method improved the transfer to the lower layers. However, with multiple layers in the model, there will always be delay and inefficiency in spreading the information.

More advanced methods have been developed to use the observation to update all levels at the same time. In order to do this we need to know how to change the subsurface properties in order to make them consistent with the surface height observation. One approach is to use statistical methods to link variations in SSH to variations in the subsurface fields. This method has been used by Hurlburt et al. (1990), Mellor and Ezer (1991), Ezer and Mellor (1994) and Ezer and Mellor (1997).

Prior to the assimilation run, statistical relationships between sea surface height and subsurface properties must be determined. These must come from historical hydrographic observations or from the model itself. The statistical correlations are then used in the assimilation run to change the model variables in response to the surface observations.

Mellor and Ezer (1991) used this method with a high resolution primitive equation model of the Gulf Stream region in a twin model experiment with good success. Ezer and Mellor (1994) and Ezer and Mellor (1997) extended this research using the same model with Geosat data and found that the method was most effective at predicting temperatures in the permanent thermocline, with greatest success at 500m depth.

These methods are quite successful but as correlations are needed for each depth and grid point, they are computationally expensive. They also require a lot of historical data to compile the statistical correlations and at the moment, hydrographic observations are still sparse and models are not yet advanced enough to provide reliable correlations.

A different approach to this problem was proposed by Haines (1991). In response to a surface observation, model fields on all levels are re-initialised. The changes to model variables that are required are determined by calculations based

on dynamical grounds rather than statistics. He found that by specifying that potential vorticity should be conserved on all levels below the surface was enough to constrain the changes to a unique solution. This work was followed up using a more complex model by Haines et al. (1993). In twin experiments, it was found that the assimilation run would converge with the control run to a reasonable degree within a year.

This method was further developed by Cooper and Haines (1996) for use with a 21-level eddy-resolving Cox model. Water column properties are conserved, but displaced vertically in response to an observed sea surface height change in order to preserve an unchanged bottom pressure. In this method, potential vorticity is again conserved on isopycnal surfaces. This is the method which is used here with climatological hydrography and is described in more detail in section 5.4. In twin experiments Cooper and Haines (1996) found that deep ocean current errors were improved by up to 60% by assimilation after a run of one year.

Oschlies and Willebrand (1996) used a similar approach of re-initialisation with a two stage assimilation process. The first stage involves relating subsurface currents to the observed geostrophic surface currents (derived from SSH observations) by predetermined correlation coefficients. Temperature and salinity changes are then obtained from an inversion of the thermal wind equation, with local T-S relationships conserved. Hence, like Cooper and Haines (1996), water mass properties are conserved on isopycnals.

In the assimilation experiments described in this chapter, we will attempt to reproduce hydrographic fields representing the ocean at the time of the altimetric observations, a 'nowcast' as they are referred to by Ezer and Mellor (1997), by assimilating SSHs with a climatological hydrography. This model-independent method is computationally inexpensive in comparison to running a model to obtain fields.

A similar attempt to produce synthetic temperature profiles in the Gulf Stream region from altimetry without using a model was made by Carnes et al. (1990). Their method used similar techniques as Ezer and Mellor. First, statistical relationships between SSH and subsurface temperature were derived from all available temperature and salinity hydrocasts from the area around the Gulf Stream after it separates from Cape Hatteras. Statistical relationships were determined for

each month of the year to take into account seasonal affects. The synthetic temperature profiles were then produced from Geosat altimetry and compared with air-dropped XBTs. They found that this method was most successful in recreating the deeper structure of the Gulf Stream and eddies below the mixed-layer and seasonal thermocline.

5.3 Sea Level Anomaly Maps

The altimeter products used have been produced by the CLS Space Oceanography Division as part of the Environment and Climate AGORA EC project (ENV4-CT9560113). The maps are produced from sea surface height data on the satellite tracks and mapped onto a 0.5°x0.5° resolution grid using objective analysis techniques. There are maps of sea level anomalies every ten days from October 1992 to October 1996. These maps show anomalies from the mean ocean level for three years from 1st January 1993 to 31st December 1995.

Each map is calculated from the altimetry data on tracks by enhanced objective analysis methods. Each grid point is determined from the tracked data using spatial and temporal correlation functions. The spatial correlation function depends on latitude, as the satellite track separation decreases further away from the equator. The function has a scale of the order of 250km near the equator decreasing to 100km at a latitude of ±60°. The temporal correlation function is a Gaussian with an e-folding time of 15 days using all data within a window of ±10 days.

An example of a sea level anomaly map of the North Atlantic is given in figure 5.3a and for the Pacific, figure 5.6.

5.4 Assimilation Scheme

Cooper (1995) and Cooper and Haines (1996) describe a method to assimilate observations of sea surface height into ocean models. The assimilation method has to be consistent with observational evidence and known physical behaviour of the ocean features whose surface signatures are being observed. The assimilation scheme is based on the observed properties of mesoscale eddies described in section 1.1.5.

5.4.1 Sea Surface height and water column mass

As referred to in section 1.1.5, with certain assumptions, the variations in sea surface height measured by altimetry can be used to determine variations in the mass of the underlying column of water. As different density distributions in a water column may give rise to the same total mass, altimetry cannot, on its own, be used to determine the subsurface state. By utilising observations and known behaviour of ocean phenomena altimetry can be used to define a probable structure of the subsurface ocean.

Local time variations in sea surface height as measured by a satellite altimeter, Δh_s, can be expressed as a local variation in pressure Δp_s at a reference level, $z = 0$, by the hydrostatic relation,

$$\Delta p_s = g\rho\Delta h_s \tag{5.1}$$

where g is the acceleration due to gravity and ρ is the density of sea water.

It follows that the pressure variation at any depth in the water column below the altimetric observation, $\Delta p(z)$, assuming hydrostatic balance, is determined by

$$\Delta p(z) = \Delta p_s + g\int_z^0 \Delta\rho(z')dz'. \tag{5.2}$$

The term on the right is the effect on the pressure at level z of changes in the mass of the water column between z and the reference level.

For a water column of cross-sectional area A and depth H the time variation of its mass, ΔM, is determined by

$$\Delta M = A\int_{-H}^0 \Delta\rho(z)dz \tag{5.3}$$

which, with equation 5.2, becomes

$$\Delta M = \frac{A}{g}(\Delta p(-H) - \Delta p_s). \tag{5.4}$$

If we assume that pressure variations on the topography are small so that $\Delta p(-H) = 0$ the above equation becomes

$$\Delta M = \frac{A}{g}\Delta p_s. \tag{5.5}$$

Hence, altimetric observations can be used to constrain the total mass of a water column. With a free surface, the assumption of no time variations of pressure on

the topography is equivalent to assuming a constant mass of water between the free surface and the bottom of the water column.

5.4.2 Vertical displacement of water columns

We have established that sea surface height variations can be used to determine changes in the mass of the water column below. However, different water column density structures may integrate to give the same total mass. The aim of assimilation, whether in a model or in this case with a climatological hydrography, is to combine the *a priori* state of the ocean with altimetric observations to produce a good estimate of the new water structure.

Changes in total mass of the water column will arise from changes in its density structure, which is a function of temperature, T, Salinity S, and depth, z. The equation of state that relates these is represented by,

$$\rho = K(T, S, z). \tag{5.6}$$

We have used the Unesco equation of state to determine density throughout this work (Unesco 1981, Millero et al. 1980, Millero and Poisson 1981).

Following from the observations of mesoscale eddies and in order to conserve potential vorticity on isopycnals, changes in the density field are achieved by vertical displacement of isopycnals and the water mass properties on them. The displacement, Δh is uniform with depth. Hence, the change in properties on each depth level are be calculated by

$$\Delta T(x, y, z) = T(x, y, z + \Delta h) - T(x, y, z) \tag{5.7}$$

$$\Delta S(x, y, z) = S(x, y, z + \Delta h) - S(x, y, z) \tag{5.8}$$

$$\Delta \rho(x, y, z) = K(T + \Delta T, S + \Delta S, z) - K(T, S, z) \tag{5.9}$$

As the profiles are defined by values on discrete levels, the new values are determined by spline interpolation from the old profiles. Due to the dependence of the equation of state on depth, the density profile is calculated from the updated properties on the depth level rather than simply displacing it as with temperature and salinity. Pressure at each level can now be calculated with equation 5.2.

Figures 5.1 and 5.2 show examples of vertical displacement of a water column and the new temperature, salinity and potential density profiles. The potential

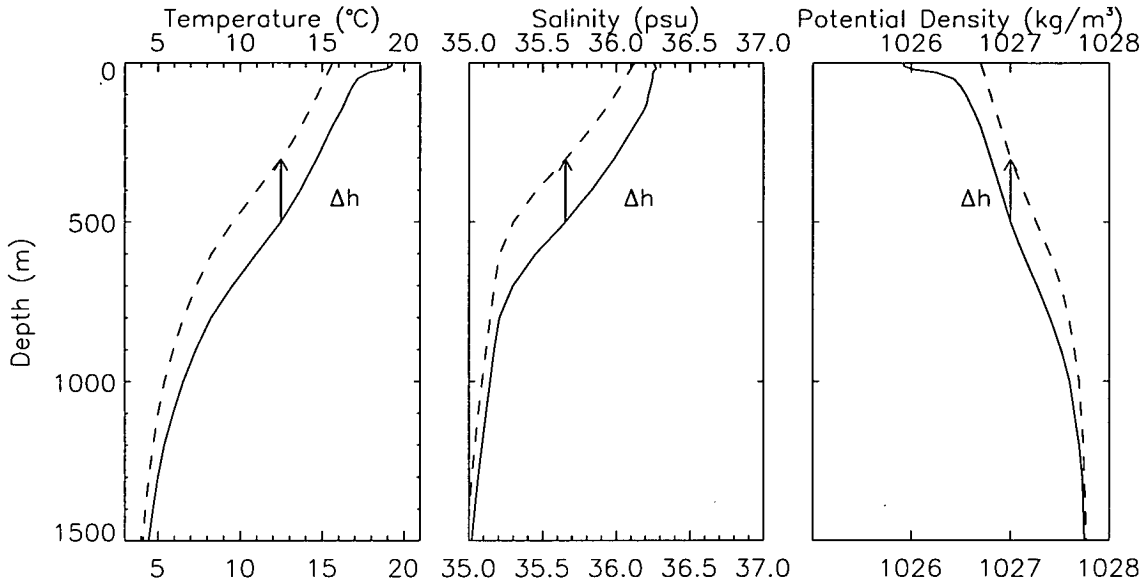

Figure 5.1: Vertical displacement of a water column in response to a low sea level anomaly. The solid line is the climatological profile and the dashed line is after displacement.

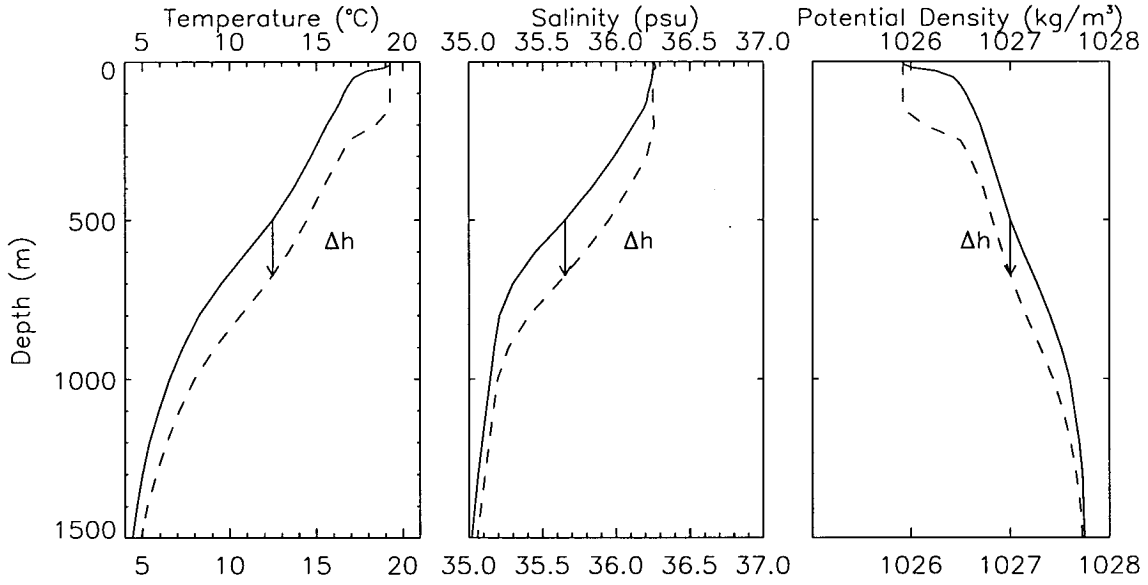

Figure 5.2: Vertical displacement of a water column in response to a high sea level anomaly. The solid line is the climatological profile and the dashed line is after displacement.

density profile is calculated from the T and S curves and referenced to the surface. When lifting, water is added to the bottom of the profile with the same properties as the existing water on the lower-most level. Water at the top of the column is lost as it is raised above the surface. As seen in figure 5.2, when the column is lowered, water is added at the surface with surface properties which leads to a deepening of the mixed layer.

The vertical displacement, Δh, is constrained by the condition that the pressure update on the deepest level is zero. The surface pressure calculated from the sea level anomaly is balanced by the change in mass of the water column by vertical displacement. Δh is calculated by an iterative procedure. Depending on the sign of the surface pressure, the water column is lifted or lowered by an estimated distance. The mass of the new water column is then calculated with equation 5.3. The bottom pressure change is then calculated from the change in mass of the water column and the observed surface pressure. Depending on the sign of this, the water column is again lifted or lowered by a distance half the previous estimated. As this procedure is iterated a number of times the bottom pressure change converges on zero and becomes negligible. The water column and surface pressure now satisfy equation 5.5.

The basis of this method, as developed by Cooper (1995), Cooper and Haines (1996), is that physical properties should be conserved when new data do not give direct information about these properties. Below the influence of the atmosphere, ocean processes are mostly adiabatic and water parcels move on isopycnal surfaces. Vertical displacement is therefore consistent with these physical ideals.

This method uses a local rearrangement of the water structure in response to an observed sea level anomaly. As described in section 1.1.5, mesoscale eddies are formed when meanders in the Gulf Stream (or another such current) pinch off, enclosing one water mass within another. Hence, the formation of an eddy involves a horizontal rearrangement of water. However, observations of eddies show that in the permanent thermocline, on isopycnal surfaces, the thickness of layers between isopycnals is nearly constant across an eddy (Cooper 1995).

In the ocean interior, ocean processes are adiabatic and mixing occurs along isopycnal surfaces. Therefore, properties vary slowly on isopycnal surfaces and this is seen in maps of temperature and salinity on potential density surfaces

(Lozier et al. 1994, Lozier et al. 1995). Since divergence and convergence of water masses are very small in geostrophic flow, the thickness of a layer between isopycnals is conserved. The horizontal movements of water that are involved in the creation of a mesoscale eddy are not large so, to a good approximation, the shape and structure of the thermocline are similar within and outside the eddy.

The main alternative approach to assimilation of altimetry is to use statistical relationships between observed sea surface height and subsurface water structure (Carnes et al. 1990, Mellor and Ezer 1991, Ezer and Mellor 1994, Ezer and Mellor 1997). These require large numbers of observations to determine the correlations which need to be collected in all parts of the ocean. Furthermore, as chapters 3 and 4 show, there is considerable long term subsurface variability in the ocean so statistical relationships determined from one period may no longer be valid for other years. The uncomplicated method of vertical displacement is therefore not only computationally cheaper than statistical methods but is also equally valid at all times.

Of course, there are limitations to this simple assimilation scheme. Where there are more dramatic changes in water masses and the structure of the thermocline is changed, vertical displacement will not perform so well. It is also likely that more subtle changes in the deep waters and currents will not be recreated by this method which is principally concerned with the permanent thermocline. In the experiments reported in this work, the performance of the assimilation method is assessed and modifications and limitations determined.

5.5 Producing new hydrographic fields

Cooper and Haines (1996) used simulated altimetric data in a twin model experiment. In simple terms, the difference between the observed sea surface pressure and the model surface pressure is used to adjust the water columns by vertical displacement.

Here, the assimilation is performed using sea level anomalies. We have altimetric data from the TOPEX/POSEIDON satellite from 1993-1995. The climatological hydrography is assumed to be a representation of the long term mean state of the ocean. It was therefore initially assumed that the mean sea level

observed by the satellite over the three years is consistent with the climatological hydrography. Thus, a sea level anomaly observed at a particular position reflects a change from the climatology of the structure of the water column below the observation.

As described in section 5.3, the altimetric data is in the form of sea level anomaly maps every ten days. The aim is to assimilate one of these fields with the climatology to give hydrographic representation of the ocean at that particular time.

The climatology is mapped onto a one-degree grid with vertical profiles at the centre of one-degree boxes. The sea level anomaly maps have half degree resolution with data at the centre of half-degree boxes. Thus, the location of a climatological profile is at the centre of a square of four SLA data points. The SLA at the position of the profile is determined by averaging the four surrounding sea level anomalies.

Figure 5.3 shows a typical sea level anomaly field from TOPEX/POSEIDON and the vertical displacement produced when it is assimilated with the smoothed Lozier hydrography. As can be seen, there is considerable spatial variability, particularly concentrated around the Gulf Stream region, reflecting the eddies and meanders associated with this current. Further downstream in the current, the activity continues but declines in magnitude as the current splits, spreads out and weakens.

The rest of the ocean is less active. In the tropics there are variations in sea level on larger spatial scales but these are of smaller magnitude than in the strong currents. North of the North Atlantic Current, in the Labrador Sea and to the south of Iceland, the variations in sea level anomaly are small.

Figure 5.3b shows the resultant vertical displacement after the assimilation of the SLA field with the smoothed Lozier hydrography. A positive sea level anomaly produces a lowering of the water column and is indicated by negative displacement on the figure. It can be seen that the vertical displacements are of opposite sign to the SLAs. In the tropics the sea level anomalies are accompanied by only small water column displacements. Conversely, in the far North, relatively small sea surface height anomalies have produced very large displacements.

Figures 5.4 shows cross-sections along Longitude 43°W of temperature through the smoothed Lozier hydrography before and after assimilation. The original

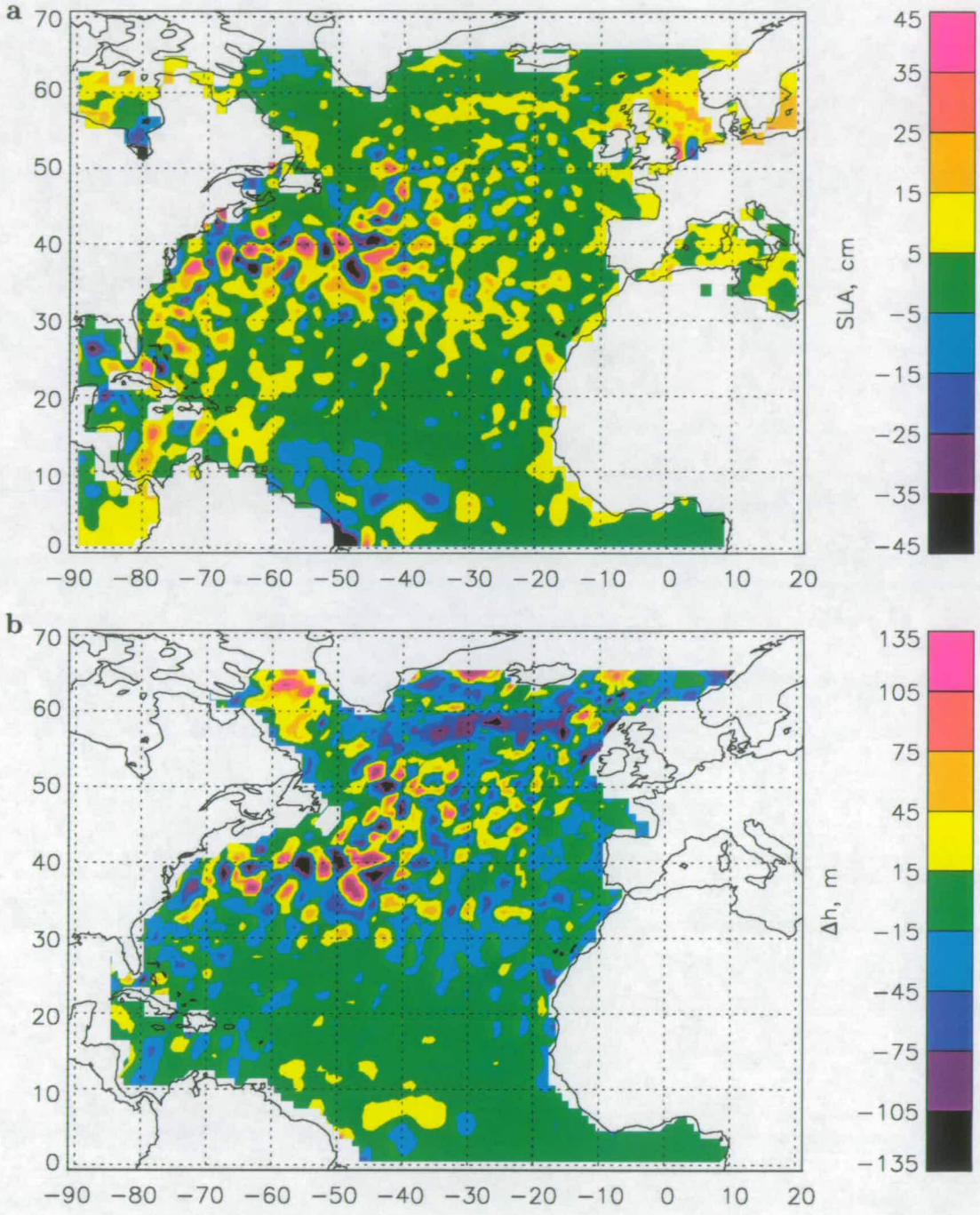

Figure 5.3: **a)** A sea level anomaly map of the Atlantic for 1/12/94 observed by TOPEX/POSEIDON and **b)** the vertical displacement (Δh) of water columns when the SLA field is assimilated with smoothed Lozier hydrography. Positive Δh indicates lifting of the water column.

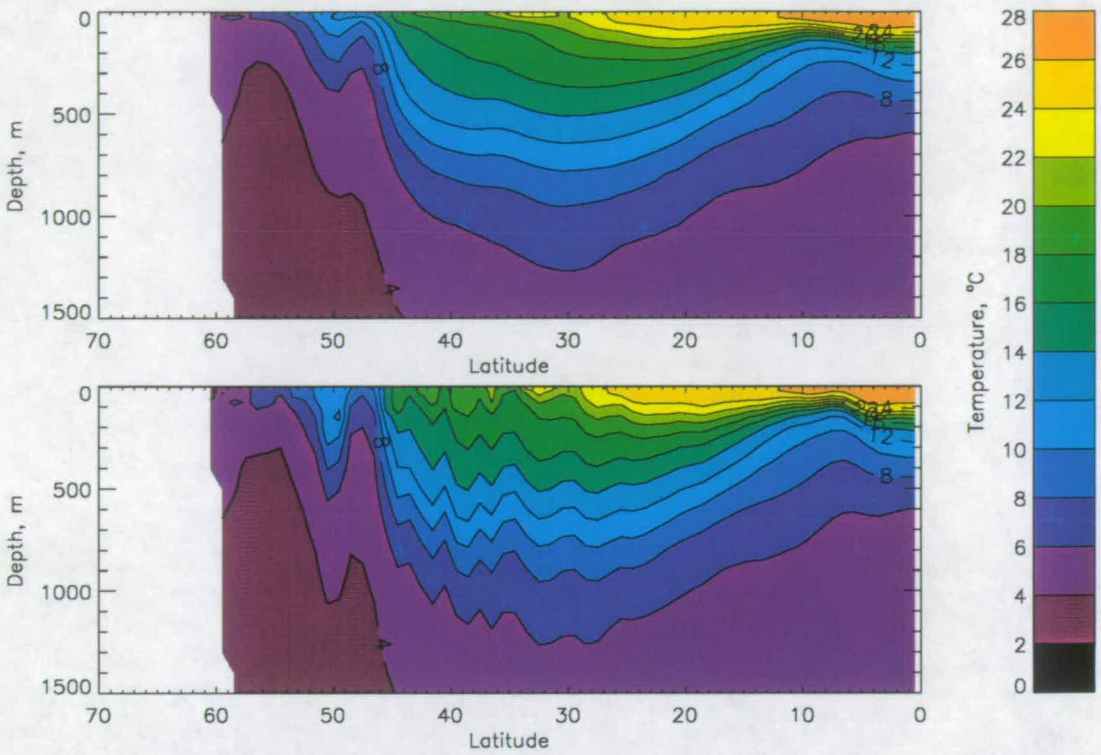

Figure 5.4: Cross-section of temperature along 43°W through the Lozier hydrography before and after assimilation.

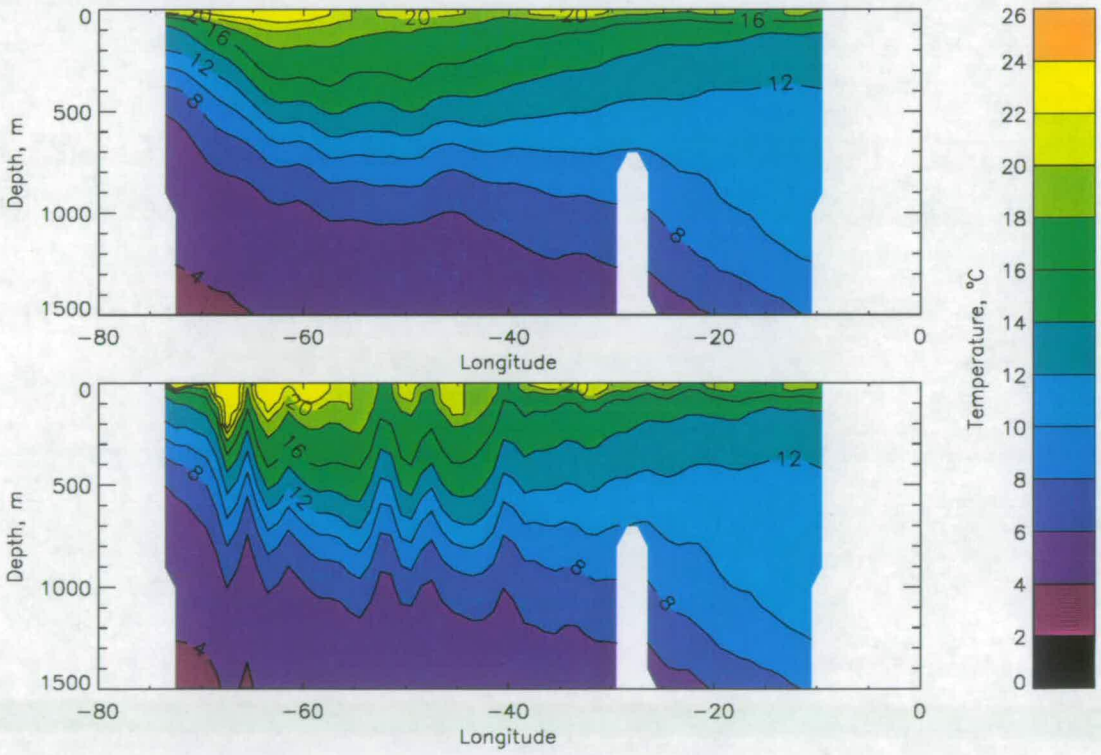

Figure 5.5: Cross-section of temperature along 38°N through the Lozier hydrography before and after assimilation.

hydrography at the top shows smooth isotherms with the front associated with the Gulf Stream obvious at 45°N. In the lower plot of the hydrography after the assimilation of altimetric data, the result of vertical displacement can be seen. Between 30° and 50°N the vertical displacements are evident, producing sharp deepening and shoaling of the isotherms.

The reason for the large displacements in the sub-arctic region is illustrated in the north-south cross-section in Figure 5.4. The assimilation scheme alters the mass of a water column to compensate for a positive sea level anomaly in order to maintain a constant bottom pressure. In the north the temperature and density of the water changes slowly with depth and the difference between the temperatures of the surface and bottom waters is relatively small. Therefore to change the mass of the water column significantly, large displacements are required. In these cases it may not be realistic to assume there are no bottom pressure changes.

In the tropics, the water is well stratified with a very steep thermocline. Consequently, the assimilation scheme will only displace water columns a little in response to even a large sea level anomaly.

In figure 5.4, at about 45°–50°N, modest SLAs have produced large lifting and lowering in the poorly stratified water, whereas between 30° and 45°N, larger SLAs have produced smaller vertical displacements in response. In the tropics, some displacements can be seen but they are quite small in the steep thermocline.

A cross-section of temperature along 38°N is shown in figure 5.5. This is a section through the Gulf Stream and the region of greatest sea surface height variability. The relatively smooth original field in the upper diagram has been greatly disturbed with large vertical displacements, some up to 300m. At some points large lifting has resulted in colder waters brought to the surface, such as at 66°W and 52°W.

Figure 5.6 are equivalent maps for the Pacific Ocean of figure 5.3. In this case, the satellite altimetry has been assimilated with Levitus (1994) climatological hydrography. As with the North Atlantic, large spatial variability is associated with strong currents. Here, these are the Kuroshio Current and Kuroshio Extension in the northern Pacific and in the south, the Antarctic Circumpolar Current. These currents are characterised by the large amplitude, but small spatial scale,

variations.

In contrast to the North Atlantic, there are also some very large scale sea level anomalies in tropical regions. At the time shown, December 1994, there is a strip of anomalously high sea level running along the equator and a strip of low sea level running parallel to the north. These are due to changes in the equatorial currents.

Thus, by assimilating the altimetric sea level anomalies, new instantaneous hydrographic fields of whole ocean basins can be constructed. These will be shown to better represent the state of the ocean at particular instants than the original climatology which can only describe the mean ocean state over the last century.

5.6 Comparison with XBTs

It is important to verify this method to discover if it is able to improve the original climatology and produce a more valid hydrography for a given time. Profiles from the hydrographies are compared with *in situ* expendable bathythermographs (XBTs) before and after assimilation. Comparison of an XBT with a climatological profile assimilated with a sea level anomaly at the time and place as the XBT measurement will allow us to assess how well the procedure performs and discover problems with the assimilation scheme. This will also be useful in evaluation of the assimilation scheme for use with ocean circulation models to determine problems, situations where the method cannot be applied and necessary adjustments to the method.

To compare an assimilation with an XBT, the SLA at the time and place of the XBT measurement is found. The SLAs are on mapped on a half degree grid, with maps at ten day intervals, so to determine a SLA appropriate to the XBT, linear interpolation in time and space is used. The nearest profile from the climatology is then displaced vertically according to this SLA.

Comparison of two XBT profiles with the climatology and post-assimilation hydrography are shown in figure 5.7. The first XBT is in the centre of the Gulf Stream. A large sea level anomaly of -631mm has been detected at the position of the XBT and when this is assimilated with the nearest climatological profile

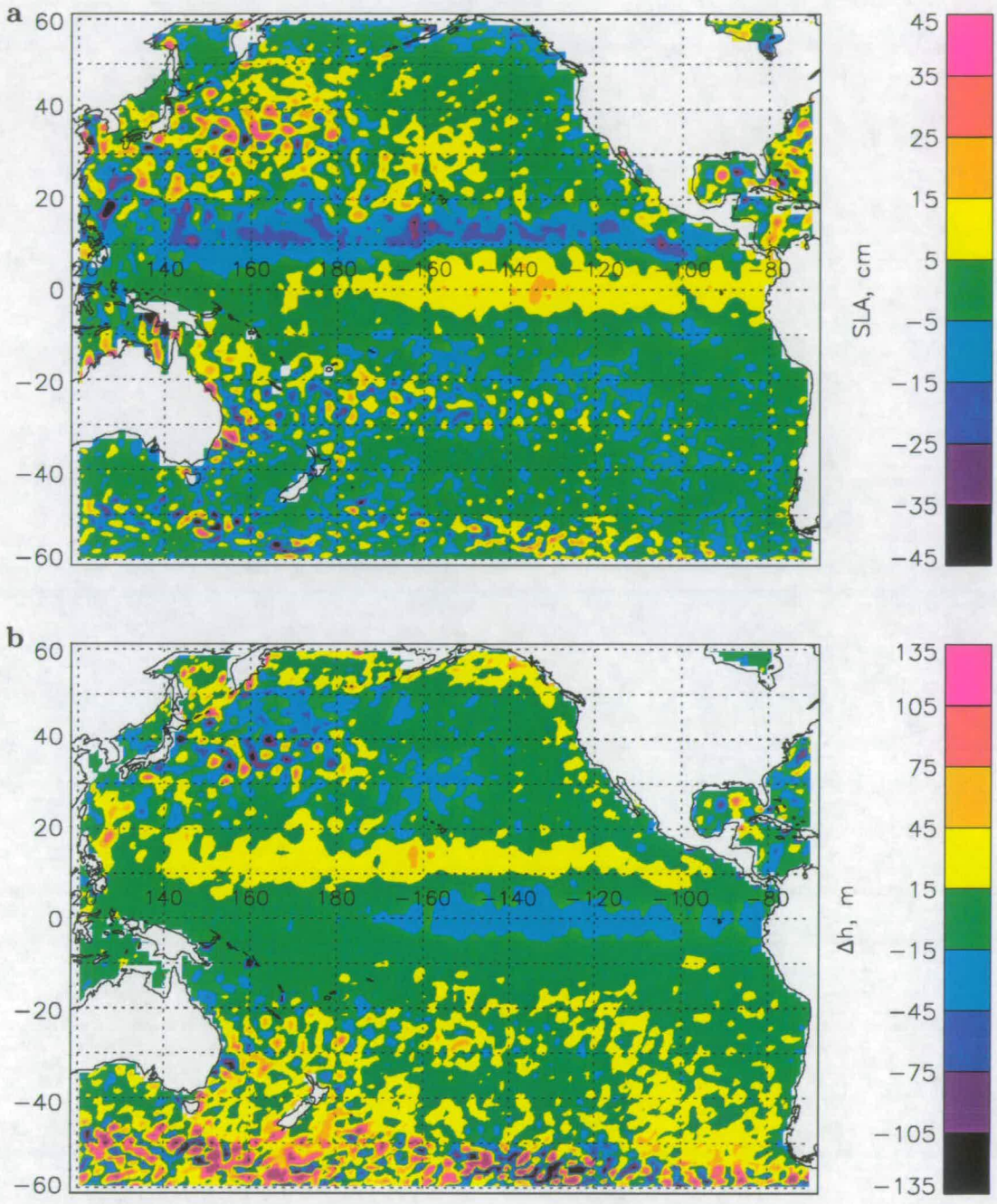

Figure 5.6: **a)** A sea level anomaly map of the Pacific Ocean for 1/12/94 observed by TOPEX/POSEIDON and **b)** the vertical displacement (Δh) of water columns when the SLA field is assimilated with Levitus (1994) hydrography. Positive Δh indicates lifting of the water column.

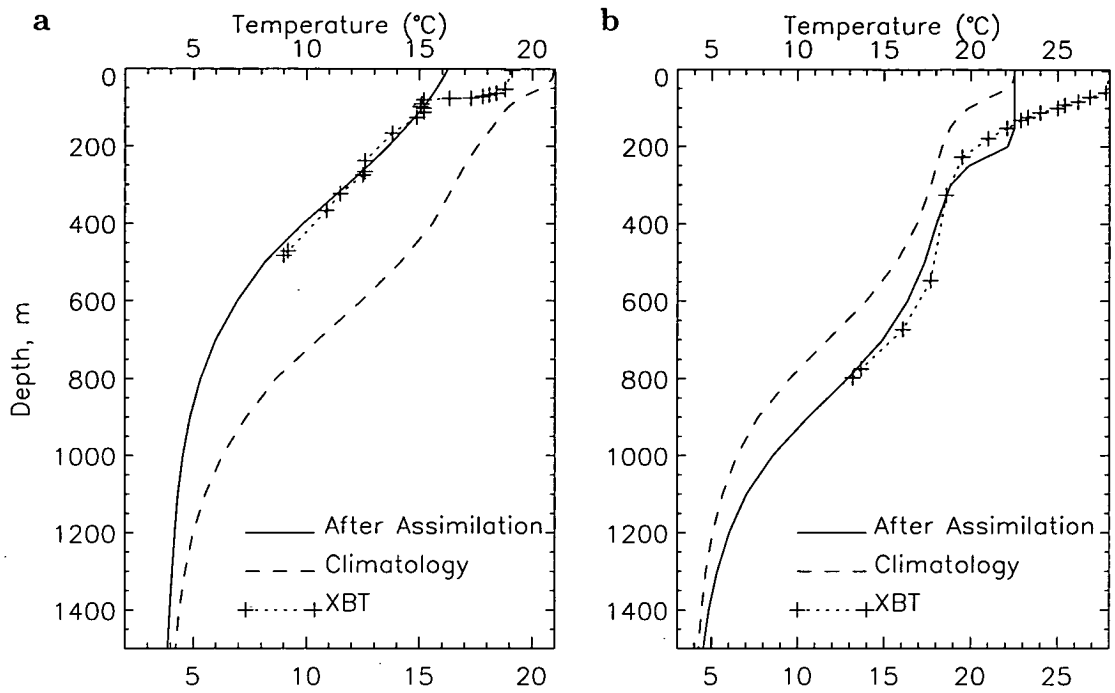

Figure 5.7: XBTs and nearest climatological profile before and after assimilation with SLA at time and position of XBT measurement. XBTs at **a)** 7/6/93 Latitude 38.62°N Longitude 56.92°W and **b)** 23/8/94 Latitude 36.37°N Longitude 61.63°W

(dashed line) results in a upward displacement if 334m. In this case, it brings the climatological profile into very close agreement with the XBT over the depths of the permanent thermocline.

The second is from just south of the Gulf Stream in the subtropical gyre. The 18°C mode water can clearly be seen in the profile. A sea level anomaly of +469mm has been detected and assimilation produces a lowering of the climatology by 150m. Again this has improved the climatological profile in comparison to the XBT. There is some disagreement in shape of the profile but it is only minor in this case.

5.6.1 Evaluation of assimilation scheme

The success of the assimilation scheme is assessed by determining how close the climatological profile is to the XBT before assimilation and then after. This is quantified by the RMS of the differences in temperature between the XBT and climatology at seven depth levels as shown in figure 5.8 and called ΔT. The seven levels are at 100m intervals from 100m to 700m. If the XBT does not

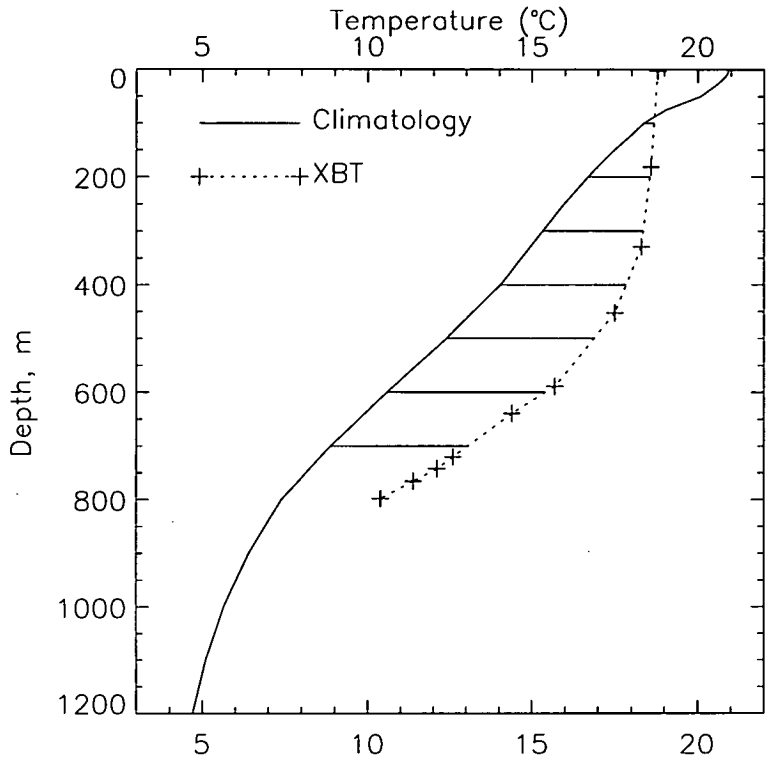

Figure 5.8: A comparison between an XBT and a climatological temperature profile showing the levels where the difference is calculated. The RMS difference is 3.42°C.

extend down as far as 700m, then the RMS of the available levels is taken. The XBT temperatures are not recorded on these standard depth levels so linear interpolation is used to determine the temperature at the required level.

With this quantitative evaluation of how well the XBTs and climatology match it is possible to assess the improvement or otherwise brought about by the assimilation. Henceforth, the RMS difference from an XBT will be referred to as ΔT_C for the original climatology and ΔT_A after assimilation. By performing assimilation on the climatology and comparing with many XBTs, statistics of the improvement at different times and locations can be analysed.

5.6.2 Amendments to the assimilation scheme

There are a number of deficiencies in the assimilation scheme that have been identified. Some have been anticipated in advance or were encountered by Cooper (1995) and Cooper and Haines (1996) and some have arisen from analysis of

the results of the experiments conducted for this work. The main problems are described here briefly but are dealt with in more detail in the next chapter, together with the results of adaptations of the assimilation scheme to account for these problems.

Climatology Problems

It has been assumed that the climatology represents the mean state of the ocean during the three years 1993–1995 and that anomalies from the three year mean sea level reflect the changes in the water structure. However, as chapters 3 and 4 have shown, variability on interdecadal time-scales is considerable. The Lozier climatology was compiled from observations taken throughout the century from 1900 to 1990. The mean sea level, from which sea level anomalies are determined, is derived only from the years 1993 to 1995. Therefore, there is a mismatch and the climatology will not accurately represent the ocean during the altimetric observation period.

This is a particular problem at this time because of the development of a very intense anomaly in the northern subtropical gyre and Gulf Stream (section 4.5.1). This began in 1988 and was still strong in 1994 and included some very large vertical displacements of the thermocline by up to 150m. This is part of the most variable region in the North Atlantic and is therefore important for the assimilation scheme.

In order to overcome this, the climatological hydrography is first altered to agree with the XBTs during 1993–95. This correction is applied before assimilation and is described in the next chapter along with results of assimilation using this 1993–95 hydrography instead of the original.

The mixed-layer

The assimilation scheme as described so far changes the hydrography by vertical displacement of water columns. However, hydrography in the ocean is also altered by interaction with the atmosphere and solar heating causing changes in the mixed-layer and seasonal thermocline. The shape of a temperature profile is changed by these effects and contribute to the sea surface height signal.

Cooper (1995) proposed a method of using sea surface temperature data to modify the mixed-layer before assimilation of the altimetry. This method has been incorporated into the assimilation scheme and tested with climatological hydrographies. Another method which has been tried is to ignore the mixed-layer and just try to filter out its contribution to the sea surface height signal. These methods and results are described in the next chapter.

Other problems which will cause errors in the results of assimilation have also been identified. One problem which occurs when the product of the assimilation is compared to an XBT for evaluation, comes from a mismatch in the position of the XBT and climatological profile. The climatological profiles are ordered on a one degree grid whereas the XBTs are irregularly scattered.

The assimilation scheme changes the water structure by simply vertically displacing water columns. Thus, the post-assimilation temperature profile is the same shape as the pre-assimilation. If, however, the actual profile has changed shape, for example by horizontal advection, the post-assimilation temperature profile cannot match the XBT observation.

A problem that was acknowledged by Cooper (1995) is that the assimilation scheme assumes that bottom pressure does not change. Cooper and Haines (1996) state that this is a good assumption in most situations except on continental shelves or on regions of strong barotropic flow. However, if there is a change in bottom currents then it may have some effect on the sea surface height signal and the assimilation.

These sources of errors are discussed in more detail and with some examples in the next chapter.

5.6.3 Best Possible Fit

Due to some of the problems mentioned above, in many cases the shape of the XBT is different from that of the climatological temperature profile. In these cases, it is not possible, by vertical displacement alone, to achieve a perfect, ($\Delta T = 0$), or even a good fit. There is a limit, therefore, to the success of the assimilation scheme to match with each individual XBT, and only a minimum ΔT is attainable.

The best possible fit by displacement alone can be determined and used as

a guide to evaluating how close the assimilation brings the climatology to the instantaneous hydrography. The best fit is achieved by lifting and lowering a water column until the ΔT is a minimum.

In order to produce a best fit, a good thermocline is required in both the XBT and climatology. On some occasions in the far north the thermocline is very shallow or has been removed by intense cooling and convective overturning. In these cases it is difficult to obtain a sensible best fit. For this reason, the best fits that are produced in the far north of the Atlantic are not reliable.

5.7 Summary

To summarise the assimilation experiment, for each XBT measurement, the nearest climatological profile is displaced in line with the observed sea level anomaly at the time and location of the XBT. The pre- and post-assimilation temperature profiles are compared to the XBT and the differences, ΔT_C and ΔT_A are calculated. This procedure is performed for all XBTs and the mean of ΔT_C and ΔT_A in various regions determined. The difference between ΔT_C and ΔT_A is referred to as the 'improvement' and will often be presented as a percentage. The improvement is positive when ΔT_A is less than ΔT_C, i.e. the post-assimilation profiles are, on average, closer to the XBTs than the pre-assimilation.

In the next chapter, the results of assimilation and comparison with XBTs are presented.

Chapter 6

Assimilation Results

6.1 Introduction

The results of assimilation and how well they recreate the state of the ocean, as shown by XBTs, are presented in this chapter. For the most part, the North Atlantic ocean is concentrated on as this is the most observed ocean in terms of XBTs. The climatology used in the North Atlantic is the smoothed Lozier climatology described in Chapter 2. Later in the chapter results of assimilation using the Levitus 1994 climatology are presented. Results from the Pacific ocean are also reported here using the Levitus 1994 climatology.

The assimilation is first tested with the smoothed Lozier climatology of the North Atlantic. The North Atlantic is also used assess the success of the assimilation scheme and determine problems. Difficulties and inadequacies of the assimilation are discussed with examples. Amendments to the assimilation scheme to overcome some problems are described and the results presented.

6.2 Atlantic Results

Figure 6.1 presents the locations of all XBTs which extend below 200m depth taken between the years 1993 and 1995 inclusive in the North Atlantic. There are high concentrations of XBTs along the shipping lanes particularly between Europe and America. The western Atlantic off the east coast of America has a good distribution of XBTs which is important as the highly variable Gulf Stream is therefore well observed. North of 50°N the coverage is poor with some large gaps. There are also gaps and areas of few observations in parts of the eastern

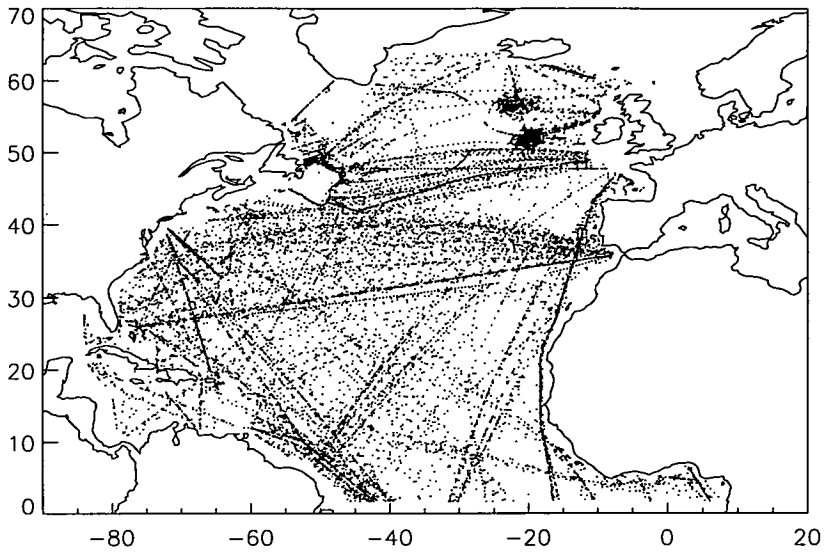

Figure 6.1: Location of XBT measurements in the North Atlantic between 1993 and 1995 inclusive.

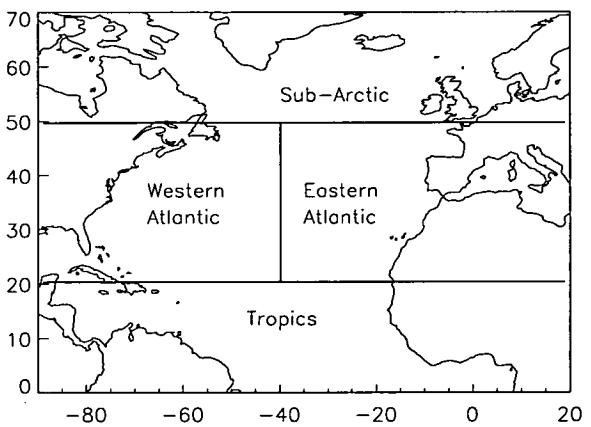

Figure 6.2: Division of the North Atlantic Ocean into regions for the study of assimilation.

side of the ocean.

The assimilation produces different results depending on water column structure. Therefore, the assimilation behaves differently in different parts of the ocean as illustrated in figure 5.3. For this reason the North Atlantic has been separated into four areas, shown in figure 6.2.

South of 20°N is defined as the tropics. The ocean here is characterised by a warm, shallow mixed-layer and a very steep thermocline. Seasonal variations are small due to more constant solar radiation than at higher latitudes. Generally, sea surface height variations are reasonably small but often large-scale.

In mid-latitudes, between 20° and 50°N, the Atlantic is split into eastern and western parts. Most of the western section is the subtropical gyre. There is a bowling down of isotherms (see figures 5.4 and 5.5), the thermocline is quite gradual and there is a large mass of 18°C mode water. The most significant feature of the Western Atlantic is the Gulf Stream and its associated front. Eddies and meanders in the Gulf Stream cause large amplitude, small-scale variations in sea surface height. This is a very important region for the assimilation scheme. The Eastern Atlantic is quieter than the west but there is still some activity causing sea level anomalies.

North of 50°N the water is poorly stratified. The difference in temperature between bottom and surface waters is smaller and in many places the thermocline is very weak and shallow. Seasonal variation is large here, with deep convection often occurring in winter in the Labrador and Greenland seas and a sharp, shallow thermocline forming in summer. Because of the smaller temperature difference between bottom and surface, modest sea level anomalies will, on assimilation, produce large vertical displacements. Sea surface height variations are quite small in this area but sometimes on very large scales.

6.2.1 Results of Assimilation

The results of assimilation of altimetry with the smoothed Lozier climatological hydrography are presented in this section. These are the results using the basic assimilation scheme only. Additions to the assimilation method and their results are described in later sections.

Statistics were compiled from the mean differences, ΔT_C and ΔT_A, between XBTs and climatology before and after assimilation. Means of the differences for each month and in each area are presented in figure 6.3. Here, all XBTs in the period 1993-1995, that reach a depth of 200m or greater, are used. The figure also shows the number of XBTs per month contributing to the mean.

In general the overall improvement after assimilation is small, but there is a slight improvement most of the time in all areas. In the Western Atlantic where the highly variable Gulf Stream has influence, the difference is greater and more variable than the other areas. There is an improvement in the overall mean difference from 1.92°C to 1.77°C. Table 6.1 lists the overall mean differences before

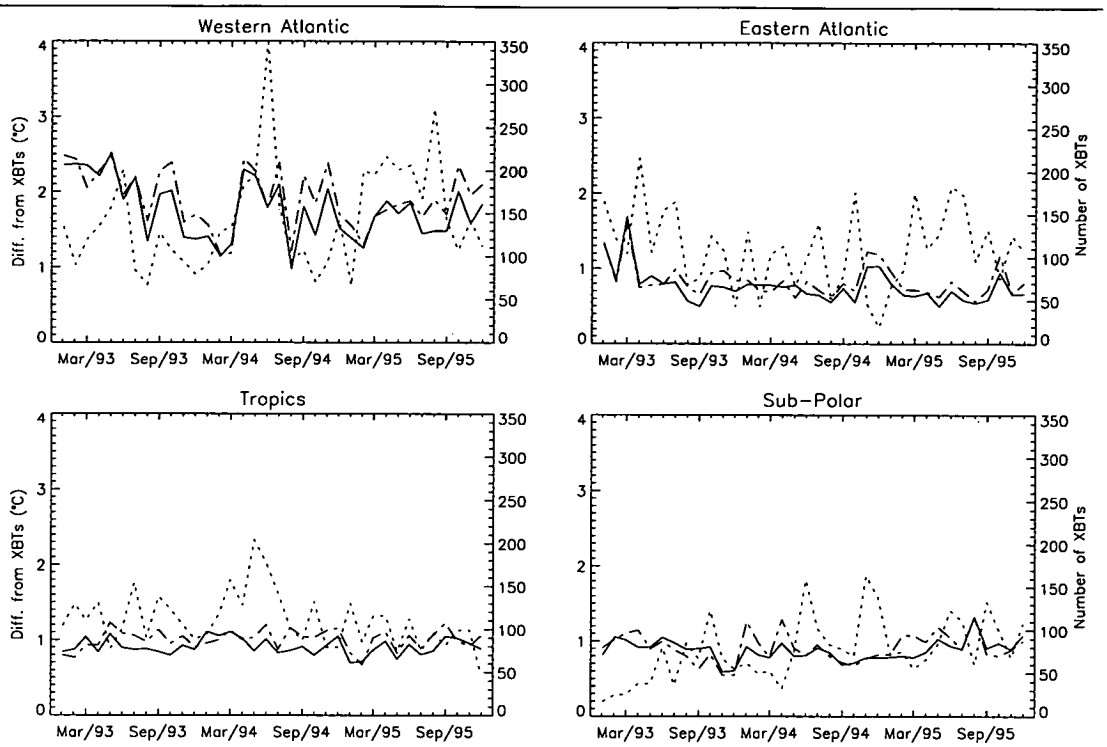

Figure 6.3: Mean difference between XBTs and climatology. The dashed line is before assimilation, the solid line is after and the dotted line and the right hand scale shows the number of XBTs used.

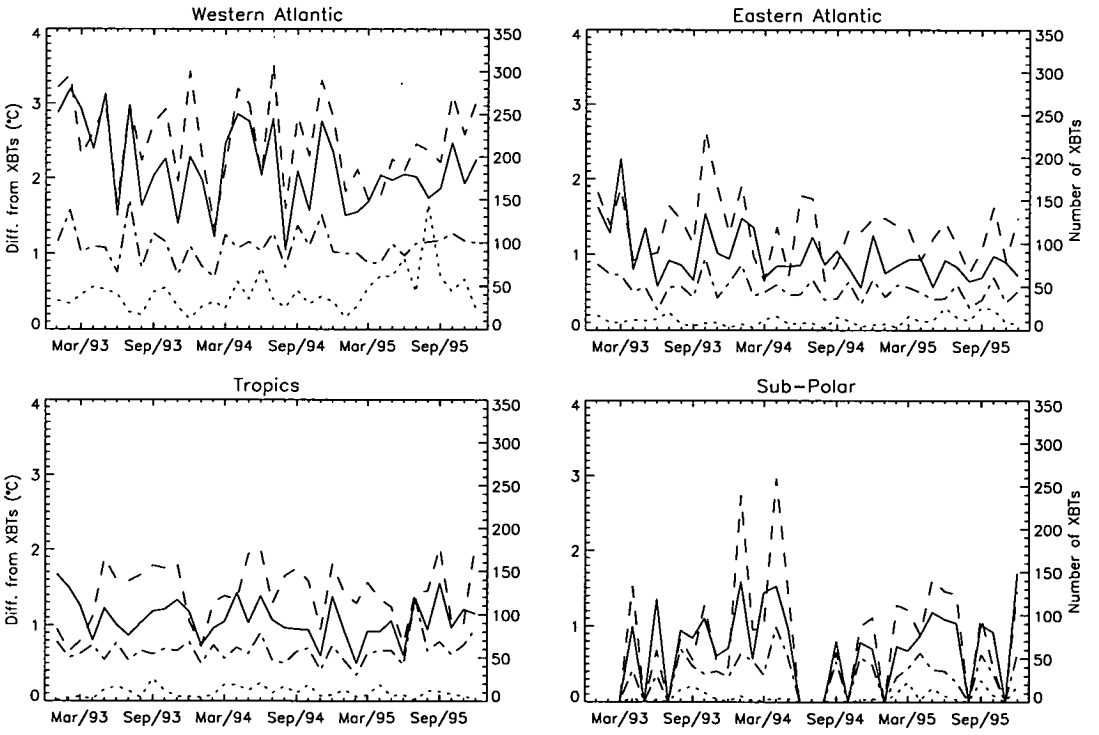

Figure 6.4: As figure 6.3 but with using only XBTs where a sea surface height anomaly of greater than 10cm has been detected. The extra dash-dot line shows the best fit attainable by vertical displacement.

		Western Atlantic	Eastern Atlantic	Tropics	Subpolar
No Limit	Original (ΔT_C)	1.92	0.84	1.00	0.92
	Assimilation (ΔT_A)	1.76	0.76	0.91	0.88
	Improvement	8.3%	8.7%	9.4%	3.8%
10cm Limit	Original (ΔT_C)	2.51	1.32	1.42	0.80
	Assimilation (ΔT_A)	2.15	0.98	1.08	0.67
	Improvement	14.2%	25.4%	23.9%	15.6%
10cm Limit	Best fit	1.09	0.54	0.67	0.33
	Improvement	56.3%	59.1%	53.1%	58.7%

Table 6.1: Overall mean temperature differencesin °C and relative improvements for the Atlantic regions.

and after assimilation with the relative improvement. The original climatology fits the observed temperature profiles best in the Eastern Atlantic and some small improvement is made by assimilation. The tropical region shows the best relative improvement of the four regions whereas it is clear that in the subpolar region the assimilation performs worst.

In the majority of assimilation experiments, the sea surface height anomaly is quite small, so only a small vertical displacement is made. This has little effect on the difference between the XBT and the climatological profile. In order to examine the assimilation scheme more effectively when the statistics are compiled, only cases where the sea level anomaly is greater in magnitude than 10cm are used. This emphasises the assimilation itself and reduces the relative influence of other factors.

Figure 6.4 shows the mean temperature differences for all XBTs where the observed SSH anomaly is greater than 10cm and the overall mean differences are in table 6.1. Also shown on figure 6.4 and in table 6.1 are the results of displacing water columns so that the temperature profiles fit best with the XBTs.

These selected cases have, as expected, a higher initial mean difference than the mean from all XBTs. Improvements are also larger, both in magnitude and relative improvement. There are more variations in the ΔT by month which is unsurprising given the smaller number of XBTs contributing. Figure 6.5 shows the mean improvement achieved by assimilation, i.e. subtraction of the mean difference after assimilation from the difference before. The best possible improvement

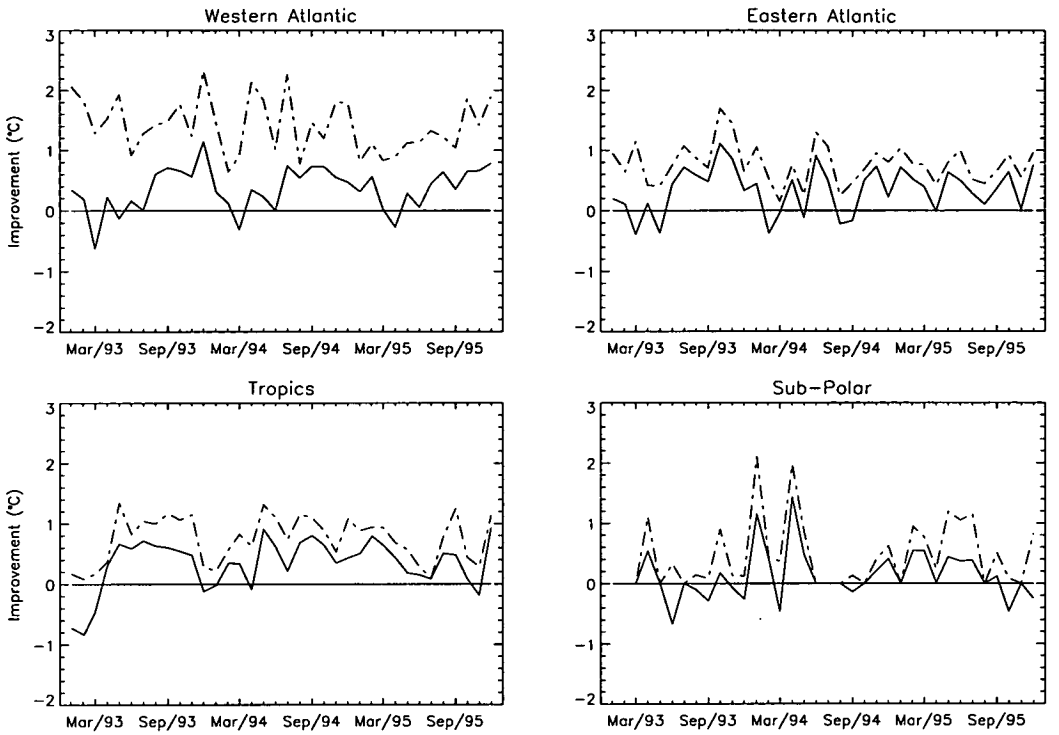

Figure 6.5: The solid line is the mean improvement in temperature differences achieved by assimilation. The dashed line shows the improvement by displacing water columns to a best fit with XBTs. Negative values indicate that the assimilation has made the fit worse.

is also shown.

The Western Atlantic is dominated by the highly variable Gulf Stream so it is unsurprising that the lines on figure 6.4 are so variable. The overall improvement is 14.2% which is lower than the other areas. This could be due to errors in the determination of sea surface anomaly as the small-scale variability in sea surface height will make mapping errors large and further errors will be introduced in the interpolation, as explained in section 6.6.3. It could also be due to the long-term hydrographic change seen in the early nineties described in chapter 4. This is discussed further in the next section. The best possible ΔT is quite uniform so more successful assimilations using vertical displacement are theoretically feasible.

The improvement shown in figure 6.5 reveals a possible seasonal variation. There are minima in March 1993, March 1994 and April 1995 while summer and autumn months have strong improvements. This seasonal effect is likely to be due to changes in the mixed-layer and seasonal thermocline. Attempts to reduce the error from seasonal variations are described in section 6.4.

The Eastern Atlantic shows very good overall improvement but results are

very variable with several months where the assimilation makes the temperature differences worse. The variations do not, however, seem to be related to an annual cycle. It is interesting to note that the improvement by assimilation quite closely follows the best possible improvement.

The figures also show that the assimilation scheme performs well in the tropics which have the highest relative improvement. There does not seem to be an annual oscillation which is to be expected because seasonal effects are small near the equator. There are a few months, particularly the first four months of 1993, where the improvements are negative. The small numbers of XBTs which qualify by the sea level amplitude criteria will increase the variation in the results.

The subpolar region is poorly covered by XBTs and these are further decreased by the 10cm lower limit on sea level anomalies. Consequently, in this area, there are several months with no data and in the other months the temperature differences are very noisy. The mean improvement is still good.

The best possible improvement shows that the assimilation scheme has its limits but that if the assimilation scheme can be modified, it may be possible to get closer to the *in situ* observations. In the next sections the results of improvements to the assimilation method are presented.

The two profiles in figure 5.7 are examples where the assimilation scheme works very well. However in most cases, assimilation makes a less dramatic improvement and there are cases where the profile after the assimilation is actually worse than before. There are also cases where the shape of the temperature profile and XBT are very different and cannot therefore be made to agree well by vertical displacement alone.

In the next section the problem of a mismatch between the climatological hydrography, compiled from observations taken between 1900 and 1990, and the mean sea surface height from 1993 to 1995 is discussed and a solution tested. In section 6.4 the problems caused by air-sea interaction and the changes in the mixed-layer are described and amendments to the assimilation scheme proposed.

6.3 Long-term variability of hydrography

So far we have assimilated anomalies from a three year mean sea level (1993–1995) with a climatological hydrography based on data taken from 1900 to 1990. The assimilation method displaces a climatological water column according to the sea level anomaly, therefore the mean sea surface height has to be consistent with the climatology. However, as has been reviewed and investigated in chapters 3 and 4, there is considerable variation in water structure on annual to decadal time-scales. We cannot expect to get good matches with XBTs where the mean hydrography for the period 1993–1995 differs significantly from the climatological hydrography.

A method was devised to determine whether, over the three years under consideration, XBTs in any region were consistently different from the climatological hydrography. This was done by using the best fit method, described earlier. For all XBTs taken during the three years from 1993 to 1995, the nearest climatological temperature profile was displaced until the RMS difference, ΔT, was at a minimum. The amount of displacement, Δh, was recorded together with the position of the XBT. Hence, for each XBT measurement we record a displacement giving a list of Δh with their locations.

All the displacements were then mapped using the method described in appendix A to produce an overall field of difference, in terms of vertical position of the thermocline, between the climatology and the observed state of the ocean in 1993–95.

Figure 6.6 shows the required mean displacement applied to the climatological hydrography to bring it into agreement with XBTs from the years 1993–1995. North of 50°N the large displacements illustrate the problem of fitting the climatological profiles with shallow thermoclines to the highly variable XBT profiles. South of 30°N, very little adjustment of the thermocline is needed. The largest displacement of concern is the region between 37° and 43°N and 40° and 60°W. The lowering of climatological water columns to align them with XBTs is large here with a maximum of about 180m.

This region is part of the large anomaly described in Chapter 3 which started in 1988 and lasted at least until 1995. When compared with the sea level anomaly

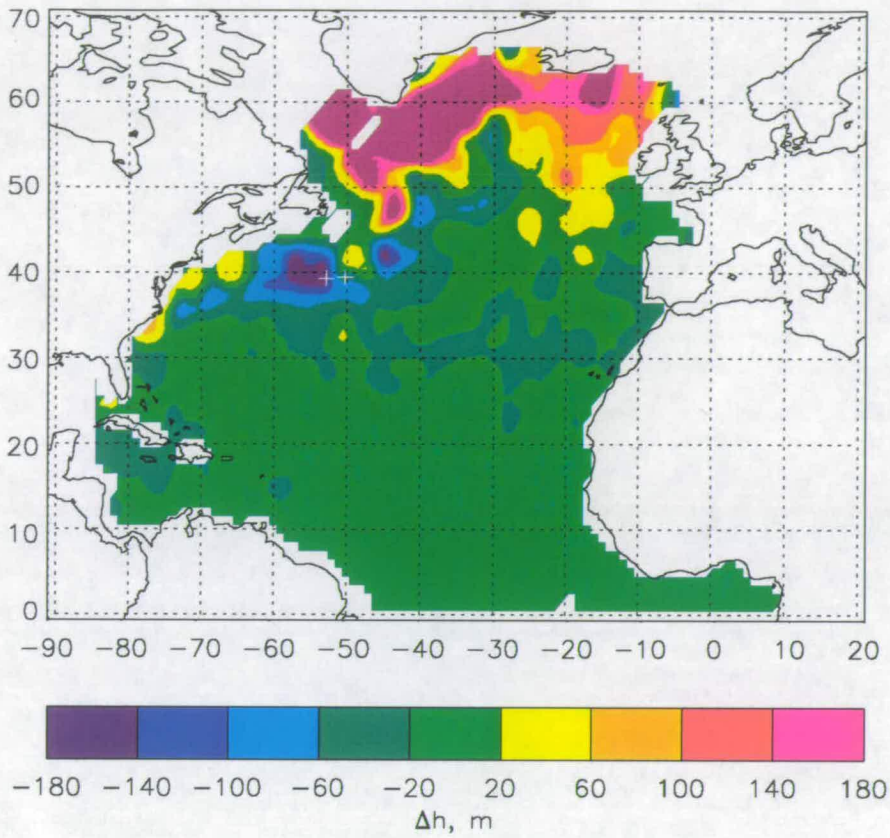

Figure 6.6: Vertical displacement of water columns from Lozier et al. (1995) climatology required to agree with XBT observations from 1993–1995. The crosses mark the positions of the XBTs in figure 6.7.

map shown in figure 5.3, it can be seen that this is also an area of high small-scale sea surface height variability. This is a region where the performance of the assimilation scheme will be put to the test most.

It is clear that adjusting the climatology to the period 1993–1995 before assimilating the altimetry should result in closer matches with XBTs. This is done simply by displacing the climatological hydrography by the amounts shown in figure 6.6 to produce a new hydrography, the 1993–95 hydrography. This new hydrography is then used as the starting point for assimilation.

The effect of using an updated hydrography as the starting point for assimilation is illustrated in Figure 6.7. Here, the climatological profile is first vertically displaced to correct for the time period discrepancy, then assimilation of altimetry is performed. In these two cases, this has resulted in good matches to the XBTs. The positions of the XBT measurements in relation to the vertical displacement

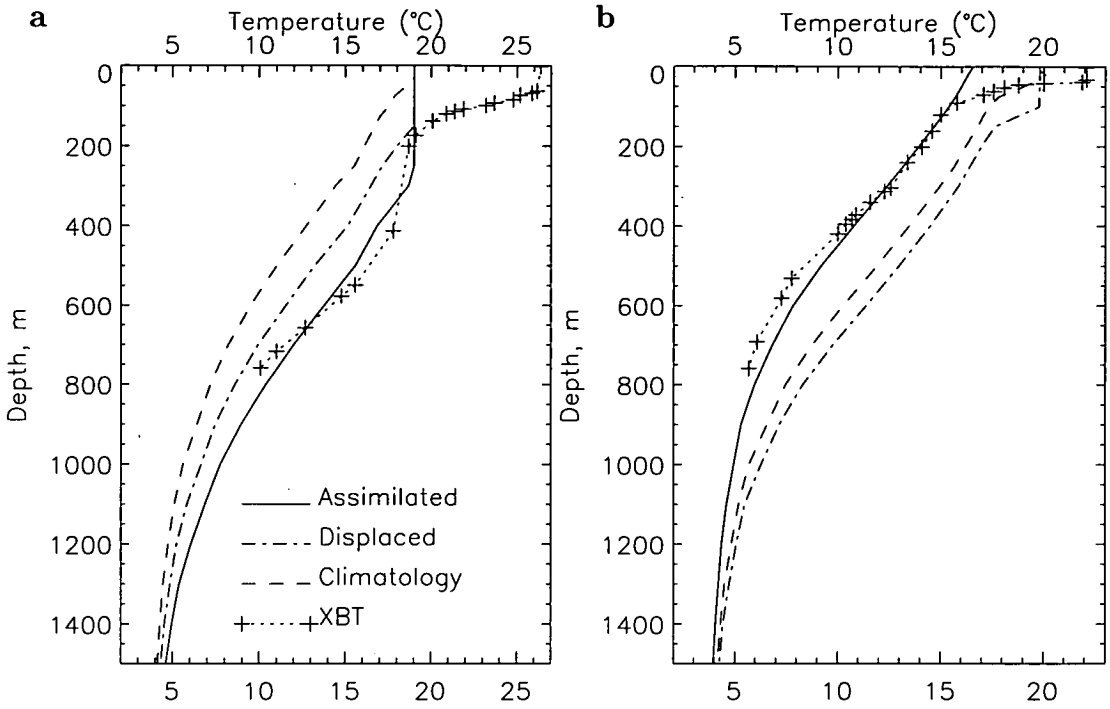

Figure 6.7: Correction of the climatology and assimilation of sea level anomalies. The dashed line is the original climatological temperature profile, the dash and dot line is after the correction for long-term variability and the solid line shows the profile after assimilation. XBTs **a)**19/7/95 39.37°N 52.85°W **b)** 19/7/95 39.48°N 50.28°W

correction field are shown in Figure 6.6.

The interdecadal correction method is likely to cause more errors in the seasonal thermocline and mixed-layer. As seen in figure 6.7 the lowering of the climatological hydrography to correct for long-term changes has artificially introduced a deep mixed-layer.

6.3.1 Results for correction of hydrography for long-term variability

Figure 6.6 showed the mean vertical displacement of climatological temperature profiles to attain a best fit to XBTs from 1993–1995. It can be seen that there is a large change in the Western Atlantic, which, in the last section, was the region that produced the smallest relative improvement after assimilation.

Figure 6.8 shows the results of assimilation on a corrected climatology. The improvements are all relative to the original climatology. Table 6.2 gives the overall average improvements in comparison to both the original climatology and

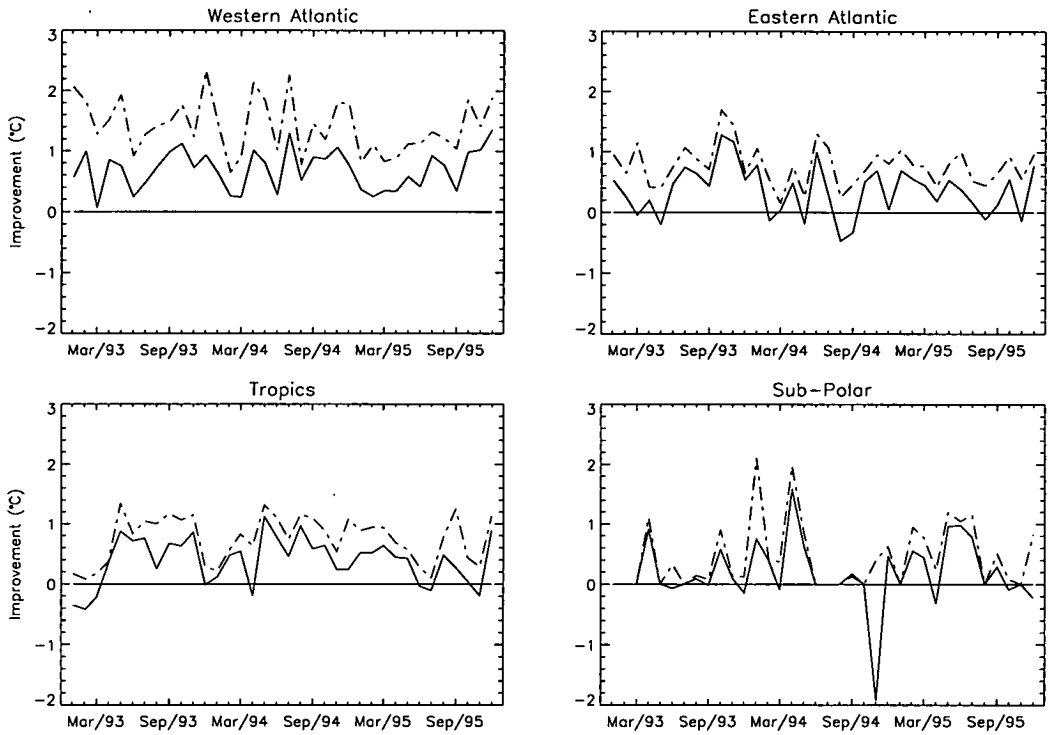

Figure 6.8: As figure 6.5 including a correction to the climatology to make it consistent with the 1993–1995 ocean state. Continuous line is after assimilation with correction and dashed line is best possible improvement.

	Western Atlantic	Eastern Atlantic	Tropics	Subpolar
Original	2.51	1.32	1.42	0.80
Correction	2.22	1.24	1.34	0.74
Assimilation	1.82	0.96	1.03	0.61
Total Improvement	27.4%	27.1%	27.2%	23.7%
Improvement relative to 93-95 climatology.	18.1%	22.6%	23.1%	18.1%
Best possible	56.3%	59.1%	53.1%	58.7%

Table 6.2: Overall mean differences in °C and improvements for the Atlantic regions including the correction for long-term change in hydrography.

the climatology after correction. All the results are from XBTs where observed sea surface height anomalies are greater than 10cm.

All regions give better overall results with the Western and Eastern zones and the Tropics all receiving improvements of 27% after correction of climatology and assimilation. The climatological correction method has had the greatest effect on the Western Atlantic region which is to be expected as XBTs showed a large difference between climatology and the hydrography during the 1993–1995 period. Not only is the overall improvement from the original climatology much better but also the improvement from the corrected climatology is considerably larger. This is very strong evidence for the need to adjust the climatological hydrography so that it represents the ocean for the period from which the mean sea level is determined by satellite altimetry. The improvement for the Western Atlantic in figure 6.8 now follows the best possible improvement more closely.

Assimilation in the Eastern Atlantic and the Tropics has also benefited from prior correction of climatology with increased overall improvement from original climatology. However, in these cases the improvement from the corrected climatology is less than the improvement due to assimilation from raw climatology.

As has been previously discussed, the process of lifting and lowering a water column to obtain best fits to XBTs is not satisfactory. The correction field shown in figure 6.6 shows very large lifting in the north which is more a symptom of the inability to fit the climatological profile to XBTs than any real hydrographic change. Thus the correction will not be as effective in this region. Nevertheless, it does show some improvement to the assimilation.

It is clear that when sea level anomalies are assimilated with a climatological hydrography, that hydrography must be representative of the period over which the mean sea level is appropriate. Correcting a climatology by the method described improves the assimilation. All procedures and results presented in later sections use adjusted climatology.

6.4 Mixed-Layer Effects

It is the permanent thermocline that we are trying to recreate in this procedure. As it is conservative, this process cannot simulate changes in the water-column

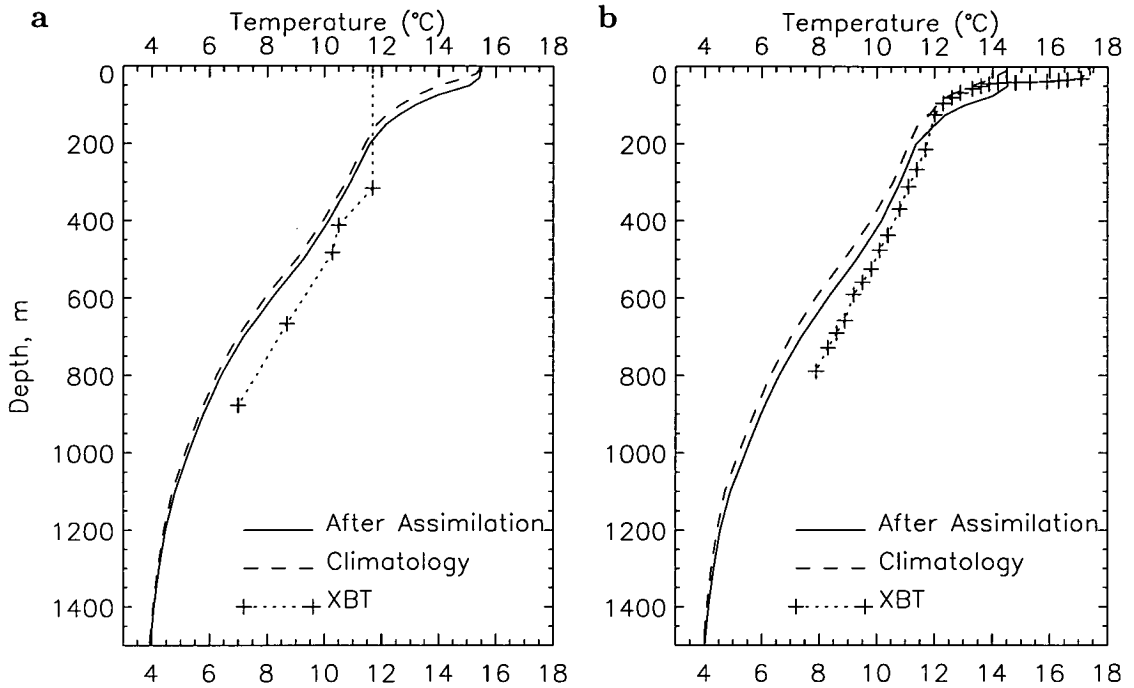

Figure 6.9: XBT and nearest climatological profile before and after assimilation with SLA at time and position of XBT measurement. XBTs were deployed on **a)** 8/2/93 at 47.5°N, 26.8°W and **b)** 26/7/93 at 49.2°N, 25.9°W.

which involve exchange of heat of salt. This is particularly a problem in the surface layer, where air-sea interactions such as heat fluxes, precipitation and evaporation are major contributors to water mass properties. Thus the mixed-layer and seasonal thermocline indicated by the XBT will not usually match that shown by the annual mean climatology.

Figure 5.7 illustrates this well. In both cases, the XBT is from the summer and so both have a shallow, warm mixed-layer which is the result of warming of the surface by incident solar radiation. Obviously, to recreate these would require creating water-masses with new properties. In figure 5.7a the lifting of the profile has brought colder waters near to the surface. The profile matches well with the XBT below 100m but the cold water has been capped with a warm layer.

The XBT in figure 6.9a is from February 1993. Heat loss at the surface has resulted in cooling of the upper layers of water. Convective overturning has entrained deeper layers into the mixed-layer producing a deep cold mixed-layer. Therefore the upper 300m of the XBT differs considerably from the climatology. Figure 6.9b shows an XBT close in position to figure 6.9a but taken in July

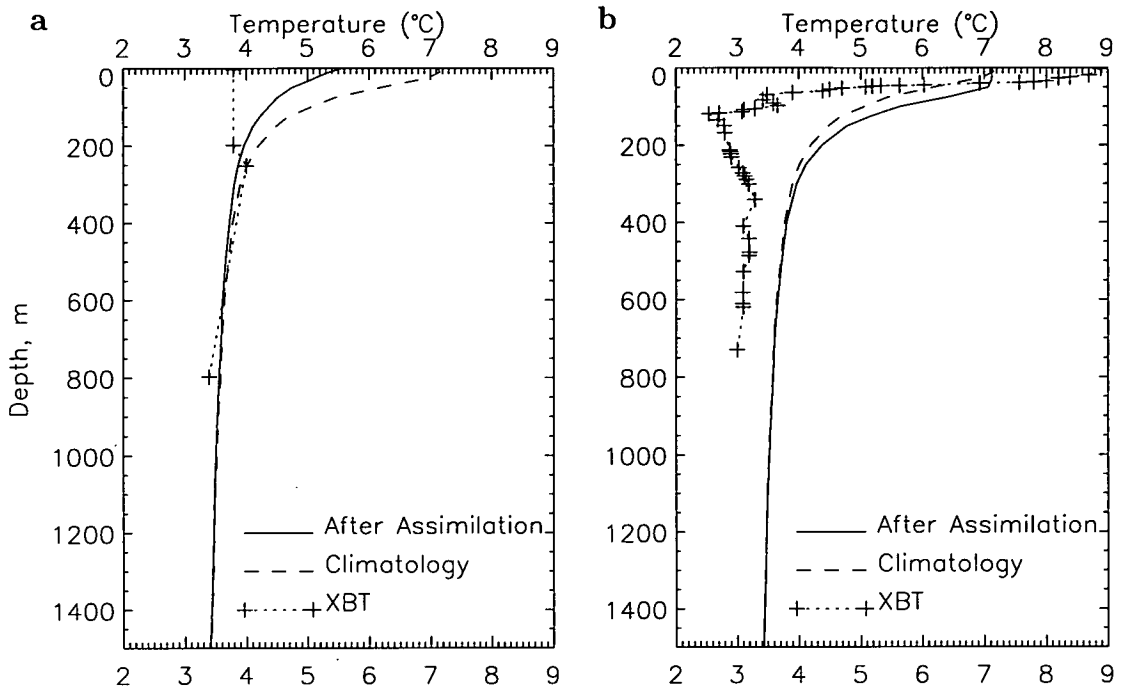

Figure 6.10: XBTs and nearest climatological profiles before and after assimilation with SLA at time and position of XBT measurement. Both XBTs were at 51°N 47°W taken on **a)** 27/1/94 **b)** 26/7/94.

1993. This water column now has a warm, shallow mixed-layer. Obviously, these diabatic changes in the structure of the water column cannot be reconstructed by assimilation.

Seasonal changes in temperature profiles are even more pronounced in the Northwestern Atlantic, in the Labrador Sea and surrounding area as illustrated by figure 6.10. The XBTs show the temperature of a water-column in summer and winter. In winter, intense cooling has produced an almost uniform temperature profile and there is no thermocline. The second XBT is from the same location six months later. During the winter further cooling and convection have resulted in colder temperatures deeper down and a temperature minimum at about 120m. The summer mixed-layer is a very thin and comparatively warm layer capping the water column.

It is clear that in this region most changes in the water-column structure are from air-sea interaction and are non-adiabatic. This is an area of deep convection and formation of North Atlantic deep water. The conservative, adiabatic assimilation scheme cannot, therefore, be expected to work here.

The seasonal warming and cooling of the surface layers will affect the sea surface height by thermal expansion and contraction of the water. This is known as the steric effect and has been observed in tidal gauge data (Pattullo et al. 1955, Pattullo 1963) and also more recently from Geosat (Jacobs et al. 1992) and TOPEX/POSEIDON observations (Stammer and Wunsch 1994, Stammer 1997).

Gill and Niiler (1973) discuss the theory of large-scale sea surface height variations. They state that the time-varying component of SSH, η, has three components and can be written as

$$\eta = \eta_s + \eta_{bc} + \frac{1}{g\rho_0} p_b \tag{6.1}$$

where η_s is the SSH anomaly due to changes in the surface layers. η_{bc} is the component of SSH change due to changes in the water below the seasonally affected layers. The third term in the equation relates to changes in barotropic currents, which for the assimilation here, is assumed to be zero.

The surface component, η_s, is determined by

$$\eta_s = \frac{1}{\overline{\rho}_0} \int_{-h}^{0} \rho'(z) dz, \tag{6.2}$$

and below the mixed-layer and seasonal thermocline,

$$\eta_{bc} = \frac{1}{\overline{\rho}_0} \int_{-H}^{-h} \rho'(z) dz \tag{6.3}$$

where the depth h is the base of the seasonal thermocline taken to be 200m by Gill and Niiler (1973). $\rho'(z,t) = \rho(z,t) - \rho_0(z)$ is the time-dependent density anomaly relative to a reference profile.

Equation 6.2 gives the component of the SSH anomaly that arises from changes in the surface layer properties and can be split into heat and salinity content:

$$\eta_s = \frac{1}{\rho_0} \left(\int_{-h}^{0} \frac{\partial \rho}{\partial T} T' dz + \int_{-h}^{0} \frac{\partial \rho}{\partial S} S' dz \right) \tag{6.4}$$

where T' and S' are changes of temperature and salinity. Estimates reported by Gill and Niiler (1973) suggest that the second term is small and the steric height anomaly is dominated by changes in the heat content of these upper waters from interaction with the atmosphere.

For our purposes, η_s can be considered to be the change in the SSH due to thermal expansion from the seasonal variation of heat fluxes. As such it does not

involve any change in mass of the water column. As steric anomalies tend to be on large scales, any resultant pressure gradients will be very small. And therefore will not be associated with currents.

The term, η_{bc}, represents the effect of density changes in the permanent thermocline which are related to changes in currents. It is these density changes that the assimilation scheme attempts to recreate. In using the assimilation method in its most basic form described so far, we use all of the observed sea level anomaly, $\eta = \eta_s + \eta_{bc}$, to vertically displace the water column. Therefore, not only may the new profile be wrong in the mixed-layer and seasonal thermocline, but also the permanent thermocline may be erroneous as only η_{bc} reflects the changes here.

At the position of the XBT shown in figure 6.9, a sea level anomaly, η, of +69mm was observed which, by assimilation, produces a downward displacement of the water column of 44m. However, the XBT reveals that winter cooling has produced a deep, cold mixed-layer. Contraction of this water will have lowered the sea surface so η_s will be negative. Therefore, η_{bc} will be greater than the observed SLA and the water column should be lowered more. This would bring it into closer agreement with the XBT.

For the assimilation to be successful, either the mixed-layer and seasonal thermocline should be estimated or the steric part of the SSH anomaly, η_s, should be identified and removed from the SSH anomaly observation. The latter case would not then attempt to reproduce the surface layer water structure. In the next sections, two methods are described for dealing with this problem. In the first, the sea surface temperatures are used to estimate mixed-layer properties and depth. In the second, an attempt is made it remove the steric effect by a filter.

6.4.1 Assimilation of Sea Surface Temperatures

Cooper (1995) devised a method of assimilating sea surface temperatures at the same time as SSHs. Radiometers on board satellites, such as ATSR and AVHRR, can now be used to provide reasonably accurate sea surface temperatures (SSTs).

Here, the same two stage process is used to assimilate sea surface height and temperature with mean annual climatology. First, the mixed layer temperature of the mean annual climatology is adjusted to the observed sea surface temper-

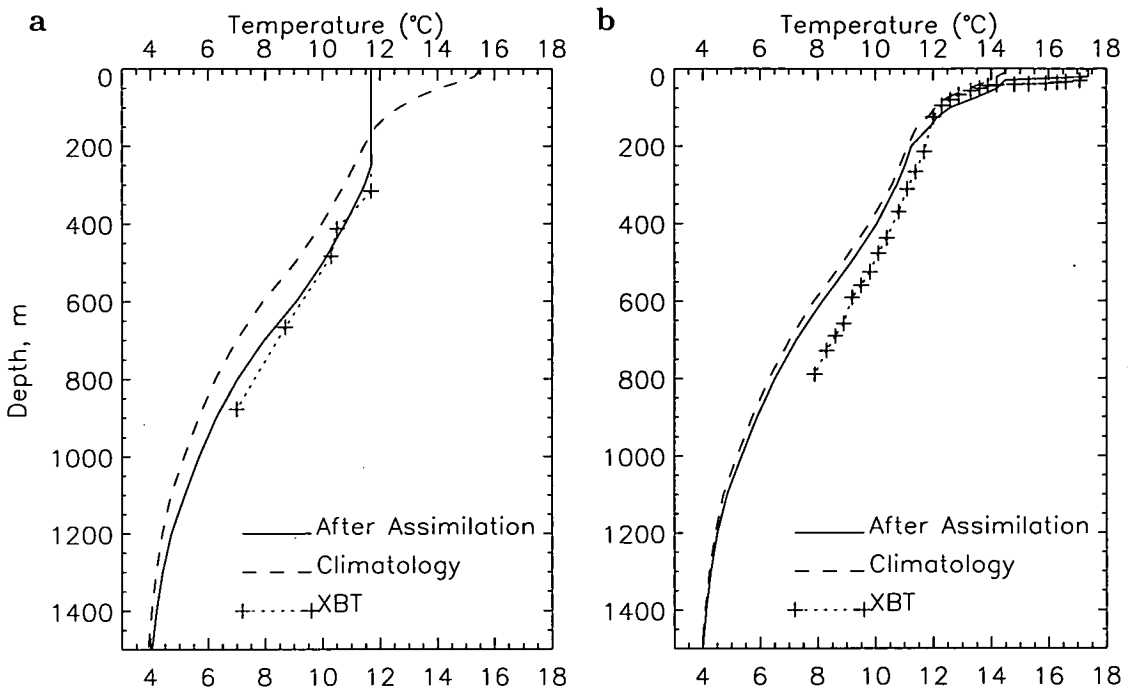

Figure 6.11: As figure 6.9 but now using surface temperature information in the assimilation together with sea surface height anomaly.

ature, and then the column is displaced vertically as before. In this case the surface temperature is taken from top of the XBT profile. If the observed sea surface temperature is less than that of the climatological profile, this is used as a maximum temperature limit for the profile. Effectively, this sets the mixed layer to the cooler observed temperature and, as some of the thermocline will be warmer than the observation, the thermocline will deepen. This is realistic as cooling will lead to convective overturning.

In the case of an observed surface temperature warmer than the model, Cooper (1995) increased all the current mixed-layer to the new temperature. However, as can be seen in the previous few figures, the climatology does not show a well defined mixed-layer. This is because it is an annual mean climatology. It is also clear from the XBTs shown that summer mixed-layer depths vary. There is, therefore, considerable difficulty producing a reasonable estimation of a warm mixed-layer from sea surface temperatures only. In many cases this results in reseting the temperature of only the top layer which may produce a deeper mixed layer if the water-column is subsequently lowered.

A major problem with the use of satellite radiometers to determine sea surface

temperatures is that the presence of cloud prevents the observation of the sea surface. This can often result in very poor coverage, particularly in regions such as the mid-latitude North Atlantic where cloud cover is common. Therefore, in order to evaluate the effectiveness of using SSTs to define a mixed-layer, when performing an assimilation and comparing the results with an XBT, the sea surface temperature indicated by the XBT is used instead of satellite observations.

Figure 6.11 shows the same XBTs as figure 6.9. The assimilation has now been performed with the new mixed-layer corrections. The XBT in figure 6.11a has a colder, deeper mixed layer than the climatology so in the first stage of the assimilation, all temperatures warmer than the XBT SST are reset to that value. This has the effect of increasing the mass of the water column so more lowering is required than before (figure 6.9). In this case the combination of SST and SSH anomaly assimilation has brought the climatological profile into good agreement with the XBT. It is a further improvement on assimilation of an SSH anomaly alone.

In the second example, the XBT shows a warmer SST than climatology. The climatology has no mixed-layer so only the uppermost layer is reset to the XBT SST. Lowering of the water column deepens this layer slightly.

There are clear problems with using this technique with a climatological hydrography. The Cooper (1995) scheme is designed to assimilate surface observations into models at regular, and short intervals of time. With a model we already have a water structure with a mixed-layer consistent with the air-sea fluxes. There may still be rapid changes required, but seasonal affects are included in the model. With a climatology representing an annual mean, the actual mixed-layer may be very different and so the assimilation may not result in a good profile. In the summer, when a warm mixed-layer must be created, this is a particular problem.

6.4.2 Filtering out the Steric Component

In the original assimilation scheme, the water column is vertically displaced according to the whole observed sea level anomaly, η, which is the sum of the steric component, η_s, and the permanent thermocline changes, η_{bc}. However, to make a correct displacement, we only want η_{bc}. As the simulation of the mixed layer has problems, it may be better to try to find a way to isolate the steric sea surface

height and remove it from the observed SSH anomaly.

The steric height anomaly is a result of the thermal expansion and contraction of the upper layer of the ocean due to net heat exchanges with the atmosphere. These heat fluxes and the resultant SSH changes vary slowly spatially (Stammer 1997) whereas, in mid-latitude regions and strong currents, changes in the permanent thermocline are dominated by smaller scale phenomena.

Figure 6.12 shows two smoothed sea level anomaly maps from March and September, the months with the extremes of steric height anomaly. The maps have been smoothed with a 20°x20° box average, which removes the small scale features. It can be seen that there is a large-scale seasonal variation, up to 14cm difference in SSH between the two months. This agrees with Stammer (1997), who compared TOPEX/POSEIDON sea level anomalies averaged over seasons. They found differences of about 12cm between spring and autumn in the northern hemisphere and 6cm in the southern hemisphere. Atmospheric seasonal variations are more extreme over land masses, hence the northern hemisphere shows greater steric variation.

The areas of largest seasonal sea surface height variation are in mid-latitudes on the western sides of the oceans. This is because summer and winter air temperatures are more extreme over continents and the prevailing westerlies at mid-latitudes bring the cold or hot continental air over the western oceans. Towards the equator, the seasonal cycle in solar radiation is less pronounced so there is less heating and cooling of the mixed-layer. The steric height anomaly is therefore much smaller in the tropical regions.

The large-scale structure shown by figure 6.12 is largely attributed to the steric height anomaly, η_s, particularly in mid-latitudes. Therefore, if we subtract this smoothed altimetric field from the original TOPEX/POSEIDON sea level anomaly map, the remaining surface height anomaly should represent η_{bc}. We have, in effect, filtered out the surface height which results from mixed-layer and seasonal thermocline changes. The baroclinic surface height anomaly, η_{bc}, can then be used to displace the water column, giving a more accurate estimate of the permanent thermocline.

The twenty degree smoothing is only an approximation of the steric height anomaly. Not all the large-scale structure seen in figure 6.12 will be the result of

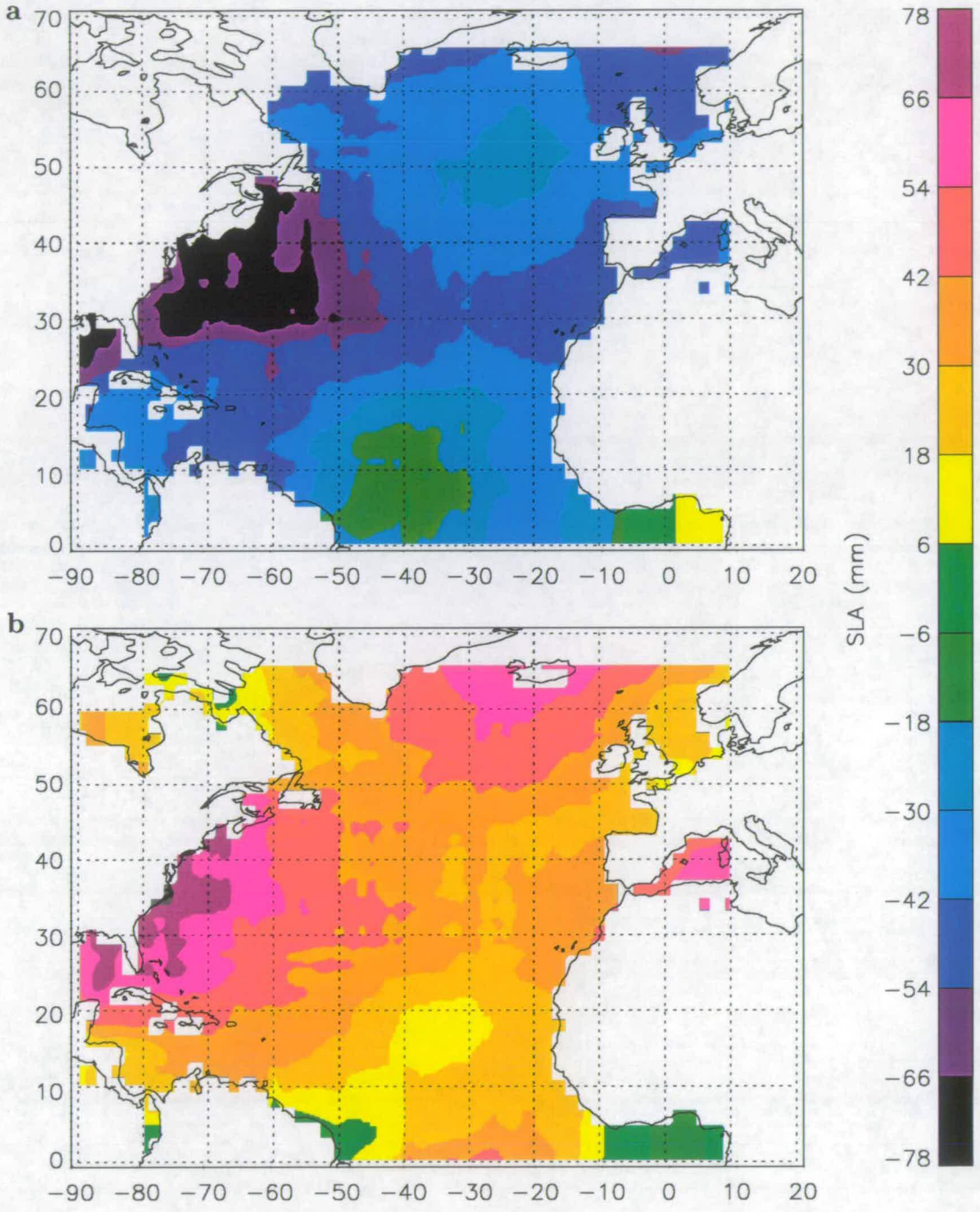

Figure 6.12: TOPEX/POSEIDON sea level anomaly maps smoothed with a 20°x20° box average. Maps are from **a)** 11/3/93 and **b)** 7/9/93.

seasonal thermal expansion. Stammer (1997) estimated seasonal average steric SSH anomalies from ECMWF net surface heat fluxes. He subtracted these from the respective seasonal average T/P SSH anomalies giving the residual dynamic component, η_{bc}. In mid-latitudes the revealed dynamic SSH structure was dominated by small-scale variations. However, in the tropics there are considerable large-scale differences between seasons. The estimated steric component is very small here and most of the variability is due to changes in wind stress. These large-scale features will be filtered out by the above method whereas they are in fact due to the dynamic height, η_{bc}.

Examples of a large-scale anomaly in the tropical Pacific can be seen in figure 5.6. Along the Equator, there is a long stretch of anomalously high sea level and also a large area of low sea surface height between 10° and 20°N. These are related to changes in wind stress and ocean currents and would be wrongly filtered out by this method.

It is likely that while the filter method will produce improvements in assimilation in mid-latitudes, in the tropics, it is more probable that it will be detrimental. The best approach may be to treat the tropical regions separately from the rest of the oceans.

6.4.3 Results of assimilation accounting for steric height changes

In the last section, the effect of seasonal heating and cooling on the upper layers of the ocean and the related changes in sea surface height were discussed. Two methods were proposed to overcome this problem. The first involves the use of sea surface temperatures to estimate a mixed-layer to adjust the climatological profile. The second is a filter to remove the variation in sea surface height due to heating and cooling of the upper layers.

Figure 6.13 and figure 6.14 show the results of assimilation with the sea surface temperature assimilation and steric filter respectively. Table 6.3 gives the overall results of assimilation with these modifications. The results also include hydrography correction and are limited to cases where the sea level anomaly is greater than 10cm.

The use of sea surface temperatures from XBTs in the assimilation produces

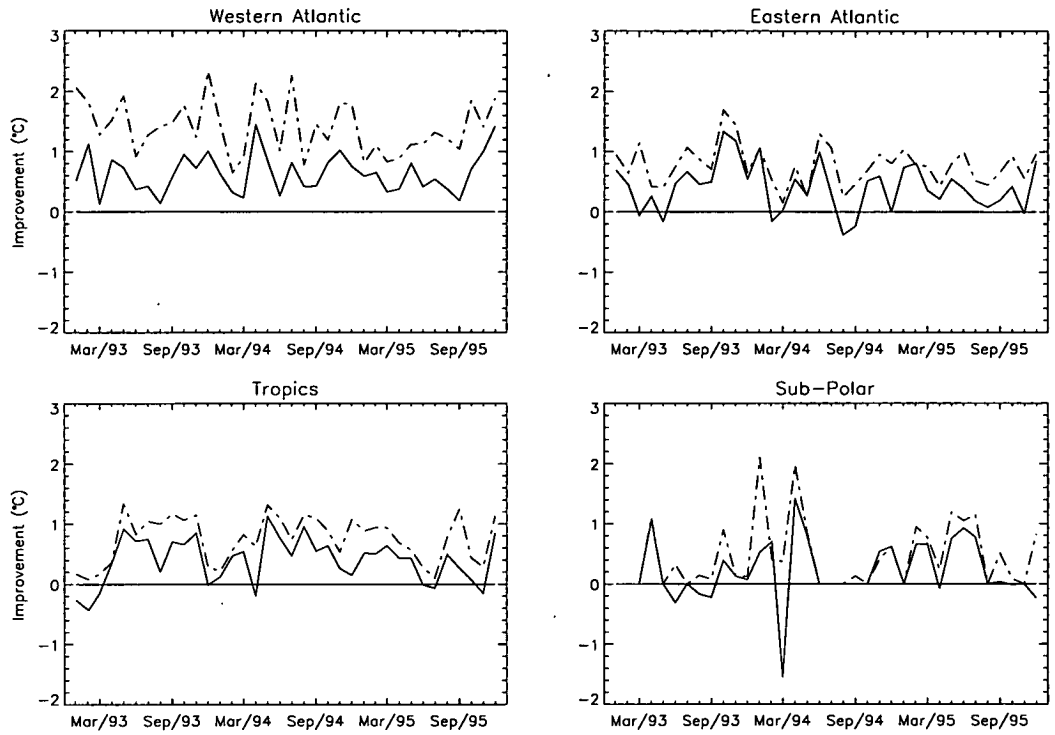

Figure 6.13: As figure 6.8 with assimilation of sea surface temperatures. Including 93-95 correction.

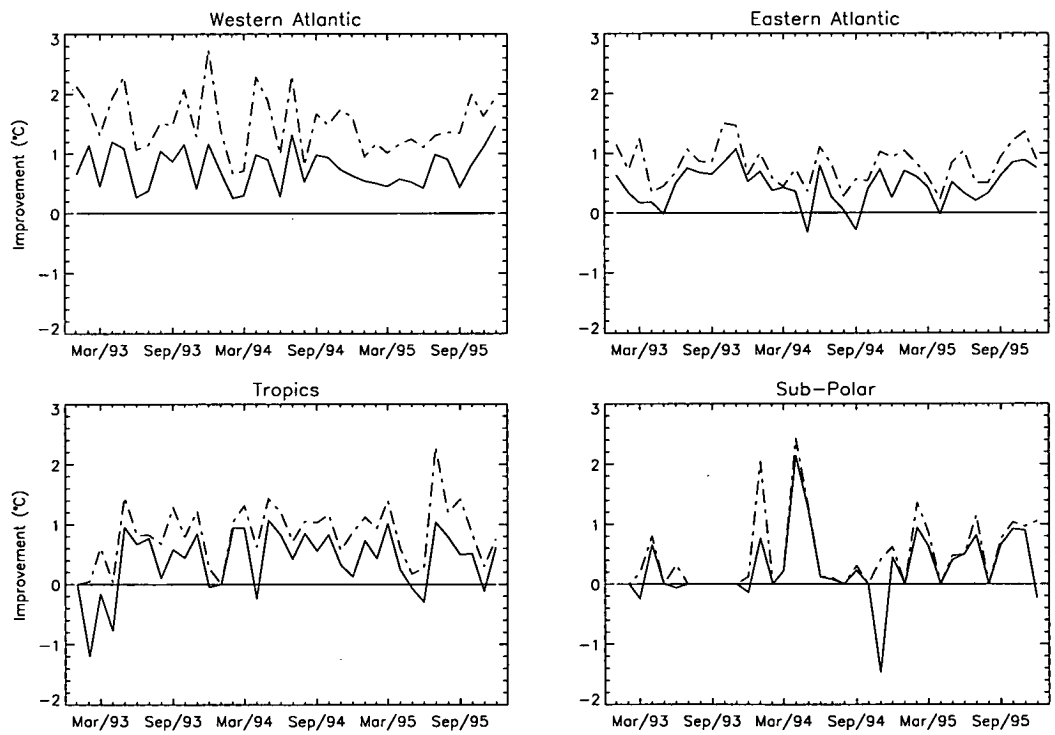

Figure 6.14: As figure 6.8 but sea level anomalies have been spacially filter to remove the steric effect. Including 93-95 correction. SSTs are not assimilated.

		Western Atlantic	Eastern Atlantic	Tropics	Subpolar
SST Assim.	Original	2.51	1.32	1.42	0.80
	Assimilation	1.87	0.91	1.03	0.59
	Improvement	25.4%	30.8%	27.6%	26.1%
Best possible		56.3%	59.1%	53.1%	58.7%
Steric Filter	Original	2.65	1.40	1.46	0.80
	Assimilation	1.90	0.95	1.06	0.53
	Improvement	28.4%	32.4%	27.2%	33.2%
Best possible		57.1%	58.5%	58.0%	61.5%

Table 6.3: Overall temperature differences (in °) for assimilation with SSTs and steric filter. The assimilation includes a pre-assimilation correction to 93–95 hydrography. A 10cm limit on SLAs in in force.

mixed results. In the Western Atlantic, the overall improvement is worse than without using SSTs but it is better in the east Atlantic and subpolar regions. In the tropics the improvement is nearly the same. There are no significant differences in the shapes of the lines in figure 6.13 compared to figure 6.8.

When the steric filter is applied to sea surface height anomalies, their values are changed. Consequently, different locations will be over the 10cm anomaly limit which is why the initial temperature differences in table 6.3 are different here than for previous assimilation tables. Therefore, it is the relative improvements that are compared.

Relative improvements are all better than both original assimilation and assimilation with SSTs, except in the tropics where the result is the same. In both western and eastern mid-latitudes, the steric filter performs well, improving the assimilation scheme significantly. In all cases, the steric filter has reduced the number of XBTs where the sea level anomaly is greater than 10cm. This probably accounts for the increased noisiness in figure 6.14. There does not appear to be a seasonal cycle but this may be hidden by the noise in the time series.

In the eastern Atlantic the improvement is excellent and is better than half of the best possible improvement. The numbers of qualifying XBTs is less with the steric filter, increasing the variation in the results. In the tropics, the overall improvement is the same as without the filter. This is not surprising, indeed a worse result might have been expected as in these regions a lot of sea surface

height anomalies are due to changes in the wind driven currents and are large-scale features. These may be taken out of the sea level anomaly used in assimilation by the filter when in fact they do reflect changes in the thermocline structure.

In the subpolar region, the number of XBTs contributing to the statistics has been further reduced by the steric filter leaving a very uneven time series of improvement. As for the tropics, many anomalies tend to be large-scale and so are reduced by filtering. One problem which may arise, particularly in the subpolar region, is that of a significant barotropic mode component to the sea surface height. Some of this barotropic mode may also be filtered out from the SSH anomalies which may account for some of the increase in improvement here.

Figures 6.15, 6.16 and 6.17 show the mean of the modulus of temperature differences between climatology and XBTs against depth for ordinary assimilation, assimilation with additional SST information and assimilation with steric filter respectively. The means have been compiled by averaging differences from all three years into four seasonal periods, January to March, April to June, July to September and October to December. The minimum sea level anomaly limit of 10cm was in force. The contributing data have come from all of the North Atlantic.

Figure 6.15 shows the results of straight assimilation of sea level anomalies. It can be seen that original differences are reasonably constant with depth except at 100m where the mean difference is larger, particularly in summer and autumn. There are good improvements with assimilation below 200m, but near the surface the improvement is reduced in summer. This is a result of seasonal changes in the mixed-layer which cannot be recreated with the original assimilation scheme.

The results of the use of SST information to supplement sea level anomalies in the assimilation are given in figure 6.16. In the winter, the errors have been reduced in the upper layers but in summer they are much worse. This is not surprising as no satisfactory method of simulating a summer state of a mixed-layer and seasonal thermocline was found. The approach of setting a maximum for the temperature profile when the observed SST is less than the climatological appear to be effective in the winter months.

Finally, figure 6.17 shows the performance of the assimilation scheme with sea surface height anomalies which have been filtered to remove the steric component.

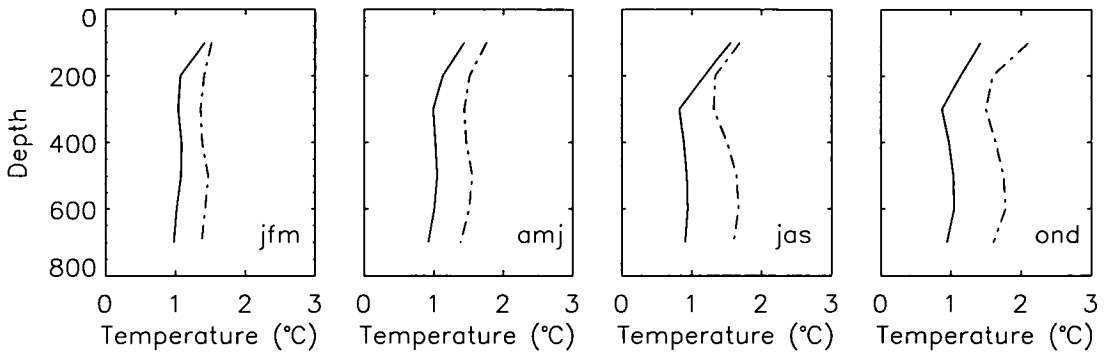

Figure 6.15: Mean of modulus of temperature differences between climatology and XBTs against depth, respectively, January–March, April–June, July–September, October–December. The dashed line is the original climatology and the continuous line is after assimilation.

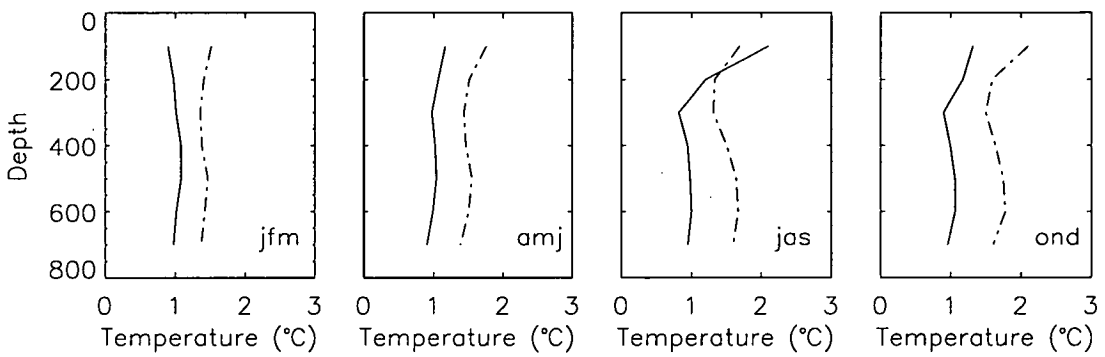

Figure 6.16: As figure 6.15 with SST information included in assimilation.

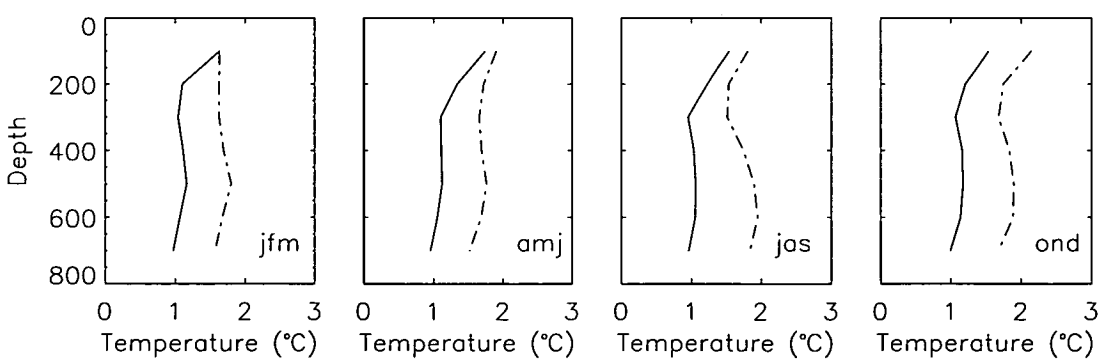

Figure 6.17: As figure 6.15 with steric filter on sea level anomalies

	Western Atlantic	Eastern Atlantic	Tropics	Subpolar
Lozier Original	1.92	0.84	1.01	0.92
Steric	1.50	0.69	0.85	0.71
Filter	21.9%	17.1%	15.5%	23.6%
Best	0.97	0.44	0.55	0.47
Possible	49.4%	47.8%	44.9%	48.9%
Levitus Original	2.19	0.84	1.01	0.84
Assimilation	1.66	0.69	0.85	0.73
+ Steric filter	24.3%	17.7%	15.6%	13.4%
Best	1.18	0.45	0.56	0.52
Possible	45.9%	46.6%	44.3%	37.8%

Table 6.4: Mean temperature differences in °C and relative improvements from original, uncorrected climatology. There is no limit in force. Assimilation results include correction and steric filter.

This method does not attempt to improve the climatological profile in the mixed-layer, but should reduce the overall error. This is reflected in these results where the shape of the difference profiles are similar to those produced by the simple assimilation but over all depths the improvement is slightly better.

6.5 Assimilation with Levitus 1994 Climatology

The Lozier et al. (1995) climatological hydrography has been employed so far but this assimilation scheme has also been used with the Levitus (1994) climatology. For the most part, Levitus is similar to Lozier, the main difference being the large smoothing scale employed by Levitus. A new mean displacement field was calculated to make the Levitus hydrography consistent with the average state of the ocean for 1993–1995. As with the Lozier climatology, the best version of the assimilation scheme was found to require the 93–95 correction and filtering the sea level anomaly fields to remove the steric height anomaly.

The overall results from assimilating altimetry with Levitus 1994 climatology are presented in table 6.4. These include 93–95 correction displacement and steric filter. The results are very similar to those with Lozier in the Eastern Atlantic and Tropics. It is interesting that in the subpolar region, Levitus starts closer to the XBTs but the end result is very similar to the Lozier result.

The main difference between Lozier and Levitus results are in the Western Atlantic. The greater smoothing of the Levitus hydrography has a large effect on the Gulf Stream where horizontal temperature and salinity gradients are steep. In this area, the large-scale smoothing of Levitus leads to a hydrography which agrees less well with XBTs than Lozier. This is illustrated by the greater initial difference between Levitus and the XBTs, and further emphasized by the best fit. After correction and assimilation, Levitus is still not as good as Lozier.

6.6 Other problems

6.6.1 Spatial differences

The climatological hydrography consists of water-columns regularly gridded on a 1° grid. Each profile is located at the centre of a 1° square, i.e. 35.5°N, 49.5°W etc. The XBTs, by contrast, are irregularly positioned. For assimilation the nearest climatological profile to an XBT has been chosen and vertically displaced according to the SSH anomaly and then compared with the XBT. Because of the resolution of the grid, the XBT will never be more than 0.7° away from a profile. However in some areas, notably frontal regions, temperature gradients can be very sharp and two temperature profiles, separated only by 1°, may be significantly different.

Figure 6.18 shows an XBT with the four immediately surrounding climatological profiles before and after assimilation. All four climatological profiles have been displaced according to the SLA, determined by interpolation from SLA gridpoints, at the position of the XBT. These are from the Gulf Stream front. The original climatological temperature profiles do have considerable differences although they are close together. For example, the difference between the surface temperatures of the North Western (a) and South Eastern (d) profiles is about 3°C. Consequently, when each profile has the SSH anomaly at the XBT assimilated with it the results are even more different.

The assimilation with the nearest profile (SE) gives a result that compares reasonable well with the XBT but the assimilation with the North Western profile makes it much worse. The XBT was located at 43.8°N 43.7°W whereas the climatological profiles are at latitudes of 43.5°N and 44.5°N and longitudes 43.5°W and

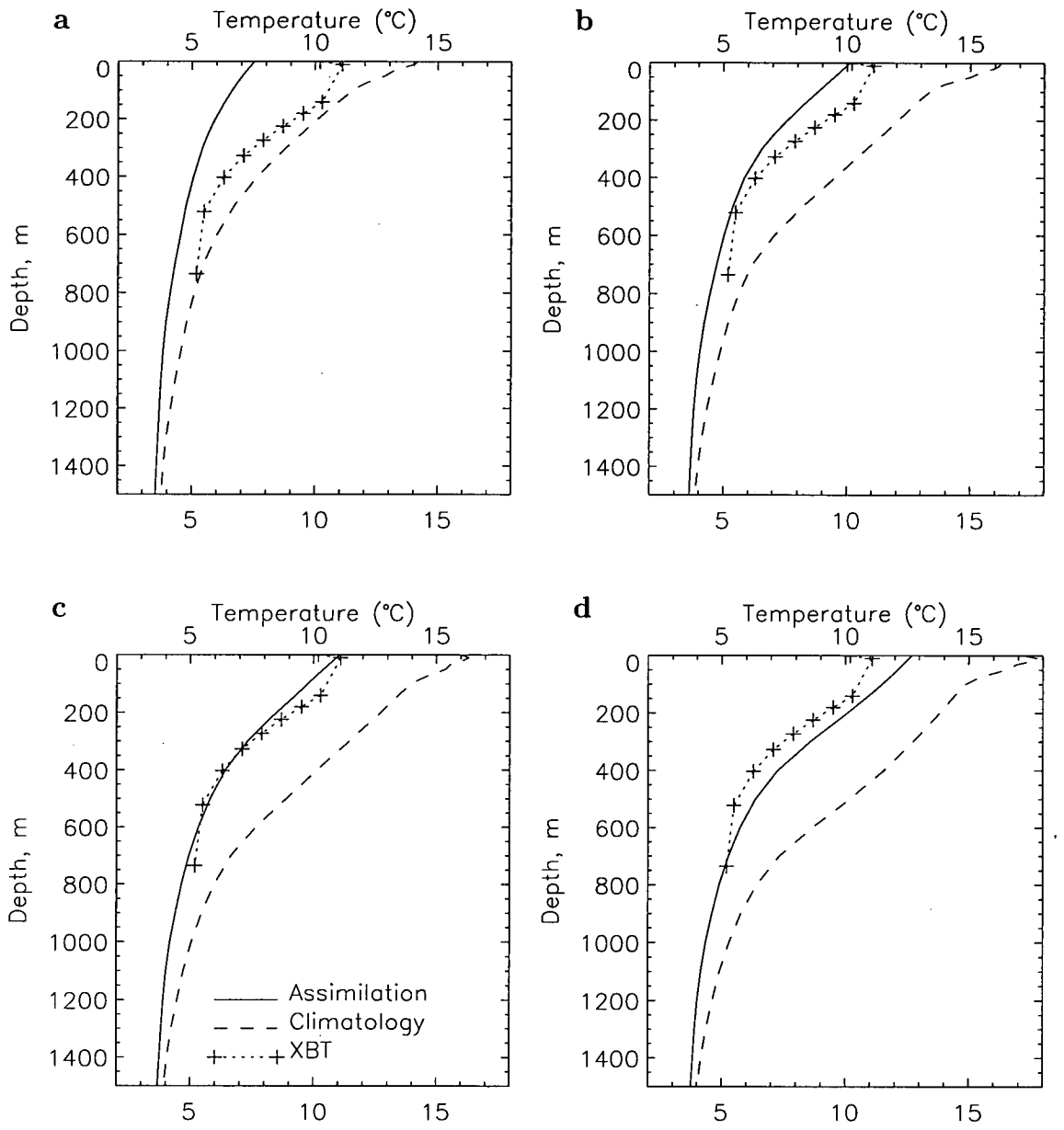

Figure 6.18: One XBT from 18/4/94 43.8°N 43.7°W compared to the four surrounding climatological temperature profiles before and after assimilation. The four figures show the same XBT and the climatological profiles **a)** NW, **b)** NE, **c)** SW, **d)** SE of the XBT position. The XBT is nearest the South Eastern profile.

44.5°W. The appropriate profile at the location of the XBT will be somewhere between the four surrounding profiles.

6.6.2 Advection

The assimilation scheme is conservative, preserving the shape and structure of a water column, by lifting and lowering it, only adding new waters at the top or bottom. However, in reality, horizontal advection and mixing of water masses may change the shape of temperature profiles. In section 6.3 it was described how long-term changes in water structure were accommodated by a mean vertical displacement of water columns to XBTs from the three years under consideration. However, if advection has occurred at one level bringing water of a different temperature, the shape of the profile may be changed completely and this cannot be accounted for by this method.

It is also the case that during the three years of assimilation, the shapes of the temperature profiles may change during this time. In assimilation of satellite altimetry into ocean general circulation models, the model will control advection and profile shape will change as a consequence. It is unlikely that the shape of profiles in the period 1993–1995 will be the same as throughout all the time from which the climatology is compiled. The climatology is a first estimate of the ocean structure but may contain data similar to the 1993–95 period.

However, it is worth noting that there is a remarkable agreement between the shapes of climatological temperature profiles and XBTs from 1993–1996. As shown by the examples so far, climatology does generally fit the shape of XBTs very well. Sometimes the climatology has a thermocline that is less steep than the XBT but this is due to the smoothing of the climatological hydrography.

In figure 6.19 there are two examples where the XBT has a different form to that of the climatological temperature profile. The profiles are from different parts of the Gulf Stream front. Both XBTs have more convex shapes than the respective climatological profiles indicating advection of warmer waters into the middle of the thermocline has occurred.

Figure 6.19b is from the edge of the subtropical gyre off the east coast of America. The shape of the XBT profile is more similar to the water-structure nearer the centre of the gyre and large amounts of 18°C water can be seen. It is

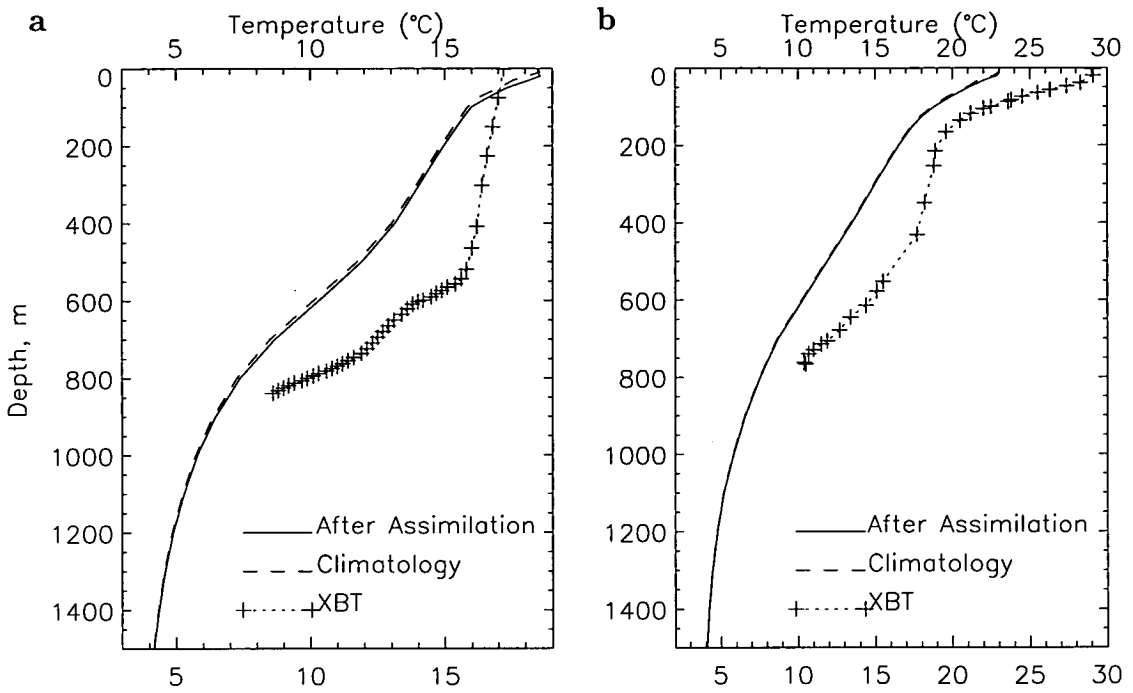

Figure 6.19: XBTs which differ in shape to the nearest climatological temperature profile **a)** 8/5/93 42.0°N 42.0°W, **b)** 10/9/93 36.8°N 72.8°W

clear that water has been advected into this region from the adjacent subtropical gyre.

In figure 6.19a, warmer water has also been advected into the middle of the thermocline. However the origin of this water is not so clear because other profiles nearby do not share the shape of this XBT. Water may have been advected within a certain depth range only, thus changing the form to a unique shape. Salinity information would perhaps help in the understanding of the origin and causes of these changes.

In the cases in figure 6.19, no discernible sea surface height anomalies have been detected and the assimilation scheme has not displaced the profiles significantly. It is not clear why the advection and changes in the water columns have not produced a signals in the sea surface height.

6.6.3 Errors in the Altimetry

Inaccuracies in the assimilation will also result from errors in the sea surface height. There are several sources of error contributing to the sea surface height anomaly maps used in this assimilation method.

The raw altimeter data from which the maps are made have two sources of error, instrument error and orbit error. These combined give an error of about 4cm r.m.s. (Mitchum 1994) on the observed sea surface height. Errors from the tidal model and inverse barometer correction are relatively small.

The maps are produced from the tracked observations by a space/time objective analysis method. There are mapping errors associated with this procedure. The error at a given grid point on a map is dependent on its position in space and time in relation to the satellite tracks and the variability of the sea surface height. Where the sea surface height is more variable, the mapping will incur greater absolute error.

When assimilating a profile to compare with an XBT, the sea surface height anomaly at the time and position of the XBT is determined from the SLA maps by linear interpolation. The SLA data used are in the form of maps for every ten days with a spatial resolution of half a degree. Interpolation between grid points and maps will introduce some errors into the result.

6.6.4 Barotropic Mode

As explained in Chapter 5, the assimilation method vertically displaces a water column thereby altering its mass in compensation for an observed sea surface height anomaly in order to preserve a constant bottom pressure. However, if there is a change in the currents at the bottom of the ocean and therefore a change in the bottom pressure then the vertical displacement that has been calculated in response to an observed SLA may be incorrect.

This assumption of no pressure change at the bottom is reasonable throughout most of the ocean where strong currents and variations are restricted to the upper 1000m. The deeper currents are both much slower and more constant. At the very bottom of a water column we can expect only small changes which are insignificant compared to upper ocean activity.

However, in the subpolar region, the water is very poorly stratified (figure 5.4) and in the winter very deep convection can occur in the Greenland and Labrador seas. Here the bottom pressure is likely to be affected by changes in the water column above it and will not remain constant. As figure 5.3 illustrates, moderate sea level anomalies often result in large displacements by the assimilation scheme

	Western Atlantic	Eastern Atlantic	Tropics	Subpolar
Original	1.92	0.84	1.01	0.92
Straight Assimilation	1.77 8.3%	0.76 8.7%	0.91 9.4%	0.88 3.8%
Correction Only	1.69 12.2%	0.76 9.0%	0.94 6.4%	0.76 16.6%
Correction + Assimilation	1.51 21.1%	0.72 13.8%	0.85 15.0%	0.70 22.6%
SST Assim.	1.61 16.1%	0.69 17.4%	0.85 15.8%	0.71 22.4%
Steric Filter	1.50 21.9%	0.69 17.1%	0.85 15.5%	0.71 23.6%
Best Possible	0.97 49.4%	0.44 47.8%	0.55 44.9%	0.47 48.9%
Levitus Original	2.19	0.84	1.01	0.84
Assimilation + Steric filter	1.66 24.3%	0.69 17.7%	0.85 15.6%	0.73 13.4%

Table 6.5: Mean temperature differences in °C and relative improvements from original, uncorrected climatology. There is no limit in force. Results from assimilation with SSTs and steric filter include correction to hydrography. Levitus assimilation results include correction and steric filter.

in high latitudes. A significant part of these anomalies are likely to be the result of either mixed-layer heating and cooling from surface exchanges as mentioned in section 6.4 or from the barotropic mode or simply advection.

6.7 Summary of Results from North Atlantic

Table 6.5 lists all the overall temperature differences between climatology and XBTs for all assimilation samples with all versions of the assimilation scheme without the 10cm limit. It shows the overall performance of the assimilation scheme in the different regions of the North Atlantic.

The assimilation scheme on its own produces an improvement, but it is clear that the correction of the climatology for long-term variability makes a significant difference in all areas. This is particularly so in the Western Atlantic where there is a large difference in the Gulf Stream between the period 1993–1995 and the climatology.

The correction also has a large effect in the subpolar region. As reported previously, there are problems with the correction and the assimilation statistics in this region. Both are based on taking differences in temperature between XBTs and climatological profiles at standard depth levels from 100m to 700m. However, in this region the main thermocline is often shallower than 100m and so the differences are based on the more uniform waters below. Consequently the differences and improvements reported here may not be a true representation of how close the climatological profiles match XBTs.

Although figure 6.6 shows that there is little difference between the original climatology and the 93–95 climatology in the Eastern Atlantic or the tropics, it still does improve the assimilation significantly.

There are mixed results from the two methods used to address the mixed layer problem. In the Western Atlantic, the steric filter method seems to make little difference to the assimilation scheme while using XBT SST actually reduces the effectiveness of the assimilation. In contrast, in the Eastern Atlantic, both methods make significant improvements to the assimilation. In the tropical and subpolar regions the effects are small. The steric filter method gives the best results overall although there is an argument for not using it in the tropics.

Figure 6.20 is a map of the mean difference, ΔT_c, between XBTs and the original smoothed Lozier climatology. The largest differences follow the Gulf Stream very closely. Most of the rest of the ocean has relatively small differences except for a region in the Western Tropics.

Figure 6.21 is the same as figure 6.20 but shows the mean difference, ΔT_A, between the hydrography after assimilation and XBTs. Figure 6.22 shows the overall improvement using all XBTs between 1993 and 1995 and figure 6.23 shows the improvement due to the 93–95 correction displacement alone. The maps were produced by averaging improvements from XBTs by the method described in appendix A with an influence radius of 5 degrees. This method gives a smooth map with coarse resolution. Finer resolution would be subject to natural temporal and small-scale spatial variability as XBTs are irregularly distributed.

These show that the best results from assimilation are located in mid-latitudes, with the majority of the ocean recording an improvement of greater than 10%. The large improvement off Greenland is almost entirely from the 93–95 correction

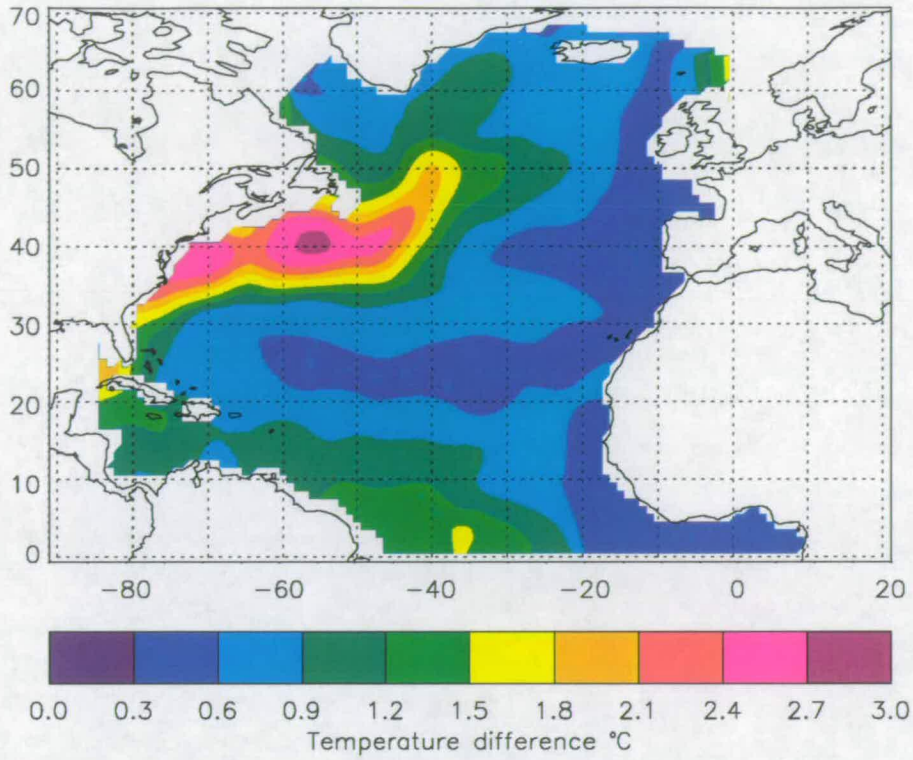

Figure 6.20: Map of mean temperature differences between XBTs and original smoothed Lozier climatological hydrography.

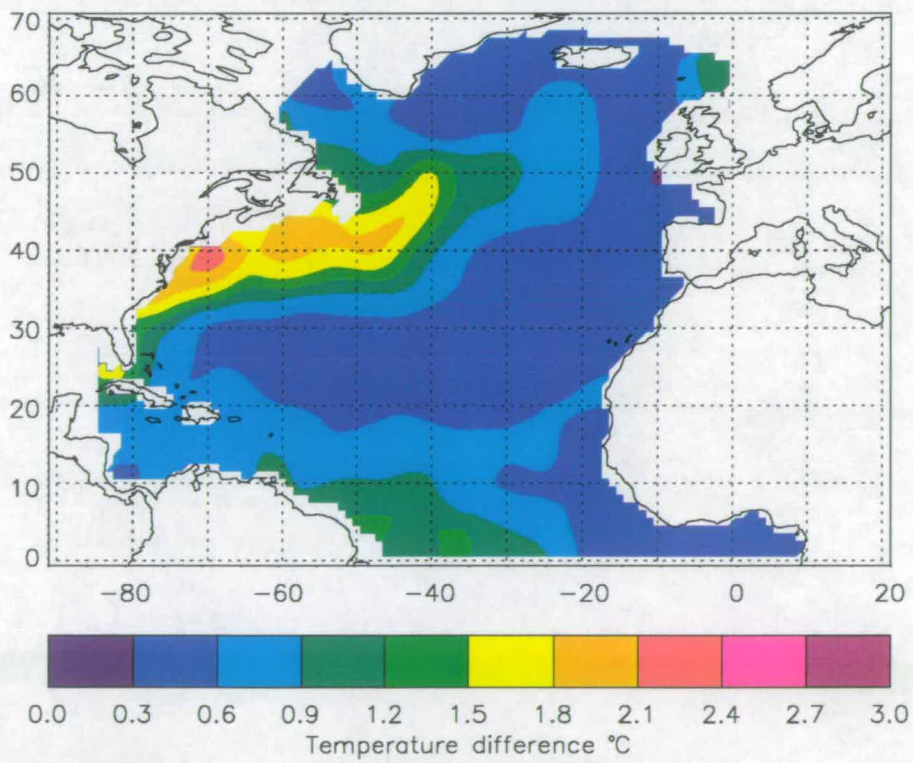

Figure 6.21: Map of mean temperature differences between XBTs and hydrography after assimilation with 93–95 correction and steric filter

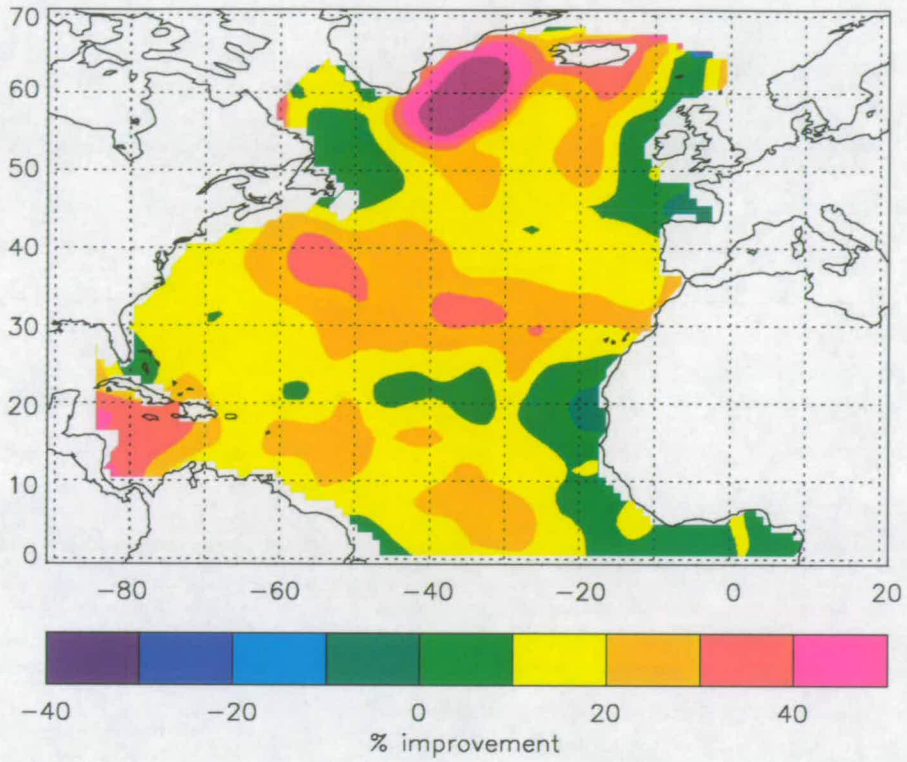

Figure 6.22: Improvement of climatology after assimilation compared to XBTs including correction displacement and employing the steric height filter.

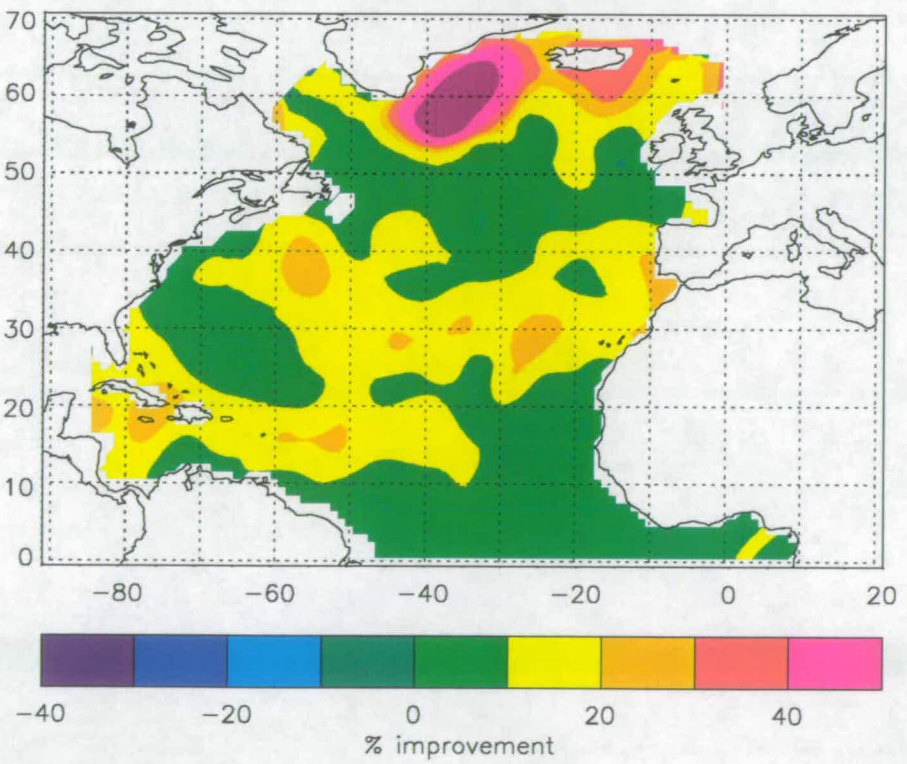

Figure 6.23: Improvement of climatology after correction displacement alone compared to XBTs.

displacement.

There is a small area off the west coast of Africa where the improvement is negative. In this area, the differences between climatological temperature profiles and XBTs are always small, the correction for long-term variability is small and sea level variability is also low. Thus, any errors in altimetry or elsewhere may have a significant effect on the results. There are no obvious reasons why this area shows a worsening of the hydrography with assimilation.

Figure 6.24 shows the mean improvement of Levitus with 93–95 correction and assimilation of filtered altimetry. Figure 6.25 gives the improvement due to 93–95 correction alone. In comparison to Lozier, more of the overall improvement can be attributed to the 93–95 correction, particularly around the Gulf Stream. Also noticeable is that less correction is required in Levitus in the area south of Iceland. It appears that Levitus gives a better representation of this part of the ocean than Lozier.

Over most of the ocean, Levitus and Lozier climatologies are very similar. However, in the sharp gradients of the Gulf Stream, Lozier temperature profiles are closer in shape to XBTs than Levitus. It has been found that, on the whole, the Lozier climatology, after correction for long-term variation, gives the best results for assimilation with sea level anomalies.

The primary conclusion to be brought from examining the mixed-layer is that this method can only recreate the permanent thermocline and that efforts to simulate a mixed-layer give unsatisfactory results. It appears that the best way is to ignore those layer affected by seasonal effects and air–sea interaction and filter out the steric component of the sea level anomaly. Hence, post-assimilation hydrography is likely to be worst in the top 100–200m.

6.8 Pacific Results

In addition to the North Atlantic trials, the assimilation was also tested in the Pacific Ocean. The climatological hydrography used was Levitus (1994) and the satellite altimetry is the same as for the North Atlantic; sea level anomalies from 1993–1995.

Figure 6.26 shows the distribution of XBTs in the Pacific for this period. As in

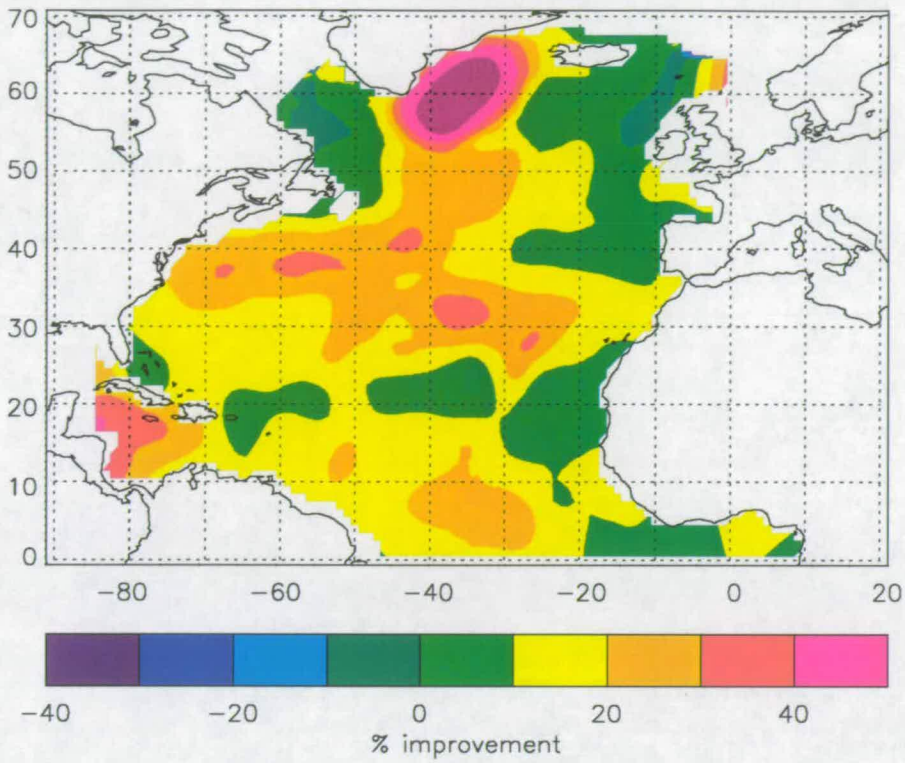

Figure 6.24: Improvement of Levitus 1994 climatology after assimilation compared to XBTs including correction displacement and employing the steric height filter.

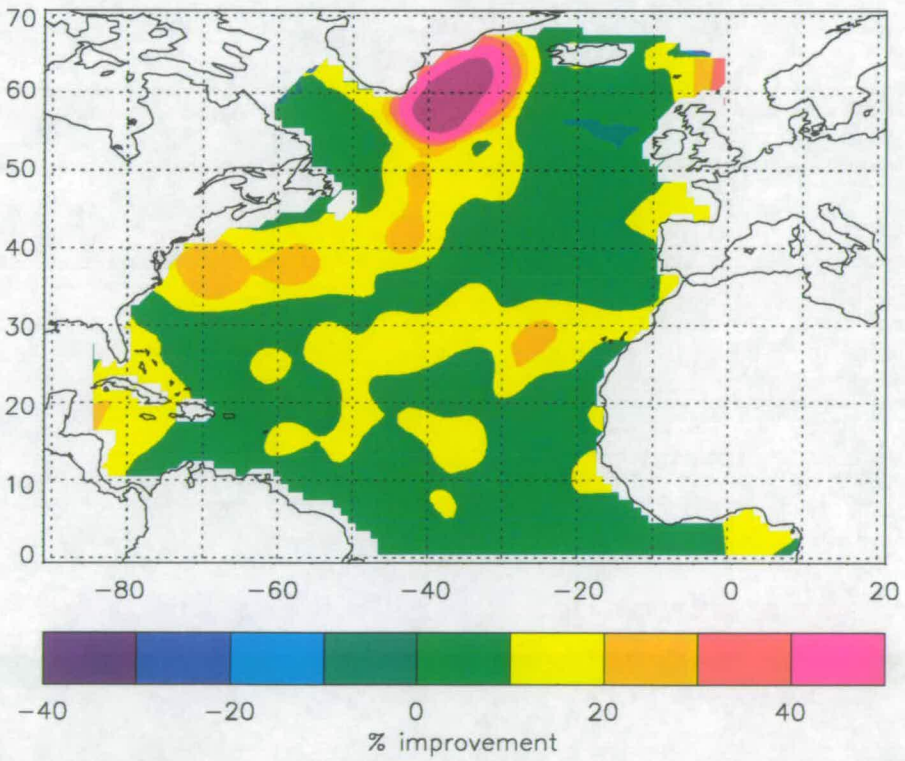

Figure 6.25: Improvement of Levitus 1994 climatology after correction displacement alone compared to XBTs.

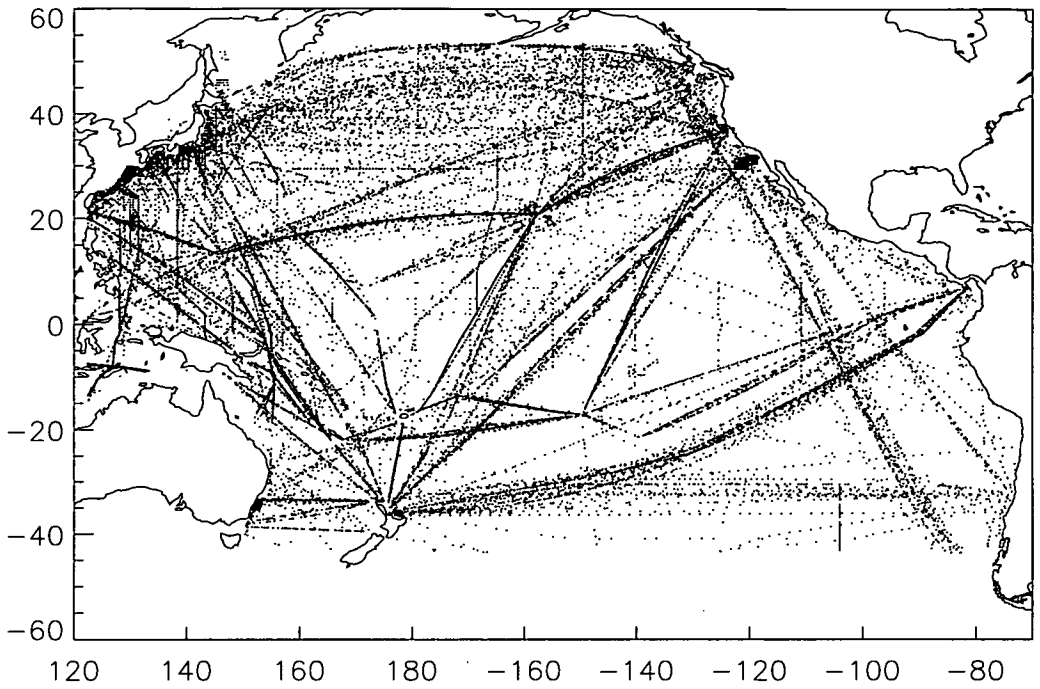

Figure 6.26: Location of XBT measurements in the Pacific Ocean between 1993 and 1995 inclusive.

the Atlantic, the pattern is dominated by lines of XBTs following major shipping lanes. XBTs are very dense off the coast of Japan and in the western Pacific. There is good coverage over most of the northern Pacific, but as the ocean is much larger, the XBTs are not as concentrated as in the North Atlantic. In the southern Pacific, XBTs are mostly restricted to the shipping lanes and there are some considerable gaps in the data. XBTs are very scarce south of 40°S.

Between 10°S and 10°N can be seen several regular meridional lines of XBTs across the full width of the ocean. Here, the ocean and atmosphere is monitored as part of the Tropical Ocean–Global Atmosphere (TOGA) project (Kessler et al. 1996). There is an array of buoys moored at fixed points along several meridians, nominally 15° of longitude apart, between 10°S and 10°N across the whole of the ocean. These measure, amongst other observations, the water temperature at standard depths down to 500m (Hayes et al. 1991). Complementing these observations, the Volunteer Observing Ship XBT program (Meyers and Donguy 1980, Smith and Meyers 1996) samples 3–4 meridional ship tracks in the tropical Pacific approximately once a month. Consequently there are a large amount of temperature profile data along these meridians at many different times through-

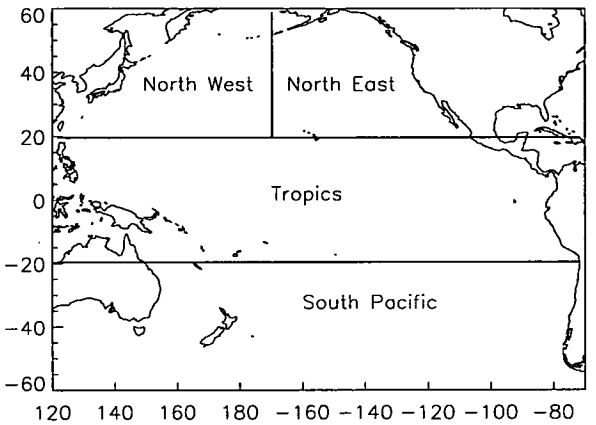

Figure 6.27: Division of the Pacific Ocean into regions to study assimilation.

out the period.

For analysis of the assimilation results, the Pacific has been divided into four regions as indicated in figure 6.27. As there are many, widely distributed XBTs in the North Pacific this has been split into eastern and western sections with the west dominated by effects associated with the Kuroshio Current. Due to the paucity of data in the south Pacific, this is considered as one region. Between 20°S and 20°N is the tropical region. This is an important region as there are large-scale variations in currents and water masses here, such as the El Niño phenomenon. There are insufficient XBTs in subpolar regions to justify a separate region for study.

Mean Displacement Field

Figure 6.28 shows the mean displacement field required to correct the Levitus 1994 hydrography to fit XBT observations during 1993-1995. This is equivalent to the North Atlantic mean displacement field of figure 6.6. It is noticeable that Pacific displacements are considerably smaller in magnitude than in the North Atlantic.

The largest displacements are a line of lifting stretching across the Pacific from north Japan to off southern Alaska. This appears to run along the northern edge of the front and is mostly a result of the smoothing in the production of the Levitus 1994 hydrography. A line of lowering south of the lifting areas supports this theory. In the tropics, there is a large region of water-column lifting. While

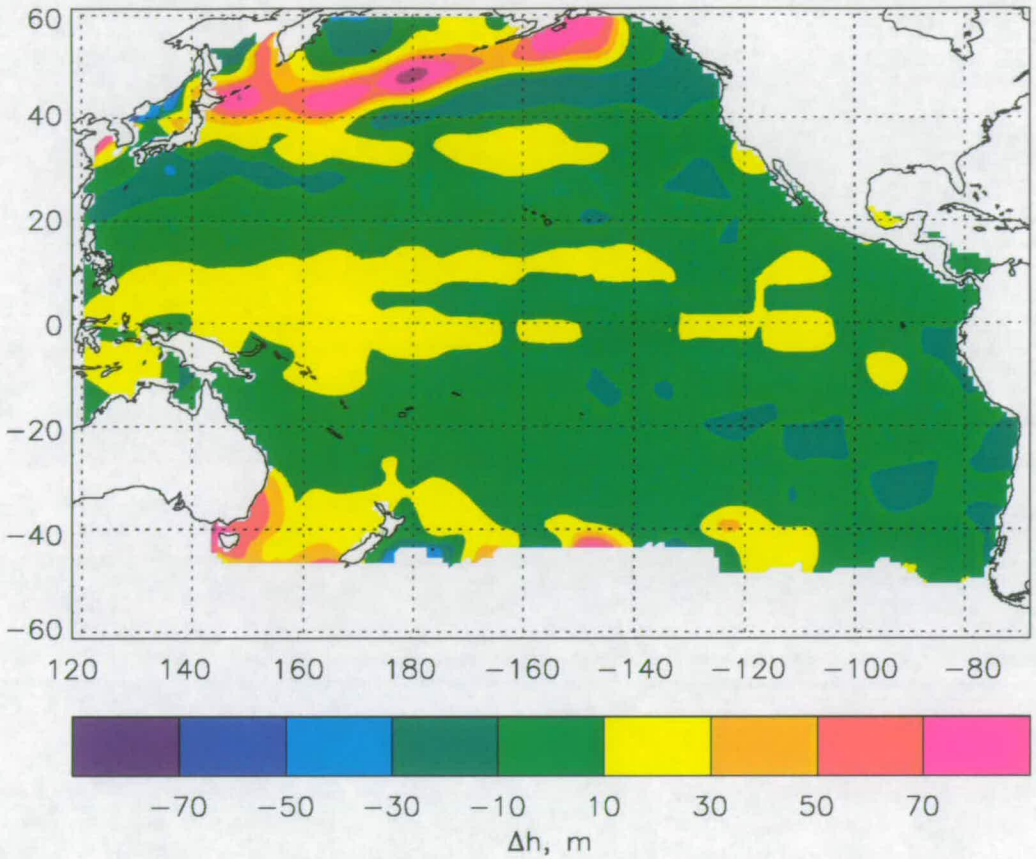

Figure 6.28: Vertical displacement of water columns from Levitus 1994 climatology required to agree with XBT observations from 1993–1995.

	North West	North East	Tropics	South
Original	1.65	0.64	1.08	0.90
Assimilation Only	1.47 10.5%	0.61 4.3%	0.95 12.2%	0.77 14.9%
Correction Only	1.61 1.9%	0.61 4.7%	0.96 11.6%	0.84 6.9%
Correction + Assimilation	1.43 13.4%	0.58 8.6%	0.80 25.9%	0.73 18.9%
Correction + Steric Filter	1.43 12.9%	0.56 12.7%	0.85 21.7%	0.73 19.2%
Best Possible	0.88 46.5%	0.38 41.1%	0.53 50.7%	0.41 54.8%

Table 6.6: Overall results for the Pacific Ocean. The table gives mean temperature differences in °C between XBTs and hydrography and the percentage improvement achieved by assimilation and modifications.

this is relatively small in magnitude it is significant as the thermocline is very steep here.

In the far south the mean displacement field is cut off where the numbers of XBTs become too few to give a reliable average. It can be seen that along the edge of this cut off, there are a few small areas of large displacement a result of compiling averages from scarce, highly variable data.

6.8.1 Results

Table 6.6 lists the mean temperature differences between hydrographies and XBTs from each region over all three years. Temperature differences refer to XBTs compared with the original Levitus 1994 hydrography, with hydrography after simple assimilation of altimetry only, with hydrography after 93–95 mean correction displacement only, after correction displacement and assimilation, and after correction with assimilation of filtered sea level anomalies. With each difference is listed the improvement from the original hydrography. Also listed are the best possible differences achieveable by displacement with improvement.

The original mean differences between hydrography and XBTs in the Pacific are mostly smaller than their equivalent in the North Atlantic. The only exception is the tropical regions where the mean difference is slightly greater than the North Atlantic.

The Pacific north west region is similar to the Western Atlantic with a strong boundary current and extension. As in the North Atlantic, this region shows the greatest difference between climatology and XBTs. The improvement by the long-term correction is quite small but when followed by assimilation, the improvement is good and greater than the sum of correction and assimilation when performed separately. The steric filter has little effect in this region. The Pacific north west behaves very similarly to the western Atlantic. The smaller overall relative improvement is due to a smaller pre-assimilation correction, improvement due to assimilation is slightly better in the Pacific.

The original climatology in the north east region is closer to XBTs than in the equivalent region in the North Atlantic and assimilation and correction give smaller relative improvement. Like in the North Atlantic, the steric filter produces the best results in this region, making a considerable improvement to the simple

assimilation scheme.

The tropics are an interesting area in the Pacific Ocean. The initial temperature error is slightly larger than in the Atlantic but improvements from both 93–95 mean correction and assimilation are larger than for any other region from either ocean. The steric filter, as expected, reduces the improvement from assimilation. This is due to the signal in the sea level anomaly from large-scale current variations being filtered out.

Assimilation and correction in the south Pacific produces good improvement in the hydrography. The improvement from the assimilation part is larger than the other regions. The steric filter does not make much difference which is similar to the North western Pacific. Figure 6.26 shows that there are more XBTs in the western south Pacific than the east, thus it is expected that these results are similar to those from the north west.

Figure 6.29 is a map of the mean temperature difference between XBTs and the original, pre-assimilation climatological water profiles. The largest differences are associated with the variable Kuroshio but there are also large errors in equatorial regions. This reflects the considerable variations in the tropical Pacific. Eastern mid-latitudes show good agreement between XBTs and climatology.

Figures 6.30 and 6.31 show relative improvements due to assimilation with normal SLAs and filtered SLAs respectively. Both include the application of the correction displacement, the improvement from which is shown in figure 6.32.

There is a strong band across the tropics where the hydrography has been greatly improved by the assimilation process. The tropics show better improvement without the steric filter whereas in mid-latitudes, the filter does have a positive effect. A possible reason for the success of the assimilation, without the steric filter, in the tropics is that as sea level anomalies are large-scale, errors introduced during mapping of the SLAs from the tracked data are small.

The prominent features of these fields are the sharply defined arcs and circles in the tropics. These are an effect of the many repeat observations on the meridional ship tracks and the mapping procedure. So many XBTs have been deployed at these locations that they dominate all grid points around them within the radius influence of the mapping routine. Thus, at the limit of the influence of one of these ship tracks, there is a sudden change in improvement value.

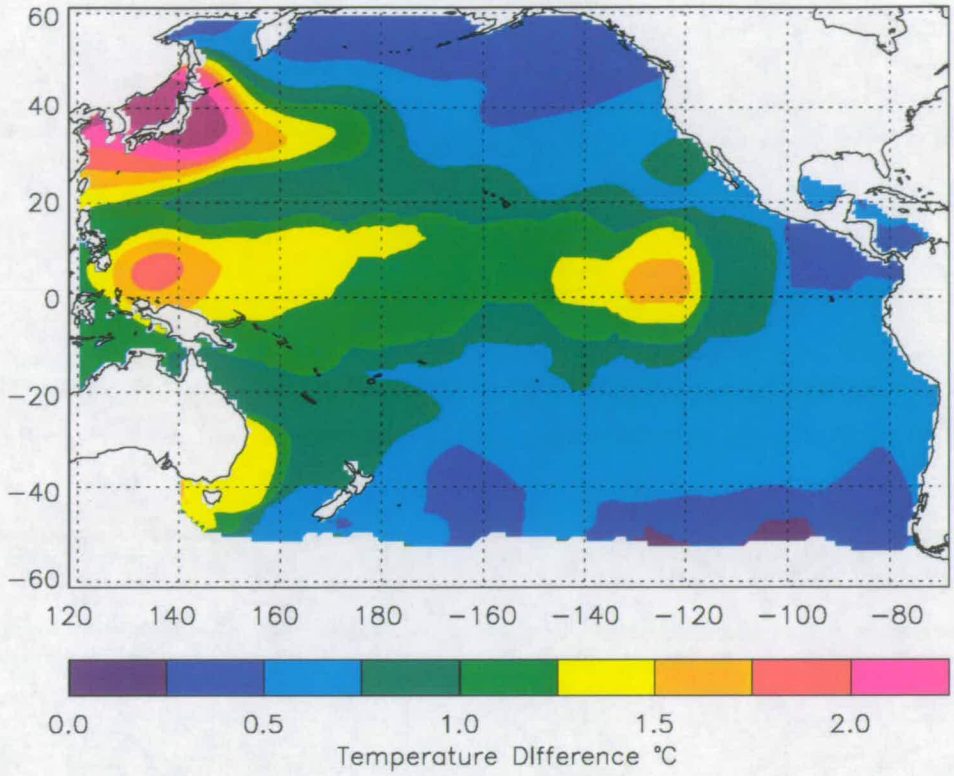

Figure 6.29: Map of mean temperature differences between XBTs and original Levitus 1994 climatological hydrography.

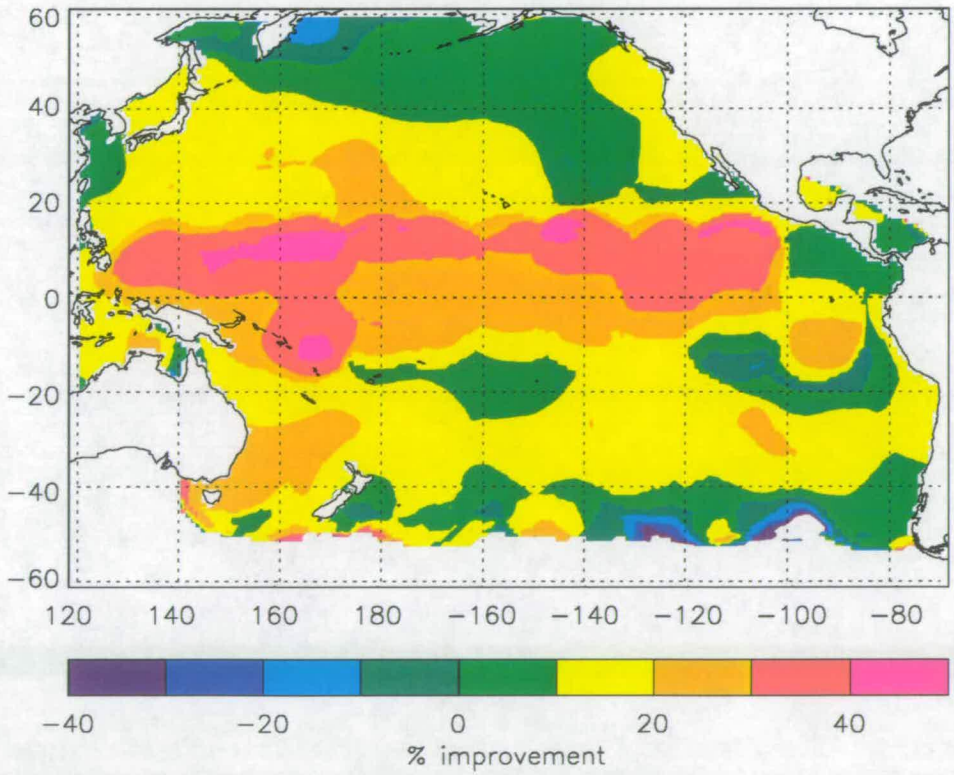

Figure 6.30: Map of relative improvement in temperature differences between XBTs and hydrography after correction displacement and straight assimilation.

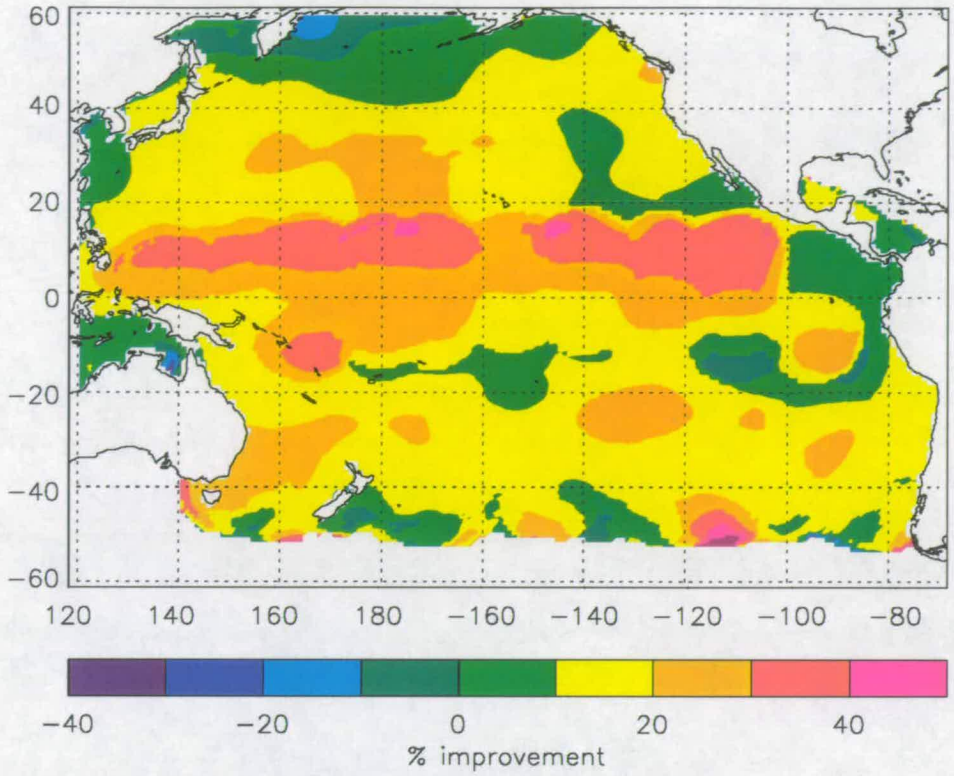

Figure 6.31: Map of relative improvement in temperature differences between XBTs and hydrography after correction displacement and assimilation of filtered SLAs.

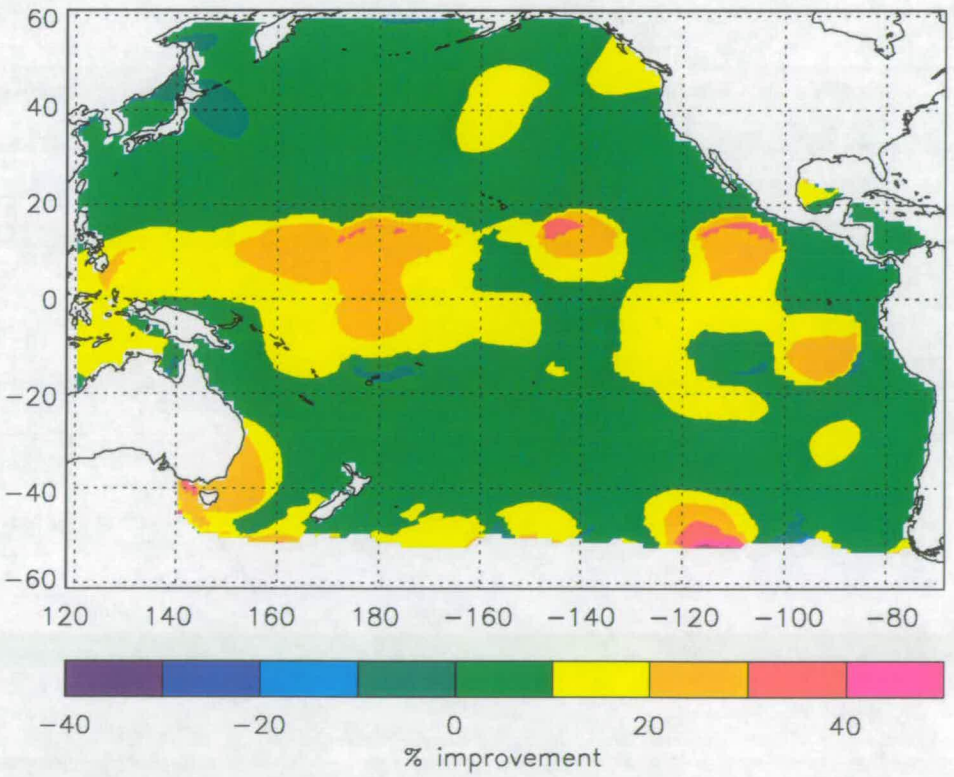

Figure 6.32: Map of relative improvement in temperature differences between XBTs and hydrography after correction displacement only.

The part of the improvement due to the pre-assimilation correction displacement is given in figure 6.32. Over most of the ocean this improvement is quite small, less than 10%, but in the tropics it is more significant. Off the east coast of northern Japan there is a small area of negative improvement which is probably due to errors from mapping of the mean displacement as it is immediately south of a small region of large water column lifting (shown in figure 6.28.)

6.9 Discussion

Sea level anomalies from satellite altimetry have been assimilated with a climatological hydrography in order to produce a hydrography of the ocean at the time of the altimeter observation, a 'nowcast'. It is difficult to compare the results with a nowcast from a model assimilation, e.g. Ezer and Mellor (1997) but it has been shown that it can significantly improve the climatology.

In the North Atlantic, the smoothed Lozier climatology is closer overall to XBTs than the Levitus (1994) both before assimilation and after. The Lozier data set is better in the Gulf Stream region where the excessive smoothing of Levitus has spread out the steep gradients of the front.

It was found that, due to longer term variability, the climatological hydrography was not consistent with the mean hydrography during the three years, 1993–95, from which the mean sea surface height was determined. It is crucial that the pre-assimilation hydrography represent the mean ocean state during this time. In order to overcome this problem, the climatological water columns were first displaced vertically in order to fit the mean temperature profiles during 93–95 determined from all XBTs from that period. This greatly improved the assimilation in all regions, even where the necessary pre-assimilation displacement was relatively small.

The long time-scale variations in hydrography may have consequences for assimilation methods based on statistical correlations between SSH and subsurface properties. The correlations must be relevant to the period of assimilation. If they are based on observations made at different time, these correlations may no longer be valid during the assimilation.

The assimilation method could not satisfactorily recreate the water column

in the upper layers where the ocean is affected by interaction with the atmosphere. The temperature and salinity profiles change shape with the deepening and cooling of the winter mixed-layer and then the creation of a thin warm summer mixed-layer. This cannot be recreated by vertical displacement alone. The use of sea surface temperature as additional information was inadequate as it tells us nothing of the depth of the mixed-layer. The best solution appears to be to ignore the mixed-layer and hope to gain good results just in the permanent thermocline.

However, a proportion of the SSH signal comes from the expansion and contraction of the surface waters. Hence, a spatial filter was used on the SLA fields to remove this part from the sea level anomalies and this did improve the results of the assimilation in the permanent thermocline. There is, however, some concern that this filter will also remove some large-scale SLA features which do arise from a displacement of the thermocline. The tropics show some large-scale SLAs which are due to large-scale circulation changes, such as El Niño, rather than seasonal effects. This is probably why the assimilation is less successful with the steric filter in the tropical Pacific than without. It may, therefore, be best to avoid using the filter in tropical regions.

The pre-assimilation displacement may also introduce errors in the mixed layer as lowering will create a deeper mixed-layer and lifting will remove the surface waters of the water column.

These problems with determining near-surface water properties from assimilation of altimetry have been recognised by both Carnes et al. (1990) and Ezer and Mellor (1997). Carnes et al. (1990) found that his synthetic temperature profiles matched XBTs best in the deeper ocean and Ezer and Mellor (1997) found that their assimilation was most effective at 500m depth, in the permanent thermocline. It does seem that in order to create a nowcast that is good for the near-surface layers as well as the deeper ocean, a more sophisticated method to estimate the mixed-layer is required.

Ezer and Mellor (1997) also stated that in the deep ocean, below the permanent thermocline, the assimilation was not as effective as in thermocline. Here, as most XBTs only go down to 800m, it is not possible to know how accurate the profiles are below. Further study using deeper temperature measurements is required to

assess the effect of the assimilation at depth.

Displacing climatological profiles to make a best possible fit with XBTs reveals that only 50% improvement can be made by vertical displacement alone. The rest of the difference between climatology and XBTs is due to difference in shape of the temperature profile. Some of this change in shape may be a long-term variation, in which case, a further correction to the original climatology may be made as well as the pre-assimilation displacement. This could be achieved by examining the thickness between set isotherms of the climatological profile and stretching or squashing these so that they match the mean thicknesses determined from XBTs throughout the assimilation period.

Some of the changes in shape of vertical profiles may come about during the assimilation period, perhaps by advection of water masses in one layer only. In this case, vertical displacement in response to an observed SLA will not work effectively. This is a limitation of the assimilation of SLAs with climatological hydrography. Assimilation into a good model may not suffer so much from this problem but these findings may indicate the need to assimilate subsurface information from XBTs and other sources as well as altimetry.

Chapter 7

Conclusions

7.1 North Atlantic Hydrography

Two climatological hydrographies of temperature and salinity in the North Atlantic have been compared, Levitus (1994) and Lozier et al. (1995). The Levitus climatology had been smoothed greatly whereas the Lozier data set was in a raw form, with several gaps and completely unsmoothed.

The gaps in the Lozier data set were filled and smoothed to produce new climatological hydrography. All processing was performed on isopycnal surfaces to avoid unrealistic mixing of water masses. This also helped preserve steep gradients of temperature and salinity as they vary more slowly on isopycnal surfaces than on depth surfaces. Smoothing scales were kept very small in order to preserve as much resolution as possible.

The resultant climatology was smooth but retained some of the small scale, but important, features that had been smoothed out in the Levitus climatology. It was notably better at representing the Gulf Stream, where the steep gradients had been smoothed too much by Levitus. In this area, temperature profiles from the smoothed Lozier climatology were closer in shape to XBT observations than were Levitus profiles.

It must be noted that the Lozier data set was processed for the purposes of this research, namely as a first guess for the objective analysis of historical subsurface temperature observations and for assimilation with altimetry. This required a good hydrography of the deep ocean. The original Lozier data set did not have any information on the shallower waters of continental shelves and this was not needed here. Also, the near surface layers, the top 50m, are not as smooth as

lower levels. These shortcomings did not affect the use of the climatology here but may need addressing if this product were to be used for other purposes.

7.2 Interdecadal Variability

Interdecadal variability in the North Atlantic was studied by objectively analysing subsurface temperature data to produce a time series of temperature anomaly maps from 1950 to 1994. The data were mostly from bathythermograph observations which have not been used much in previous research on variability. It has been shown that these data can be used to examine the development and evolution of large scale temperature anomalies in the upper 500m of ocean.

Evidence was found for the progression of temperature anomalies from one region of the North Atlantic to others. Three paths of movement of anomalies have been tentatively identified. The first is from the northern subtropical gyre along the Gulf Stream and North Atlantic Current into the northeastern Atlantic. The second is a path, apparently following the Irminger and Greenland Currents, from the northeastern Atlantic into the Labrador Sea. Finally, a warm anomaly was seen to smoothly move westwards across the ocean following the return flow of the southern subtropical gyre. These transitions were not always smooth and it is not clear how they progress from one region to another. The movement is similar in paths and manner to that of SST anomalies reported by Hansen and Bezdek (1996).

It was found that a dipole pattern existed during most of the period. When the western subtropical gyre was occupied by a temperature anomaly, the ocean north of 50°N was occupied by an anomaly of the opposite sign. It was also found that these regions appeared to show a cycle of approximately 30 years but the data record is not long enough to determine whether this is an oscillation or just a feature of this particular period.

Two strong temperature anomalies in the subtropical gyre were identified. The first, in 1966–72, was a cold anomaly and was characterised by a lifting of isotherms and a lessening of the temperature gradients across the Gulf Stream front. This suggests that the gyre circulation has lessened. During the second anomaly, a very warm event in 1988–94, the Gulf Stream front steepened con-

siderably and strong bowling of isotherms was seen in the subtropical gyre. This implies a stronger Gulf Stream and recirculation. The warm event produced temperature anomalies, greatest at a depth of 500–700m, more intense than any other since 1950.

These events may be caused by spinning-up or slowing down of the gyre circulation. The cold anomaly occurred at the end of period of low North Atlantic Oscillation index characterised by reduced westerly winds over the mid-latitude North Atlantic. The warm period coincided with high NAO index with strong westerlies and trade winds. This strongly suggests that the subtropical gyre has responded to the wind fields acting on the sea surface which lead to the observed events.

7.2.1 Further work

We have identified several large anomalies in subsurface temperature fields of the North Atlantic but the causes and mechanisms behind most of them are still not well understood. Although an explanation has been found for the cold and warm anomalies in the subtropical gyre, other anomalies and their evolution and propagation require further investigation.

The temperature data could be analysed further by investigating changes in the thickness of layers of water between isotherms. This may help to determine the source of temperature changes. Another source of information which may help the investigation is to look at salinity data from CTDs. The drawback is that they may be too scarce to be of sufficient use. Salinity will also help to determine the origin of water masses which may be useful in understanding the causes of the variability.

At the end of the data in 1994, the warm anomaly in the subtropical gyre was still very strong. It was also showing signs of spreading along the North Atlantic Current. It would be very interesting to obtain data from the following years to see how the anomaly evolves and whether it has further affects on the rest of the ocean.

Clearly one of the major problems facing research into oceanic variability is the limited amount of data available. These data only go back to 1950 and this is evidently not long enough to study interdecadal variability. Good spatial

coverage, observing the ocean to reasonable depths, and repeated year after year is required to study long-term variations and to monitor climatic change.

7.3 Assimilation of altimetry with climatological hydrography

Sea level anomalies from 1993–95, derived from the TOPEX/POSEIDON satellite altimeter, were assimilated with climatological hydrography in the North Atlantic and the Pacific. This model-independent and computationally inexpensive method was used to create new hydrographic fields to represent the ocean at the time of altimetric observation. Such fields could be used where one might normally use a climatology but would be more relevant to a particular time. The hydrography might also be used to estimate geostrophic currents.

The hydrographies, pre- and post-assimilation, were compared with XBT observations to evaluate the effectiveness of the assimilation scheme. In the North Atlantic, the smoothed Lozier and the Levitus (1994) climatologies were tested. Throughout most of the ocean both performed similarly, however, in the Gulf Stream region, the Lozier data set was considerably better both before and after assimilation. This is due to the excessive smoothing of properties in the steep gradients of the Gulf Stream in the Levitus climatology.

A persistent discrepancy between both climatological hydrographies and the XBTs from 1993–95 was found. This is due to the warm anomaly in the northern subtropical gyre described earlier. In order for the assimilation to work, the hydrography must be consistent with the years from which the mean altimetric sea surface height is derived. Therefore, before assimilation, the climatology is adjusted by vertically displacing water columns so that they fit closely to the mean XBT observations from 1993–95. This correction improved results of the assimilation significantly.

The assimilation gave the best results in reproducing the permanent thermocline but could not recreate the mixed-layer and waters influenced by interaction with the atmosphere. Attempts to use SST as additional information to constrain the mixed-layer were unsuccessful as the depth of the mixed-layer is still unknown. More sophisticated methods may be necessary to define this region. In

order to increase the success of the assimilation in the permanent thermocline, a spatial filter was applied to the SLA fields before assimilation to remove the effect on the sea surface height of heating and cooling of the mixed-layer. However, this was found to be detrimental in the tropics where large-scale SLAs are often due to large scale circulation changes.

The assimilation scheme was evaluated by calculating mean temperature differences over 100–700m depth between XBTs and pre- and post-assimilation profiles from the climatological hydrography. In the North Atlantic, using the smoothed Lozier climatology, the western Atlantic, with the Gulf Stream and associated meanders and eddies, was the region with the largest differences, but also showed the largest improvement with assimilation. The initial mean difference in this region was 1.9°C, which was reduced to 1.7°C with the pre-assimilation correction to bring the climatology into agreement with the mean 93–95 hydrography. The assimilation of sea level anomalies, filtered to remove steric height changes, further improved the mean difference to 1.5°C. This is an overall improvement of 22%. The eastern Atlantic was improved from 0.84°C to 0.76°C by 93–95 mean correction and to 0.69°C by assimilation, with an overall improvement of 17.1%. In the tropics the improvements were from 1.01°C to 0.94°C to 0.85°C respectively and overall, 15.5%.

The subpolar region showed good improvement from 0.92°C to 0.76°C with 93–95 mean correction and a smaller improvement to 0.71°C with assimilation. Inspection of individual cases, however, showed problems with vertical displacement and the evaluation method in this region. This far north, the XBTs show a shallow mixed-layer and thermocline with poorly stratified water below. Seasonal variations in the shape of profiles were extreme, from a very shallow mixed-layer in summer to deep winter convection which in some places removed the thermocline altogether. Vertical displacements could not take into account these large seasonal variations so it is concluded that the effectiveness of this assimilation approach is limited in high latitude regions.

The assimilation scheme was also applied to a Levitus (1994) climatological hydrography of the Pacific. The assimilation was most successful in the tropics where an overall improvement of 26% was achieved. In the tropical Pacific, changes in circulation often occur on large scales, giving rise to large-scale sea

level anomalies. These signals will be removed by the steric filter, which reduces the success of the assimilation here. As seasonal changes are small in the tropics, the best assimilation results are achieved without the steric filter. In the rest of the ocean, mean overall improvement was between 13% and 19%.

These figures show that the assimilation scheme has not reached its full potential. Some other problems with the scheme that have been identified are: errors in the altimetry and in the mapping of sea level anomalies from data on satellite tracks, changes in barotropic currents and differences in temperature profile shapes due to changes in advection and water masses. However, considering the simplicity of the method, the results show some significant improvement.

The mean best possible improvement by vertical displacement alone in the North Atlantic was 48%. This shows that only half of the difference between the XBTs and the climatology is due to a vertical displacement. The rest is from differences in shape of the profile, either from the mixed-layer and seasonal thermocline or changes in the shape of the thermocline. Such changes in subsurface structure cannot be inferred from sea surface observations alone, the only way to determine them is with in situ measurements such as XBTs. This indicates the need for the assimilation of XBTs in models as well as surface observations to constrain the subsurface structure.

Appendix A

Mapping Technique

In several parts of the work, I have irregularly spaced observations or data that I wish to map onto a regular grid. The most common example of this is where I have data from expendable bathythermograph observations. These are deployed from ships, or sometimes by air, crossing the oceans. Sometimes these are specific oceanographic cruises but often XBTs are deployed from merchant ships. Consequently, these are unevenly distributed over the oceans, in both space and time. It is desired that these observations are averaged and mapped onto a regular grid, usually a 1°x1° grid.

Figure A.1 illustrates the problem. Data are spread in an irregular pattern, shown as crosses, which we wish to present on the regular grid. To assign a value to the gridpoint marked, all points within the influence radius, R, are averaged. Data are weighted according to distance from the gridpoint by a Gaussian function:

$$w_s = \exp\left(-\frac{r_s^2}{(R/2)^2}\right) \tag{A.1}$$

where r_s is the distance of data point s from the gridpoint. The term $R/2$ determines the scale width of the function. Here it is chosen so that a data point at the edge of the influence radius is given a weighting of 2% of a point at the centre. At the radius $R/2$, the data is weighted by $1/e$ =37%.

Data and gridpoints are defined in terms of latitude and longitude. However, the distance between lines of longitude decreases closer to the poles so the calculation of distance between gridpoint and data point has to account for this.

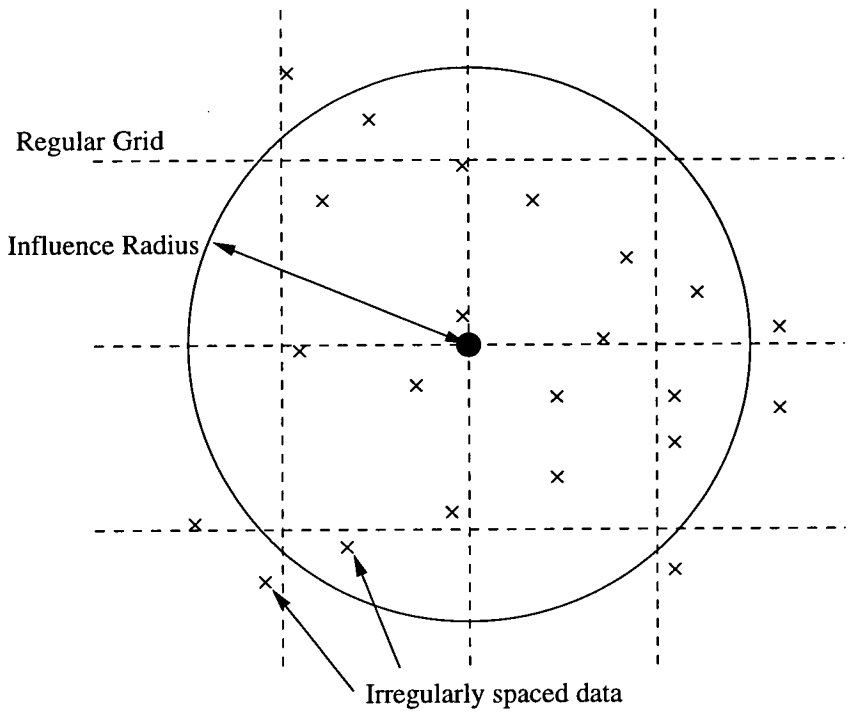

Figure A.1: Irregularly spaced data points which must be mapped onto a regular grid.

Thus, the property value of the gridpoint, A_{ij}, is determined by,

$$A_{ij} = \frac{\sum_{s=1}^{N} a_s w_s}{\sum_{s=1}^{N} w_s} \tag{A.2}$$

where a_s is the property of the data point s. The data $s = 1$ to N are those points within the influence radius. There is also usually a lower limit to the number of data points within the circle, below which the gridpoint will be given a null value.

This mapping scheme averages and smoothes the data at the same time. The advantage of it is that if there are large gaps in the data these can be filled with estimate values from the nearest surrounding data. However, there are some disadvantages to it. It is indiscriminate as to where within the influence radius the available data may lie. It is possible that there will be more on one side that another so, particularly if there are strong gradients, the data may be biased to one side. If there is a cluster of repeat observations in one place they may dominate the mapping onto those gridpoints within the influence radius.

Bibliography

Andersen, O. B., Woodworth, P. L. and Flather, R. A.: 1995, Intercomparison of recent ocean tide models, *J. Geophys. Res.* **100**, 25261–25282.

Antonov, J. I.: 1993, Linear trends of temperature at intermediate and deeplayers of the North Atlantic and North Paciic oceans: 1957–1981, *J. Climate* **6**, 1928–1942.

Barnston, A. G. and Livezey, R. E.: 1987, Classification, seasonality and persistence of low-frequency atmospheric circulatioon patterns, *Mon. Wea. Rev.* **115**, 1083–1126.

Belkin, I. G. and Levitus, S.: 1996, Temporal variability of the subarctic front near the Charlie-Gibbs Fracture Zone, *J. Geophys. Res.* **101**, 28317–28324.

Berry, P. J. and Marshall, J. C.: 1989, Ocean modelling studies in support of altimetry, *Dyn. Atmos. Oceans* **13**, 269–300.

Bjerknes, J.: 1964, Atlantic air-sea interaction, *Adv. Geophys.* **10**, 1–82.

Blayo, E., Verron, J. and Molines, J. M.: 1994, Assimilation of TOPEX/POSEIDON altimeter data into a circulation model of the North Atlantic, *J. Geophys. Res.* **99**, 24691–24705.

Bretherton, F. P., Davis, R. E. and Fandry, C. B.: 1976, A technique for objective analysis and design of oceanographic experiments applied to MODE-73, *Deep-Sea Res.* **23**, 559–582.

Bryden, H. L., Griffiths, M. J., Lavin, A. M., Millard, R. C., Parrilla, G. and Smethie, W. M.: 1996, Decadal changes in water mass characteristics at 24°N in the subtropical North Atlantic Ocean, *J. Climate* **9**, 3162–3186.

Carnes, M. R., Mitchell, J. L. and deWitt, P. W.: 1990, Synthetic temperature profiles derived from GEOSAT altimetry: Comparison with air-dropped expendable bathythermograph profiles, *J. Geophys. Res.* **95**, 17979–17992.

Cartwright, D. E. and Ray, R. D.: 1990, Oceanic tides from Geosat altimetry, *J. Geophys. Res.* **95**, 3069–3090.

Cartwright, D. E. and Ray, R. D.: 1991, Energetics of global ocean tides from Geosat altimetry, *J. Geophys. Res.* **96**, 16897,16912.

Cheney, R. E.: 1995, Preface to the Journal of Geophysical Research special edition on TOPEX/POSEIDON, *J. Geophys. Res.* **100**(C12), 24893.

Cooper, M. C.: 1995, *A dynamical method for assimilation of altimeter data into ocean models*, PhD thesis, University of Edinburgh.

Cooper, M. C. and Haines, K.: 1996, Altimetric assimilation with water property conservation, *J. Geophys. Res.* **101**(C1), 1059–1077.

Curry, R. G., McCartney, M. S. and Joyce, T. M.: 1998, Oceanic transport of subpolar climate signals to mid-depth subtropical waters, *Nature* **391**, 575–577.

Delworth, T., Manabe, S. and Stouffer, R. J.: 1993, Interdecadal variations of the thermohaline circulation in a coupled ocean-atmosphere model, *J. Climate* **6**, 1993–2011.

Deser, C.: 1996, A century of North Atlantic data indicates interdecadal change, *Oceanus* **39**(2), 11–13.

Deser, C. and Blackmon, M. L.: 1993, Surface climate variations over the North Atlantic Ocean during winter: 1900-1989, *J. Climate* **6**, 1743–1753.

Dewar, W. K.: 1986, Mixed layers in Gulf Stream rings, *Dyn. Atmos. Oceans* **10**, 1–29.

Dickson, R. R.: 1997, From the Labrador Sea to global change, *Nature* **388**, 649–650.

Dickson, R. R., Meincke, J., Malmberg, S. A. and Lee, A. J.: 1988, The 'Great Salinity Anomaly' in the northern North Atlantic 1968–1982, *Prog. Oceanogr.* **20**, 103–151.

Dietrich, G., Kalle, K., Krauss, W. and Siedler, G.: 1975, *General Oceanography, 2nd Ed.*, John Wiley, New York.

Drakopoulos, P. G., Haines, K. and Wu, P.: 1997, Altimetric assimilation in a Mediterranean general circulation model, *J. Geophys. Res.* **102**, 10509–10523.

Drinkwater, K. F., Myers, R. A., Pettipas, R. G. and Wright, T. L.: 1994, Climatic data for the northwest Atlantic: the position of the shelf/slope front and the northern boundary of the Gulf Stream between 50°W and 75°W, 1973–1992, *Can. Data Rep. Hydrogr. Ocean Sci.* **125**, 103.

Ezer, T. and Mellor, G. L.: 1994, Continuous assimilation of GEOSAT altimeter data into a three-dimensional primitive equation Gulf Stream model, *J. Phys. Oceanogr.* **24**, 832–847.

Ezer, T. and Mellor, G. L.: 1997, Data assimilation experiments in the Gulf Stream region: how useful are satellite derived surface data for nowcasting the subsurface fields?, *J. Atmos. Oceanic Technol.* **14**, 1379–1391.

Fu, L. L., Christensen, E., Lefebvre, M., Menard, Y., Yamarone, C. A., Dorrer, M. and Escudier, P.: 1994, TOPEX/POSEIDON mission overview, *J. Geophys. Res.* **99**(C12), 24369–24381.

Gaspar, P. and Ponte, R. M.: 1997, Relation between sea level and barometric pressure determined from altimeter data and model simulations, *J. Geophys. Res.* **102**, 961–971.

Gill, A. E. and Niiler, P. P.: 1973, The theory of the seasonal variability in the ocean, *Deep Sea Res.* **20**, 141–177.

Greatbatch, R. I., Fanning, A. F. and Goulding, A. D.: 1991, A diagnosis of interpentadal circulation changes in the north atlantic, *J. Geophys. Res.* **96**(C12), 22009–22023.

Grötzner, A., Latif, M. and Barnett, T. P.: 1998, A decadal climate cycle in the North Atlantic Ocean as simulated by the ECHO coupled GCM, *J. Climate* **11**, 831–847.

Haines, K.: 1991, A direct method for assimilating sea surface height into ocean models with adjustments to the deep circulation, *J. Phys. Oceanogr* **21**, 843–868.

Haines, K., Melanotte-Rizzoli, P., Young, R. E. and Holland, W. R.: 1993, A comparison of two methods for the assimilation of altimeter data into a shallow water model, *Dyn. Atmos. Oceans* **17**, 89–133.

Halliwell, G. R.: 1998, Simulation of North Atlantic decadal/multidecadal winter SST anomalies driven by basin-scale atmospheric circulation anomalies, *J. Phys. Oceanogr.* **28**, 5–21.

Hansen, D. V. and Bezdek, H. F.: 1996, On the nature of decadal anomalies in North Atlantic sea surface temperature, *J. Geophys. Res.* **101**, 8749–8758.

Hayes, S. P., Mangum, L. J., Picaut, J., Sumi, A. and Takeuchi, K.: 1991, TOGA-TAO: A moored array for real time measurements in the tropical Pacific Ocean, *Bull. Amer. Meteor. Soc.* **72**, 339–347.

Helland-Hansen, B.: 1934, The Sognefjord section: Oceanographic observations in the northernmost part of the North Sea and the southern part of the Norwegian Sea, *James Johnson Memorial Volume*, University of Liverpool Press, pp. 257–274.

Helland-Hansen, B. and Nansen, F.: 1909, *The Norwegian Sea, Report on Norwegian Fishery and Marine Investigations*, Vol. II, No. 2, Kristiania, Bergen.

Holland, W. R. and Melanotte-Rizzoli, P.: 1989, Assimilation of altimeter data into an ocean model: Space verses time resolution studies, *J. Phys. Oceanography* **19**, 1507–1534.

Hoskins, B. J.: 1983, *Large Scale Dynamical Processes in the Atmosphere*, Academic, London.

Hurlburt, H. E.: 1986, Dynamical transfer of simulated altimeter data into subsurface information by a numerical ocean model, *J. Geophys. Res.* **91**, 2372–2400.

Hurlburt, H. E., Fox, D. N. and Metzger, E. J.: 1990, Statistical inference of weakly correlated subthermocline fields from satellite altimeter data, *J. Geophys. Res.* **95**, 11375–11409.

Hurrell, J. W.: 1995, Decadal trends in the North Atlantic Oscillation: Regional temperatures and precipitation, *Science* **269**, 676–679.

Jacobs, G. A., Born, G. H., Parke, M. E. and Allen, P. C.: 1992, The global structure of the annual and semiannual sea surface height variability from Geosat altimeter data, *J. Geophys. Res.* **97**, 17813–17828.

Joyce, T. M.: 1984, Velocity and hydrographic structure of a gulf stream warm-core ring, *J. Phys. Oceanogr.* **14**, 936–947.

Joyce, T. M. and Robbins, P.: 1996, The long-term hydrographic record at Bermuda, *J. Climate* **9**, 3121–3131.

Kessler, W. S., Spillane, M. C., McPhaden, M. J. and Harrison, D. E.: 1996, Scales of variability in the equatorial Pacific inferred from the Tropical Atmosphere-Ocean array, *J. Climate* **9**, 2999–3024.

Krauss, W.: 1986, The North Atlantic Current, *J. Geophys. Res.* **91**, 5061–5074.

Kushnir, Y.: 1994, Interdecadal variations in North Atlantic sea surface temperature and associated atmospheric conditions, *J. Climate* **7**, 141–157.

Latif, M. and Barnett, T. P.: 1994, Causes of decadal climate variability over the North Pacific and North Atlantic, *Science* **266**, 634–637.

Latif, M. and Barnett, T. P.: 1996, Decadal climate variability over the North Pacific and North America: dynamics and predictability, *J. Climate* **9**, 2407–2423.

Levitus, S.: 1982, *Climatological atlas of the world ocean.*, NOAA Prof. Pap., Natl. Oceanic and Atmos. Admin., Washington D.C.

Levitus, S.: 1989a, Interpentadal variability of salinity in the upper 150m of the North Atlantic Ocean, 1970–1974 versus 1955–1959, *J. Geophys. Res.* **94**, 9679–9685.

Levitus, S.: 1989b, Interpentadal variability of temperature and salinity at intermediate depths in the North Atlantic Ocean, 1970–1974 versus 1955–1959, *J. Geophys. Res.* **94**, 6091–6131.

Levitus, S.: 1989c, Interpentadal variability of temperature and salinity in the deep North Atlantic Ocean, 1970–1974 versus 1955–1959, *J. Geophys. Res.* **94**, 16125–16131.

Levitus, S.: 1994, World ocean atlas 1994 cd-rom sets., *National Oceanographic Data Center Informal Report.*

Levitus, S. and Antonov, J. I.: 1995, Observational evidence of interannual to decadal scale variability of the subsurface temperature-salinity structure of the world ocean, *Climatic Change* **31**, 495–514.

Levitus, S., Antonov, J. I. and Boyer, T. P.: 1994, Interannual variability of temperature at a depth of 125 meters in the North Atlantic Ocean, *Science* **266**, 96–99.

Lozier, M. S., McCartney, M. S. and Owens, W. B.: 1994, Anomalous anomalies in averaged hydrographic data, *J. Phys. Oceanogr.* **24**, 2624–2638.

Lozier, M. S., Owens, W. B. and Curry, R. G.: 1995, The climatology of the North Atlantic, *Progress in Oceanography* **36**, 1–44.

Luyten, J. R., Pedlosky, J. and Stommel, H.: 1983, The ventilated thermocline, *J. Phys. Oceanogr.* **13**, 292–309.

Marshall, J., Dobson, F., Moore, K., Rhines, P., Visbeck, M., d'Asaro, E., nad S Chang, K. B., Davis, R., Fisher, K., Garwood, R., Guest, P., nad C Herbaut, R. H., Holt, T., Lazier, J., Legg, S., McWilliams, J., Pickart, R., Prater, M., Renfrew, I., Schott, F., Send, U. and Smethie, W.: 1998, The Labrador Sea deep convection experiment, *Bull. Amer. Meteor. Soc.* **79**, 2033–2058.

McCartney, M. S. and Talley, L. D.: 1982, The subpolar mode water of the North Atlantic Ocean, *J. Phys. Oceanogr.* **12**, 1169–1188.

McCartney, M. S., Curry, R. G. and Bezdek, H. F.: 1996, North Atlantic's transformation pipeline chills and redistributes subtropical water, *Oceanus* **39**, 19–23.

Mellor, G. L. and Ezer, T.: 1991, A Gulf Stream and an altimetry assimilation scheme, *J. Geophys. Res.* **96**, 8779–8795.

Meyers, G. and Donguy, J. R.: 1980, An XBT network with merchant ships, *Trop. Ocean-Atmos. Newslett.* **2**, 6–7.

Millero, F. J. and Poisson, A.: 1981, International one-atmosphere equation of state for seawater, *Deep-Sea Res.* **28A**, 625–629.

Millero, F. J., Chen, C.-T., Bradshaw, A. and Schleicher, K.: 1980, A new high pressure equation of state for seawater, *Deep-Sea Res.* **27A**, 255–264.

Mitchum, G.: 1994, Comparison of TOPEX/POSEIDON sea surface heights and tide gauge sea levels, *J. Geophys. Res.* **99**, 24541–24554.

Molinari, R. L., Mayer, D. A., Festa, J. F. and Bezdek, H. F.: 1997, Multi-year variability in the near-surface temperature structure of the midlatitude western North Atlantic Ocean, *J. Geophys. Res.* **102**, 3267–3278.

Nerem, R. S., Lerch, F. J., Marschall, J. A., Pavlis, E. C., Putney, B. H., Tapley, B. D., Eanes, R. J., Ries, J. C., Schutz, B. E., Shum, C. K., Watkins, M. M., Klosko, S. M., Chan, J. C., Luthcke, S. B., Patel, G. B., Pavlis, N. K., anf R H Rapp, R. G. W., Biancale, R. and Nouel, F.: 1994, Gravity model development for TOPEX/POSEIDON - Joint Gravity Model-1 and Model-2, *J. Geophys. Res.* **99**, 24421–24447.

Nouël, F., Berthias, J. P., Deleuze, M., Guitart, A., Laudet, P., Piuzzi, A., Pradines, D., Valorge, C., CDejoie, Susini, M. F. and Taburiau, D.: 1994, Precise Centre National d'Etudes Spatiales orbits for TOPEX/POSEIDON: Is reaching 2 cm still a challenge?, *J. Geophys. Res.* **99**, 24405–24419.

Oschlies, A. and Willebrand, J.: 1996, Assimilation of geosat altimeter data into an eddy-resolving primitive equation model of the North Atlantic Ocean, *J. Geophys. Res.* **101**, 14175–14190.

Parrilla, G., Lavin, A., Bryden, H., Garcia, M. and Millard, R.: 1994, Rising temperatures in the subtropical north atlantic ocean over the past 35 years, *Nature* **369**, 48–51.

Pattullo, J. G.: 1963, Seasonal changes in sea level, in *The Sea*, M. N. Hill (ed.), Vol. 2, Wiley Intersci., New York, pp. 485–496.

Pattullo, J. G., Munk, W. H., Revelle, R. and Strong, E.: 1955, The seasonal oscillation in the sea level, *J. Mar. Res.* **14**, 88–155.

Rapp, R., Wang, Y. M. and Pavlis, N. K.: 1991, The Ohio State 1991 geopotential & sea surface topography harmonic coefficient model, *Dept. Geodetic Science and Surveying Report No.410*, Ohio State University, p. 64.

Reverdin, G., Cayan, D. and Kushnir, Y.: 1997, Decadal variability of hydrograhy in the upper northern North Atlantic in 1948–1990, *J. Geophys. Res.* **102**, 8505–8531.

Rhines, P. B. and Young, W. R.: 1982, A theory of wind-driven circulation: I. Mid-ocean gyres, *J. Mar. Res.* **40 (Suppl)**, 559–596.

Roemmich, D.: 1983, Optimal estimation of hydrographic station data and derived fields, *J. Phys. Oceanogr.* **13**, 1544–1549.

Roemmich, D. and Wunsch, C.: 1984, Apparent changes in the climatic state of the deep North Atlantic Ocean, *Nature* **307**, 447–450.

Schmitz, W. J. and McCartney, M. S.: 1993, On the North Atlantic circulation, *Rev. Geophys.* **31**, 29–49.

Schwiderski, E. W.: 1980a, Ocean tides, 1, global ocean tidal equations, *Mar. Geod.* **3**, 161–217.

Schwiderski, E. W.: 1980b, Ocean tides, 2, a hydrodynamical interpolations model, *Mar. Geod.* **3**, 218–257.

Shum, C. K., Woodworth, P. L., Andersen, O. B., Egbert, G. D., Francis, O., King, C., Klosko, S. M., Le Provost, C., Li, X., Molines, J.-M., Parke, M. E., Ray, R. D., Schlax, M. G., Stammer, D., Tierney, C. C., Vincent, P. and Wunsch, C. I.: 1997, Accuracy assessment of recent ocean tide models, *J. Geophys. Res.* **102**, 25173–25194.

Smith, N. R. and Meyers, G.: 1996, An evaluation of expendable bathythermograph and Tropical Atmosphere-Ocean Array data for monitoring tropical ocean variability, *J. Geophys. Res.* **101**, 28489–28501.

Stammer, D.: 1997, Steric and wind-induced changes in TOPEX/POSEIDON large-scale sea surface topography observations, *J. Geophys. Res.* **102**, 20987–21009.

Stammer, D. and Wunsch, C.: 1994, Preliminary assessment of the accuracy and precision of TOPEX/POSEIDON altimetry data with respect to the large scale ocean circulation, *J. Geophys. Res.* **99**, 25584–25604.

Stommel, H.: 1979, Determination of water mass properties of water pumped down from the Ekman layer to the geostrophic flow below, *Pro. Natl. Acad. Sci* **79**, 3051–3055.

Sutton, R. T. and Allen, M. R.: 1997, Decadal predictability of North Atlantic sea surface temperature and climate, *Nature* **388**, 563–567.

Talley, L. D.: 1984, Meridional heat transport in the pacific ocean, *J. Phys. Oceanogr.* **14**, 231–241.

Talley, L. D. and McCartney, M. S.: 1982, Distribution and circulation of Labrador Sea water, *J. Phys. Oceanogr.* **12**, 1189–1205.

Talley, L. D. and Raymer, M. E.: 1982, Eighteen degree water variability, *J. Mar. Res.* **40 (Suppl.)**, 757–775.

Tapley, B. D., Chambers, D. P., Shum, C. K., Eanes, R. J., Ries, J. C. and Stewart, R. H.: 1994, Accuracy assessment of the large-scale dynamic ocean topography from TOPEX/POSEIDON altimetry, *J. Geophys. Res.* **99**, 24605–24617.

Tapley, B. D., Watkins, M. M., Ries, J. C., Davis, G. W., Eanes, R. J., Poole, S. R., Rim, H. J., Schutz, B. E., Shum, C. K., Nerem, R. S., Lerch, F. J., Marshall, J. A., Klosko, S. M., Pavlis, N. K. and Williamson, R. G.: 1996, The joint gravity model 3, *J. Geophys. Res.* **101**, 28029–28049.

Taylor, A. H.: 1995, North-south shifts of the Gulf Stream and their climatic connection with the abundance of zooplankton in the UK and its surrounding seas, *J. Mar. Sci.* **52**, 711–721.

Taylor, A. H.: 1996, North-south shifts of the Gulf Stream: Ocean-atmosphere interactions in the North Atlantic, *Int. J. Climatol.* **16**, 559–583.

Taylor, A. H. and Stephens, J. A.: 1980, Latitudinal displacements of the Gulf Stream (1966 to 1977) and their relation to changes in temperature and zooplankton abundance in the northeast Atlantic, *Oceanol. Acta* **3**, 145–149.

Taylor, A. H. and Stephens, J. A.: 1998, The North Atlantic Oscillation and the latitude of the Gulf Stream, *Tellus* **50A**, 134–142.

Unesco: 1981, Background papers and supporting data on the International Equation of state of seawater 1980, *Unesco technical papers in marine science.*

van Loon, H. and Rogers, J. C.: 1978, The seesaw in winter temperatures between Greenland and Northern Europe part 1: General description, *Mon. Wea. Rev.* **106**, 296–310.

Verron, J.: 1992, Nudging satellite altimeter data into quasi-geostrophic ocean models, *J. Geophys. Res.* **97**, 7479–7491.

Walker, G. T. and Bliss, E. W.: 1932, World weather V, *Mem. Roy. Meteor. Soc* **4**, 53–84.

Williams, R. G.: 1988, Modification of ocean eddies by air-sea interaction, *J. Geophys. Res.* **93**, 15523–15533.

Williams, R. G.: 1989, The influence of air-sea interaction on the ventilated thermocline, *J. Phys. Oceanogr.* **19**, 1255–1267.

Worthington, L. V.: 1959, The 18° water in the Sargasso Sea, *Deep-Sea Res.* **5**, 297–305.

Worthington, L. V.: 1976, *On the North Atlantic Circulation*, The John Hopkins University Press, Baltimore, Md.

Wunsch, C. and Stammer, D.: 1997, Atmospheric loading and the oceanic "inverted barometer" effect, *Rev. Geophys.* **35**, 79–107.

Wyrtki, K., Magaard, L. and Hager, J.: 1976, Eddy energy in the oceans, *J. Geophys. Res.* **81**, 2641–2646.

Zorita, E. and Frankignoul, C.: 1997, Modes of North Atlantic decadal variability in the ECHAM1/LSG coulped ocean–atmosphere general circulation model, *J. Climate* **10**, 183–201.